WAR DEPARTMENT
CORPS OF ENGINEERS
ENGINEER DEPARTMENT

DEPARTMENT OF COMMERCE
WEATHER BUREAU
HYDROMETEOROLOGICAL SECTION

HYDROMETEOROLOGICAL REPORT NO. 1

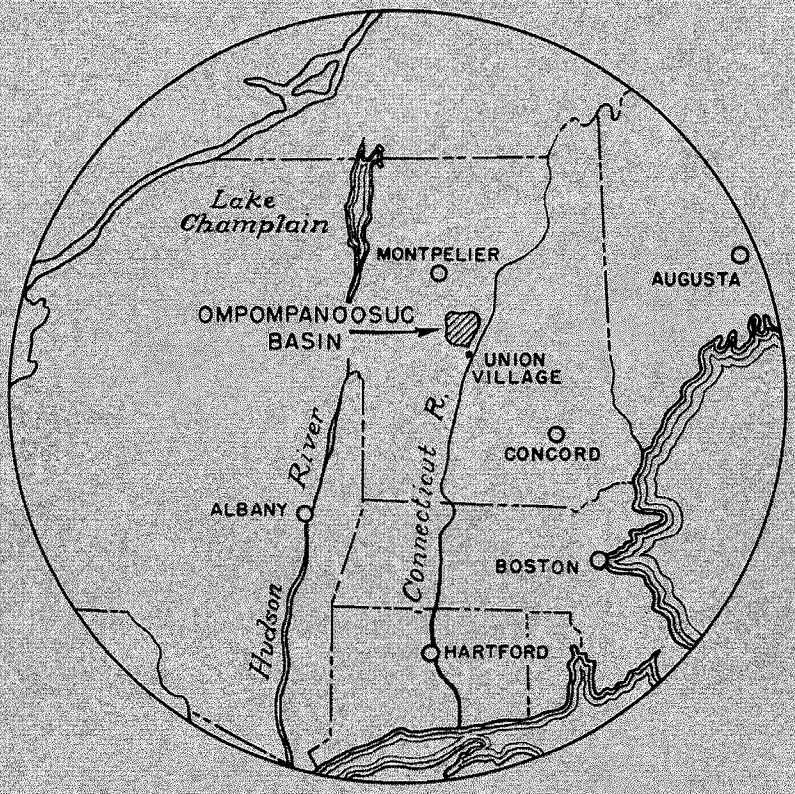

MAXIMUM POSSIBLE PRECIPITATION

OMPOMPANOOSUC BASIN

ABOVE UNION VILLAGE

VERMONT

Department of Commerce
Weather Bureau
Hydrometeorological Section

War Department
Corps of Engineers
Engineer Department

Hydrometeorological Report No. 1

MAXIMUM POSSIBLE PRECIPITATION

OVER THE OMPOMPANOOSUC BASIN ABOVE UNION VILLAGE, VERMONT

A Study of Meteorological Causes of Record
Storms and Quantitative Estimates of
Critical Precipitation Rates

Prepared by

The Hydrometeorological Section of the Weather Bureau

in cooperation with

The Corps of Engineers, U. S. Army

and submitted

March 18, 1940

454

Published at
U. S. Waterways Experiment Station
Vicksburg, Mississippi
1943

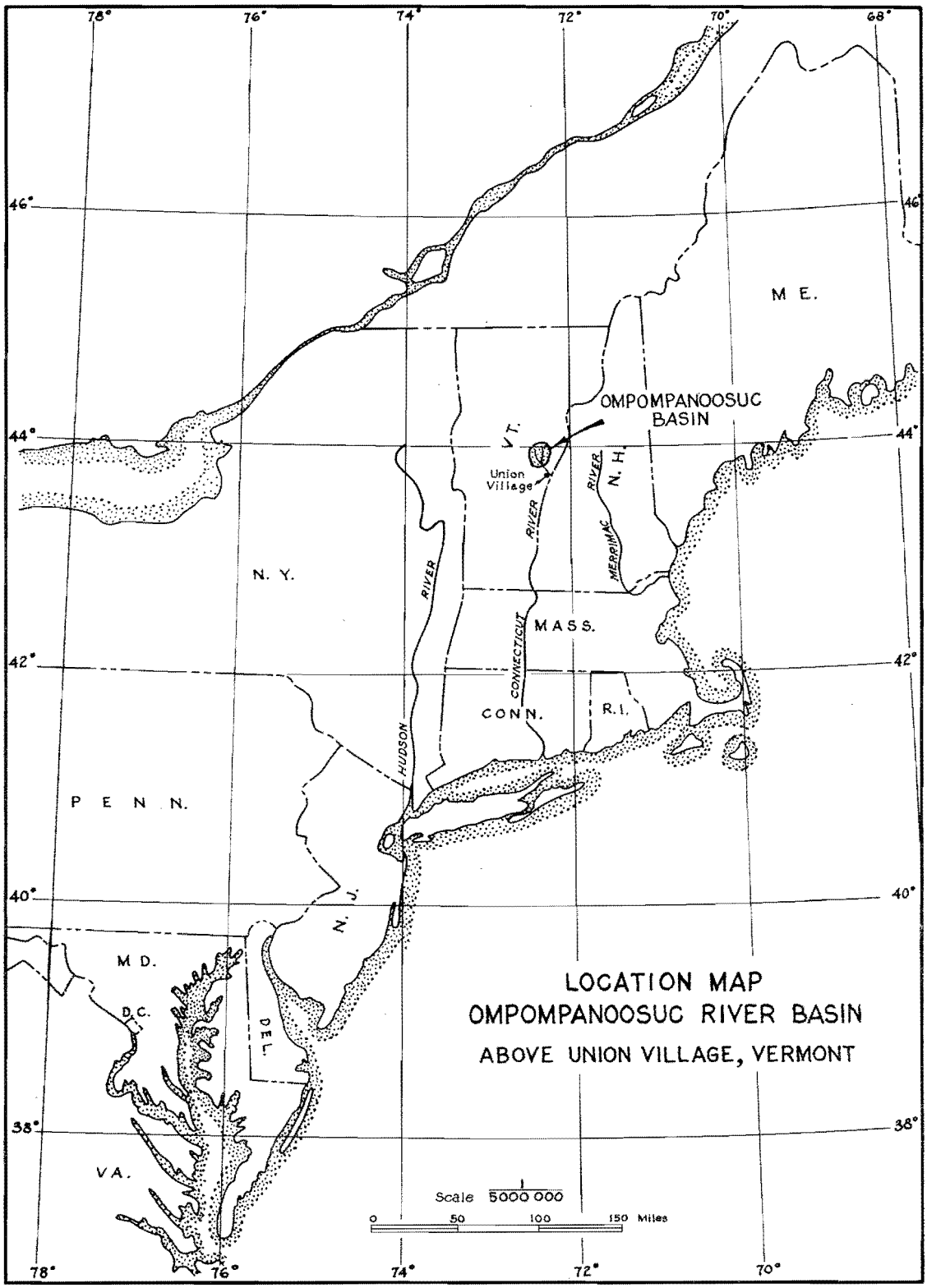

Frontispiece

TABLE OF CONTENTS

LIST OF FIGURES

LIST OF FIGURES (Cont.)

LIST OF FIGURES (Cont.)

INTRODUCTION

When this study was undertaken by the Hydrometeorological Section of the Weather Bureau at the request of the Office of the Chief of Engineers, it was to apply only to the Ompompanoosuc Basin above Union Village, Vermont. However, after it was under way, due to the similarity of conditions that would produce the maximum possible precipitation over much of the northeastern section of the United States, it was decided to include all the Atlantic drainage from the Kennebec to the Hudson River Basin, inclusive. It was also decided to make the study applicable to areas of from 100 to 1,000 square miles.

Reports prepared by the Division and District Offices of the U. S. Engineer Department, containing precipitation data, isohyetal maps, and mass rainfall curves for a large number of major storms in the central and eastern United States, have formed a broad basis for the study of storm patterns and precipitation characteristics. In addition to published records, such reports include all precipitation data and miscellaneous information on storms obtainable from the manuscripts of original records, files of municipal agencies, newspapers, testimony of witnesses, and similar sources. Data assembled and organized by the Engineer Offices are reviewed by the Hydrometeorological Section and are supplemented by meteorological analyses. There has been profitable collaboration with representatives of the Office of Chief of Engineers

and with personnel visiting the Section from District and Division Offices of the Engineer Department.

The following members of the Hydrometeorological Section contributed to the preparation of the final report under the direction of Merrill Bernard, Principal Hydrologist:

D. C. Cameron, Meteorologist in Charge
E. Bellay, Associate Meteorologist
A. K. Showalter, Associate Meteorologist
H. C. S. Thom, Associate Hydrologic Engineer
G. N. Brancato, Assistant Meteorologist
F. R. Jones, Assistant Meteorologist
F. W. Kenworthy, Assistant Meteorologist
P. Light, Assistant Hydrologic Engineer
S. B. Solot, Assistant Meteorologist
J. S. Sweet, Assistant Hydrologic Engineer
W. T. Wilson, Assistant Hydrologic Engineer
C. Woo, Assistant Hydrologic Engineer
J. T. Bray, Junior Meteorologist
C. G. Gilbert, Junior Meteorologist
H. K. Gold, Junior Meteorologist
J. R. Rosenthal, Junior Meteorologist
A. L. Shands, Junior Meteorologist

Very capable assistance was rendered by the sub-professional and clerical staff.

As snow melt is a vital factor in producing floods in this region, the storms were divided into two groups: (1) storms that occur when no snow is present, and (2) storms that occur when snow is present; the runoff from snow melt is added to that from storm rainfall. The maximum amount of water that can be present in the form of snow and the maximum rate at which it can melt is a problem that will require more research and study than has been possible in this report. An examination of snow melt literature discloses a paucity of data and lack of adequate technique for determining rates of snow melt. In this report, however, an approach has been made by estimating snow melt rates from a study of the

March 1936 records of snow cover, precipitation, discharge, and other data for various New England basins.

After all the basic data were completed, enveloping duration-depth and area-depth curves were prepared. These curves were verified through comparison with the enveloping curves derived by increasing the storms on the basis of the maximum amount of precipitable water.

This report, originally issued March 18, 1940, is reprinted in its original form. More thorough treatments of the problems of snow melt and theoretical adjustments of storm rainfall are contained in subsequent reports entitled "Maximum Possible Precipitation over the Ohio River Basin above Pittsburgh, Pennsylvania" and "Maximum Possible Precipitation over the Sacramento Basin of California."

CHAPTER I

PHYSICAL FEATURES

Topographic influences

The Ompompanoosuc Basin is located in the upper Connecticut River watershed in east-central Vermont. This area lies in the upper Appalachian Mountain chain, between the White and Green Mountains; the extreme upper reaches of the Ompompanoosuc Basin are a part of the former range. Elevations above mean sea level within the basin range from 550 feet at the dam site to 2,412 feet at the summit of Colton Hill near the northwest edge of the basin. The terrain is extremely hilly and irregular, but can hardly be termed mountainous.

The general area while located well within the northern Appalachian highlands is not particularly affected by orographic influences, since nearly all precipitation in New England is produced by cyclonic or frontal action and the relatively low mountain ranges are a minor factor in augmenting or diminishing precipitation. The exceptions may be found in some headwater regions of the principal rivers of New England where the valley is open to the southeast or south and is flanked by mountains which crest between 4,000 and 6,000 feet, such as the Merrimac Basin. In the warm sector of a cyclone, convergence of the very moist tropical air at the heads of such valleys may result in an appreciable increase in the local precipitation as compared with the general isohyetal

pattern of the storm.

Climatology

This general summary includes the climatology of the Atlantic drainage area of New England and the Hudson River drainage area in New York State.

The entire region is so situated geographically that it receives a maximum frequency of visitation of cyclonic storm activity through the entire year, in fact, this area eventually comes under the influence of the majority of cyclonic disturbances which affect the United States. No seasonal variation in precipitation is important, annual rainfall being evenly distributed throughout the months. In general, short period rainfall intensities are greatest in late spring and summer and excessive rains of longer durations occur in late summer and early fall. The extremes of average annual precipitation in New England range from 35 inches in northern Vermont and New Hampshire, with the exception of Mt. Washington where it is considerably higher due to orographic effects in the White Mountains, to 47 inches in southwestern Connecticut and 48 inches on the central coast of Maine. Excessive 24-hour amounts during winter months, December to March, of more than three inches are rare, but summer rainfall excesses are more frequent because of high intensities experienced in thunderstorms. A very even distribution of thunderstorm occurrence makes all parts of the region liable to high short-period rainfall intensities during the summer months.

Since great accumulations of snow may occur and since the types of cyclonic disturbances which visit this region may result in rapid melting, snow is an extremely important factor in flood production. At

Boston, Massachusetts, the average annual snowfall is 43.8 inches, with extremes of 96.4 inches during the winter of 1873-74 and 10 inches during the winter of 1875-76. The average seasonal snowfall at first order Weather Bureau stations ranges from 50.4 inches at Albany, New York, 60.4 inches at Portland, Maine, and 73.0 inches at Concord, New Hampshire, to 38.6 inches at New Haven, Connecticut, and 32.4 inches at Providence, Rhode Island. The greatest average seasonal snowfall from any reporting station is 168.3 inches at Pittsburgh, New Hampshire.

CHAPTER II

TYPES OF STORMS

There are four types of storms which could produce heavy rainfall over small areas in New England:

Stationary frontal type

Rapidly moving intense cyclones

Hurricanes

Thunderstorms, local or frontal

Stationary frontal type

When a continued supply of cold air at upper levels develops a cyclonic circulation centered near the Lakes region, a stationary frontal zone tends to develop parallel to the Atlantic Coast. This stationary front marks the boundary between two northward-moving currents with sharply contrasting heat and moisture properties. On the left is a cold dry current, and on the right a warm moist current which must have a greater northward velocity than the cold air under conditions of balanced flow. (Brunt, D., Physical and Dynamical Meteorology, 2nd Edition, Chapter X.) At the surface a cold anticyclone tends to develop beneath the upper cold cyclone, and a trough of low pressure tends to develop beneath the upper warm moist tongue. There is also a tendency for cyclogenesis to occur near the southern end of the stationary trough. The combination of all these factors results in the

establishment of an inverted V-shaped pressure trough over New England. Convergence is very pronounced in such a trough and creates a typical flood situation.

V-shaped troughs pointing northward have also been noted as factors in the production of flood rains in the Sinai Peninsula (Ashbel, D., Great Floods in Sinai Peninsula, Quarterly Journal of the Royal Meteorological Society). However, Ashbel states that V-shaped troughs are not found in North America; this is contrary to our findings.

Such inverted V troughs with a stationary front may develop to the north of a hurricane as well as an extratropical disturbance. The heaviest rains occur when the moist air mass to the right is potentially unstable and usually occur prior to the passage of the main cyclonic center.

Rapidly moving intense cyclones

When a mass of cold polar air pushes far south of its normal position and develops a cyclonic circulation aloft there is a pronounced tendency for surface cyclogenesis to occur at some distance east of the center of the cold cyclone aloft. This happened during the November 1927 storm, and also during March 1936.

If the cyclones which develop do not become too large, they may move rapidly northward and produce heavy rain with their passage. In some cases, such as March 17, 1936, the cyclone deepens rapidly, occludes, and tends to develop a stationary trough to the north.

Hurricanes

The normal path of northward moving hurricanes carries them some distance off-shore at the latitudes of New England. (Mitchell, C. L.,

West Indian and Other Tropical Cyclones of the North Atlantic Ocean. Monthly Weather Review Supplement No. 24, 1924.) However, under the influence of intense cold cyclonic circulation aloft over the Great Lakes, a hurricane can movely directly over New England. Usually the very effect which caused the hurricane to move inland will cause its northward velocity to be accelerated. In other words, the hurricane comes under the influence of a strong cyclonic gradient aloft and tends to be deflected to the left of its normal path with an accelerated motion. This is an effect similar to that explained for a northward moving moist tongue in the discussion of the March 1936 storm (Chapter IV). It is now fairly well established that hurricanes move with the speed and direction of the "parent" moist tongue at intermediate levels so it is to be expected that they would show similar trajectories under the influence of a strong cyclonic gradient. The September 1938 hurricane furnishes an excellent example of accelerated motion with deflection to the left of the normal path. The cold cyclone aloft at that time was centered near Sault Sainte Marie, Michigan.

Hurricanes tend to move through the stationary frontal zone or inverted V pressure trough, so they can be treated in the same category as intense cyclonic disturbances.

Thunderstorms, local or frontal

Local thunderstorms are produced under relatively quiet conditions. Because of New England's geographical location between the relatively cool waters of the Atlantic Ocean and the Great Lakes, local thunderstorms do not usually attain any great intensity. Frontal thunderstorms attain considerable intensity in this region when associated with

conditions described in the discussion of stationary frontal types and rapidly moving intense cyclones.

CHAPTER III

ADJUSTMENT OF STORMS ON BASIS OF PRECIPITABLE WATER

There are two principal types of motion which produce lifting of air masses to heights sufficient to result in condensation and precipitation. First a large scale movement up an inclined surface which may be either a mountain barrier or a dome of colder air. The second type of motion is almost directly vertical due to convergence of air into a vortex which may be either moving or stationary.

If a steady state is assumed, and if all moisture condensed over a region is precipitated over that region and no suspended water (cloud particles) is carried into or away from the area, the rates of precipitation can be analyzed as follows:

Consider the first case, namely motion up an inclined surface:

FIGURE a

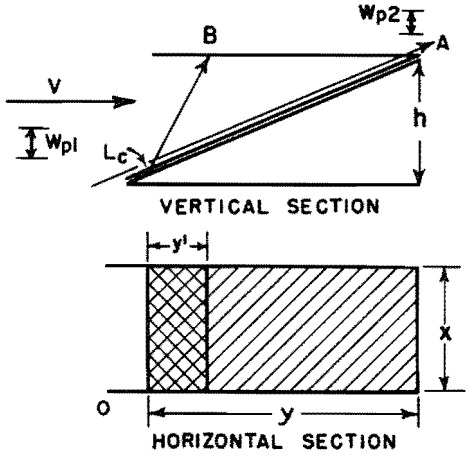

If v = mean horizontal velocity parallel to the major axis of the

basin,

W_{p1} = depth of precipitable water in air column on entering above basin

W_{p2} = depth of precipitable water in air column on leaving basin

$(W_{p1} - W_{p2})$ = depth condensed and precipitated over the basin

h = height of maximum lift

L_c = level of condensation for entire column.

Then each column of unit cross section will deposit $(W_{p1} - W_{p2})$ inches of precipitation in moving from point L_c to level h. If the current takes trajectory A, the precipitation can be assumed to be deposited uniformly over the area xy. If the current undergoes convection and takes trajectory B, the precipitation will be deposited over the area xy'.

The intensity of precipitation can be expressed in terms of v, W_p, x, y, as follows:

If i = the intensity of precipitation in inches per hour

W_p = precipitable water in inches

v = wind velocity in m.p.h.,

$$i = \frac{x\, v\, (W_{p1} - W_{p2})}{x\, y} = \frac{v\, (W_{p1} - W_{p2})}{y}$$

This gives the average intensity over the area xy. However, if the air mass should become unstable and undergo convection along the trajectory B the moisture would be deposited in the distance y' and the average intensity over the area xy' would equal

$$\frac{v\, (W_{p1} - W_{p2})}{y'}$$

In either case the average intensity of precipitation is directly proportional to the precipitable water removed which in turn is proportional to the amount in the column before condensation.

The actual relationship for a given slope and horizontal distance would be a relationship as indicated graphically below:

FIGURE b

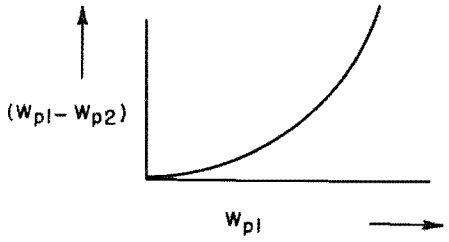

Within narrow limits therefore a linear relationship can be assumed.

The second type of lift is caused by convergence and can be treated as inflow across the circumference of a circle.

FIGURE c

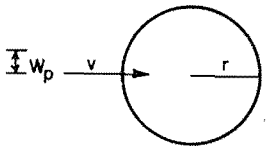

v = velocity of inflow, m.p.h.

r = radius in miles

W_p = depth of precipitable water in column

i = intensity of precipitation

$$i = \frac{2\pi r\, v W_p}{\pi r^2} = \frac{2v\, W_p}{r}$$

In this case the average intensity of precipitation is again directly proportional to the precipitable water. This convergence toward a point is more nearly the true pattern when convection obtains than is trajectory B illustrated in the upglide flow in Figure (a). This simple upglide motion probably never produces more than light rains. In the actual case straight parallel flow does not exist during moderate rains, but rather a convergent flow which produces an added component to the inflow velocity.

For very large areas undoubtedly the general upglide flow accompanied by horizontal convergence for long periods tends to produce the greater amounts of rainfall. However, within the general upglide flow local instability may produce scattered areas of the convective type of precipitation. But these small concentrations will not affect the average depths over large areas because concentration over very small areas occurs at the expense of the surrounding region.

The average intensity of rainfall over a large area therefore depends on the quantity of moisture available and the rate at which the moisture bearing air can be brought into the rain zone. Not all the moisture can ever be precipitated from an air mass and quantities of suspended liquid water can bring only temporary increases in intensity when released. If a given intensity is to be maintained over a large area for an appreciable time, the intensity of precipitation must be directly proportional to the rate of inflow of precipitable water.

In connection with variations in the rate of inflow it is important to remember that most of the moisture for precipitation comes from the warm moist current which is usually a maritime tropical mass moving

northward. As explained later, in the discussion of the March 1936 storm, the immediate control of the circulation intensity seems to lie in the cold air west of the moist tongue. If the northward velocities of the moist current are to undergo accelerations, there must be a prior increase in the circulation activity or cyclonic vorticity of the cold air aloft to the west or northwest of the moist tongue. This results in an increase in the rate of eastward translation of the cold air which displaces the rain zone eastward and reduces the possibility of further critical rainfall rates over one basin unless that basin is so oriented that the center of most intense rainfall could move downstream with the flood crest.

The above explanation of the dynamic processes which tend to cause rainfall to cease if the rates become too intense has of course been adequately demonstrated by hydrologists in statistical studies of intensity-duration relationships (see Meyer, Yarnell, Bernard, etc.).

For very small areas the rate of inflow depends on the isallobaric component (see Brunt and Douglas) which according to Petterssen probably has a maximum value of about 15 m.p.s. Further, the rate of deepening of a cyclonic system which controls the isallobaric component is directly related to the rate of occlusion of the system. When the system is completely occluded, the high rates of precipitation tend to diminish rapidly. Thus the known intensity-duration relationships are again demonstrated to be entirely consistent with what is known of meteorological dynamics.

It is quite obvious that over very large basins the upglide formula is the better approximation and over very small basins the

convergence formula more nearly fits the problem. For extremely small basins and for very short durations the amount of liquid water in suspension must be considered an important factor. The maximum possible depth of precipitable water in a column of air 5 km. deep is approximately 3.00 inches for very warm moist tropical air. A fall of 1.00 inch in one minute has been observed at Opid's Camp, California. The maximum rate of fall for very large water droplets has been shown to be about 8 m.p.s. This means that the observed 1.00 inch in one minute must have fallen from a layer 480 meters or approximately 1,500 feet deep. In other words, this column of air must have carried enough suspended liquid water to produce the equivalent of approximately 300% saturation. Neglecting the possibility of abnormally large hailstones it can be seen that a rate of one inch per minute could not be sustained much longer than 3 minutes since by that time practically all the liquid water above the station would have been released and there would be some time required for the reproduction of the cycle.

Any computation as to how rapidly such phenomenal rates could be repeated would be pure fiction. However, the area must be of the order of magnitude of an intense cumulonimbus cloud.

In most flood-producing storms over average size basins it must be considered that both convergence and upglide are intermittently operative over the basin. The quantities of precipitable water can be considered to be approximately constant and the variations in average intensity over the basin can be considered a function of the rate of northward transport of warm moist air into the basin and of the rate of convergence and lift of that air mass. The variation in localized

intensities can be considered a function of the rates of inflow into localized convective zones.

If the depths of precipitable water during an actual storm can be obtained, it is relatively easy to estimate whether or not the depths of precipitable water might have been greater for the region and season. If it is demonstrated that the depths of precipitable water could have been greater, a proportionate linear increase in the volume of precipitation can be assumed. In other words, if only a small increase is made, it can be assumed that the solenoidal field and the energy from latent heat will not be appreciably affected. Both these factors would tend to produce increased circulation which would accelerate the intensities beyond the rates obtained by extrapolation; and further, this increased activity would result in shortening the duration. However, when adjustments on a percentage basis are applied to the duration-depth curve of the storm, some of the obvious discrepancies are eliminated.

Increasing the intensity of circulation usually results in producing a greater concentration of the rainfall and a shortening of the duration and thus for a very large area the resultant average depth might remain approximately the same. Considering the general deficiency of storm data, and the logical relationships between rainfall rates and precipitable water as demonstrated by seasonal trends in both, the precipitable water method seems the best available approach.

It is feasible to make an estimate of the maximum possible depths of precipitable water. Since it can be shown that warm air masses pick up their moisture by evaporation from the surface, the surface dew point in a saturated air mass can not exceed the temperature of the moist

surface. If the dew point were higher, condensation rather than evaporation would occur. During heavy rain situations the precipitation falls from the warm moist air mass which has picked up most of its moisture by evaporation over tropical ocean surfaces. Ocean water temperatures do not vary much and rarely exceed 82°F. in midsummer; relative humidity does not reach 100% in air at those temperatures. Assuming a saturated adiabatic lapse rate with the maximum possible surface dew point of 80°F. the maximum possible depth of precipitable water between sea level and 5 km. can be computed.

For different localities and different seasons it can be statistically determined what surface dew point can be considered a maximum during a rainy period and the depth of W_p for that maximum dew point can be computed. This computed depth can be compared to the observed or estimated depth of W_p during a major storm period and the actual storm values can be extrapolated proportionately.

In the absence of upper air soundings for a major storm a very close approximation can be made by assuming a saturated adiabatic lapse rate with surface temperature equal to the representative dew point in the warm sector, because if intense convergence and convection are present the warm air at the surface in the warm sector will eventually be contributing its moisture as precipitation, and the final saturated adiabatic lapse rate will be determined by the initial surface dew points.

Shown in Table I is a comparison of W_p as computed from the representative dew points with that computed from actual soundings when they were available for the storms used in this study. W_p was also

TABLE I

Storm	Representative Dew Point °F.	Maximum Possible Dew Point °F.	W_{p1} from Observed Dew Point inches	W_{p2} Computed from Sounding inches	W_{p3} from Maximum Dew Point inches	% Increase Using $\frac{W_{p3} - W_{p1}}{W_{p1}}$	% Increase Using $\frac{W_{p3} - W_{p2}}{W_{p2}}$
Oct. 6-11, 1903	67	70	1.84	--	2.07	12	--
Nov. 1-6, 1927	62	67	1.44	--	1.84	28	--
Sept. 15-17, 1932	67	71	1.84	--	2.18	18	--
July 6-10, 1935	68	73	1.91	1.93	2.40	25	24
Sept. 17-21, 1938	68	71	1.91	*	2.18	14	--
March 9-13, 1936	54	60	0.95	0.90	1.27	34	41
March 16-19, 1936	56	60	1.07	1.00	1.27	19	27

* W_p from sounding at Washington, D. C., for the 20th was 1.56 in. The center of the moist tongue was off the coast so that this value cannot be used for comparative purposes.

Note: The March 1936 storms occurred with the ground snow-covered; the other storms shown in the table occurred with no snow present.

computed using the maximum dew point possible and assuming a saturated adiabatic lapse rate as explained in the previous paragraphs. Finally the percentile increase of the volume of precipitation on the basis of increased precipitable water is shown; a comparison is shown of the increase using W_p as computed from the observed and maximum possible dew point and also using W_p from the actual soundings when available and the maximum possible dew points. It can be shown that during flood conditions if soundings are made in or near the center of the moist tongue the values of W_p as computed from the representative dew point and that computed from the actual sounding will be approximately the same.

CHAPTER IV

MAJOR STORMS

Storm of October 6-11, 1903. (See Weather Maps in Appendix.)

On the morning of October 6 a deep low was centered in southern Alberta. An extensive mass of transitional polar air covered most of the eastern half of the United States and was rapidly becoming tropical maritime air over the western Gulf states. The deep low progressed regularly eastward and occluded and on the morning of the 8th was centered near White River, Ontario, with the cold front extending south and southwestward from Ontario to northwest Florida. Active convergence and lifting of the tropical maritime air by the colder air resulted in showers and thunderstorms in and near the frontal zone.

Since the rate of decrease of pressure with elevation varies inversely as the temperature, the most rapid decrease of pressure with elevation existed in the colder air mass. The pressure was therefore lower at intermediate levels over the cold air, and the strong cyclonic circulation which developed aloft caused the tropical air to be deflected to the left as it was lifted. This produced horizontal convergence, vertical divergence, and decreasing stability. The deflection of a moist current to the west with horizontal convergence is apparently compensated by horizontal divergence and falling pressure to the east, since rapid southward thrusts of cold air are frequently accompanied by

cyclogenesis some distance to the eastward. In this case marked cyclogenesis occurred near the North Carolina Coast and was followed by the development of a major wave along the front.

The two sets of special reports from coastal stations at 1 and 4 p.m. of October 8th showed the marked development of this wave. By the evening of the 8th it had deepened considerably and was centered about 75 miles east of Kitty Hawk, North Carolina. The cold front which had been progressing regularly eastward to the north of this developing disturbance came under its influence and became an effective warm front, becoming practically stationary near the coast. As the cyclonic disturbance developed, increasing amounts of moist tropical air were forced up the frontal surface and caused almost continuous heavy rain immediately west of the front. Heavy rain continued until the afternoon of the 9th, with the maximum 24-hour amount occurring between 1 p.m. of the 8th and 1 p.m. of the 9th. During the afternoon of October 9, as the cyclone deepened, the cold air swept around it, thus occluding the system and diminishing the intensities of rainfall.

The evening map of October 8 showed the disturbance had begun to fill and its northward movement was blocked by a cold mass of air. Ship reports for the morning of the 10th indicated that either a tropical disturbance had moved into the vicinity south of the filling low or that cyclogenesis had occurred, since a well-developed disturbance was centered about 200 miles southeast of Cape Hatteras.

From the morning of October 10 to the evening of October 11 this new disturbance moved north-northeastward and filled slowly. The amount of precipitation produced at coastal stations due to this storm was

comparatively light.

This storm is a good example of a combination of events which could produce the maximum possible storm for either large or small areas for the northeastern section of the country. These events are: (a) the occurrence of heavy rain over a given area due to an extra-tropical disturbance and the combination of elements such as occurred on the 8th and 9th; (b) the following of the first storm within a short time by a tropical disturbance such as the one that developed by the morning of the 10th. It should also be mentioned that one of the factors necessary to sustain the first storm was the supply of cold air to the northwest and north which also was effective in causing the tropical disturbance to move northeastward so that comparatively light amounts of precipitation fell along the coast. It can, however, be assumed in the limiting case that the combination of elements could have been such as to allow the path of the center to be along the coast, thus producing moderate to heavy rain within six or twelve hours after the first storm. Such a sequence actually occurred during September 1938 but as is well known the arrival of the tropical storm over the rain zone resulted in an acceleration of the general circulation and a cessation of the rainfall.

Storm of November 1-7, 1927. (See Weather Maps and Upper Air Data in Appendix.)

This storm was characterized by a cold front in an elongated pressure trough which moved relatively slowly eastward during November 1 and 2, finally becoming a quasi-stationary front from Georgia to Maine by the morning of November 3.

The air aloft behind this front was quite cold and a cyclonic

circulation was indicated at 10,000 and 14,000 feet above sea level over the Lakes region on the morning of November 3. Upper air temperature data were limited to a few scattered kite observations, but a sounding for the morning of November 3 showed a temperature of -21°C. at 4,740 m. above sea level over Royal Center, Indiana. The circulation at 14,000 feet indicated that Royal Center was probably not at the center of lowest pressure and temperature, so it is assumed that it must have been unusually cold aloft behind the quasi-stationary front.

The warm air mass to the east of the stationary front was quite moist and unstable as evidenced by the existence of a tropical storm and by the fact that cyclogenesis took place so readily. However, it should be emphasized that the tropical storm itself never merged with the pressure trough; quantities of water vapor in the moist current could have been much greater if they had merged.

The processes which lead to the development of a quasi-stationary front and cyclogenesis will be covered in the discussion of the March 1936 storm.

During the day of November 3, 1927, two small cyclones developed along the Atlantic Coast and moved quite rapidly northward along the quasi-stationary front through Vermont. The precipitation as a whole was produced by the gradual lifting of warm moist air as it moved northward over cooler and more stable air. The concentration and intensification of rainfall was caused by the general convergence associated with the inverted V-shaped pressure trough and the local convergence accompanying the passage of the small intense cyclones.

There is an important feature of this and all other storms which

should be emphasized: As long as the cold air aloft to the rear of the front was moving in at a slow rate the cold front moved slowly eastward with no centralization of activity. But when the cold air aloft suddenly pushed rapidly southward, as evidenced by a drop of temperature of 10°C. at 4,000 m. from November 2 to November 3 above Royal Center, waves began to develop along the quasi-stationary front.

Another important feature of the synoptic situation on the morning of November 3 was that the supply of cold air aloft had been brought into close proximity to the supply of warm moist air over the Atlantic Ocean. This increased the intensity of the solenoidal field and caused an increase in circulation intensity (see March 1936 discussion). As the circulation accelerated, the warm moist current moved northward at a more rapid rate, cyclonic activity increased, and precipitation became more intense. However, the west to east velocities of the cold dry air behind the front also increased and the axis of the moist tongue and heavy rainfall was pushed eastward. Thus it is evident that there are very good dynamic reasons for the intensity-duration relationships that have been statistically demonstrated. An increase in intensity of precipitation demands an acceleration of flow in the warm moist air which is accompanied by an acceleration of the west to east flow of cold air thus limiting the duration of rain when the intensity increases.

Storm of September 15-17, 1932. (See Weather Maps in Appendix.)

The heavy precipitation in this storm was associated primarily with the tropical disturbance that had its origin in the southwest Gulf of Mexico on September 9th. This storm progressed very slowly northward and northeastward until the evening of the 14th when it was over

Appalachee Bay. It crossed northern Florida during the night of the 14th-15th, and by the evening of the 15th was centered about 100 miles southeast of Wilmington, North Carolina, moving north-northeastward about 25 miles per hour.

High pressure was centered over Nova Scotia with a wedge of relatively cool air extending southwestward over most of New England. A region of low pressure was centered over northern Ontario with a weak cold front which extended from the center southward along a line just east of Toronto and Cleveland and thence southwestward through southern Indiana and Illinois.

By the morning of the 16th the tropical disturbance was centered about 150 miles east of Norfolk, Virginia. The disturbance over Ontario had moved eastward so that its trough extended southward through eastern New York toward the tropical storm. The surface front associated with the low had moved eastward with the trough but was not very sharp and could not be identified south of the St. Lawrence River. However, the upper air soundings made at Cleveland on the 16th and 17th show a marked cooling off at intermediate levels with the temperature of -18.3°C. at 5 km. on the 17th being the coldest ever observed at that elevation above Cleveland in September.

The inflow of colder air into the northwest quadrant of the tropical storm induced cyclonic vorticity in the tropical air ahead of it which resulted in the deepening of the disturbance as it moved northward. The path of the storm after it crossed Florida was far enough from land so that little energy was lost due to friction. These effects caused the strong horizontal convergent flow in the trough just north of the

disturbance which resulted in vertical divergence, decreasing stability, and heavy rainfall in that area as far north as northern Maine.

On the evening of the 16th the isobars over New England showed marked convergent flow over the area of heaviest rainfall. As the storm moved inland, the effect of friction dissipated its energy and also the intensity of the rain.

The effect of the colder air to the west was still apparent on the morning of the 17th. The disturbance was centered south of Eastport, Maine, and filling rapidly but a region of marked cyclogenesis and a developing low center existed in the vicinity of Father Point, Quebec. Frontogenesis in the trough from this center southward through eastern Maine was also evident.

Storm of July 6-10, 1935. (See Weather Maps and Upper Air Data in Appendix.)

On the morning of July 6 comparatively low pressure covered most of the eastern half of the United States. One weak center was over the Carolinas and another center over Sault Sainte Marie, Michigan. In connection with the latter, a weak frontal system extended eastward through New England into a minor wave off the New England Coast. North of this frontal system was an extensive mass of cool polar air. While the surface map was characterized by relatively weak circulation, the isentropic chart showed that the cool air from the region north of the Great Lakes extended southward as a ridge into the Gulf of Mexico. East of the ridge was a trough with a tongue of moist tropical air extending northward from Florida into New York. Thunderstorms were reported generally in the area covered by the moist tongue.

Throughout the series of maps from the morning of the 6th to the morning of the 8th, no significant changes in the surface pressure distribution had taken place. The low that was centered over Sault Sainte Marie on the morning of the 6th moved slowly southeastward and was centered over northwestern Pennsylvania on the 8th. The isentropic charts however showed that the trough with the attending moist tongue and convectively unstable air had pushed northward into the St. Lawrence Valley but had remained nearly stationary over the Atlantic states. Thunderstorms with varying amounts of rain were general throughout this entire area and were heaviest over New York State due to the steeper

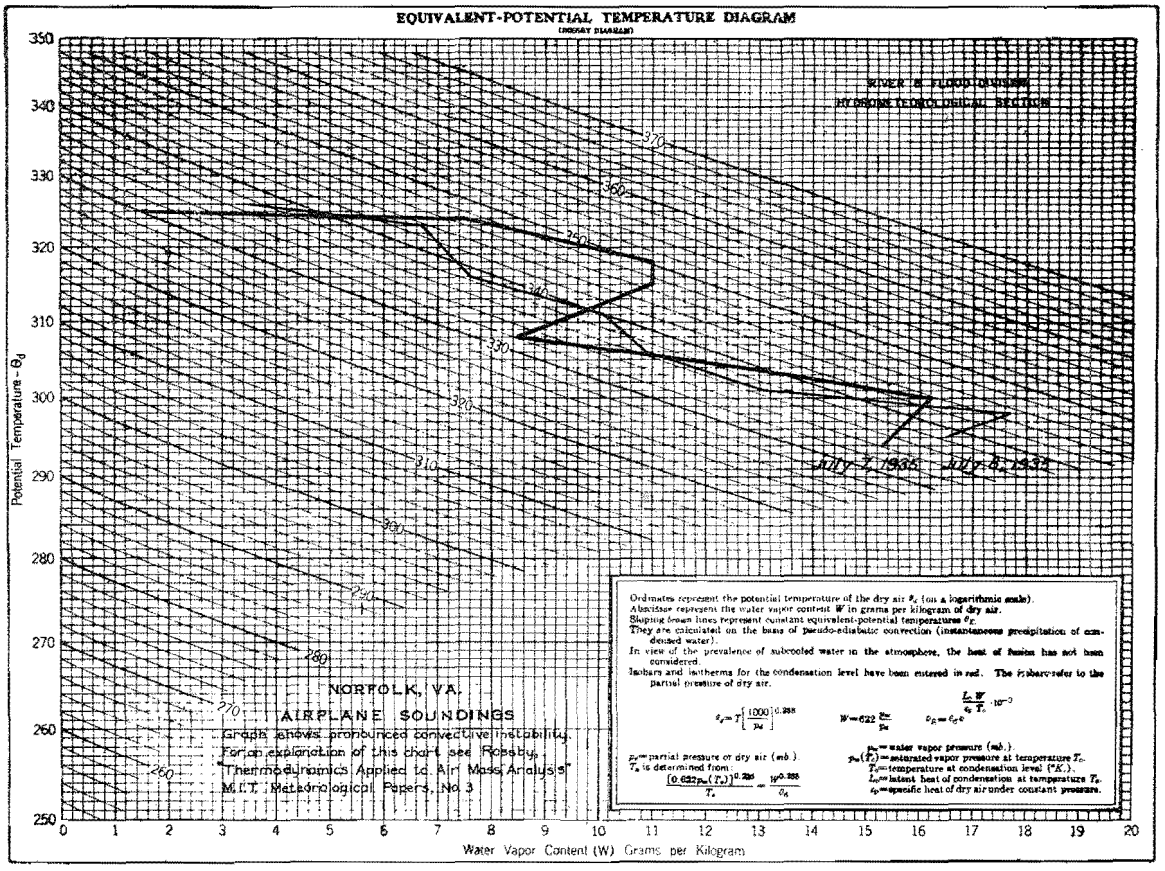

Figure 1

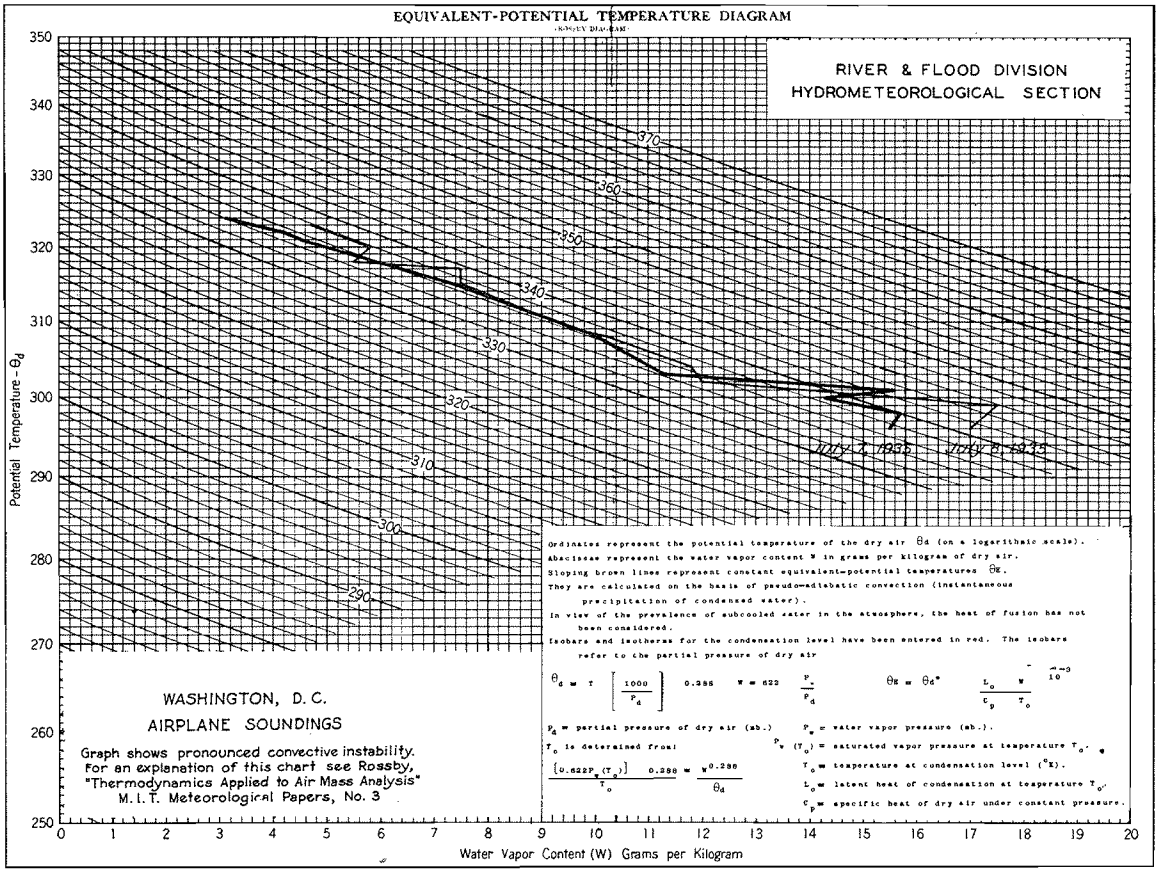

Figure 2

slope of the cold air over this region. The torrential rains in west-central New York State were coincident with this stage of the development.

The tropical air associated with these thundershowers was nearly as moist and convectively unstable as has ever been observed. (See Rossby diagrams - Figures 1 and 2, and Table 1 on page 19.) A small amount of heating from below or a slight lifting of the air mass would have been enough to release the convective energy and set off widespread thunderstorm activity. It has been shown by Rossby (1) that the

(1) Rossby, C.G. Thermodynamics Applied to Air Mass Analysis, Massachusetts Institute of Technology Meteorological Papers, Vol. 3, No. 3, 1932.

convective instability of an air mass is determined by the vertical distribution of the equivalent-potential temperature. If the equivalent-potential temperature decreases with height in the layer, then, when the entire air mass is lifted, the lower part of the air mass will reach saturation first and assume a slower rate of cooling after condensation begins, while the upper part of the air mass will continue to cool at the dry adiabatic rate. Additional lifting therefore tends to steepen the lapse rate and make the air mass unstable and capable of internal convection. Figures 1 and 2, which are soundings of July 7 and 8 for Norfolk and Washington, respectively, plotted on Rossby diagrams, show not only a rapid decrease of equivalent-potential temperature for various layers but also a lower equivalent-potential temperature at the top of the flight than at the surface in each case, which means that the entire column was convectively unstable.

The map for the evening of the 8th shows the development of a weak wave near Norfolk and by the morning of the 9th it was centered off the New Jersey Coast, having united with the dissipating weak system that was over northwestern Pennsylvania on the morning of the 8th. The upper air charts for the a.m. of the 9th show the very slow eastward displacement of both the tongue of moist air and the wedge of cold air with the resultant eastward displacement of the area of heavy rainfall into New England.

This storm serves well to illustrate a combination of circumstances which could produce a more intense storm. These can be enumerated as follows: (1) stagnation of the circulation systems such as to allow a tongue of moist and convectively unstable air to remain over a

particular region with a series of storms of the convective type; (2) higher moisture content; and (3) an arrangement of the isentropic pattern such as to give steeper slopes over the region. This would necessarily require the maintenance of a supply of colder air to the northwest and would result in more rapid displacement of the systems but would also produce rainfall of greater intensity.

Storms of March 9-22, 1936. (See Weather Maps and Upper Air Data in Appendix.)

There were three separate periods of heavy rainfall during March which had their peaks on the 9th to the 13th, the 16th to the 19th, and the 20th to the 22nd. The antecedent conditions have been discussed in some detail in U. S. Geological Survey Water-Supply Papers 798, 799, and 800, so that this discussion will be confined to a comparison of the surface and upper air data during the three storm periods.

The first period was characterized by the formation of a deep cold cyclone over the Lakes region with a development of secondary wave disturbances on the cold front along the Atlantic Coast. The 8:00 a.m. map for March 12 illustrates the synoptic situation which produced the heavy rains over New England. The horizontal cross section (see Appendix) at 5 kilometers for March 12 showed the center of lowest pressure and likewise of lowest temperature over the upper Mississippi Valley. This produced a strong gradient from north to south over the Middle Atlantic States in the upper levels of the troposphere. The horizontal cross section at 3,000 meters for the same date also showed this south to north flow over the Atlantic States. The high values of the potential temperature of the dew point show that there was a maximum of moisture

along the Atlantic Coast. The decrease of potential temperature from south to north over New England implies the necessity for upglide motion of warm moist air in that vicinity. The upglide motion is better illustrated by the isentropic chart for March 12 (see Appendix). This chart identifies the distribution of moisture on the potential temperature surface of 295°A. The significance of the chart lies in the fact that masses of air maintain the same potential temperature, regardless of lifting or lowering, as long as radiation or condensation processes are not active. The order of magnitude of radiation processes is so small that they can be neglected for 24-hour changes. The charts are drawn on the assumption that if the flow pattern of the moist currents can be identified before condensation takes place, a reasonable extrapolation of the flow patterns after condensation takes place can be obtained from the shape of the area of condensation. The solid lines of pressure are almost a direct measure of the elevation of the potential temperature surface. The distribution of moisture on the potential temperature surface is best identified by specific humidity. The specific humidity is a weight ratio between the mass of water vapor and the mass of air and is usually expressed in grams of moisture per kilogram of moist air. Since for any given potential temperature surface a given value of specific humidity can have only one pressure at which saturation will result, the lines of specific humidity can be labeled in terms of the pressure at which saturation will be reached. (Byers, H. R., On the Thermodynamic Interpretation of Isentropic Charts. Monthly Weather Review, Volume 66, March 1938, pp. 63-68.)

On the isentropic chart for March 12 the orientation of the lines

of elevation and moisture showed a maximum of moisture moving upslope over the Atlantic Coast and, since the lines of elevation pressure and condensation pressure intersected over eastern Pennsylvania, condensation was indicated for that region. Upper air information was rather limited for the New England States on this day and it seems probable that the actual area of condensation on the 295°A. potential temperature surface was much more extensive than indicated.

The synoptic situation as portrayed on the maps of March 12 is quite typical of the three major storm periods. The immediate causes of this type of situation are believed to be as follows: A strong southward thrust of cold air acquires an increased cyclonic circulation because of its southward movement. This development of a cyclonic circulation is accompanied by the development of a center of low pressure in the upper elevations. An examination of the hydrostatic equation for the rate of decrease of pressure with height, $dp = -\rho g dz$, shows that the greater the density, the more rapidly does pressure decrease with height. In other words, pressure decreases most rapidly with height in the colder air mass. This offers a simple explanation for the lowest pressure at high elevations being coincident with the region of low temperature. In fact, a very good correlation can be obtained between low pressure and low temperature at 5000 meters above sea level. Results of such

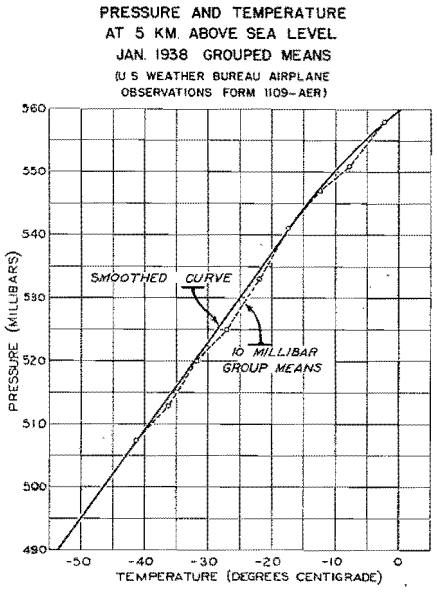

Figure 3

a correlation are shown graphically in Figure 3. However, it must not be construed that the simple hydrostatic relationships can be considered the sole cause for the development of a strong cyclonic circulation above a mass of cold air. According to the latest developments by Rossby (as yet unpublished) a southward moving current acquires an increasing cyclonic or positive vorticity if its lapse rate remains constant, and a northward moving current under the same conditions would acquire an increasing anticyclonic or negative vorticity.

If Z = the vorticity (positive for cyclonic circulation)

k = a constant

D = the depth of the air mass

f = the Coriolis, or deflective force of the earth's rotation,

then $Z = kD - f$

The Coriolis force f increases with increasing latitude, and if D remains constant, Z or the positive vorticity decreases for northward motion. If D increases without a compensating increase in latitude, the positive vorticity or cyclonic tendency also increases.

If the lapse rate does not remain constant during a purely adiabatic process, the change in lapse rate must be due to an increase or decrease in the horizontal extent of the air mass with an accompanying decrease or increase in the vertical depth of the air mass. In other words, horizontal divergence is accompanied by vertical convergence and tends to stabilize the lapse rate and cause an increase in the anticyclonic or negative vorticity. Horizontal convergence is accompanied by vertical divergence and tends to decrease the stability and cause the air mass to acquire a cyclonic or positive vorticity. During

flood situations the initiating impulse seems to be a rapid southward thrust of cold air with very little change in its lapse rate. The cold air mass therefore brings with it low pressuresaloft and the air mass acquires an increasing cyclonic circulation as it moves southward.

As Rossby has explained (Rossby, C. G., Sears Foundations, Journal of Marine Research, Volume I, No. 1, 1937. On the Mutual Adjustment of Pressure and Velocity Distribution in Certain Simple Current Systems), there is an interdependence of the dynamic and the hydrostatic processes. A strong current of air tends by dynamic process to develop a balancing pressure distribution in much the same manner as the pressure distribution will develop a balancing circulation. The southward moving cold air mass tends to circulate cyclonically about the center of low pressure and the increase in cyclonic circulation tends to produce a pressure system which will bring about balanced flow conditions. The southward thrust of cold air at high elevations therefore distorts the entire circulation pattern at higher elevations and produces a compensating northward flow of warm moist air some distance to the eastward. The distribution and circulation of the air mass in the lower levels will not be so much affected by this abnormal distortion of the circulation pattern aloft and this results in a greater latitudinal displacement of air masses aloft than in the lower levels. This causes a very active northward movement of warm moist air gliding upward over the more stable cold air in the lower levels. Such a process of course leads to condensation and precipitation.

As explained earlier, northward moving air should tend to acquire anticyclonic vorticity and increasing stability. However in the flood

situations the intensifying cyclonic circulation in the cold air west of the warm air mass seems to induce an effect similar to the isallobaric effect explained by Brunt and Douglas. (Brunt and Douglas, Memoirs of the Royal Meteorological Society, 3 No. 22.) The deepening pressure distribution tends therefore to produce convergence in the warm moist current which enables it to maintain its stability as it moves northward. In unusual cases, such as during these storm periods of March 1936, the deepening effect was so pronounced as to cause the northward moving warm moist current to acquire increasing cyclonic vorticity and decreasing stability as it moved northward. This can be seen by the cyclonic curvature of the moisture lines on the isentropic charts for March 12, 15, 18, and 21. The rain results from the lifting of masses of warm moist air and the intensities of precipitation are increased because of the development of instability which creates internal convection in the air mass.

In some storms such as during January 1937, the southward advance of cold air occurs as a more gradual and sustained movement with the tendency for the development of a quasi-stationary cold cyclone aloft. In such a case the instantaneous deepening effect is never very pronounced and not much convergence occurs in the northward moving warm moist air mass. However, if the northward moving warm moist current is conditionally unstable, not much convergence is required and if the air mass is convectively unstable (Byers, H. R., Synoptic and Aeronautical Meteorology), then all that is required to develop convection is a lifting of the air mass. In fact, in a convectively unstable air mass lifting plus horizontal divergence tends to increase the convective

instability.

The period from March 9 to March 12 was characterized by very intense circulation aloft. In other words, the mean velocities from west to east in the upper levels were greater than normal for the season. Superimposed on this intense west to east circulation was a series of very active perturbations which produced oscillations of cold air far to the south and of warm moist air far to the north. But since the mean west to east velocities remained high, the disturbances moved rather rapidly from west to east until they reached the Atlantic Coast. Along the coast the increased temperature contrast between land and water surfaces seemed to develop a solenoidal field (V. Bjerknes, J. Bjerknes, H. Solberg, and T. Bergeron, Physikalische Hydrodynamik, p. 672; 1933) which intensified the cyclonic activity.

The actual sequence of events was as follows: The first southward thrust occurred on March 11 and was clearly evident on all the charts for March 12 as a cold cyclonic circulation center over the upper Mississippi Valley. The surface synoptic situation has been discussed in the opening paragraphs. The next major southward thrust of cold air occurred on March 15 and was evident as a cyclonic circulation aloft on that date centered over Minnesota. From March 15 to the morning of March 16 this cold cyclone remained relatively stationary but during March 16 the cold dome of air with its increasing cyclonic circulation moved rapidly southward and by the morning of March 17 was centered over northern Alabama. As is usual with a rapid southward thrust of cold air, active cyclogenesis took place some distance to the eastward and the cyclone which was over northern Georgia at 8 p.m., March 16, intensified

considerably and moved northward along the Atlantic Coast producing a period of heavy rain.

In the inverted V-shaped pressure trough north of the center the cold front became stationary and developed warm front characteristics early on March 17. Active convergence and warm front lifting in this trough caused moderate to heavy precipitation from the moist tropical air which was moving northwestward over the North Atlantic States. The stagnation of the trough maintained a strong persistent flow of warm tropical air which supplied considerable heat for melting the deep snow cover which had been ripened by the rainfall and warm air during the preceding storm. The inverted V pressure trough and its stationary front were maintained in practically the same position until March 19.

The next southward thrust of cold air was first identified as a cold cyclone aloft over North Dakota on the morning of March 19. This cold mass pushed rapidly southward and by the morning of March 20 was centered over northern Alabama. Cyclogenesis again took place and the low pressure system developed over southern Indiana and moved slightly eastward with a secondary development along the Atlantic Coast which moved northward causing another series of moderate rains. A comparison was made of the intensities of precipitation during each of the three storm periods with the amounts of precipitable water available and with the rates at which the air containing this moisture was being transported northward. These comparative data are shown in Table II. The peak 24-hour rainfall amounts over all of the sub-basins in the major storms discussed in Geological Survey Water-Supply Papers 798, 799, and 800 were used as a measure of intensity of precipitation during the three

TABLE II

MARCH 1936 STORM - COMPARATIVE DATA

		March 10-13	March 16-19	March 20-22
1.	Lowest Pressure at Surface (Inches)	29.2	29.2	29.1
2.	Lowest Pressure at 5 Km.(Millibars)	516	528	526
3.	Lowest Temperature at 5 Km. Observed During the Three Storm Periods	-29.8°C.	-25.3°C.	-28.6°C.
	Station and Date	Washington D.C. Mar.13	Montgomery, Ala. Mar.17	Dayton,O. March 21
	Lowest Temperature Ever Recorded at These Same Stations at 5 Km. During March	-30.3°C.	-25.3°C.	-29.4°C.
4.	Average Maximum 24-Hour Amounts of Rainfall Over All Sub-Basins (Inches)			
	(a) New England	2.8	2.9	1.1
	(b) Potomac and Rappahannock	1.2	3.4	1.1
	(c) Hudson and Susquehanna	2.0	2.2	1.0
5.	Means of All Three Areas	2.0	2.8	1.0
6.	Ratio of Geostrophic Winds at 5 Km. over Virginia. N-S Gradient	21 to	30 to	15
7.	Representative Dew Points in Warm Sector	54°F.	56°F.	50°F.
8.	W_p Surface to 5 Km. from APOB Data	0.90	1.00	0.80
9.	W_p for Saturated Adiabatic Lapse Rate Surface to 5 Km. for Observed Dew Points	0.94	1.07	0.79
10.	Row 6 x Row 9	18.9	30.0	12.0

W_p = Depth of precipitable water in inches.

storm periods. The average over all sub-basins was considered a fair estimate of the large-scale intensity of rainfall during each storm period. Depths of precipitable water from the surface to 5 kilometers were computed from the aerological soundings and compared with the amounts that would have been present in a completely saturated air mass with a pseudo-adiabatic lapse rate and a surface temperature equal to the dew point actually observed in the warm sector. As seen in the table, these values agree quite well. However, since the rates of precipitation were also considered to be a function of the rate at which the moist air was being transported northward, the pressure gradients at 5 kilometers were used as a measure of the rate of northward flow. This is considered reasonable because it is quite safe to say that at an elevation of 5 kilometers over Virginia on the dates used the observation would be well within the warm moist current.

As mentioned earlier, internal convection within the air mass may produce locally intense showers and therefore the comparative data, as computed above, could not be expected to apply consistently for small areas. However, in a large-scale continuing process the effects of increased transport and more available moisture tend to produce greater amounts over large areas. During the two storm periods March 9-13 and 16-19, the greatest amounts over large areas for all durations occurred during the latter period. However, over small areas for durations of 36 hours and less, the intensities were greater during the period March 9-13. It seems reasonable to expect therefore that if the original column of air during the first storm period had contained as much moisture as did the column in the second period, the amounts of precipitation during

the first storm would have been greater.

Storm of September 17-21, 1938

The heaviest rainfall in this storm occurred just prior to the New England hurricane. The major features of the weather during this period have been discussed by C. H. Pierce in "The Meteorological History of the New England Hurricane of September 21, 1938," Monthly Weather Review, Volume 67, August 1939. Figure 5-c on page 252 of Pierce's article, the isentropic chart for September 20, 1938, is typical of the major features of the storm. A deep cold cyclonic circulation central over Lake Michigan was inducing a pronounced northward flow of warm moist air over New England. The weather map for 7:30 p.m., September 20, 1938, shows the typical inverted V pressure trough over central Connecticut and Massachusetts, and it was near the front in this trough that the heaviest rain occurred. The circulation which caused the front to stagnate over New England also caused the hurricane to move through the frontal zone. High intensities of rainfall were caused by strong wind velocities aloft which also caused the hurricane to move rapidly through New England. Therefore it would not be logical to assume the same intensities of rainfall to be followed by a more slowly moving hurricane which would deposit more rainfall than did the one of September 21, 1938.

CHAPTER V

NEW ENGLAND SNOW MELT RUNOFF RATES

Introduction and summary

An examination has been made of precipitation and stream discharge records for a number of basins in northeastern United States in connection with the March 1936 floods.

Snow melt runoff rates were obtained by deducting computed rainfall runoff and estimated base flow from the observed total discharge in six-hour increments.

Reversing the normal procedure, the resulting snow melt hydrograph was analyzed by a distribution graph for each basin, giving the average effective rates of snow melt on the basin.

After a careful consideration of factors relating to snow melt, in the light of existing as compared with maximum possible conditions, extrapolations were made, giving the rates shown in Table III. Subject to limitations of the present knowledge of snow melt hydrometeorology, these rates are believed to be the maximum possible for the shaded area shown on Figure 4.

Basin records

An enveloping curve of snow melt vs. area of basin in northeastern United States in the second March 1936 storm is shown in Figure 5.

The data plotted are from U. S. Geological Survey Water-Supply

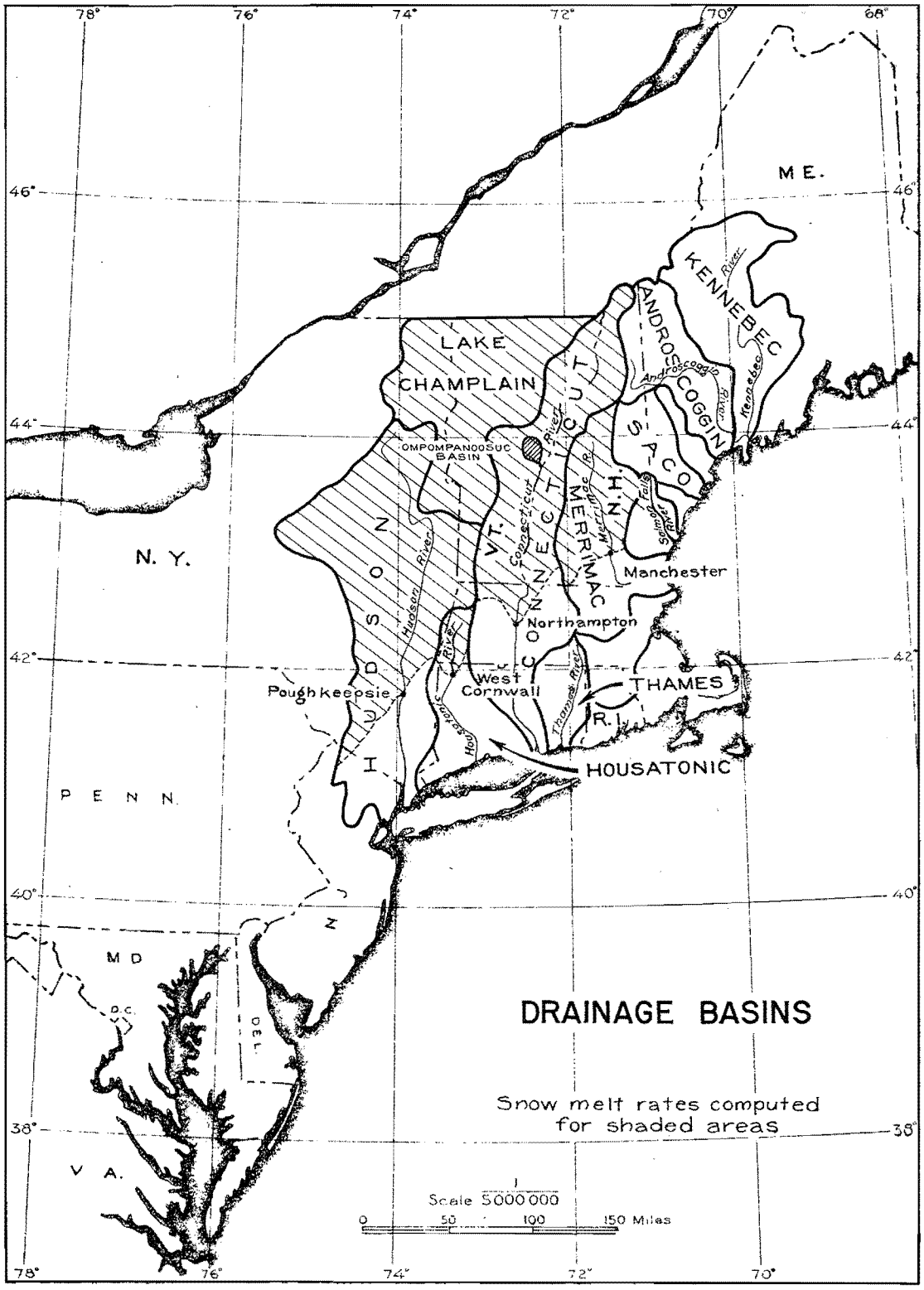
78°
76°
74°
72°
70°
68°
46°
44°
42°
40°
38°
ME.
N. Y.
PENN
MD
D.C.
DEL
VA.
LAKE CHAMPLAIN
OMPOMPANOOSUC BASIN
CONNECTICUT
VT.
N.H.
MERRIMAC
SACO
ANDROSCOGGIN
KENNEBEC
Androscoggin River
Kennebec River
Connecticut River
Merrimack River
Saco River
Ompompanoosuc River
Winooski River
Lamoille River
White River
Otter Creek
Hudson River
Mohawk River
Housatonic River
Thames River
Manchester
Northampton
West Cornwall
Poughkeepsie
THAMES R.
HOUSATONIC
DRAINAGE BASINS
Snow melt rates computed for shaded areas
Scale 5000000
0 50 100 150 Miles

Figure 4

TABLE III

ACCUMULATIVE AVERAGE DEPTHS OF SNOW MELT IN INCHES

Time in Hours	Basin Area in Square Miles			
	100	200	500	1,000
6	1.9	1.6	1.3	1.1
12	3.8	3.2	2.6	2.2
18	5.6	4.8	3.8	3.2
24	7.4	6.3	5.0	4.2
30	9.2	7.8	6.2	5.2
36	11.0	9.3	7.4	6.2
42	12.7	10.7	8.5	7.1
48	14.3	12.1	9.6	8.0

Papers 798, 799, and 800. Data for basins with less than two inches of snow melt were not plotted. No points were plotted for basins with areas exceeding 800 square miles because storage corrections had not been made. The second storm discharge was used because of the fact that on many basins the first storm set the stage by loading the snow cover with water so that the effect of the second storm was almost that of two simultaneous storms plus heavy snow melt.

Five basins were studied in detail:

Saco River at Conway, New Hampshire

Dog River at Northfield Falls, Vermont

Mad River at Moretown, Vermont

Pemigewasset River at Plymouth, New Hampshire

East Branch of the Pemigewasset River at Lincoln, New Hampshire.

Data from the last two basins have been used in defining the enveloping depth of snow melt vs. basin area curve, and the analysis of the latter basin follows:

East Branch of the Pemigewasset River at Lincoln, New Hampshire

This basin is in north-central New Hampshire, has an area of 104 square miles, and is similar to the Ompompanoosuc Basin in all important respects.

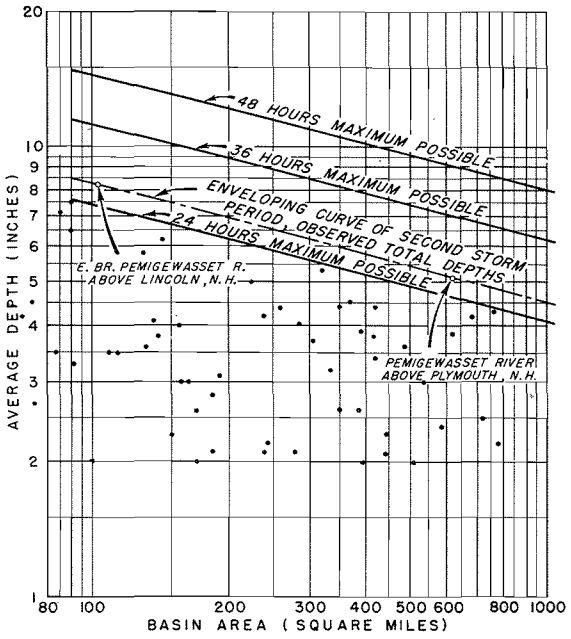

Figure 5

Northeastern United States snow melt runoff depths in second storm period of March 1936 (from U. S. Geological Survey Water-Supply Papers 798, 799, and 800)

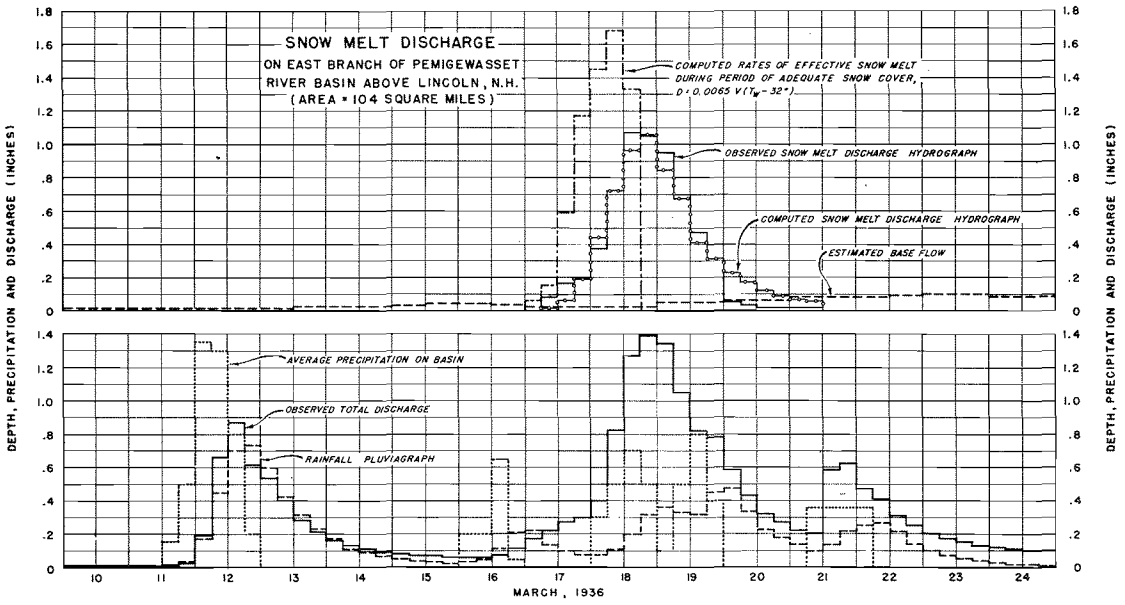

Figure 6

Figure 6 shows average precipitation over the basin, stream discharge, rainfall pluviagraph, and estimated base flow in six-hour increments for the period March 10 through 24, 1936. Average precipitation over the basin was determined by means of mass curves and isohyetal maps. Stream discharge figures are from Water-Supply Paper 798. The pluviagraph is based on a synthetic unit hydrograph developed by the Snyder method and on the assumption that representative infiltration rates are those of frozen ground conditions. The correspondence of the pluviagraph to the observed stream flow of March 12 can be seen. Soil priming by excessive fall rains followed by a hard winter freeze indicates very nearly 100% runoff. The soil was frozen during the entire month of March.

A correction for two inches of infiltration during the storm period is included in the base flow estimates, which otherwise would have more closely followed a ground water depletion curve. The final result would be no different if the infiltration had been handled as runoff deficit instead of as base flow accretion. Further, due to the small magnitude of the infiltration and base flow relative to total discharge, ordinary errors in infiltration and base flow estimates are not serious.

In Figure 6 reference is made to the observed snow melt discharge hydrograph, computed snow melt discharge hydrograph, and the observed rates of effective snow melt for the period March 17 through 20. The observed snow melt discharge is obtained by deducting, by 6-hour increments, estimated base flow and the rainfall pluviagraph from the observed total discharge. The computed snow melt discharge hydrograph is obtained by applying the basin distribution graph to computed rates

of effective snow melt for the period during which appreciable snow cover remains on the ground. Effective snow melt is the water actually released from the snow mantle. The correspondence of the observed to the computed snow melt hydrograph serves as a check on the method of computing the rate of snow melt. Snow melt rates on the other four basins were determined in a similar manner.

Thermodynamics of snow melt

The following discussion includes the derivation of the snow melt formula by means of which rates of snow melt have been computed and can be extrapolated.

Five factors related to snow melt are as follows:

1. Insolation.

   This can be ignored during heavy storms.

2. Heat conduction from underlying soil.

   In March 1936 the soil was frozen, and frozen soil is a necessary assumption for the maximum possible flood, thus eliminating conduction from the soil as a significant cause of snow melt.

3. Heating effect of warm rain.

   This can be shown most simply in the formula $D = P \frac{T - 32}{144}$

   D is rate of snow melt in inches of water per hour.
   P is rate of precipitation in inches per hour.
   T is Fahrenheit temperature of rain falling on snow surface.

4. Conduction of heat from passage of air over snow surface.

   This can be expressed in terms of the ordinary convection formula: $D = K_1 (T - 32) (1 + K_2 V)$

   D is rate of snow melt in inches of water per hour.
   T is air temperature, ^{o}F.
   V is wind velocity in appropriate units.
   K_2 is a velocity factor, giving the necessary conversion of units and including an empirical convection coefficient.

K_1 is a proportionality factor of rate of snow melt to heat supplied, conversion of units, and heat transfer coefficients.

5. Condensation - Latent heat of vaporization liberated by water vapor condensing on the cold snow surface.

An extension of Dalton's law expresses this as follows:

$$D = K_3(1 + K_4V)\ (e_1 - e_2).$$

D, K_3, V and K_4 are defined as corresponding units in the convection formula above. e_1 and e_2 are vapor pressures of the air passing over the snow, and of saturated air at 32°F., respectively.

Referring to these formulas for convection and condensation, it can be shown that for the range of wind velocities involved, $(1 + K_2V)$ is very nearly proportional to V. It can also be shown that for the range of temperatures involved, the expression $(e_1 - e_2)$ is nearly proportional to $T_w - 32^\circ$, where T_w is wet bulb temperature of the air.

Therefore these two formulas can be combined and reduced to the following simple form:

$$D = KV(T_w - 32^\circ)$$

During the second March 1936 storm period the wet and dry bulb temperatures were not greatly different. Maximum possible conditions would include 100% relative humidity.

This formula involves data that are nearly always available. It remains to evaluate K and to compare the results of this formula with field observations to determine whether or not the assumptions made permit results to be within reasonable limits of accuracy for the purpose involved.

This is the formula used in computing the rates of snow melt referred to previously, and can be evaluated by examination of Figure 6.

Neglecting the heating effect of the warm rain is evidently justifiable. Maximum flood conditions require rain, and the fact that rain runoff and snow runoff are usually concurrent is well known. The thermal effect of rain is relatively small, and may be compensated for by the heat transmitted to the frozen soil. It can be assumed that the original snow temperature is not far from 32° throughout, and maximum possible conditions can require this as a prerequisite.

Mechanics of snow melt

Figure 7 shows the effect of melting on snow depth, density, and depth of suspended liquid water in a hypothetical column of one gram of snow, originally 10 cm. high, assuming no drainage from the column. The snow is said to ripen as its density increases due to melting. Field

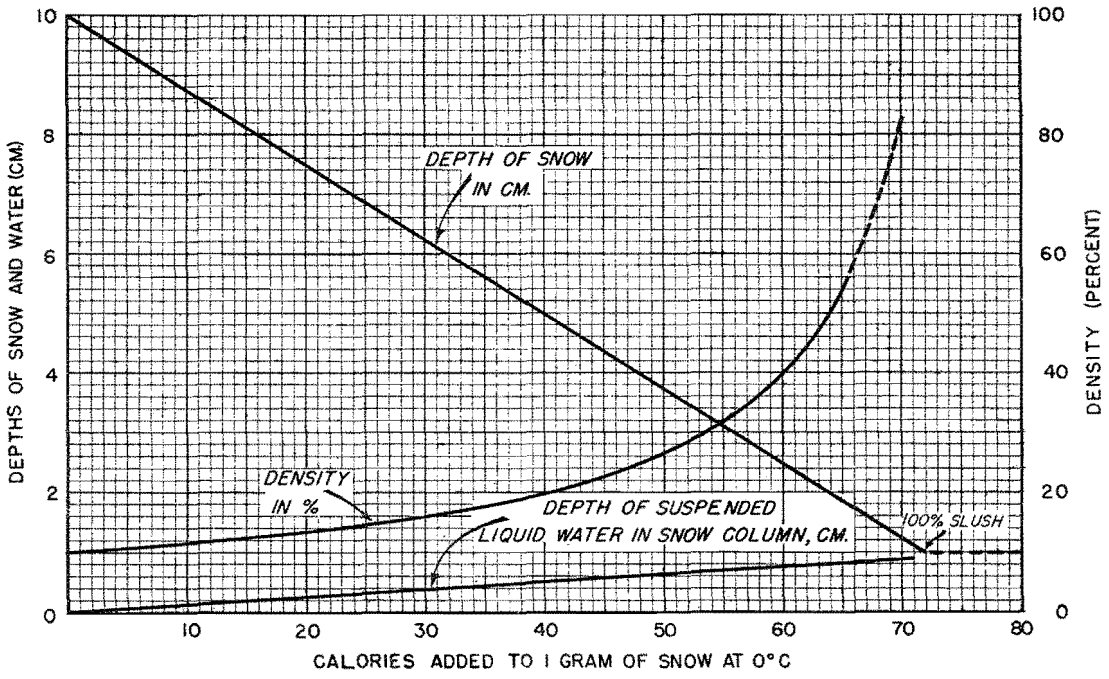

Figure 7

Ripening of 10 cm. column of snow with original density of 10% and 0°C. initial temperature

observations and laboratory experiments show that as snow melts, the water percolates downward through the snow column and builds up a capillary head.

Discharge of the suspended water does not occur until the capillary head is balanced by gravity. This head is rarely greater than one to two inches, its magnitude being related to the snow density, which seldom exceeds 50%. Figure 7 shows that, after antecedent melting has increased the snow density to 40%, the conversion of snow entirely to water requires only 20 cal./gram. This is only 25% of the total heat of fusion. Actually, it can be reduced further, because, as slush is formed, the snow structure becomes very unstable and with very little additional energy the snow structure fails. At this point, snow particles are carried by the water and contribute to runoff before completely melting. Under these conditions ripe snow can be a prerequisite to the maximum possible winter flood.

The time coordination of snow melt runoff with rainfall runoff appears to involve the process of flushing or eroding the snow structure. As the weakened snow structure erodes, the suspended water is released and augments the volume and further eroding power of the runoff water. Percolation and other flow through the snow structure erodes and melts channels in the snow, increasing the size of the capillary pores, thus decreasing the capillary storage. This is reflected in momentary rates of discharge from the snow column which exceed the average melting rate, and is accompanied by a decrease in density.

Maximum rates of snow melt

Maximum rates for 104 square miles were obtained by extrapolation

of observed rates of snow melt on the East Branch of the Pemigewasset River Basin above Lincoln, New Hampshire, by means of the formula $D = KV(T_w - 32^o)$. In the March 1936 storm the observed maximum T_w was 51.5^o and maximum V was 13.5 m.p.h. For a 36-hour period, under maximum conditions, with snow cover and heavy precipitation, the average temperature could be as high as $55^oF.$, relative humidity 100%, and average wind velocity 15 m.p.h. Higher wind velocities could not be maintained without decreasing the storm duration over a given basin. From the 36th to the 48th hour, the average temperature would have to be less, probably going down to 50^o at the end of the 48-hour period.

Figure 8 shows the observed values of wind and temperature at nearby Northfield, Vermont, this being the best available source of the

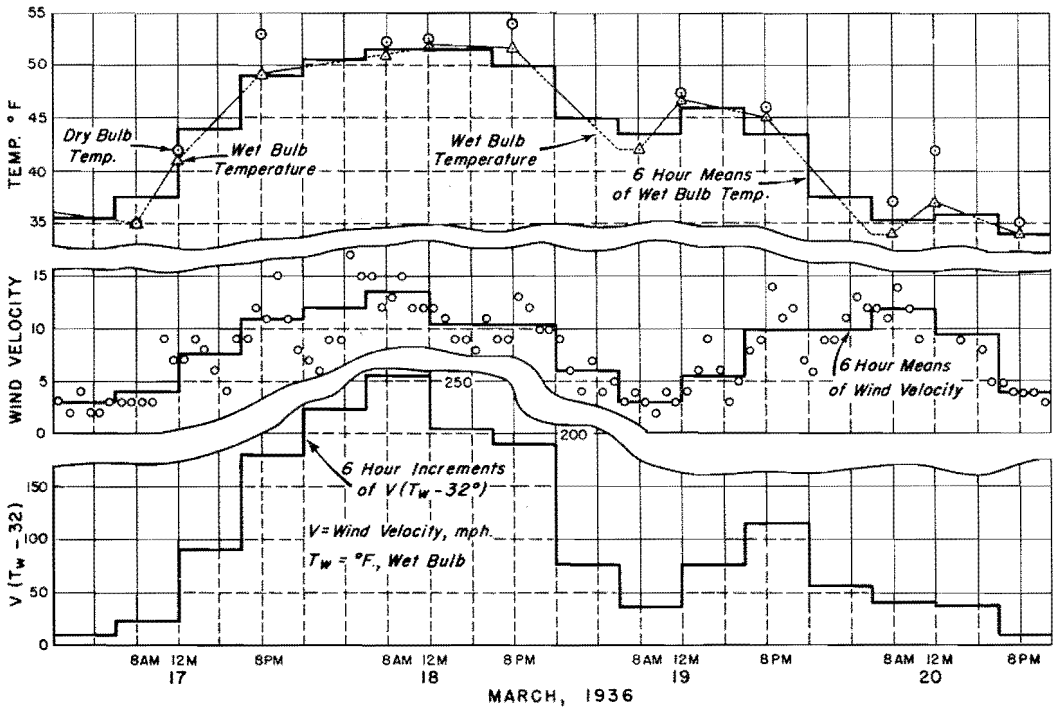

Figure 8

Observations of temperature and wind velocity at Northfield, Vermont

necessary data. Careful attention was given to exposure of the instruments and observations at other stations. The results of the analysis of the Dog River Basin above Northfield Falls, which includes Northfield in the basin, indicate that the data are applicable.

The value for K of 0.0065 for the East Branch of the Pemigewasset River is believed to result from optimum conditions favoring rapid snow melt and is not increased in the synthesis of the maximum possible rate of snow melt. North of this basin snow remained after the critical storm, and south of this basin snow melt occurred over too long a period. No other determined values of K even approach the value found for the East Branch of the Pemigewasset.

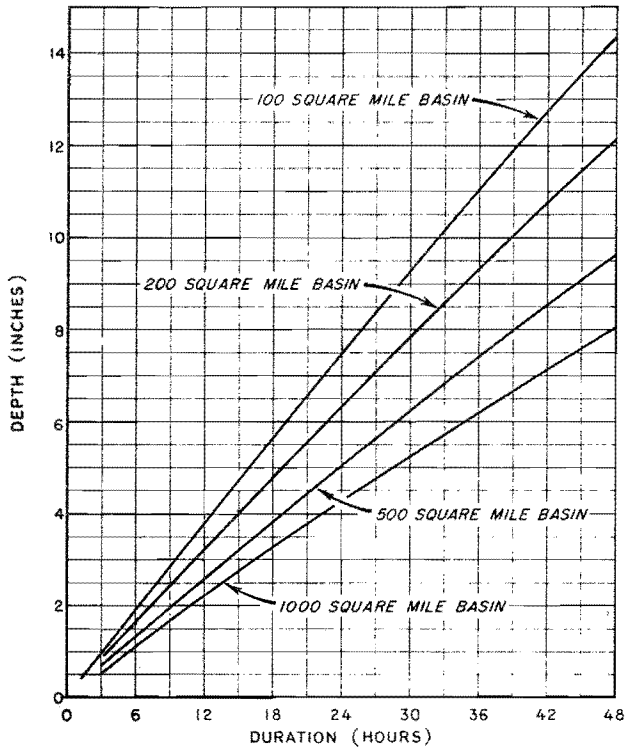

Figure 9

Duration-depth curves of maximum possible snow melt over selected basins in the New England region

Figure 9 shows duration-depth relationships for 100, 200, 500, and 1,000 square miles, and Figure 10 shows area-depth curves in 6-hour increments up to 48 hours. These curves have been obtained by straight line interpolation and extrapolation on log paper of the values for 104 and 622 square miles. (See Figure 5.)

Records indicate that

15 inches average depth of water on the ground, in the form of snow and as water suspended in the snow, is a distinct possibility for the Ompompanoosuc Basin. For other areas in the Connecticut River Basin above Northampton, Massachusetts; in the Merrimac River Basin above Manchester, New Hampshire; in the Hudson River Basin above Poughkeepsie, New York; in the Housatonic River Basin above West Cornwall, Connecticut; and in the Lake Champlain area, the total amounts required in Table III were present in 1936 or at other times and can occur again for the sizes of areas shown.

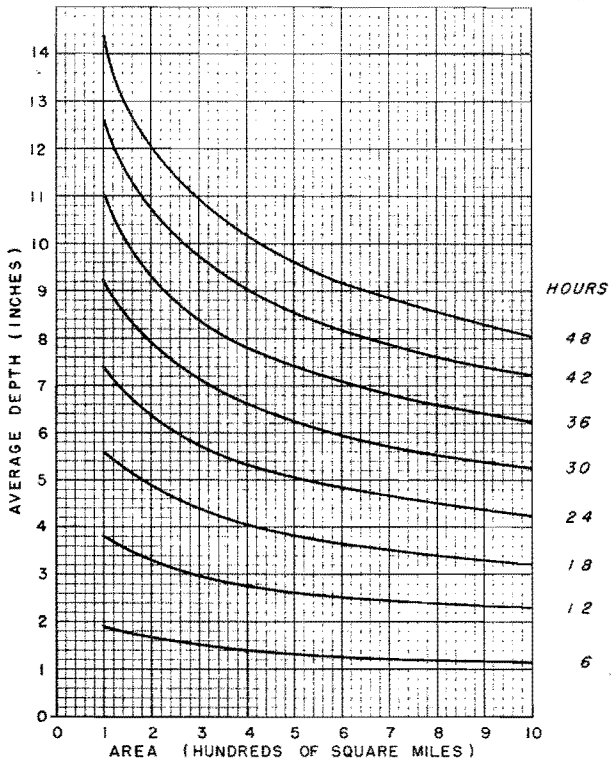

Figure 10

Area-depth curves of maximum possible snow melt over selected basins in the New England region

References

1. The Melting of Snow. R.E. Horton, Monthly Weather Review, Vol. 43, pp. 599-605; 1915.

2. Elements of Hydrology. A.F. Meyer, pp. 325-341; pp. 429-432.

3. Snow Survey and Stream Run-Off Forecast in Nevada for 1923. J.E. Church, Jr., Engineering News-Record, Vol. 90, p. 1001, 1923.

4. High Density of Snow Accelerates Its Melting and Runoff. Engineering News-Record, Vol. 99, p. 553; 1927.

5. Evaporation from Snow. R.E. Horton, Monthly Weather Review, Vol. 42, p. 99; 1914.

6. Snow Density in Relation to Runoff. J.E. Church, Jr., Engineering News-Record, Vol. 92, p. 234; 1924.

7. Some Field Experiments on Evaporation from Snow Surfaces. F.S. Baker, Monthly Weather Review, Vol. 45, p. 363; 1917.

8. Snow-Surface Temperatures. R.E. Horton and H.R. Leach, Monthly Weather Review, Vol. 62, p. 128; 1934.

9. The Accumulation and Rate of Melting of Snow as Influenced by Vegetation. Journal of Forestry, Vol. 83, pp. 564-569; 1935.

10. The Determination of Evaporation from Land and Water Surfaces. C.W. Thornthwaite and B. Holzman, Monthly Weather Review, Vol. 67, pp. 4-11; 1939.

11. Evaporation and Condensation. Engineering News-Record, Vol. 78, No. 4, pp. 196-199; 1917.

12. An Examination of Snow Deposits. British Ski Yearbook, Vol. VI, No. 13; 1932.

13. Forests and Floods in New Hampshire. Baldwin and Brooks, Publication No. 47, New England Regional Planning Commission; December 1936.

14. Improvements in the Methods of Forecasting Stream Flow. Carl Elges, American Geophysical Union, Transactions, 1939. Part I, page 62.

15. Melting Snow as a Flood Factor in the Sierra Nevada, E.H. Fletcher, American Meteorological Society Bulletin, p. 59. February 1940.

16. Snow Melting Characteristics. George D. Clyde, Utah Agricultural Experiment Station. Bulletin # 231 (technical). August 1931.

17. - 20. Water-Supply Papers Nos. 798, 799, 800, and 801.

CHAPTER VI

MAXIMUM POSSIBLE RAINFALL OVER THE OMPOMPANOOSUC BASIN

Area-depth curves

Representing as it does the functional relationship between average depth and accumulated area beginning with the largest isohyet, the area-depth curve has the property that the average depths defined by it increase in reliability with area. Thus, in a storm area having a station network density of one gage per 200 square miles, an isohyet having an enclosed area of 1,000 square miles will have five gages defining the average depth within it, whereas an isohyet having an area of 400 square miles will have only two gages defining the average depth within it. In order to correct for the inaccuracy in the average depths for small areas, it is logical to extend the area-depth curve to smaller areas by the same functional relationship which fits the data for larger areas.

Studies of area-depth curves engaged in by this section for about 100 storms occurring in different parts of the country show that an exponential function (straight line on semi-log paper) of the average depth fits area-depth data very well for durations of less than 48 hours and for areas greater than about 10 percent of the storm areas considered. No case was found where the average depth for small areas near the center of the storm exceeded the extended exponential curve fitted to average depths for the larger areas embraced by the storm.

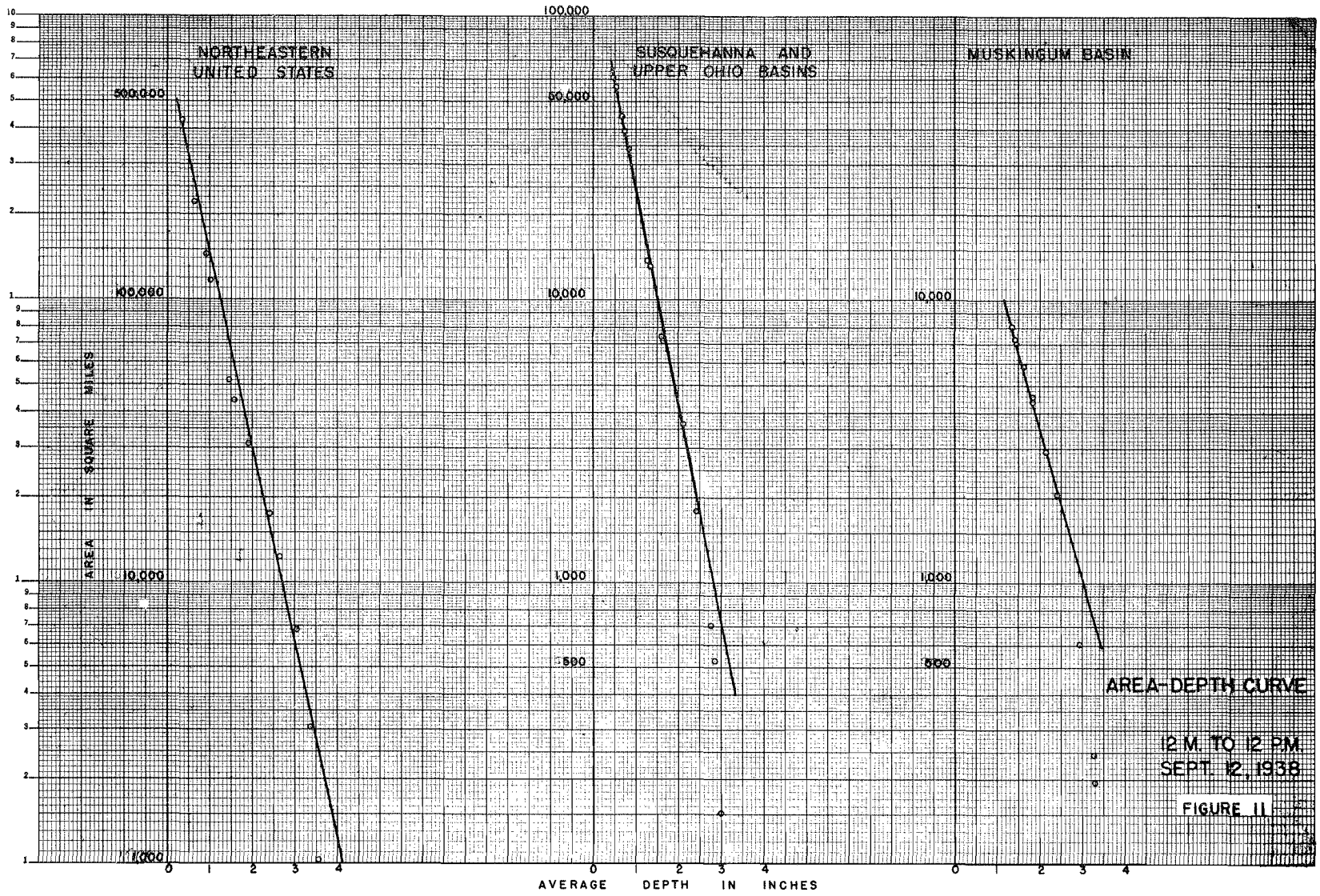
NORTHEASTERN UNITED STATES
SUSQUEHANNA AND UPPER OHIO BASINS
MUSKINGUM BASIN
AREA IN SQUARE MILES
500,000
100,000
10,000
1,000
50,000
10,000
1,000
500
10,000
1,000
500
0 1 2 3 4
AVERAGE DEPTH IN INCHES
AREA-DEPTH CURVE
12 M. TO 12 P.M.
SEPT. 12, 1938

FIGURE 11

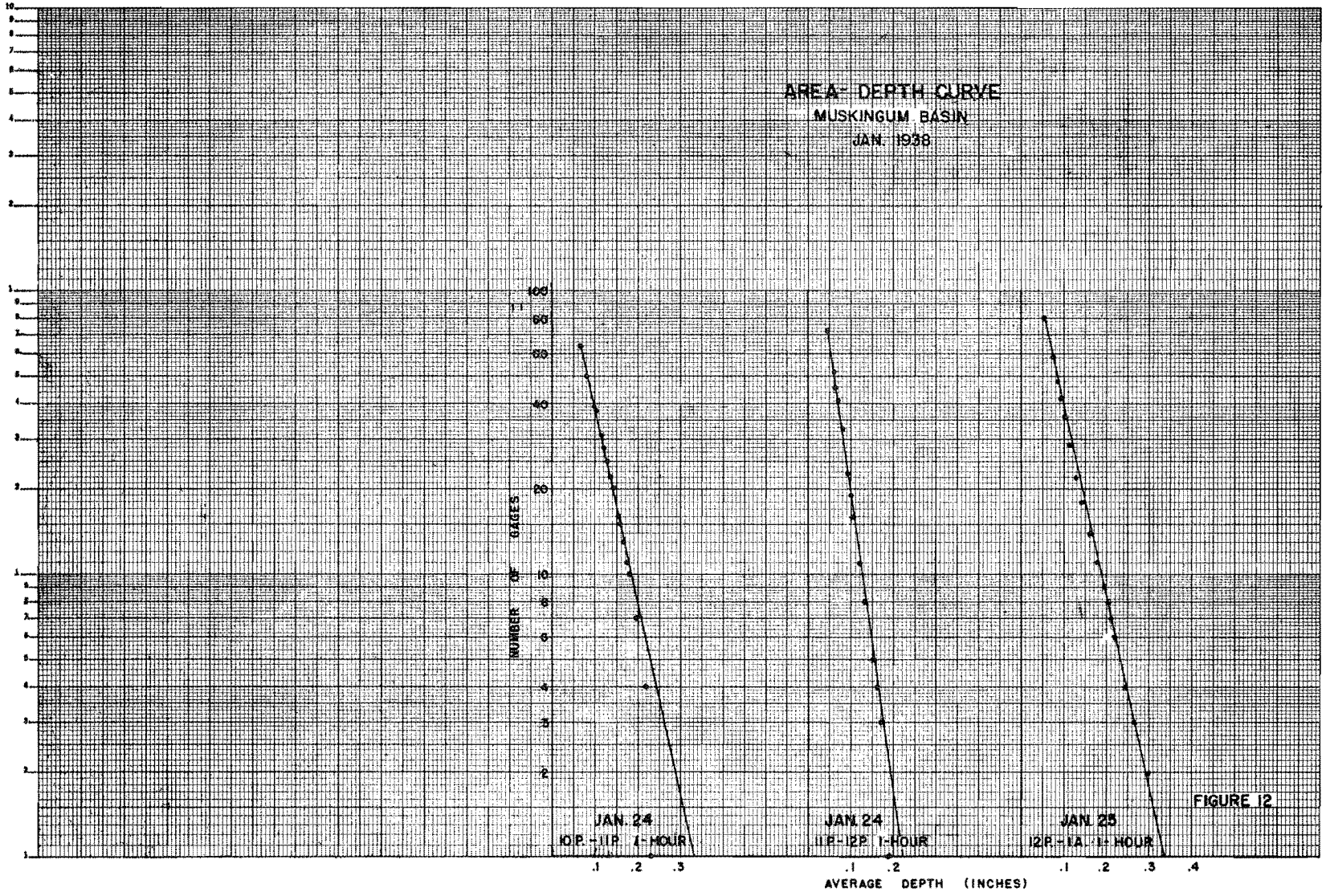
AREA- DEPTH CURVE
MUSKINGUM BASIN
JAN. 1938
NUMBER OF GAGES
100
60
40
20
10
6
4
2
JAN. 24
10 P. - 11 P. 1-HOUR
JAN. 24
11 P. - 12 P. 1-HOUR
JAN. 25
12 P. - 1 A. 1-HOUR
.1
.2
.3
.4
AVERAGE DEPTH (INCHES)

FIGURE 12

Figure 11 shows area-depth data plotted on semi-log paper for the storm of September 12, 1938, for various size areas ranging from 500,000 square miles for the northeastern United States to 8,000 square miles for the Muskingum Basin. In Figure 12 are shown average depths plotted against number of gages for a portion of the Soil Conservation Service Muskingum network for three consecutive hours on January 24-25, 1938. The departure of the curve from the plotted points is always positive and is believed to represent a reasonably small increase due to failure of the maximum measurement to coincide exactly with the storm center.

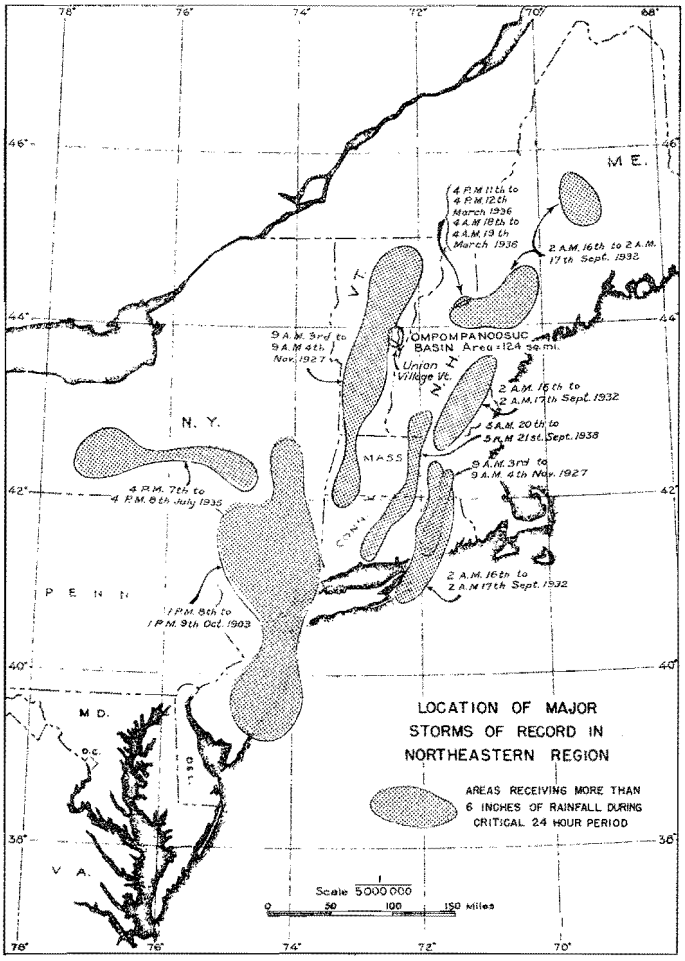

Figure 13

The gages in the Muskingum network are so evenly distributed that their number may be considered directly proportional to area.

The exponential function, therefore, seems to be a convenient and satisfactory relationship for comparing and extending area-depth curves. The curve of maximum possible rainfall for the Ompompanoosuc Basin has been developed on the basis of the

seven larger storms located as shown in Figure 13, namely the October 1903, November 1927, September 1932, July 1935, March 9-13, 1936, March 16-19, 1936, and September 1938 storms. Maximum 6, 12, 18, 24, 36, and 48 hour periods were selected in each storm and isohyetal maps were drawn for the area in the vicinity of the center. Area-depth values for these storms were computed and plotted on semi-log paper as shown in Figures 14-20, inclusive. Straight lines were fitted to points of equal duration, more weight being given to values for large areas. In all cases the area-depth curves arrived at in this manner conform to or exceed values obtained from isohyetal maps for areas greater than 100 square miles. It should be noted that the differences in value between curve and plotted points, expressed as percentages of total depth, are relatively small. This is in accordance with the procedure of semi-log extrapolation of area-depth curves, as previously explained.

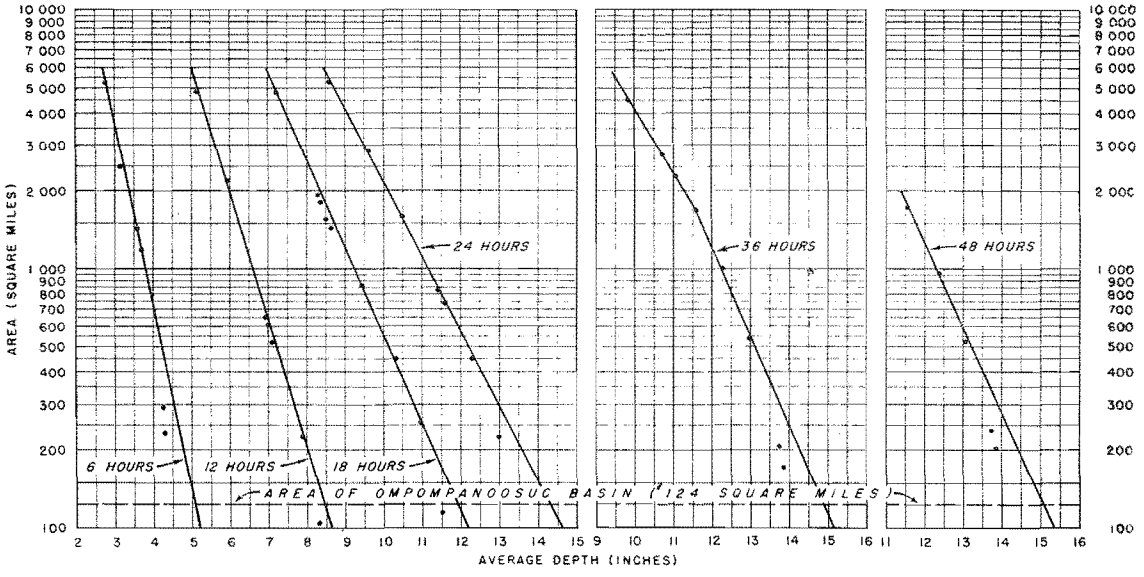

Figure 14

Area-depth curves, October 1903

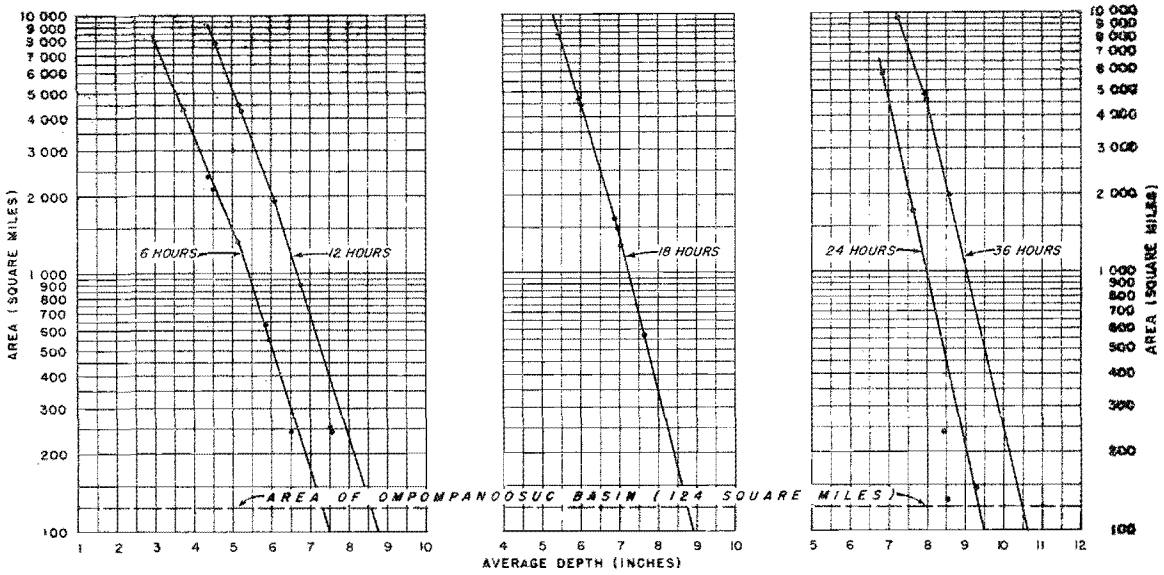

Figure 15

Area-depth curves, November 1927

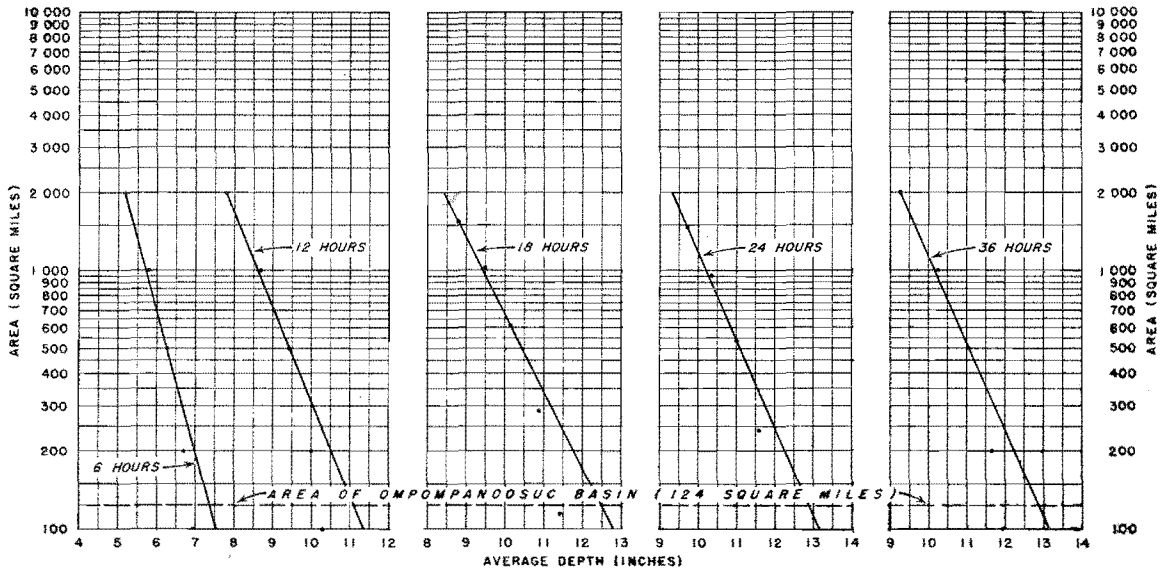

Figure 16

Area-depth curves, September 1932

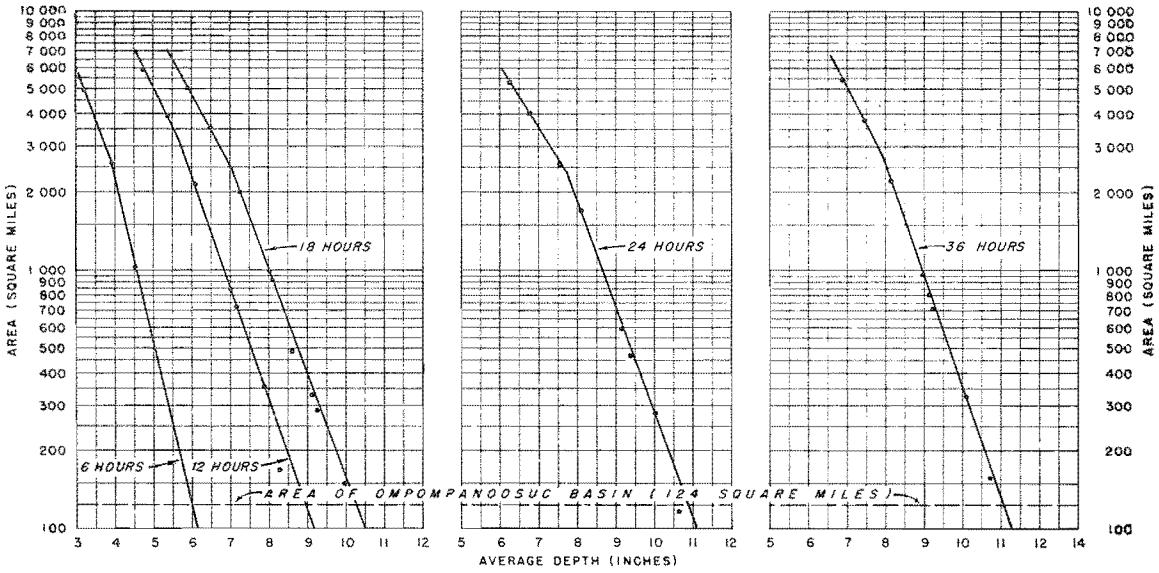

Figure 17

Area-depth curves, July 1935

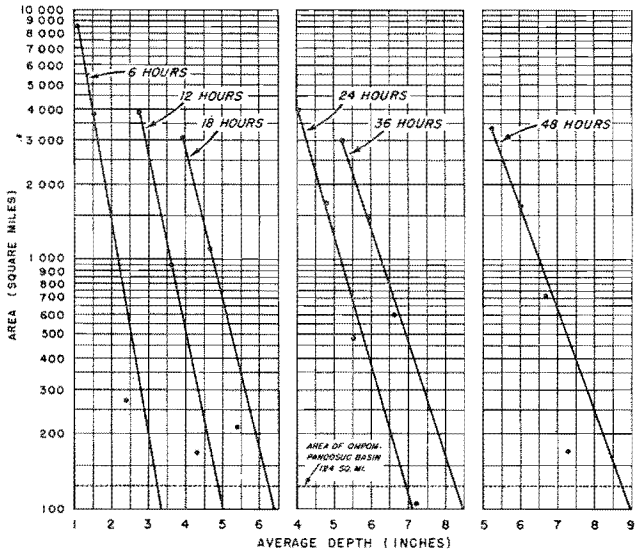

Figure 18

Area-depth curves,
March 10-13, 1936

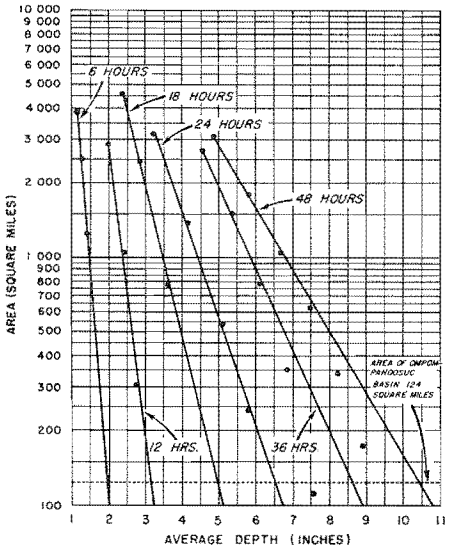

Figure 19

Area-depth curves,
March 17-19, 1936

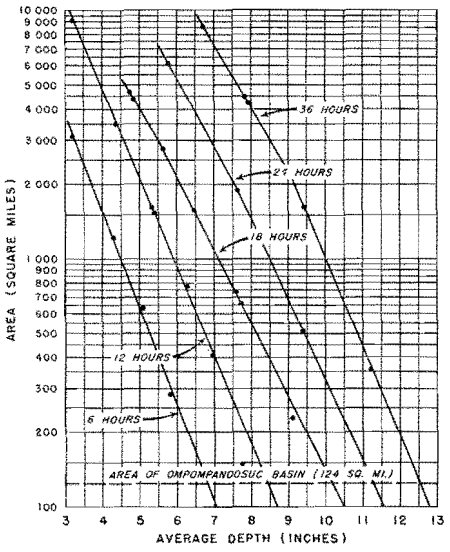

Figure 20

Area-depth curves,
September 1938

curve of maximum rainfall, viz., the September 1932 and October 1903 storms.

Reliability factor

The reliability factor accounts for three sources of error involved in the analysis of storm rainfall, namely (1) the error in construction of the mass curve due to the deficiency in the number of points defining the curve, (2) error due to inadequacy

Maximum recorded rainfall

Average depths for 124 square miles, the area of the Ompompanoosuc Basin, have been obtained by constructing a horizontal line denoting that particular area and reading off values at the points of intersection with the area-depth curves. These depths were plotted against duration in Figure 21 and Curve A drawn enveloping maximum points. Two storms gave values which served to determine this enveloping

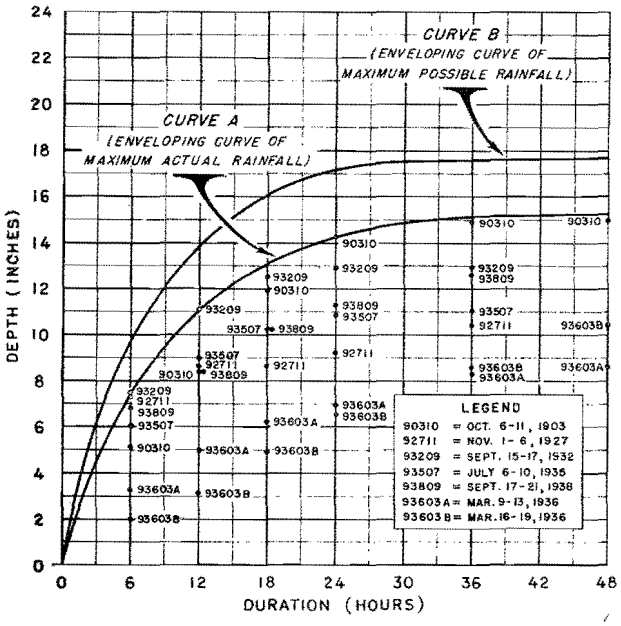

Figure 21

Enveloping duration-depth curves of maximum possible rainfall for the Ompompanoosuc Basin, (124 sq. mi.) above Union Village, Vermont

in the number of rainfall stations to define the storm pattern, and (3) the usual errors in measuring and recording precipitation. In a given storm study the total mass curve error depends on the relative number of recording gages in the network, the quality of non-recording station records, and the magnitude of the storm. The error is maximum for short durations and obviously becomes zero for the total storm period. After consideration of all these factors it was decided that a logarithmic curve descending from 20% at 6 hours to 5% for a 48-hour duration represented a reasonable estimate of the mass curve inaccuracy.

In the determination of the error due to inadequacy of rainfall stations use was made of Soil Conservation Service Muskingum records to determine the order of its magnitude. Half-hourly precipitation data from 470 recording gages within an area of 8,000 square miles were available. The arithmetic averages of this network, which can be assumed to represent the true average depth of rainfall, have been compared for the same storm periods with an average of 24 gages evenly distributed throughout the same area. The latter network corresponds roughly with the network of stations from which values are derived in this study. The results showed differences of 1% to 3% between the two sets of values. Taking into account the greater variability in the rainfall close to a storm center it

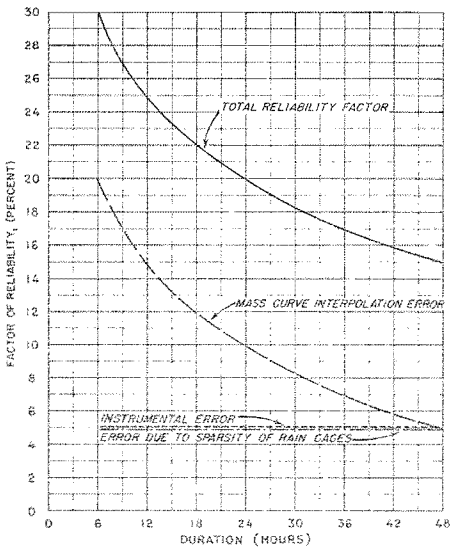

Figure 22

Reliability factors applied to maximum record rainfall

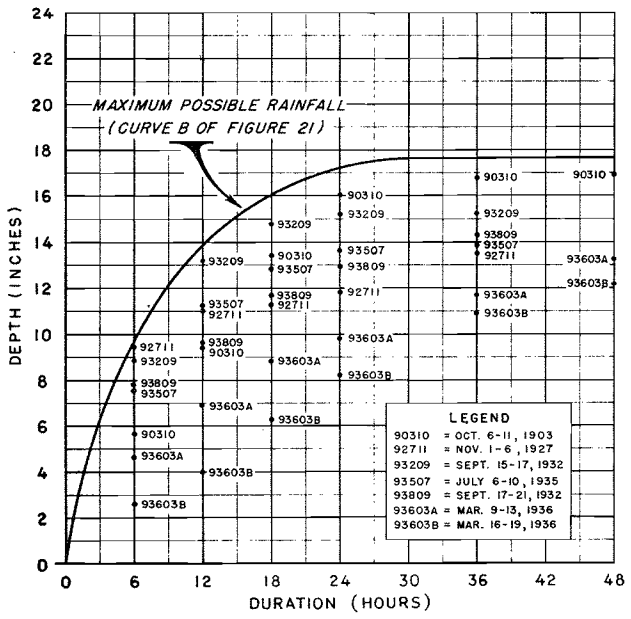

Figure 23

Duration-depth values adjusted for greater possible depth of precipitable water for the Ompompanoosuc Basin (124 sq.mi.), above Union Village, Vt.

was decided to assign a constant factor of 5% as the inadequacy of data error.

An instrumental error of 5%, constant for all durations, has been added to the other components and a total reliability factor obtained as shown in Figure 22, this factor varying from 30% to 15%.

Maximum possible rainfall

Curve B of Figure 21, representing the enveloping duration-depth curve of maximum possible rainfall, was obtained by increasing values of Curve A by the variable factor of reliability. This curve is shown again in Figure 23 together with duration-depth values representing actual rainfall amounts increased by the precipitable water adjustment discussed under "Adjustment of Storms on Basis of Precipitable Water."

The table shown on page 65 summarizes the results.

Point rainfall

The question arose early in the study as to the use to be made of point rainfall records which exceed amounts from record storms. In Figure 24 all the extreme rainfall amounts for various durations known to have been recorded in the United States are plotted on log-log paper.

TABLE IV

Duration Hours	Maximum Actual Depths Inches	Curve A Inches	Reliability Factor %	Curve B Inches	Increments Inches
6	7.40	7.4	30	9.6	9.6
12	11.10	11.1	25	13.9	4.3
18	12.45	13.1	22	16.0	2.1
24	14.30	14.3	20	17.2	1.2
30	-	-	-	17.5	0.3
36	14.90	15.0	17	17.6	0.1
42	-	-	-	17.6	0.0
48	15.05	15.3	15	17.6	0.0

One curve has been drawn enveloping all the points and another enveloping rainfall in the New England region. The latter duration-depth curve

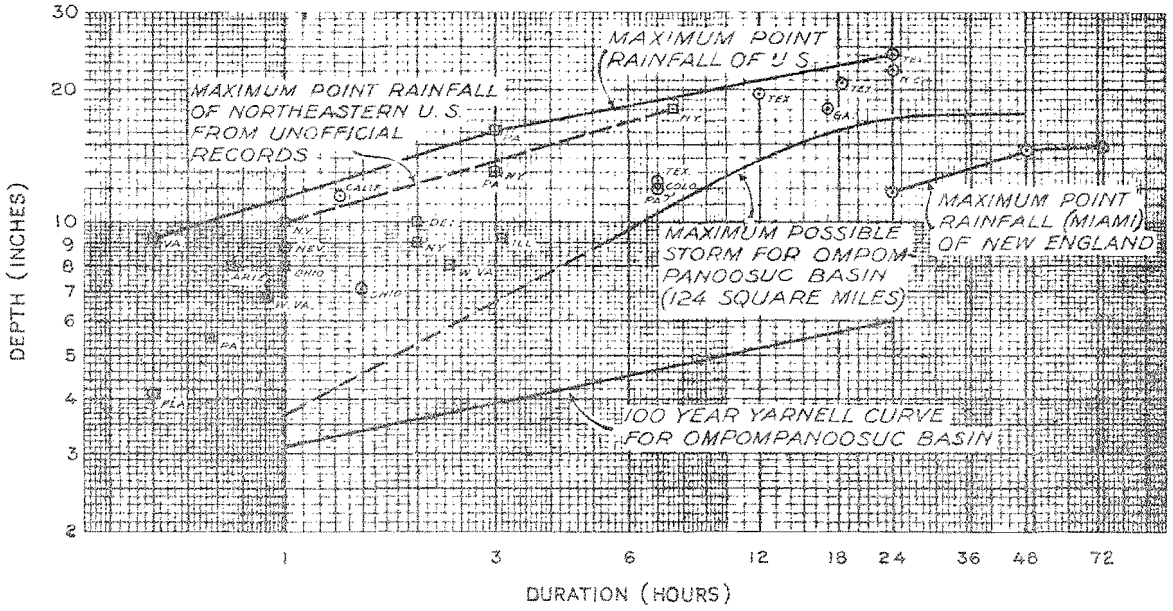

Figure 24. Duration-depth curves of point rainfall

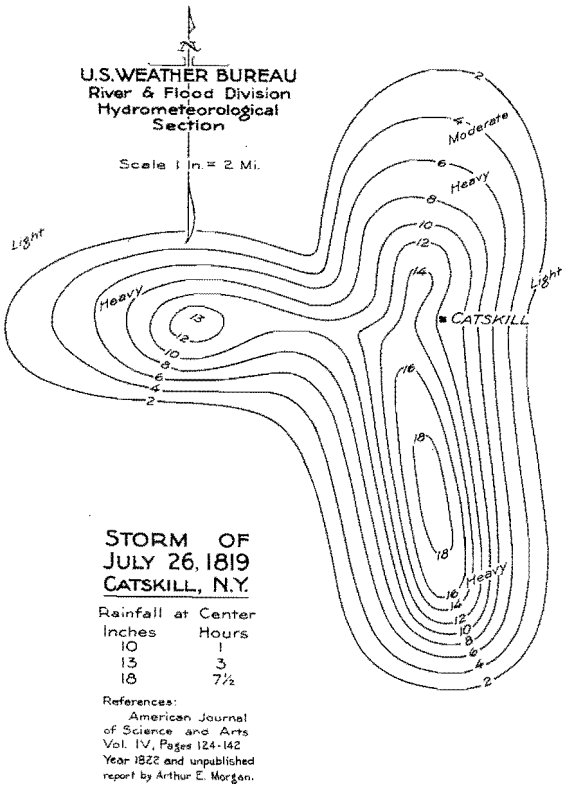

Figure 25

shown in Figure 26 which gives a lower value for 80 square miles than the September 1932 storm for a similar period.

On the basis of the analysis of the July 1819 storm it was decided that a high-intensity, short-duration storm of this type would not be the most critical over the Ompompanoosuc Basin. Also plotted in Figure 24 are maximum rainfall values from Miami Conservancy data from 7,561 station-years of record in the New England States, and the

is determined by the Catskill, New York, storm of July 26, 1819, which is reported to have lasted 7-1/2 hours and produced 18 inches of rain at the center. Fortunately a description of this storm is available which gives estimates of rain at several points and outlines the limits of heavy rainfall. From these data it was possible to prepare an isohyetal map which is reproduced in Figure 25. An area-depth curve was derived as

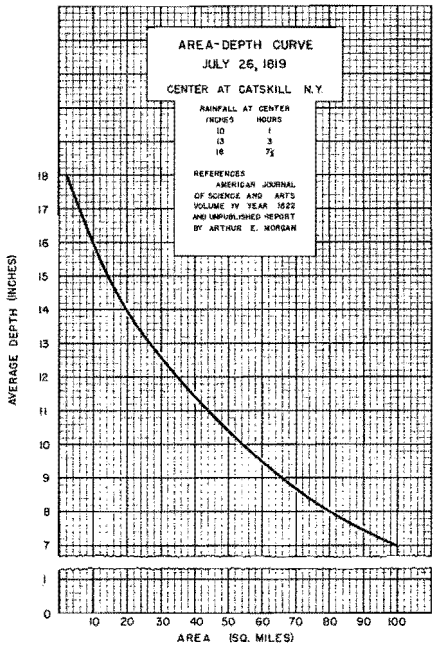

Figure 26

100-year Yarnell frequency curve derived from coefficients for the territory in which the basin is located. The maximum possible storm for 124 square miles, drawn for comparison, exceeds both of these curves.

CHAPTER VII

MAXIMUM POSSIBLE PRECIPITATION PLUS SNOW MELT OVER THE OMPOMPANOOSUC BASIN

Of the critical storms considered in this study only two, those of March 1936, occurred during a period of melting snow or in a season when antecedent meteorological conditions permitted the existence of a critical snow cover. The rainfall analysis of these storms formed the basis for determining maximum possible precipitation coincident with maximum rate of discharge from a snow cover. From area-depth curves of Figures 18 and 19 average depths of rainfall over 124 square miles were obtained and plotted against duration in Figure 27. Curve A was drawn enveloping actual values of rainfall. Duration-depth values adjusted for greatest possible depth of precipitable water were derived by increasing actual values of rainfall by the adjustment factors given in Table I, and discussed in the chapter on "Adjustment of Storms on Basis of Precipitable Water." These rainfall amounts are also

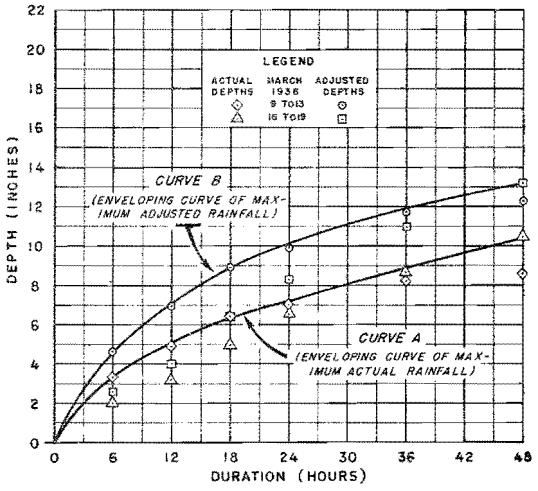

Figure 27

Enveloping duration-depth curves of maximum rainfall for the Ompompanoosuc Basin (124 sq. mi.) above Union Village, Vermont

plotted in Figure 27, and Curve B drawn enveloping these values.

As in previous reports, the inadequacies in data and uncertainties in analysis have been evaluated and combined into a reliability factor by which the amounts to be added to Curve A in Figure 27 are determined. The same procedure was followed in the consideration of maximum possible rainfall shown in Figure 21 of this report. Storms of great magnitude have admittedly a lower frequency for the colder seasons in New England. Hence, there exists a relatively shorter history of intense storms during the winter months than for the warmer seasons. It has been concluded, therefore, that a larger reliability factor should be applied to storms that occur during seasons with snow on the ground.

It is difficult to evaluate the difference between the reliability factors for the two seasons; but since the adjustment for precipitable water for those storms not involving snow runoff agreed well with the increases in the form of a reliability factor, and as this curve, (B), enveloped all values fixing the position of a reliability curve as ordinarily defined, it was accepted as absorbing the uncertainties entailed in the inadequacies of basic data and analytical methods. For these reasons Curve B is accepted as the enveloping curve of maximum possible rainfall.

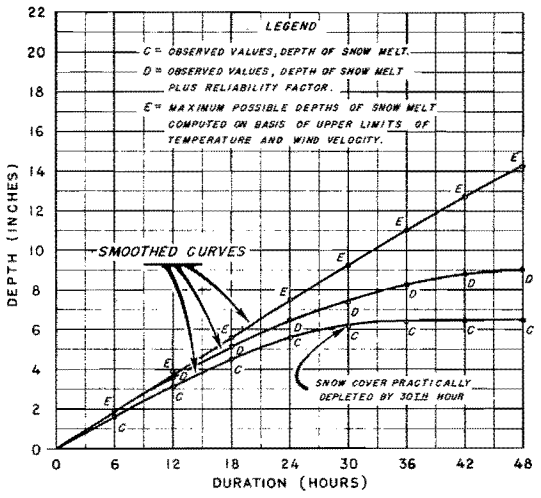

Figure 28

Enveloping duration-depth curves of snow melt on East Branch of Pemigewasset River Basin above Lincoln, N.H. (area = 104 sq.mi.)

Figure 28 shows the enveloping duration-depth curves of snow melt on the East Branch of the Pemigewasset River Basin above Lincoln, New Hampshire (drainage area = 104 square miles).

Curve C indicates the observed values of depth of snow melt.

Curve D shows the observed values plus reliability factor.

Curve E shows the maximum possible depth of snow melt computed on the basis of upper limits of temperature and wind velocity.

The value of the reliability factor has been determined by studying the effects of errors in stream discharge measurements, in base-flow and infiltration estimates, in rainfall observations, and in the selection of the distribution graph. The reliability factor used is 15% for the first 24 hours, and increases to 40% by the 48th hour as shown in Figure 28.

It can be seen that Curve E envelops Curve D. It has been determined that this is also true for the other values of area considered. Curve E has been used in the interpolation of maximum possible duration-depth curves to areas other than 104 square miles. Figure 29 shows the corresponding curve, namely Curve E, for the Ompompanoosuc Basin of 124

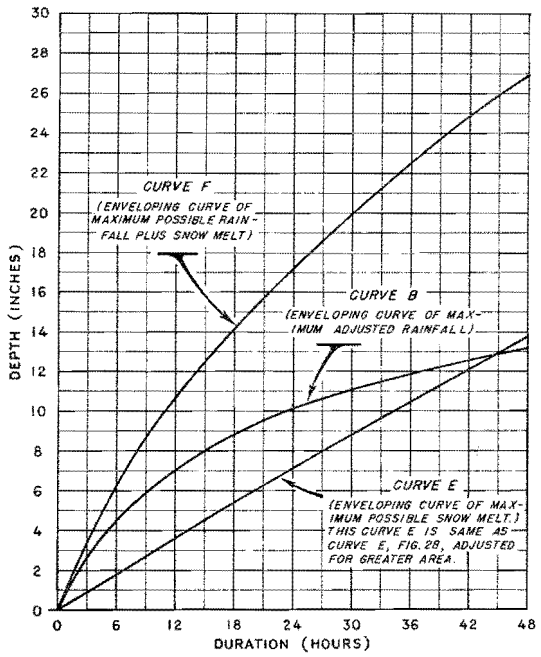

Figure 29

Enveloping curves of rainfall and snow melt for the Ompompanoosuc Basin, (124 sq. mi.) above Union Village, Vermont

square miles.

Values of Curves B and E, representing maximum possible rainfall and snow melt respectively, have been combined to obtain maximum possible rainfall plus snow melt over 12^{4} square miles given by Curve F.

Table V shown on the following page summarizes the results.

TABLE V

Duration Hours	Maximum Actual Rainfall Inches	Values of Curve A Inches	Reliability Factor %	Curve A + Reliability Inches	Precipitation Maximum Adjusted Depths - Inches	Values of Curve B Inches	Curve E Snow Melt Inches of Water	Curve F Rainfall Plus Snow Melt Inches	Increments Inches
6	3.25	3.3	30	4.3	4.60	4.6	1.8	6.4	6.4
12	4.90	5.1	25	6.4	6.90	7.0	3.6	10.6	4.2
18	6.25	6.3	22	7.7	8.80	8.8	5.4	14.2	3.6
24	6.95	7.2	20	8.6	9.80	10.1	7.1	17.2	3.0
30	-	-	-	9.5	-	11.1	8.8	19.9	2.7
36	8.60	8.8	17	10.3	11.70	11.9	10.5	22.4	2.5
42	-	-	-	11.2	-	12.6	12.1	24.7	2.3
48	10.40	10.4	15	12.0	13.20	13.2	13.7	26.9	2.2

CHAPTER VIII

MAXIMUM PRECIPITATION OVER SELECTED DRAINAGE AREAS IN THE NEW ENGLAND REGION

By utilizing data prepared for the Ompompanoosuc study it has been possible to determine rainfall and snow melt potentialities for other basins ranging in area from 100 to 1,000 square miles located in the drainage basins shown by the shaded area in Figure 4. The results given here are applicable to the Connecticut River Basin above Northampton, Massachusetts; the Hudson River Basin above Poughkeepsie, New York; the Housatonic River Basin above West Cornwall, Connecticut; the Merrimac River Basin above Manchester, New Hampshire; and the Lake Champlain Basin. The principal difficulty in extending the area of applicability is whether sufficient water may ever be available in snow deposits along the coastal regions of New England to maintain maximum rates of snow melt for 48 hours. This is a problem for future study.

The method of developing duration-depth curves of maximum rainfall for the Ompompanoosuc Basin was used for the region under consideration. Areas of 100, 200, 500, and 1,000 square miles were selected as convenient units. In the case of maximum possible rainfall, values of rainfall depth were taken from the area-depth curves of Figures 14 to 20, inclusive, and maximum points plotted as shown in Figure 30. Enveloping curves were drawn representing maximum actual rainfall. The

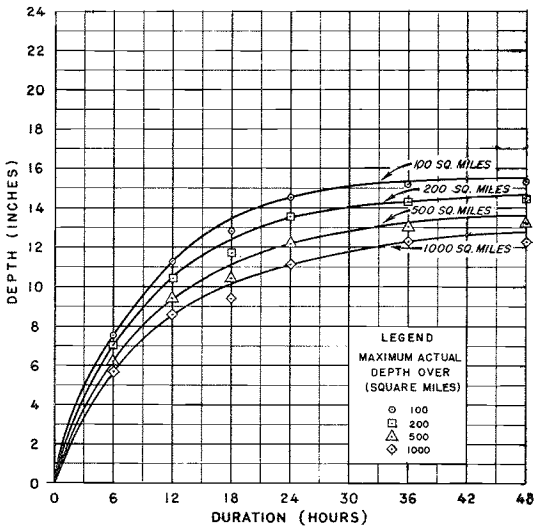

Figure 30

Enveloping duration-depth curves of maximum actual rainfall from record storms in the New England region

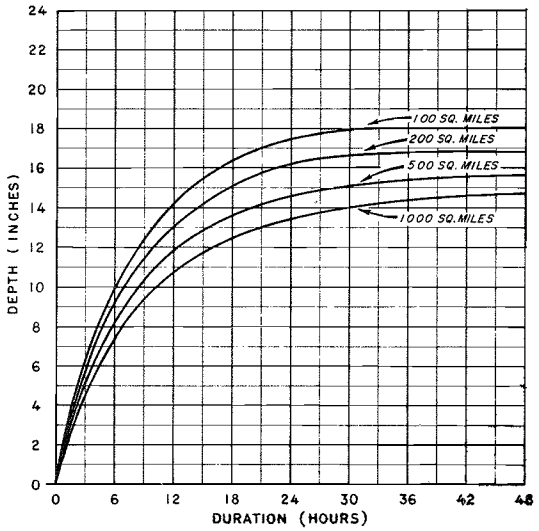

Figure 31

Enveloping duration-depth curves of maximum possible rainfall over selected basins in the New England region

reliability factors of Figure 22 were applied and the curves of maximum possible rainfall shown in Figure 31 were obtained. The same reliability factors were applied to each curve for the following reason: average depths for areas of 1,000 square miles and less having been determined by the extrapolation method described earlier, the results for areas of all values considered here are dependent on the same data and the reliability factor should be constant with area.

The enveloping duration-depth curves of maximum possible rainfall were replotted separately in Figures 32 to 35, inclusive, together with duration-depth values obtained by increasing the actual values by precipitable water adjustments corresponding to the particular storms. As before, these curves are confirmed by the fact that in all cases they envelop the adjusted values of rainfall.

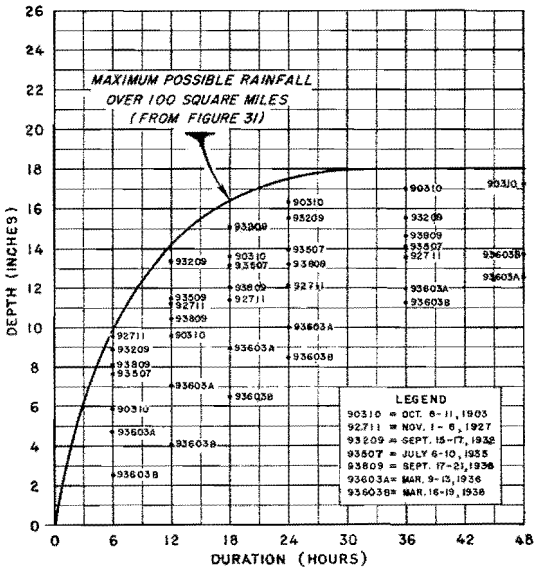

Figure 32

Duration-depth values for 100 square miles adjusted for greater possible depth of precipitable water

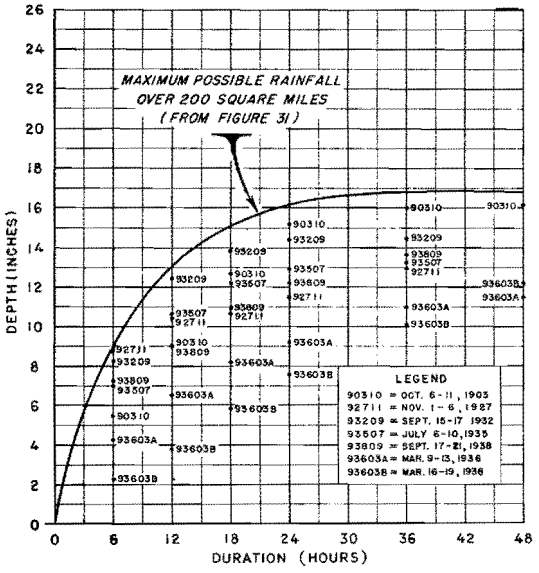

Figure 33

Duration-depth values for 200 square miles adjusted for greater possible depth of precipitable water

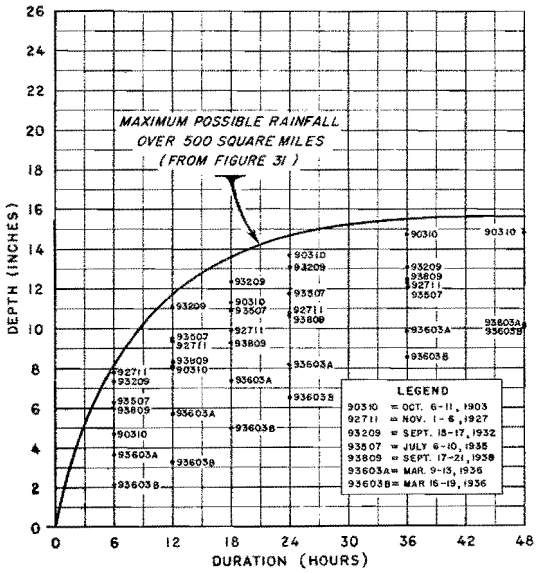

Figure 34

Duration-depth values for 500 square miles adjusted for greater possible depth of precipitable water

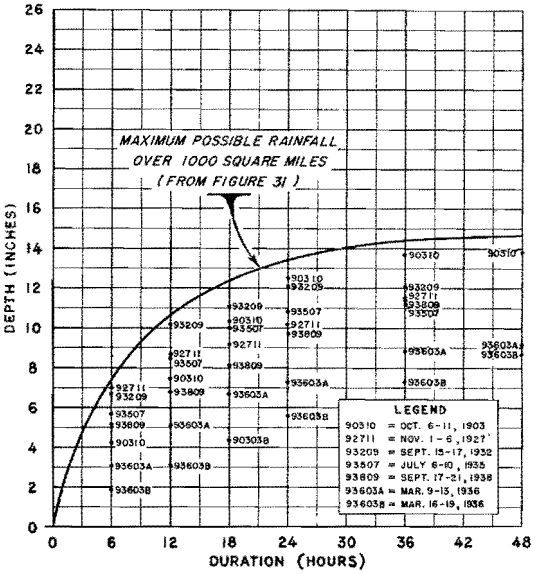

Figure 35

Duration-depth values for 1,000 square miles adjusted for greater possible depth of precipitable water

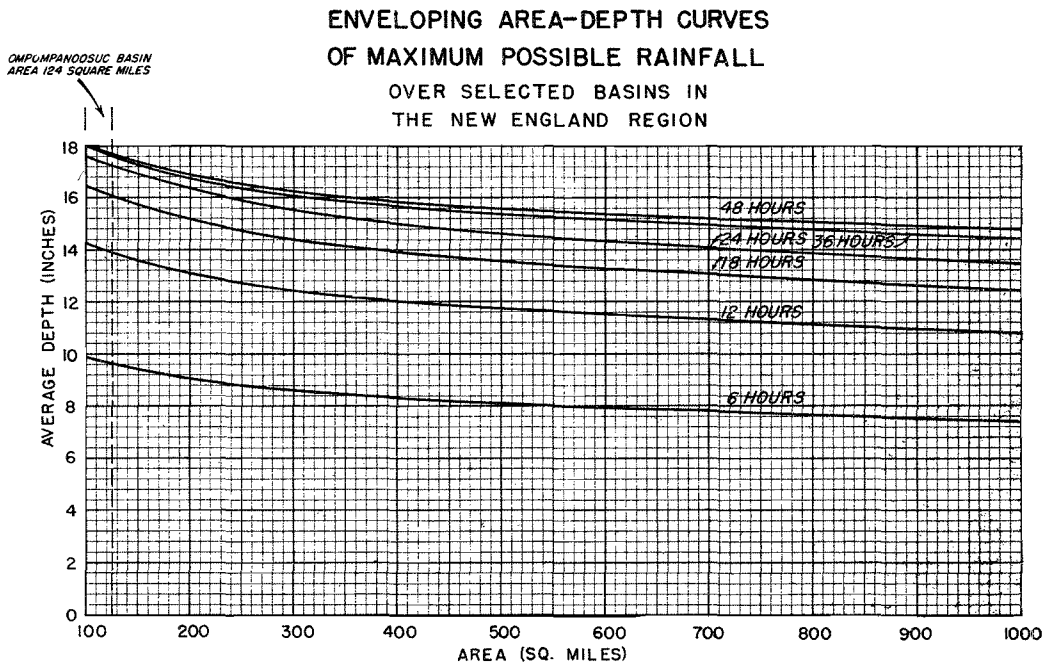

Figure 36

Enveloping area-depth curves of maximum possible rainfall for successive durations of 6 to 48 hours were derived from the corresponding duration-depth curves and are reproduced in Figure 36 for convenience in interpolating values to any size drainage basin. A table of values is shown as Table VI.

Time patterns of maximum possible rainfall, as block diagrams of six-hour increments, are shown in Figure 36-a for areas of 100, 200, 500, and 1,000 square miles. For situations requiring consideration of snow melt plus rainfall, similar flexibility in arrangement can be utilized, Figure 36-a serving as an example.

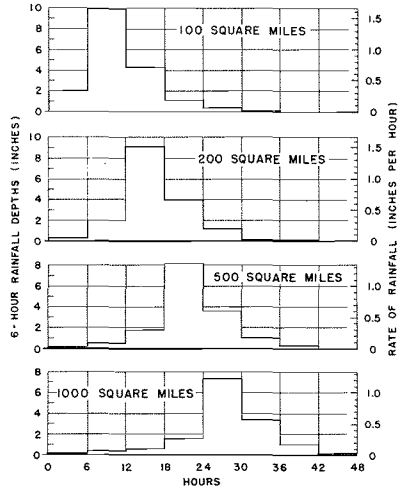

Figure 36-a

Arrangements of maximum possible rainfall over drainage areas of various sizes

TABLE VI

(For Storms Without Snow Cover)

Duration Hours	Area Square Miles	Maximum Actual Depths Inches	Enveloping Curve of Actual Rainfall - Inches	Reliability Factor %	Maximum Possible Depths Inches
6	100	7.55	7.6	30	9.9
	200	7.00	7.0	30	9.1
	500	6.25	6.3	30	8.2
	1,000	5.70	5.7	30	7.4
12	100	11.35	11.4	25	14.2
	200	10.50	10.5	25	13.1
	500	9.40	9.4	25	11.8
	1,000	8.60	8.6	25	10.8
18	100	12.80	13.4	22	16.4
	200	11.75	12.4	22	15.1
	500	10.40	11.1	22	13.6
	1,000	9.40	10.2	22	12.4
24	100	14.60	14.6	20	17.5
	200	13.55	13.6	20	16.3
	500	12.20	12.2	20	14.6
	1,000	11.15	11.2	20	13.4
30	100	-	-	-	17.9
	200	-	-	-	16.6
	500	-	-	-	15.1
	1,000	-	-	-	14.0
36	100	15.20	15.4	17	18.0
	200	14.30	14.3	17	16.7
	500	13.10	13.2	17	15.4
	1,000	12.25	12.3	17	14.4
42	100	-	-	-	18.0
	200	-	-	-	16.8
	500	-	-	-	15.6
	1,000	-	-	-	14.6
48	100	15.35	15.6	15	18.0
	200	14.40	14.6	15	16.8
	500	13.20	13.6	15	15.6
	1,000	12.30	12.8	15	14.7

Curves of maximum rainfall to be applied to snow melt were determined by utilizing the area-depth curves of the two March 1936 storms (Figures 18 and 19). Values were increased by the precipitable water adjustments for the respective storms. Figures 37 to 40, inclusive, show the actual rainfall depths, adjusted rainfall depths, and enveloping curves of maximum possible rainfall (shown as Curve A in each case). Duration-depth curves of snow melt of Figure 9 are reproduced as Curves B. Curves C, maximum possible precipitation and snow melt, have been obtained by summing up the values of Curves A and B. For convenience again, enveloping area-depth curves were determined and are shown in Figure 41. Table VII summarizes the results for maximum rainfall and snow melt.

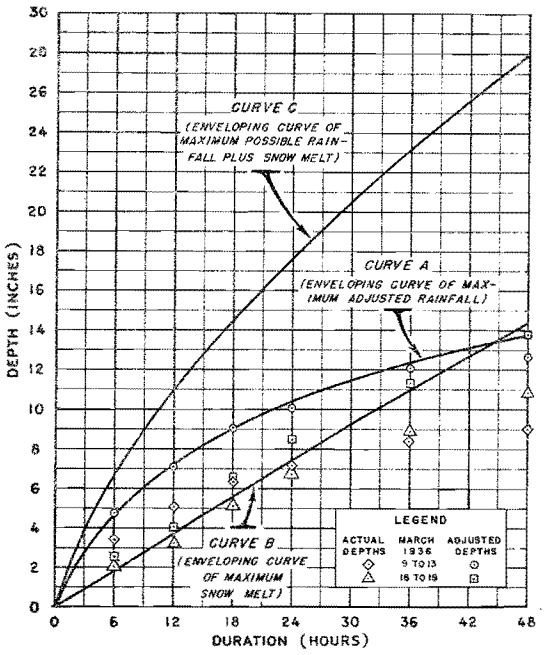

Figure 37

Enveloping curves of rainfall and snow melt over 100 square miles for selected basins in the New England region

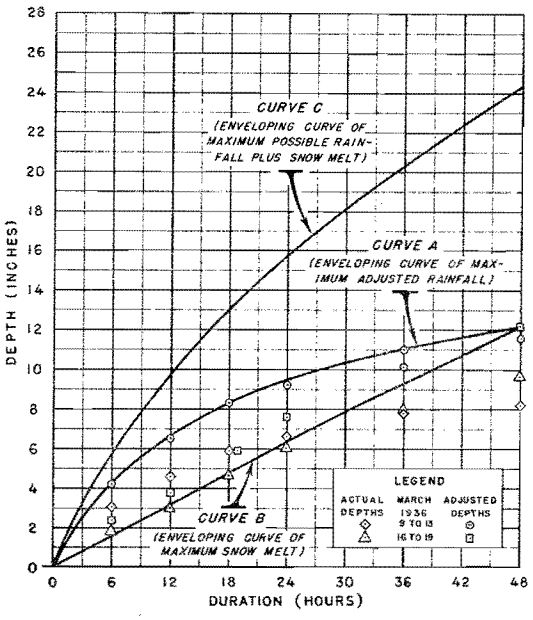

Figure 38

Enveloping curves of rainfall and snow melt over 200 square miles for selected basins in the New England region

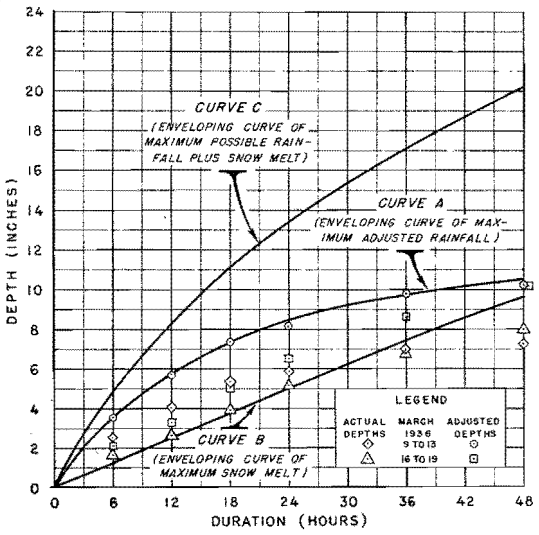

Figure 39

Enveloping curves of rainfall and snow melt over 500 square miles for selected basins in the New England region

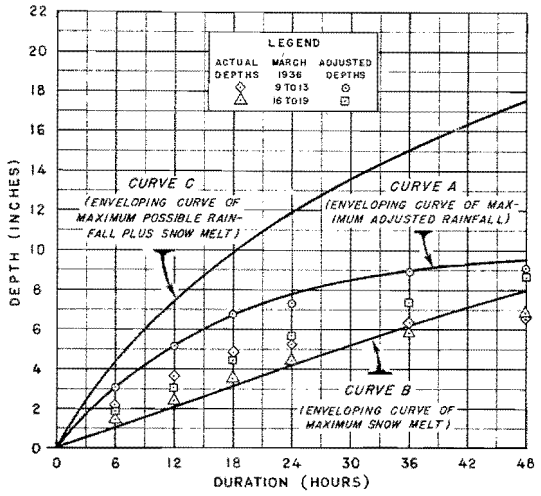

Figure 40

Enveloping curves of rainfall and snow melt over 1000 square miles for selected basins in the New England region

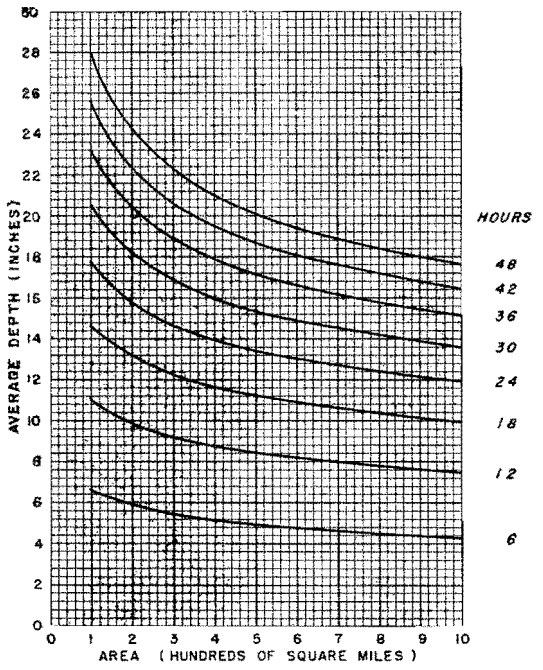

Figure 41

Enveloping area-depth curves of maximum possible rainfall plus snow melt over selected basins in the New England region

TABLE VII

(For Storms With Snow Cover)

Duration Hours	Area Square Miles	Maximum Adjusted Rainfall Depths Inches	Enveloping Curve of Adjusted Rainfall Inches	Snow Melt Inches	Maximum Possible Rainfall and Snow Melt Inches
6	100	4.70	4.7	1.9	6.6
	200	4.25	4.3	1.6	5.9
	500	3.60	3.6	1.3	4.9
	1,000	3.10	3.1	1.1	4.2
12	100	7.10	7.2	3.8	11.0
	200	6.50	6.6	3.2	9.8
	500	5.70	5.8	2.6	8.4
	1,000	5.10	5.2	2.2	7.4
18	100	9.00	9.0	5.6	14.6
	200	8.30	8.3	4.8	13.1
	500	7.40	7.4	3.8	11.2
	1,000	6.70	6.7	3.2	9.9
24	100	10.10	10.3	7.4	17.7
	200	9.25	9.4	6.3	15.7
	500	8.20	8.4	5.0	13.4
	1,000	7.35	7.7	4.2	11.9
30	100	-	11.4	9.2	20.6
	200	-	10.3	7.8	18.1
	500	-	9.2	6.2	15.4
	1,000	-	8.4	5.2	13.6
36	100	12.00	12.2	11.0	23.2
	200	11.00	11.0	9.3	20.3
	500	9.80	9.8	7.4	17.2
	1,000	8.90	8.9	6.2	15.1
42	100	-	13.0	12.7	25.7
	200	-	11.6	10.7	22.3
	500	-	10.2	8.5	18.7
	1,000	-	9.3	7.1	16.4
48	100	13.70	13.7	14.3	28.0
	200	12.20	12.2	12.1	24.3
	500	10.20	10.5	9.6	20.1
	1,000	9.15	9.6	8.0	17.6

CHAPTER IX

CONCLUSIONS

The limitations inherent in the physical analysis embraced by the foregoing discussion have made it necessary to develop this study in terms of average rainfall depths over the basin for six-hour periods only. It is well known that on larger basins the natural equalizing influences of retention and channel storage permit the application of results expressed in increments of time as great as six hours. On basins as small as the Ompompanoosuc, however, physiographic and hydrologic influences may produce excessive concentration within periods of less than six hours. While increments for lesser periods could be taken directly from the mass curves, such procedure would reflect a far greater dependability in the data and in the techniques of plotting mass curves than actually exists. It is therefore necessary to resort to a procedure not based on a physical analysis of the data themselves.

In the typical duration-depth curve, characteristic of a point or locality, average rainfall varies as a power function of the duration for intervals of at least twelve hours. Such a portion of the curve can be extrapolated from the 6-hour to the 1-hour duration and remain consistent with the probable time pattern of rainfall. It is possible, therefore, to obtain the most probable breakdown of the 6-hour amounts into hourly increments by adopting a distribution through time fixed by

the duration-depth curve. This extrapolation has been made for the range of areas involved, and is illustrated for the Ompompanoosuc Basin by the dashed line in Figure 24. The first 6-hour period of the duration-depth curves shown in Figures 23 and 31 have been replotted in Figure 42 after expanding the time scale. In Figure 43 the time pattern of 6-hour increments for 124 square miles has been resolved into hourly increments by the above procedure.

Table VIII (page 84) provides the data for preparing time patterns of maximum possible rainfall for basins with areas of 100, 200, 500, and 1,000 square miles. A similar table can be prepared for rainfall plus snow melt by means of the technique described above.

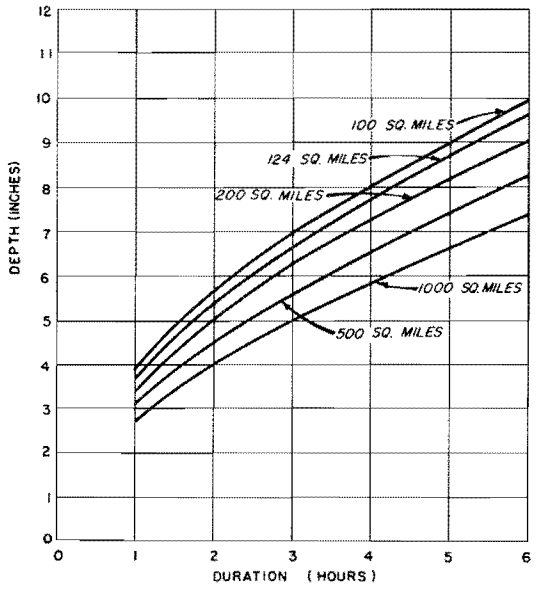

Figure 42

Enveloping duration-depth curves of maximum possible rainfall for durations of 1 to 6 hours over the Ompompanoosuc Basin and other selected drainage areas in the New England region

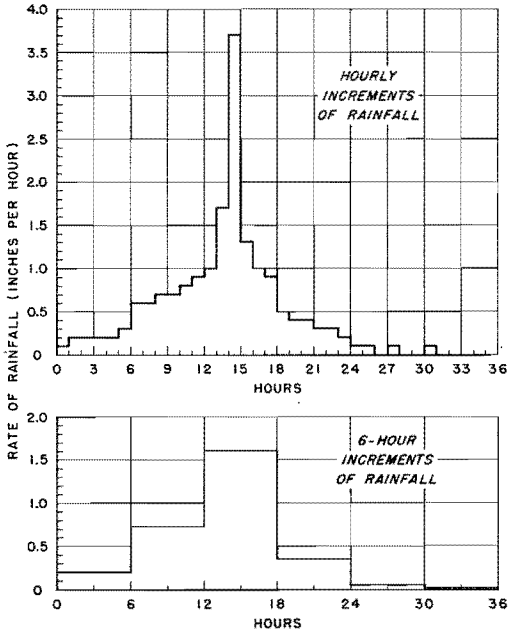

Figure 43

Maximum possible rainfall over the Ompompanoosuc Basin (124 sq. mi.) above Union Village, Vt.

In Figure 44 are shown area-depth curves for durations of 1 to 5 hours, inclusive, for convenience in determining duration-depth values for areas other than those shown in Figure 42.

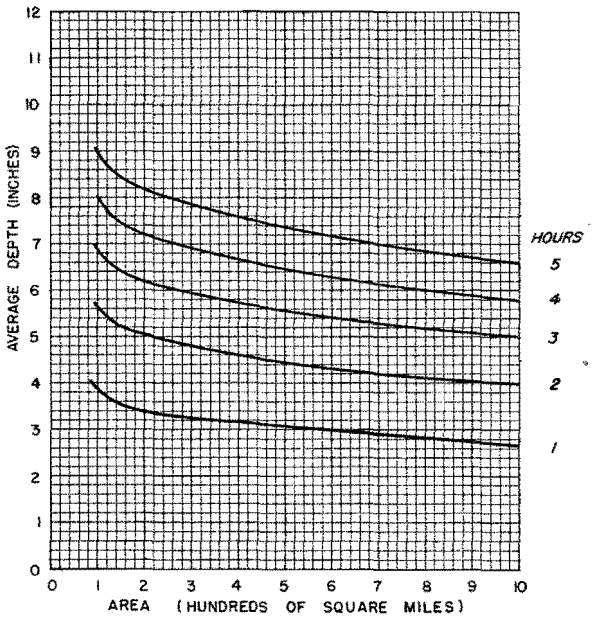

Figure 44

Enveloping area-depth curves of maximum possible rainfall for short durations over selected basins in the New England region

TABLE VIII

ACCUMULATED DEPTHS AND INCREMENTS OF THE MAXIMUM POSSIBLE STORM FOR DURATIONS OF 1 TO 48 HOURS, INCLUSIVE, FOR VARIOUS AREAS

Durations Hours	100 sq.mi.		124 sq.mi.		200 sq.mi.		500 sq.mi.		1000 sq.mi.	
	Acc.	Inc.	Acc.	Inc.	Acc.	Inc.	Acc.	Inc.	Acc.	Inc.
1	3.9	3.9	3.7	3.7	3.4	3.4	3.1	3.1	2.7	2.7
2	5.7	1.8	5.4	1.7	5.1	1.7	4.5	1.4	4.0	1.3
3	6.9	1.2	6.7	1.3	6.2	1.1	5.6	1.1	5.0	1.0
4	8.0	1.1	7.7	1.0	7.2	1.0	6.5	0.9	5.8	0.8
5	9.0	1.0	8.7	1.0	8.2	1.0	7.4	0.9	6.6	0.8
6	9.9	0.9	9.6	0.9	9.1	0.9	8.2	0.8	7.4	0.8
7	10.8	0.9	10.5	0.9	9.9	0.8	8.9	0.7	8.1	0.7
8	11.6	0.8	11.3	0.8	10.7	0.8	9.6	0.7	8.7	0.6
9	12.4	0.8	12.0	0.7	11.4	0.7	10.2	0.6	9.3	0.6
10	13.1	0.7	12.7	0.7	12.0	0.6	10.8	0.6	9.9	0.6
11	13.7	0.6	13.3	0.6	12.6	0.6	11.3	0.5	10.4	0.5
12	14.2	0.5	13.9	0.6	13.1	0.5	11.8	0.5	10.8	0.4
13	14.7	0.5	14.4	0.5	13.5	0.4	12.2	0.4	11.1	0.3
14	15.2	0.5	14.8	0.4	13.9	0.4	12.6	0.4	11.4	0.3
15	15.6	0.4	15.2	0.4	14.2	0.3	12.9	0.3	11.7	0.3
16	15.9	0.3	15.5	0.3	14.5	0.3	13.2	0.3	12.0	0.3
17	16.2	0.3	15.8	0.3	14.8	0.3	13.4	0.2	12.2	0.2
18	16.4	0.2	16.0	0.2	15.1	0.3	13.6	0.2	12.4	0.2
19	16.6	0.2	16.3	0.3	15.3	0.2	13.8	0.2	12.6	0.2
20	16.8	0.2	16.5	0.2	15.5	0.2	14.0	0.2	12.8	0.2
21	17.0	0.2	16.7	0.2	15.7	0.2	14.2	0.2	13.0	0.2
22	17.2	0.2	16.9	0.2	15.9	0.2	14.4	0.2	13.2	0.2
23	17.4	0.2	17.1	0.2	16.1	0.2	14.5	0.1	13.3	0.1
24	17.5	0.1	17.2	0.1	16.3	0.2	14.6	0.1	13.4	0.1
25	17.6	0.1	17.3	0.1	16.4	0.1	14.7	0.1	13.5	0.1

TABLE VIII(Cont.)

Durations Hours	100 sq.mi.		124 sq.mi.		200 sq.mi.		500 sq.mi.		1000 sq.mi.	
	Acc.	Inc.	Acc.	Inc.	Acc.	Inc.	Acc.	Inc.	Acc.	Inc.
26	17.7	0.1	17.4	0.1	16.5	0.1	14.8	0.1	13.6	0.1
27	17.8	0.1	17.5	0.1	16.5	0.0	14.9	0.1	13.7	0.1
28	17.8	0.0	17.5	0.0	16.6	0.1	15.0	0.1	13.8	0.1
29	17.9	0.1	17.5	0.0	16.6	0.0	15.1	0.1	13.9	0.1
30	17.9	0.0	17.6	0.1	16.6	0.0	15.1	0.0	14.0	0.1
31	17.9	0.0	17.6	0.0	16.6	0.0	15.2	0.1	14.1	0.1
32	17.9	0.0	17.6	0.0	16.7	0.1	15.3	0.1	14.2	0.1
33	18.0	0.1	17.6	0.0	16.7	0.0	15.3	0.0	14.3	0.1
34	18.0	0.0	17.6	0.0	16.7	0.0	15.4	0.1	14.3	0.0
35	18.0	0.0	17.6	0.0	16.7	0.0	15.4	0.0	14.4	0.1
36	18.0	0.0	17.6	0.0	16.7	0.0	15.4	0.0	14.4	0.0
37	18.0	0.0	17.6	0.0	16.8	0.1	15.5	0.1	14.4	0.0
38	18.0	0.0	17.6	0.0	16.8	0.0	15.5	0.0	14.5	0.1
39	18.0	0.0	17.6	0.0	16.8	0.0	15.6	0.1	14.5	0.0
40	18.0	0.0	17.6	0.0	16.8	0.0	15.6	0.0	14.5	0.0
41	18.0	0.0	17.6	0.0	16.8	0.0	15.6	0.0	14.5	0.0
42	18.0	0.0	17.6	0.0	16.8	0.0	15.6	0.0	14.6	0.1
43	18.0	0.0	17.6	0.0	16.8	0.0	15.6	0.0	14.6	0.0
44	18.0	0.0	17.6	0.0	16.8	0.0	15.6	0.0	14.6	0.0
45	18.0	0.0	17.6	0.0	16.8	0.0	15.6	0.0	14.6	0.0
46	18.0	0.0	17.6	0.0	16.8	0.0	15.6	0.0	14.6	0.0
47	18.0	0.0	17.6	0.0	16.8	0.0	15.6	0.0	14.7	0.1
48	18.0	0.0	17.6	0.0	16.8	0.0	15.6	0.0	14.7	0.0

APPENDIX

INDEX TO APPENDIX

SYMBOLS USED ON SYNOPTIC CHARTS

(Maps and charts arranged in chronological order as indicated below)

Horizontal Cross Sections (Fixed Level Charts)
3 Km. above Sea Level, March 12 to March 21, 1936.
5 Km. above Sea Level, March 12 to March 21, 1936.

Cross Sections Through the Atmosphere
Oklahoma City to Lakehurst, March 17, 1936.
San Antonio to Lakehurst, March 17, 1936.

SYMBOLS USED ON SYNOPTIC CHARTS

TEMPERATURE

TEMPERATURE at time of observation is shown at *right* of station circle, thus: 72

WEATHER

WEATHER at time of observation is shown at *left* of station circle thus: 32 *(Snow)*

- • *Rain*
- ❟ *Drizzle*
- △ *Sleet*
- ▲ *Hail*
- ✱ *Snow*

} *Number of symbols indicates relative intensity of precipitation*

- *Rain* } *Showers*
- *Snow* }
- = *Light to Moderate Fog*
- ≡ *Dense Fog*
- ≝ *Ground Fog*

PAST WEATHER is shown near, and generally at *left* of station circle, thus: 78 *(Thunderstorm within last 12 hours)*

SKY

SKY COVERING is shown *within* the station circle, thus: ○ ◔ ◑ ◕ ●

(Amount of circle shaded indicates approximate amount of sky covered by clouds)

WIND

DIRECTION AND FORCE OF WIND is shown by the **BEAUFORT** symbol, projecting from the station circle. In this symbol, only the shaft and one side of the tail of the arrow are shown; the arrow flies with the wind. The number of barbs and half-barbs on arrow-tail indicates wind force as shown in the following table:

BEAUFORT SCALE AND SYMBOLS

FORCE	M. P. H.	SYMBOL	WIND
0	Less than 1	○	*Calm*
1	1 to 3		*Light*
2	4 to 7		
3	8 to 12		*Gentle*
4	13 to 18		*Moderate*
5	19 to 24		*Fresh*
6	25 to 31		*Strong*
7	32 to 38		
8	39 to 46		*Gale*
9	47 to 54		
10	55 to 63		*Whole Gale*
11	64 to 75		
12	Over 75		*Hurricane*

MAXIMUM WIND VELOCITY (M. P. H.) within last 12 hours, and **DIRECTION**, are shown in parenthesis below the station circle, thus: 72 (↘60)

54 (↘62)

A TYPICAL STATION with symbol designations would appear as in the accompanying diagram:

FIGURE A-1

UPPER FRONTS

SURFACE FRONTS

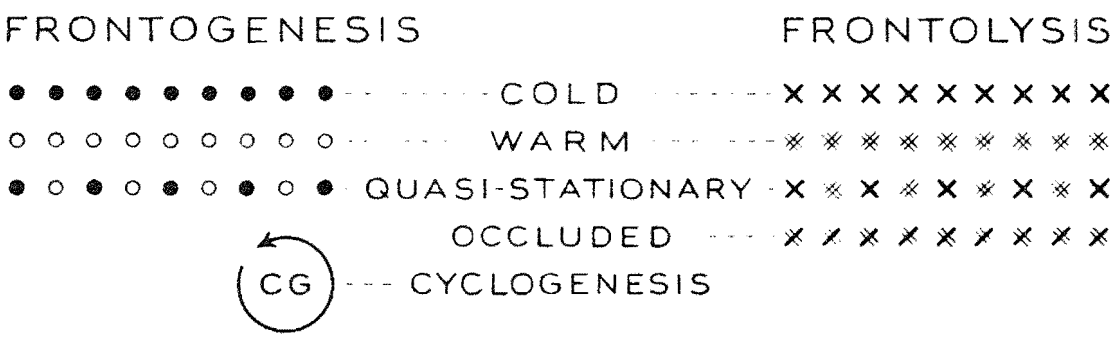

AIR MASSES *

cAw - CONTINENTAL ARCTIC AIR, warmer than the surface over which it lies *(stable in the lower layers).*

cAk - CONTINENTAL ARCTIC AIR, colder than the surface over which it is passing *(steep lapse rate in the lower layers)*

mAk MARITIME ARCTIC AIR, colder than the surface over which it is passing *(steep lapse rate).*

cPw - CONTINENTAL POLAR AIR, warmer than the surface over which it is passing *(stable in the lower layers).*

cPk - CONTINENTAL POLAR AIR, colder than the surface over which it is passing *(steep lapse rate).*

mPw - MARITIME POLAR AIR, warmer than the surface over which it is passing *(stable in the lower layers).*

mPk - MARITIME POLAR AIR, colder than the surface over which it is passing *(steep lapse rate).*

mTw - MARITIME TROPICAL AIR, warmer than the surface over which it is passing *(stable in the lower layers).*

mTk - MARITIME TROPICAL AIR, colder than the surface over which it lies or is passing *(steep lapse rate).*

S --- SUPERIOR AIR, which includes all air masses that appear warm and very dry because of, principally, subsidence and divergence.

** SEE MONTHLY WEATHER REVIEW, VOL. 67, JULY 1939, pp. 204-218.*

FIGURE A-2

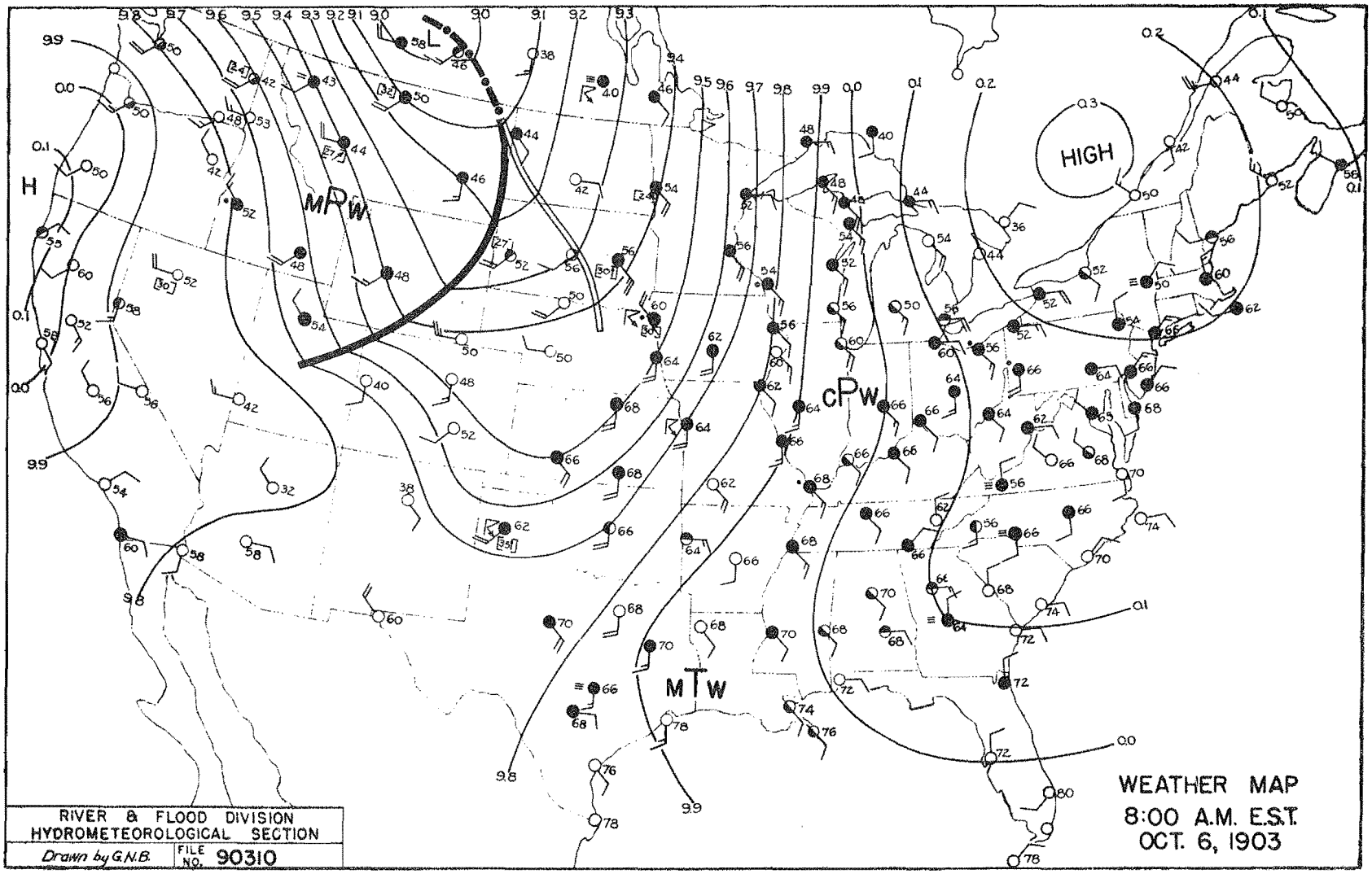
H
mPw
cPw
mTw
HIGH
L
WEATHER MAP
8:00 A.M. E.S.T.
OCT. 6, 1903
RIVER & FLOOD DIVISION
HYDROMETEOROLOGICAL SECTION
Drawn by G.N.B.
FILE NO. 90310

FIGURE A-3

FIGURE A-4

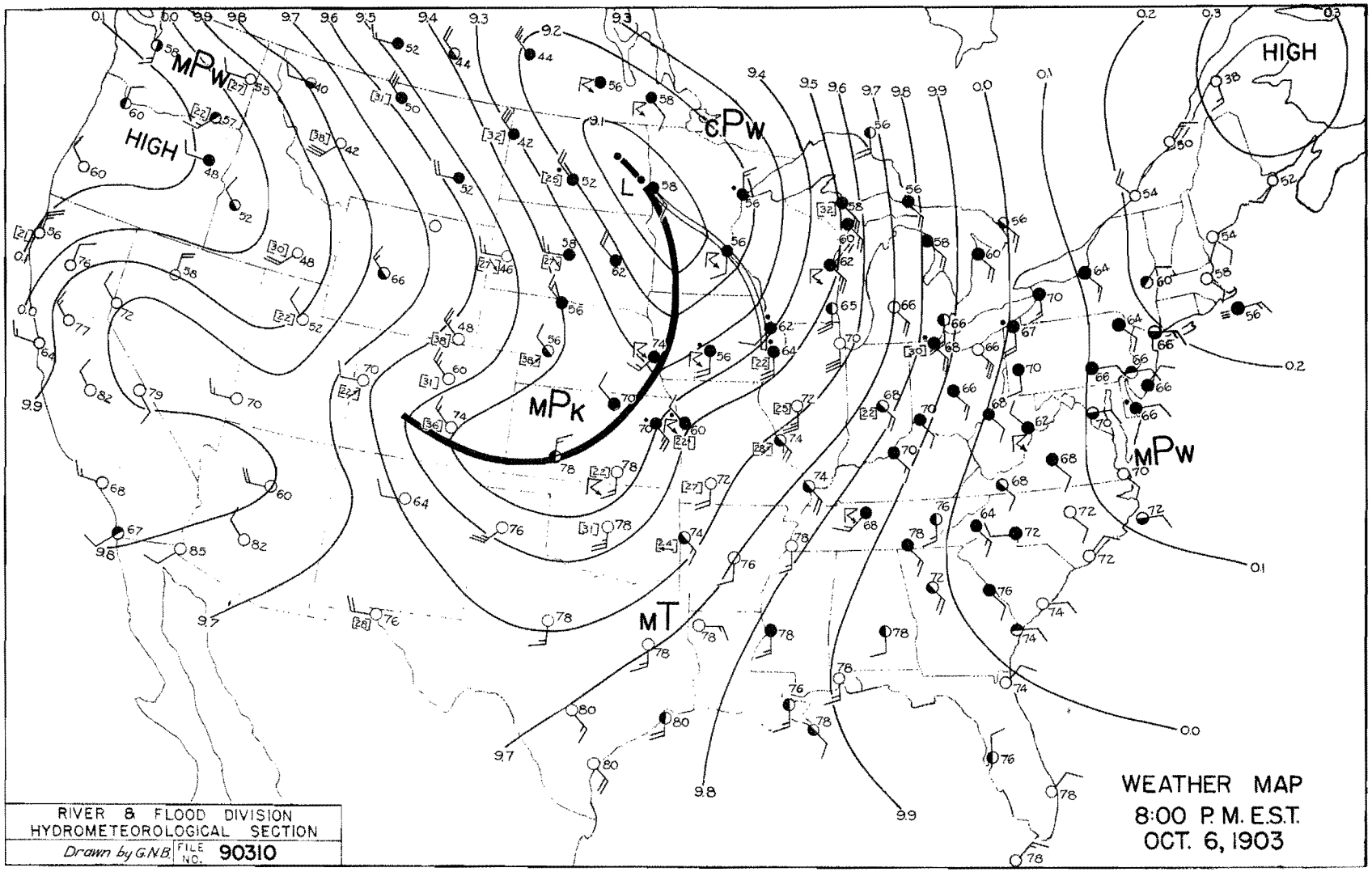
mPw
HIGH
cPw
L
mPk
mT
mPw
HIGH
WEATHER MAP
8:00 P.M. E.S.T.
OCT. 6, 1903
RIVER & FLOOD DIVISION
HYDROMETEOROLOGICAL SECTION
Drawn by G.N.B.
FILE NO. 90310

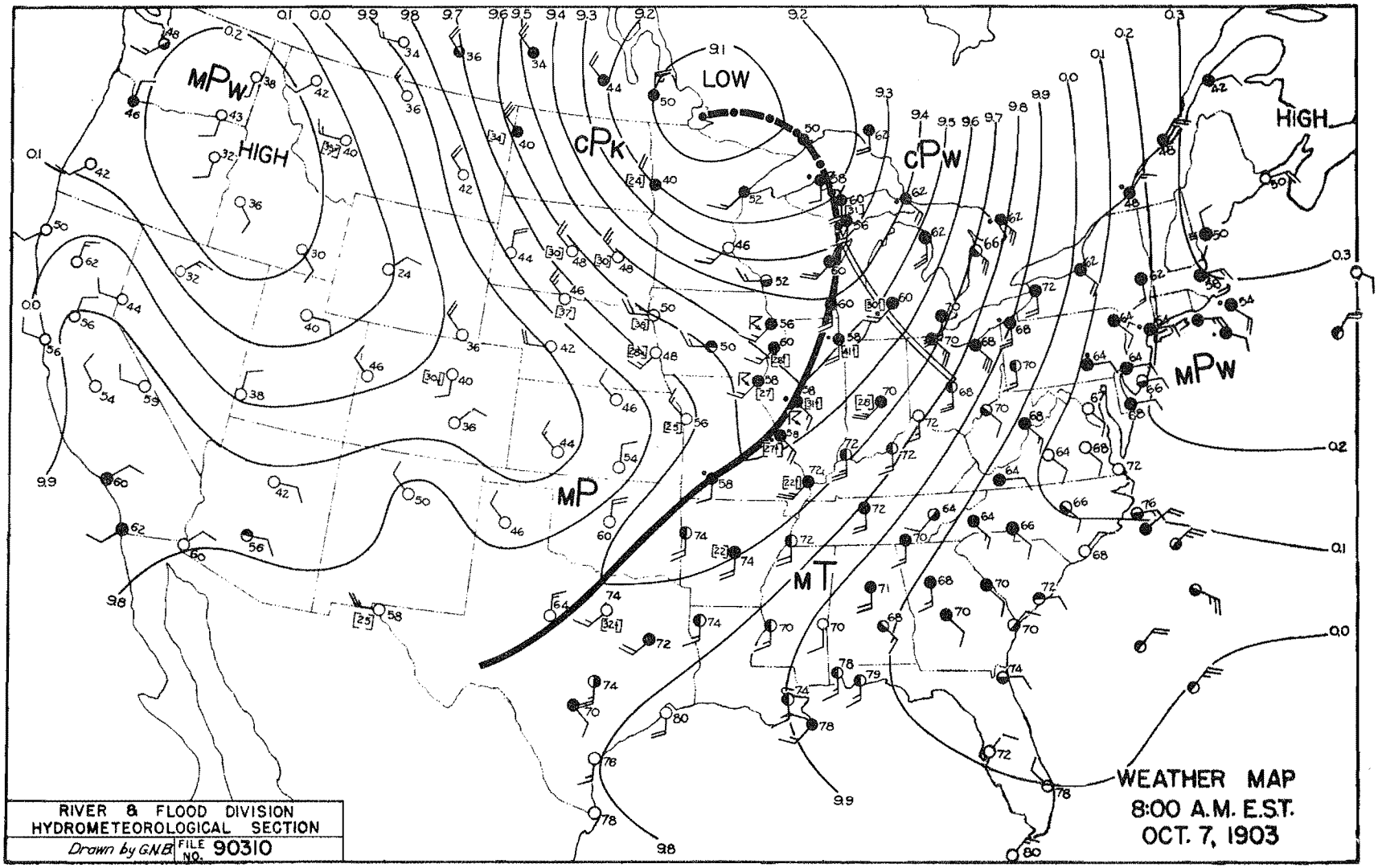
mPw
HIGH
cPk
LOW
cPw
HIGH
mPw
mP
mT
WEATHER MAP
8:00 A.M. E.S.T.
OCT. 7, 1903
RIVER & FLOOD DIVISION
HYDROMETEOROLOGICAL SECTION
Drawn by GNB
FILE NO. 90310

FIGURE A-5

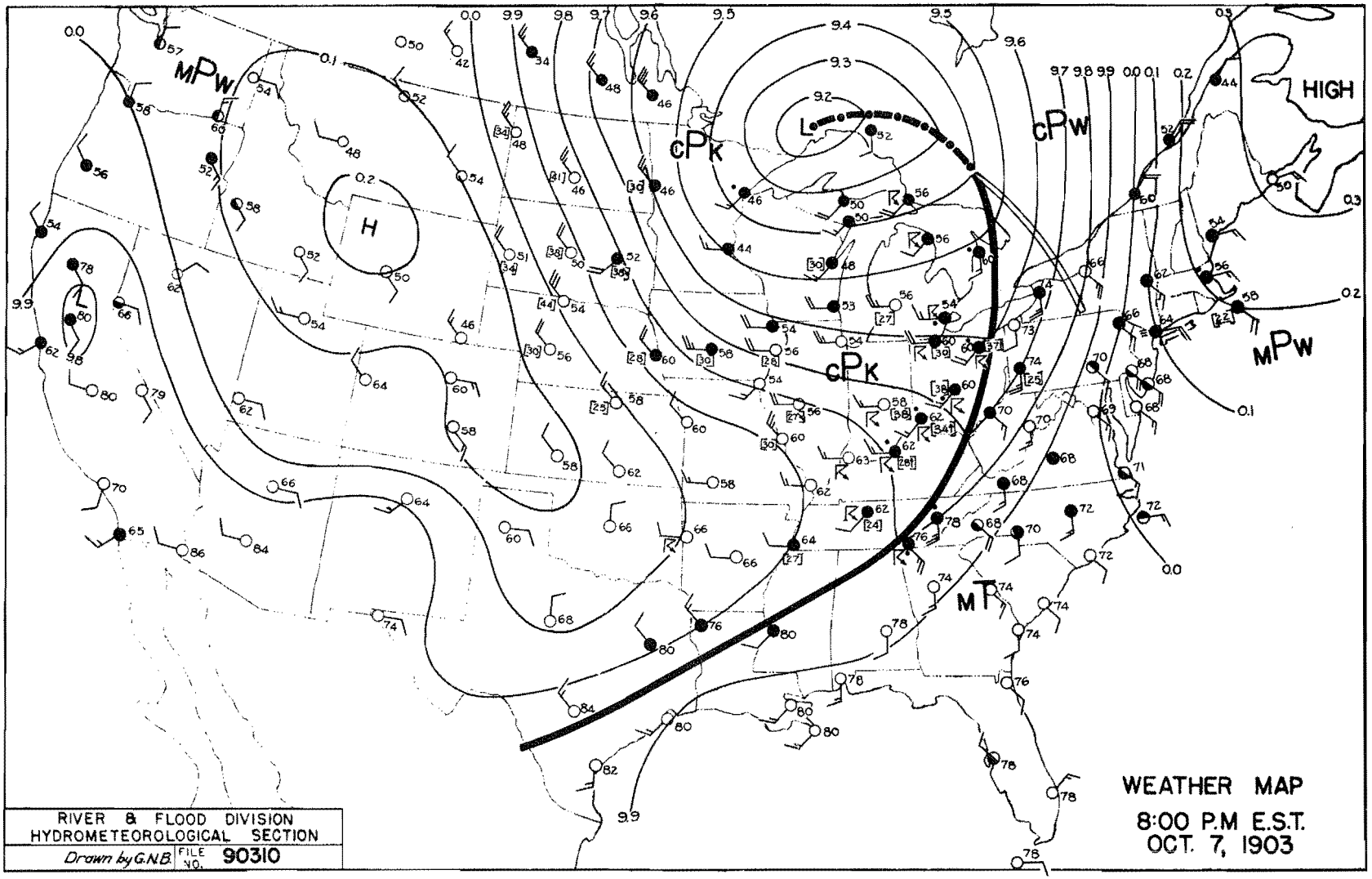
mPw
cPk
cPw
H
L
HIGH
mT
WEATHER MAP
8:00 P.M E.S.T.
OCT. 7, 1903
RIVER & FLOOD DIVISION
HYDROMETEOROLOGICAL SECTION
Drawn by G.N.B.
FILE NO. 90310

FIGURE A-6

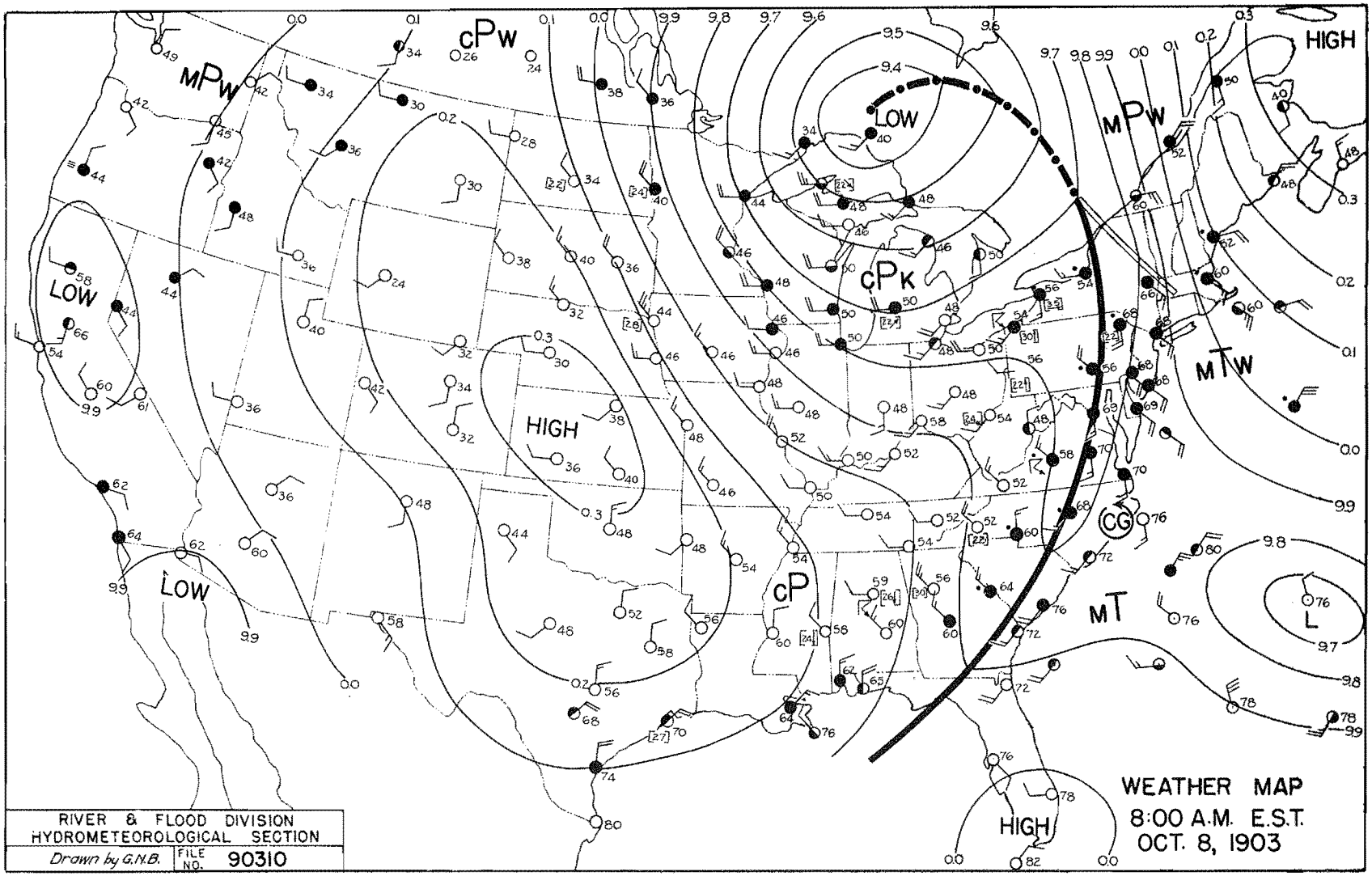
cPw
mPw
LOW
HIGH
cPk
mPw
HIGH
LOW
LOW
mTw
HIGH
cP
CG
mT
L
HIGH
WEATHER MAP
8:00 A.M. E.S.T.
OCT. 8, 1903
RIVER & FLOOD DIVISION
HYDROMETEOROLOGICAL SECTION
Drawn by G.N.B.
FILE NO. 90310

FIGURE A-7

FIGURE A-8

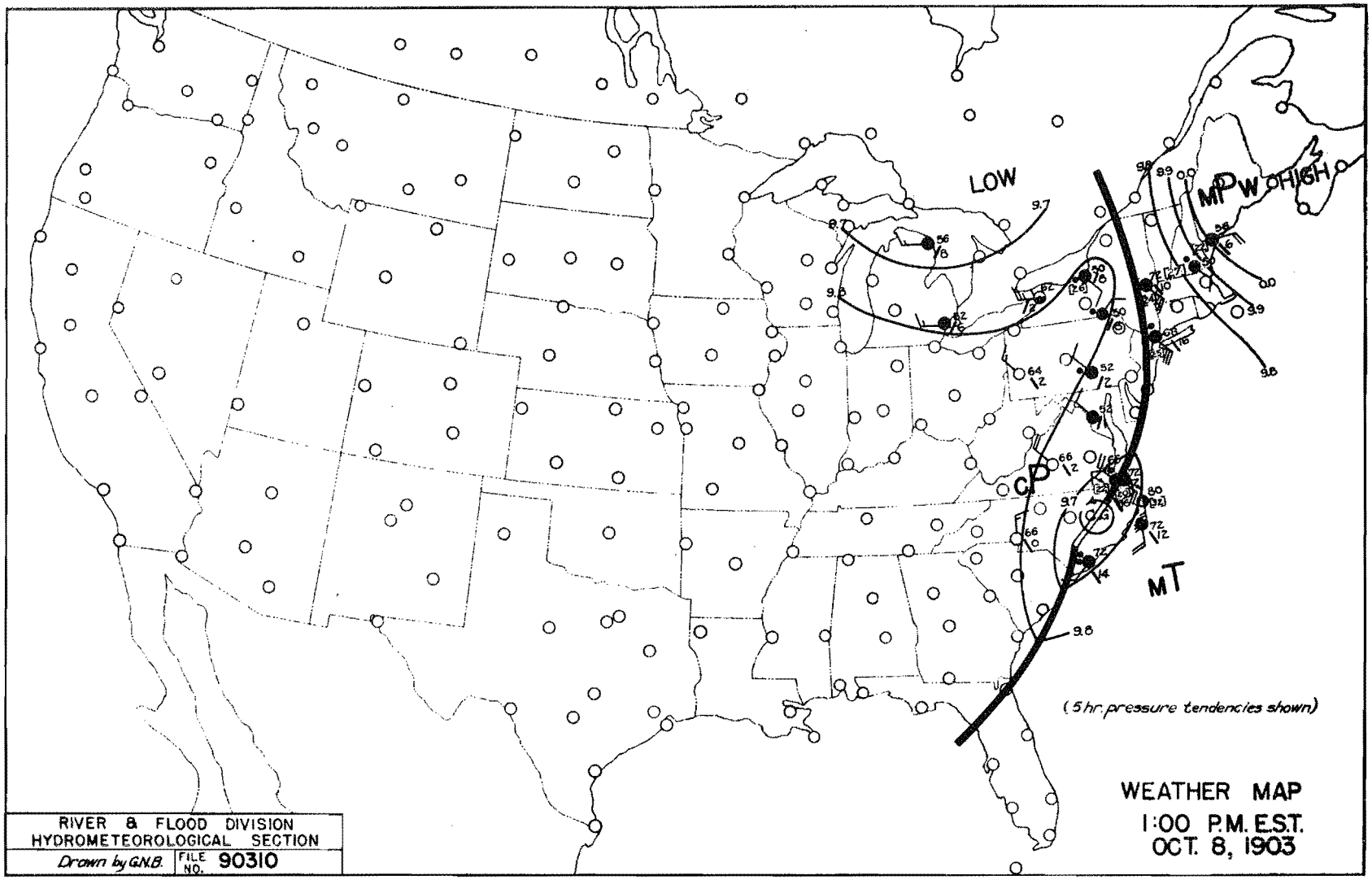
LOW
MPW HIGH
CP
MT
9.7
9.8
9.9
10.0
(5 hr. pressure tendencies shown)
WEATHER MAP
1:00 P.M. E.S.T.
OCT. 8, 1903
RIVER & FLOOD DIVISION
HYDROMETEOROLOGICAL SECTION
Drawn by G.N.B.
FILE NO. 90310

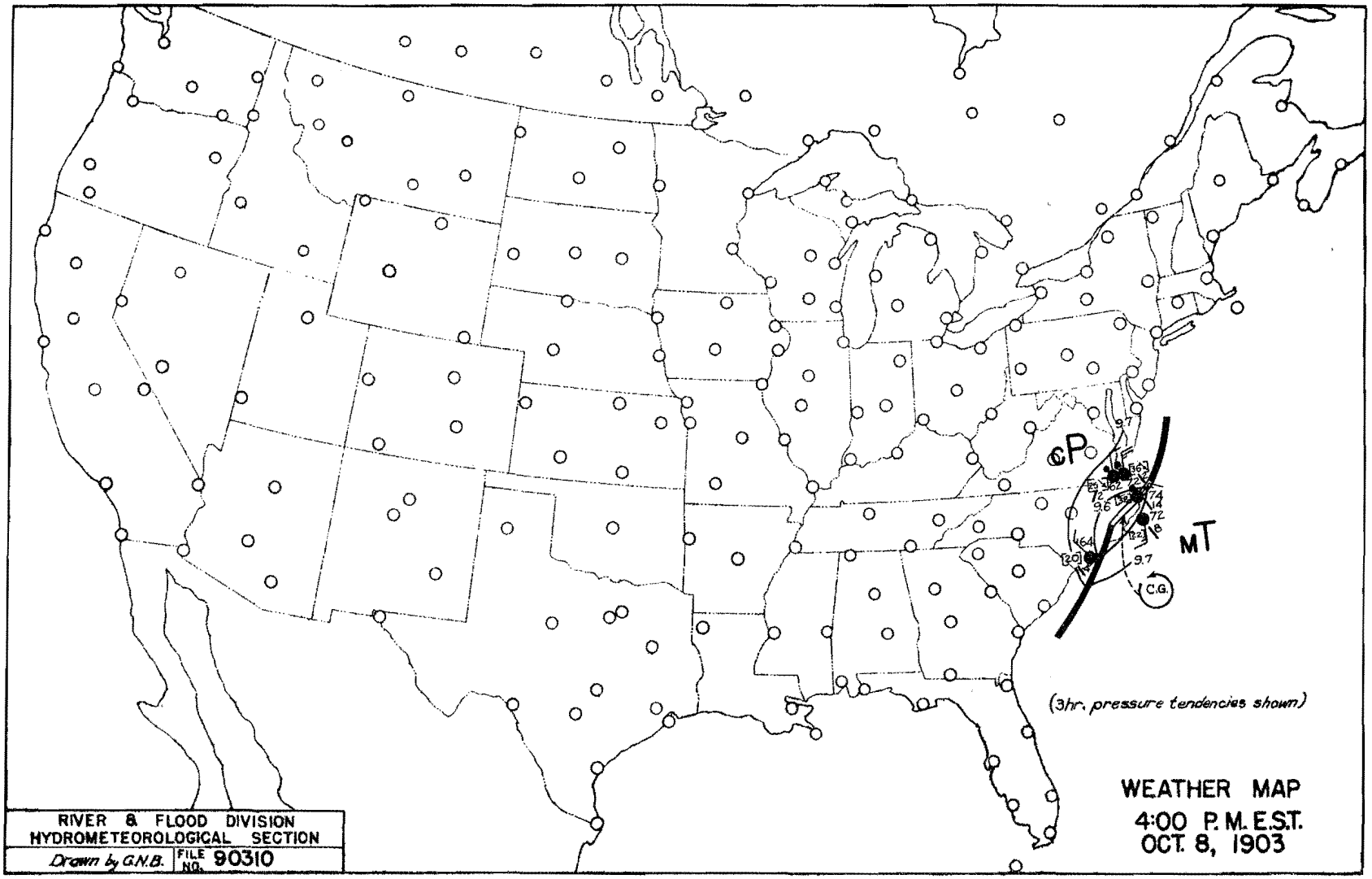
cP
mT
9.7
9.6
9.7
C.G.
(3hr. pressure tendencies shown)
WEATHER MAP
4:00 P.M. E.S.T.
OCT. 8, 1903
RIVER & FLOOD DIVISION
HYDROMETEOROLOGICAL SECTION
Drawn by G.N.B.
FILE NO. 90310

FIGURE A-9

FIGURE A-10

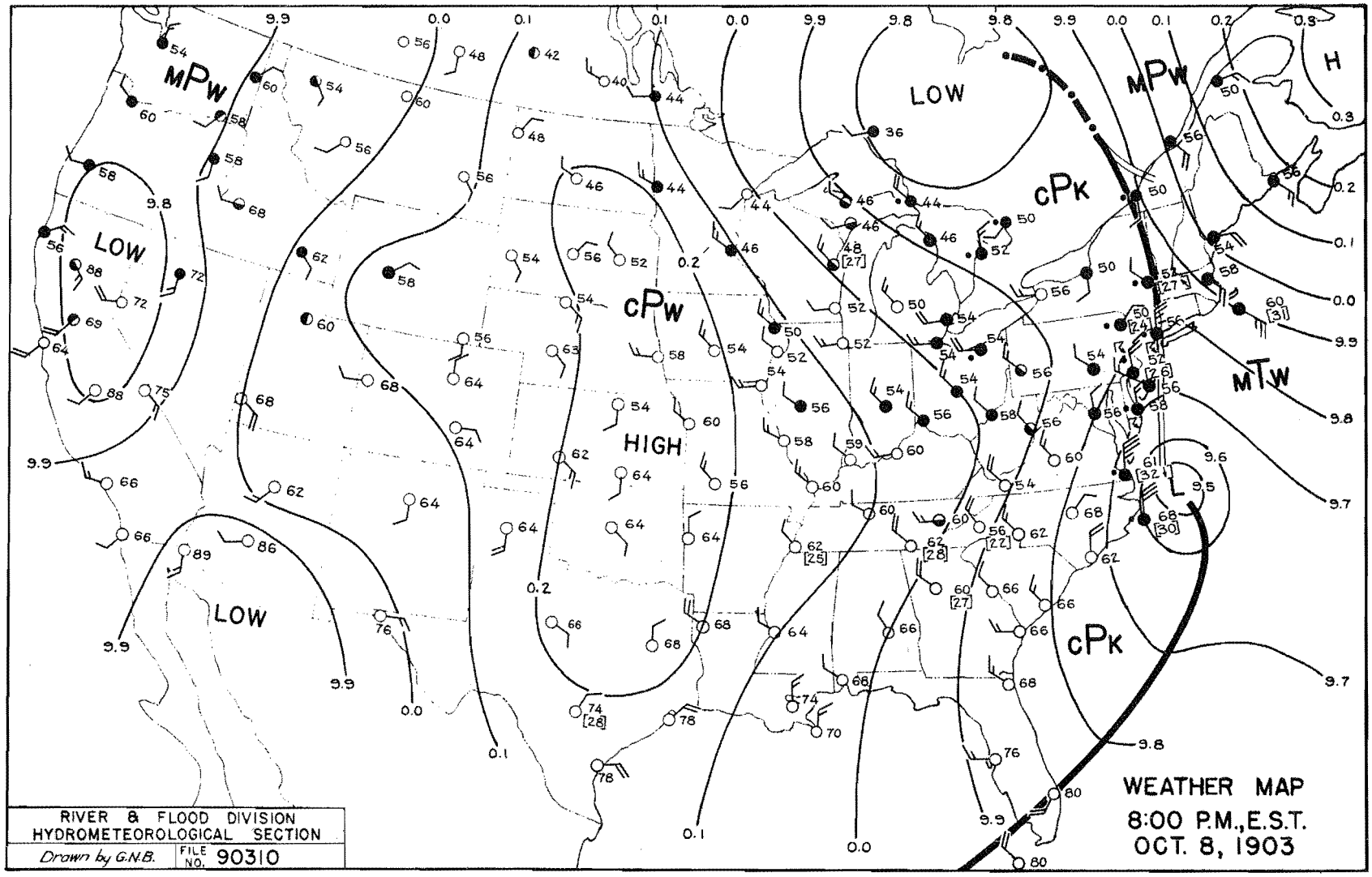
mPw
LOW
cPw
HIGH
LOW
LOW
cPk
mPw
H
cPk
mTw
L
WEATHER MAP
8:00 P.M., E.S.T.
OCT. 8, 1903
RIVER & FLOOD DIVISION
HYDROMETEOROLOGICAL SECTION
Drawn by G.N.B.
FILE NO. 90310

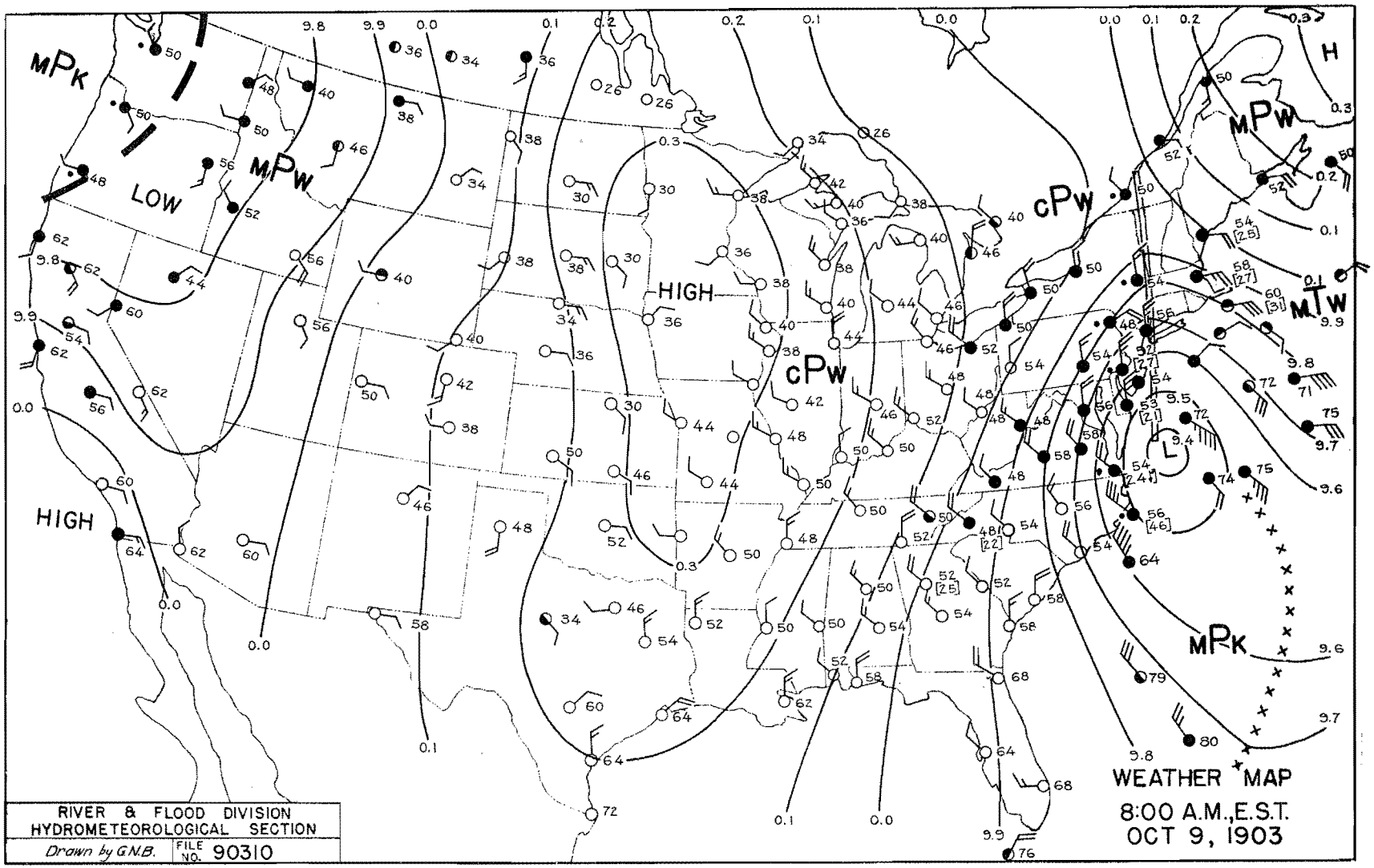
mPK
LOW
mPW
HIGH
cPW
cPW
mPW
H
mTW
HIGH
mPK
L
WEATHER MAP
8:00 A.M.,E.S.T.
OCT 9, 1903
RIVER & FLOOD DIVISION
HYDROMETEOROLOGICAL SECTION
Drawn by G.N.B.
FILE NO. 90310

FIGURE A-11

FIGURE A-12

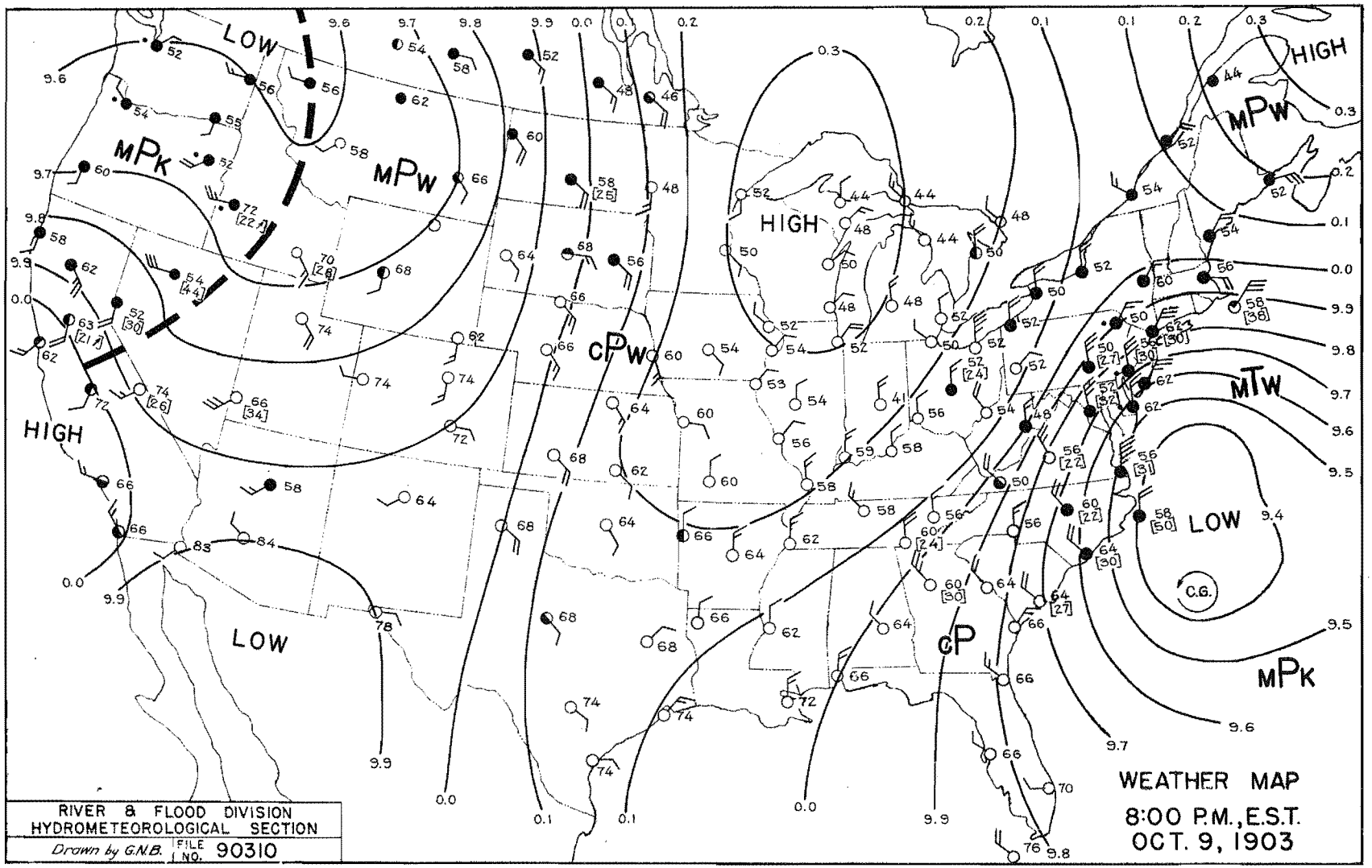
LOW
HIGH
HIGH
LOW
LOW
mPK
mPW
mPW
cPW
cP
mTW
mPK
C.G.
WEATHER MAP
8:00 P.M., E.S.T.
OCT. 9, 1903
RIVER & FLOOD DIVISION
HYDROMETEOROLOGICAL SECTION
Drawn by G.N.B.
FILE NO. 90310

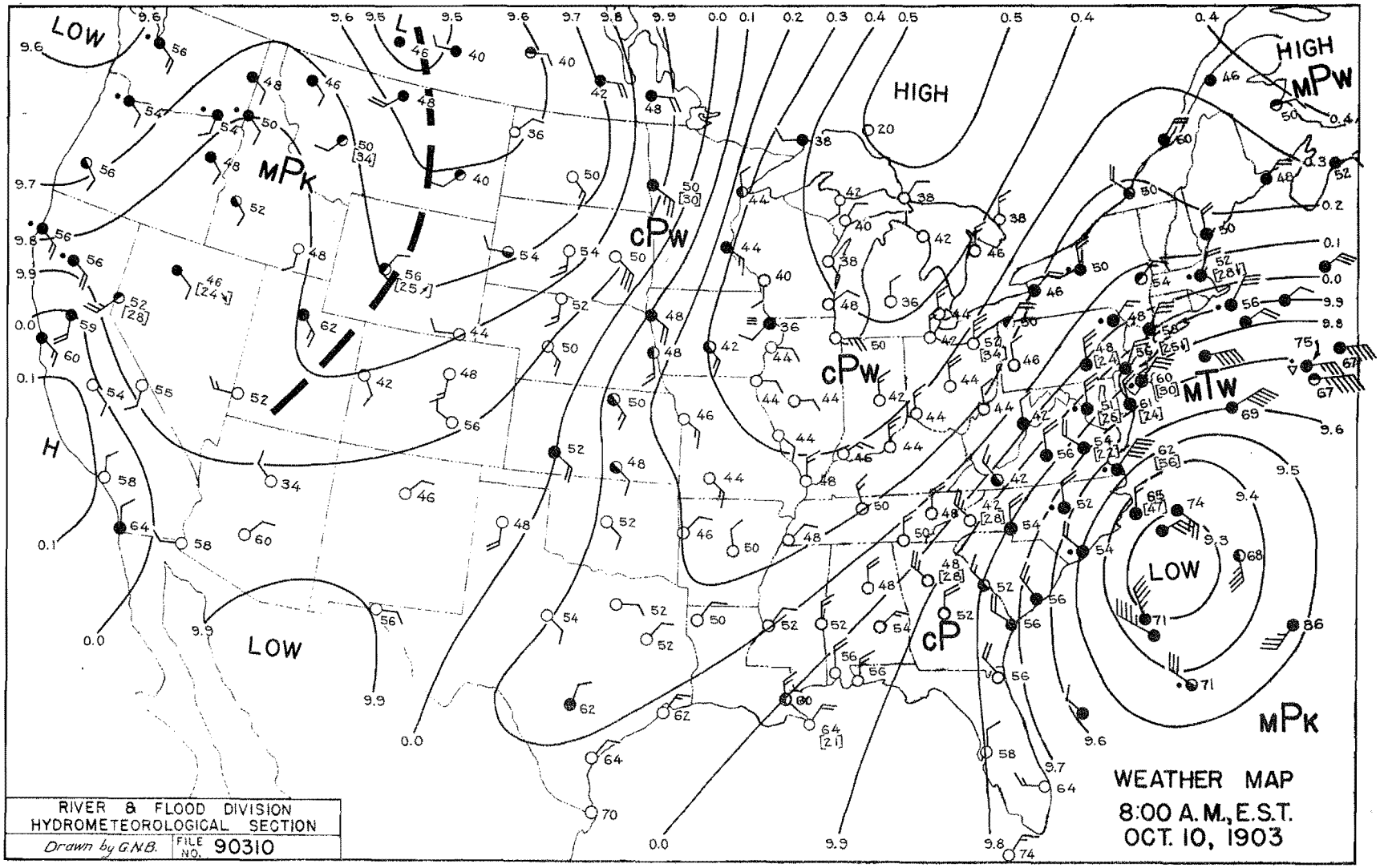
LOW
HIGH
mPK
cPW
HIGH
mPW
cPW
mTW
H
LOW
cP
LOW
mPK
WEATHER MAP
8:00 A.M., E.S.T.
OCT. 10, 1903
RIVER & FLOOD DIVISION
HYDROMETEOROLOGICAL SECTION
Drawn by G.N.B.
FILE NO. 90310

FIGURE A-13

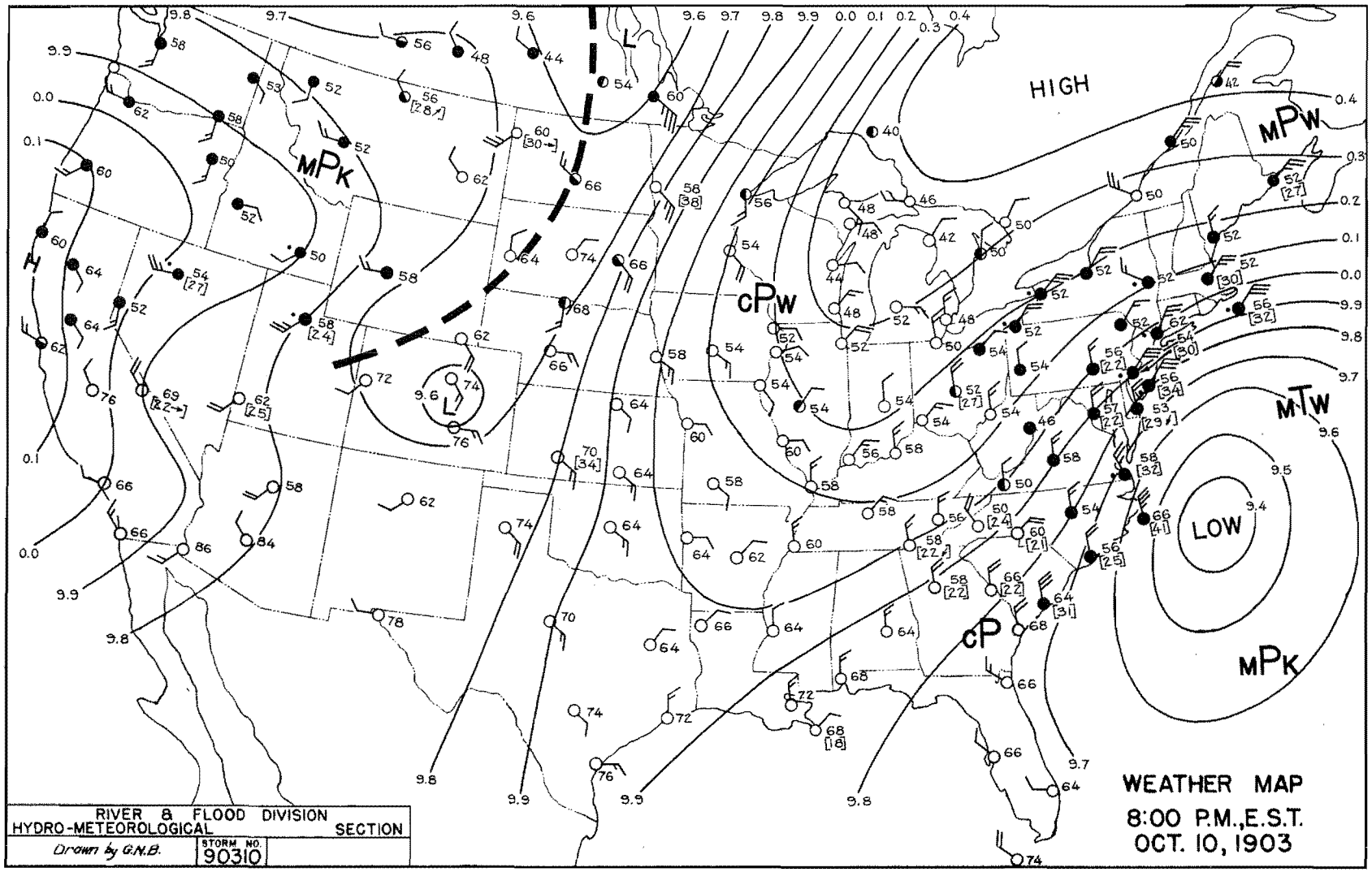
HIGH
LOW
mPw
mPk
cPw
mTw
cP
mPk
WEATHER MAP
8:00 P.M.,E.S.T.
OCT. 10, 1903
RIVER & FLOOD DIVISION
HYDRO-METEOROLOGICAL SECTION
Drawn by G.N.B.
STORM NO. 90310

FIGURE A-14

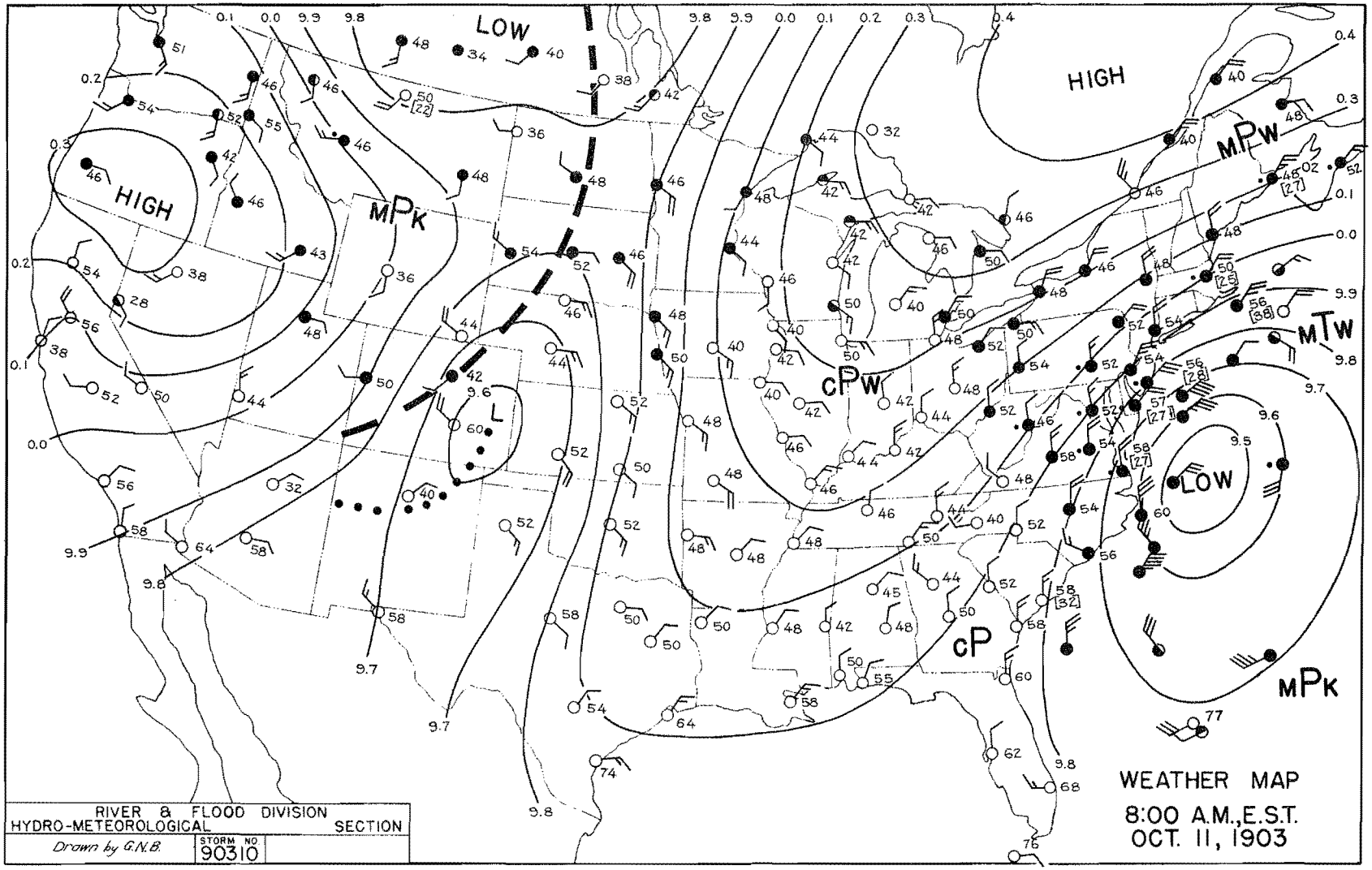
LOW
HIGH
HIGH
MPK
cPW
MPW
MTW
L
LOW
cP
MPK
WEATHER MAP
8:00 A.M.,E.S.T.
OCT. 11, 1903
RIVER & FLOOD DIVISION
HYDRO-METEOROLOGICAL SECTION
Drawn by G.N.B.
STORM NO
90310

FIGURE A-15

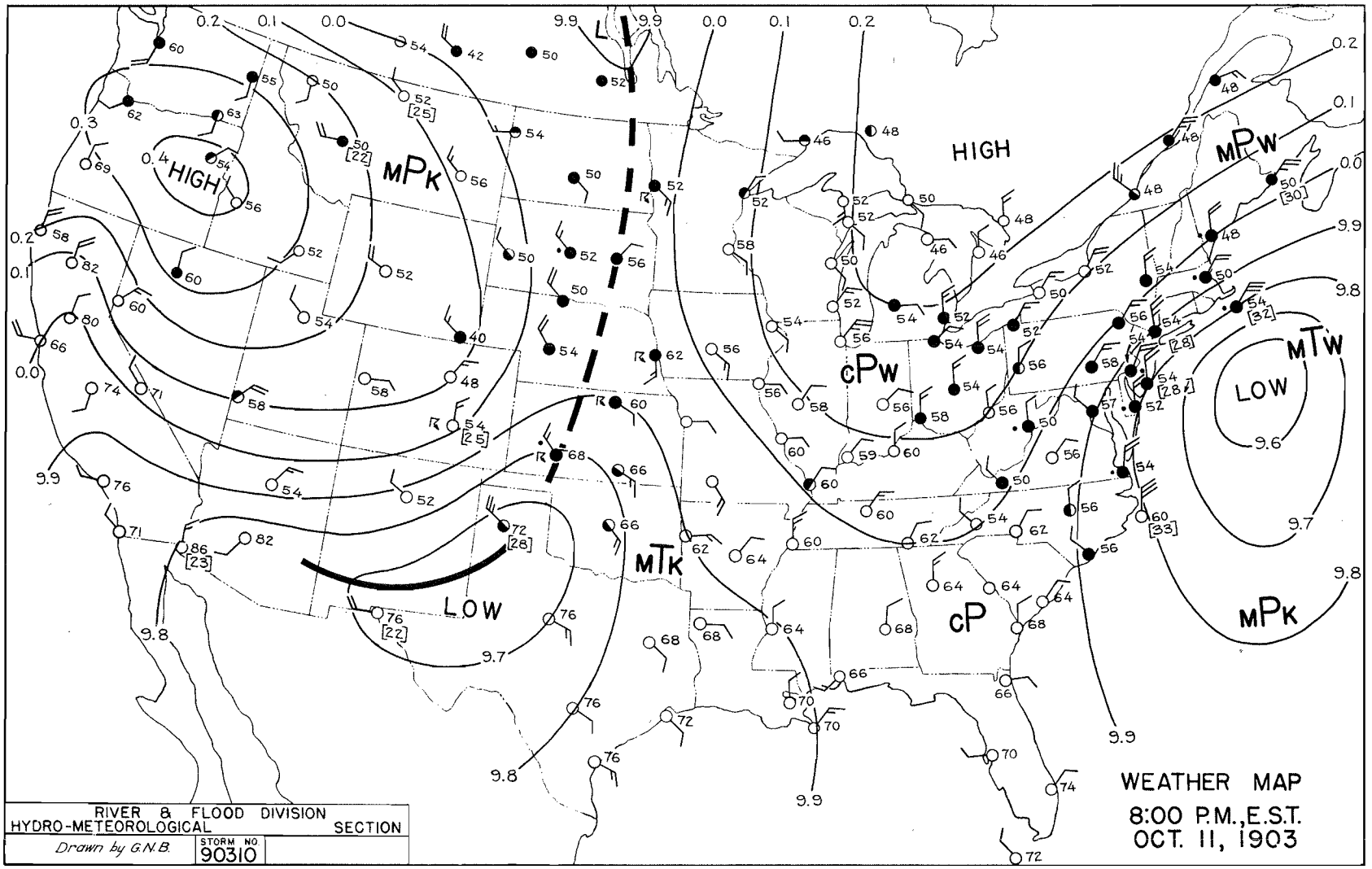
HIGH
mPK
HIGH
mPW
cPW
mTW
LOW
9.6
LOW
mTK
cP
mPK
9.9
9.8
9.7
WEATHER MAP
8:00 P.M., E.S.T.
OCT. 11, 1903
RIVER & FLOOD DIVISION
HYDRO-METEOROLOGICAL SECTION
Drawn by G.N.B.
STORM NO.
90310

FIGURE A-16

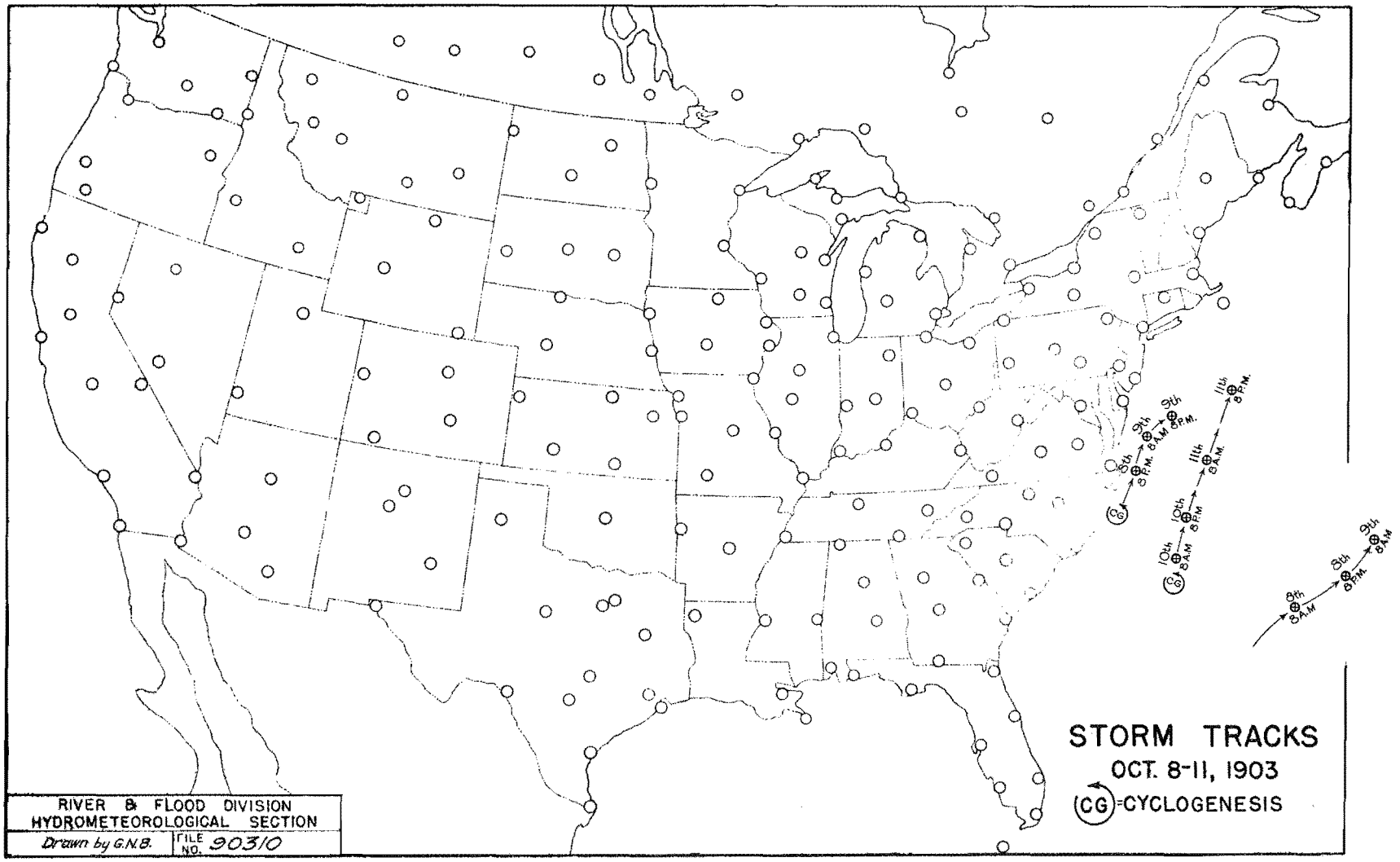
STORM TRACKS
OCT. 8-11, 1903
(CG)=CYCLOGENESIS
RIVER & FLOOD DIVISION
HYDROMETEOROLOGICAL SECTION
Drawn by G.N.B.
FILE NO. 9031O
CG
8th 8 P.M.
9th 8 A.M.
9th 8 P.M.
10th 8 A.M.
10th 8 P.M.
11th 8 A.M.
11th 8 P.M.
8th 8 A.M.
8th 8 P.M.
9th 8 A.M.

FIGURE A-17

FIGURE A-18

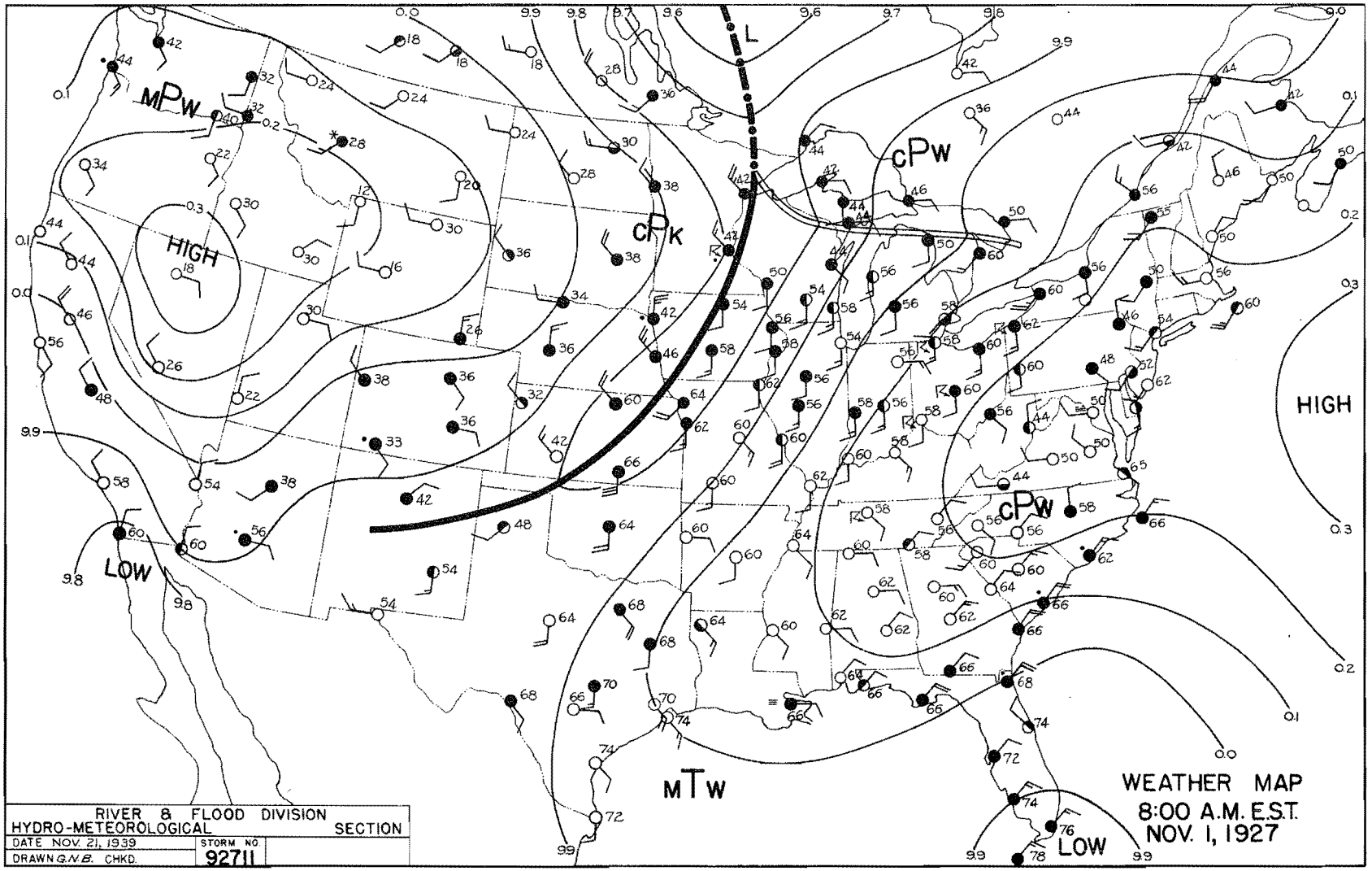
mPw
HIGH
cPk
L
cPw
cPw
HIGH
LOW
mTw
LOW
WEATHER MAP
8:00 A.M. E.S.T.
NOV. 1, 1927
RIVER & FLOOD DIVISION
HYDRO-METEOROLOGICAL SECTION
DATE NOV. 21, 1939
STORM NO. 92711
DRAWN G.V.B. CHKD.

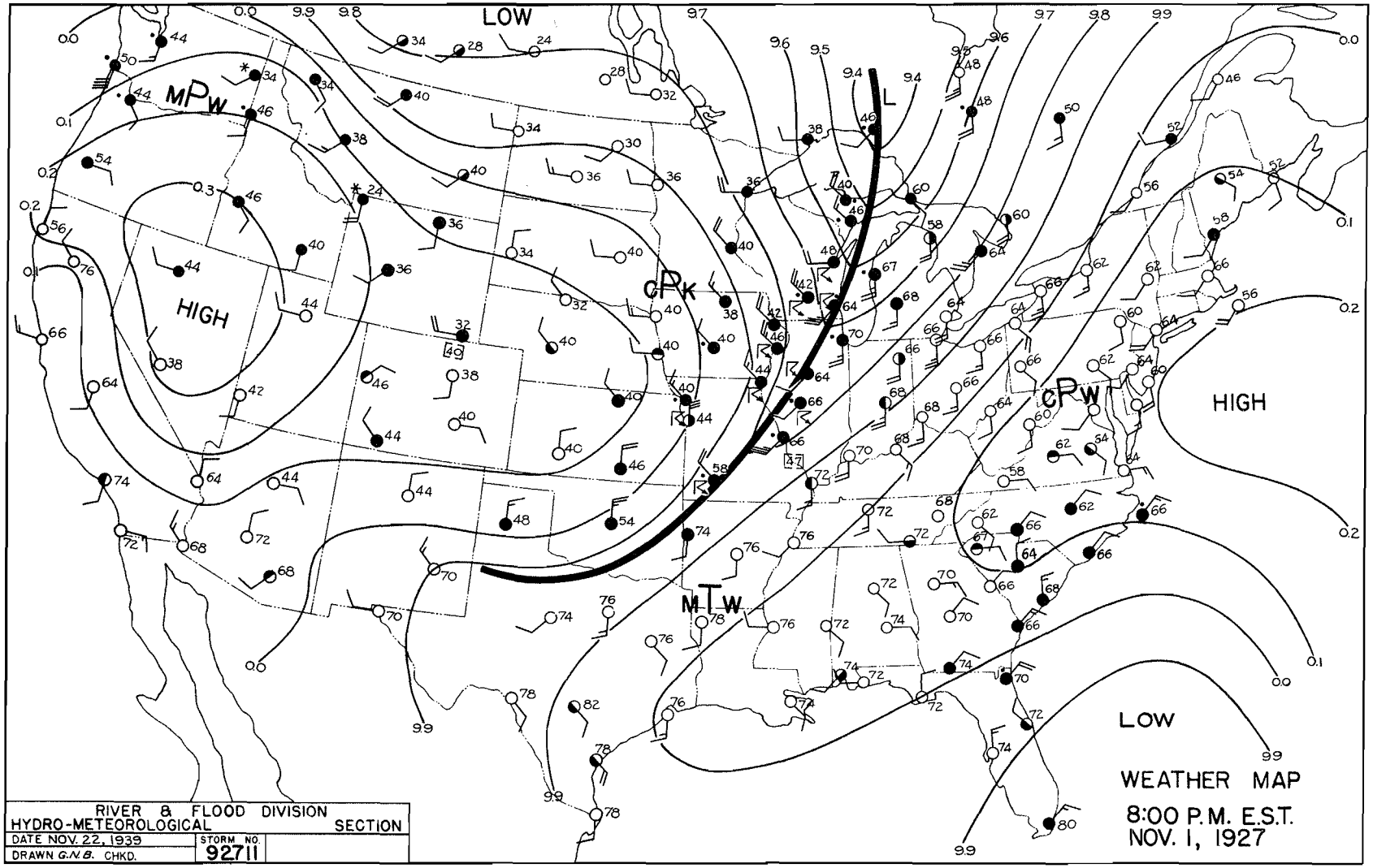
LOW
mPw
L
HIGH
cPk
cPw
HIGH
mTw
LOW
WEATHER MAP
8:00 P.M. E.S.T.
NOV. 1, 1927
RIVER & FLOOD DIVISION
HYDRO-METEOROLOGICAL SECTION
DATE NOV. 22, 1939
STORM NO. 92711
DRAWN G.N.B. CHKD.

FIGURE A-19

FIGURE A-20

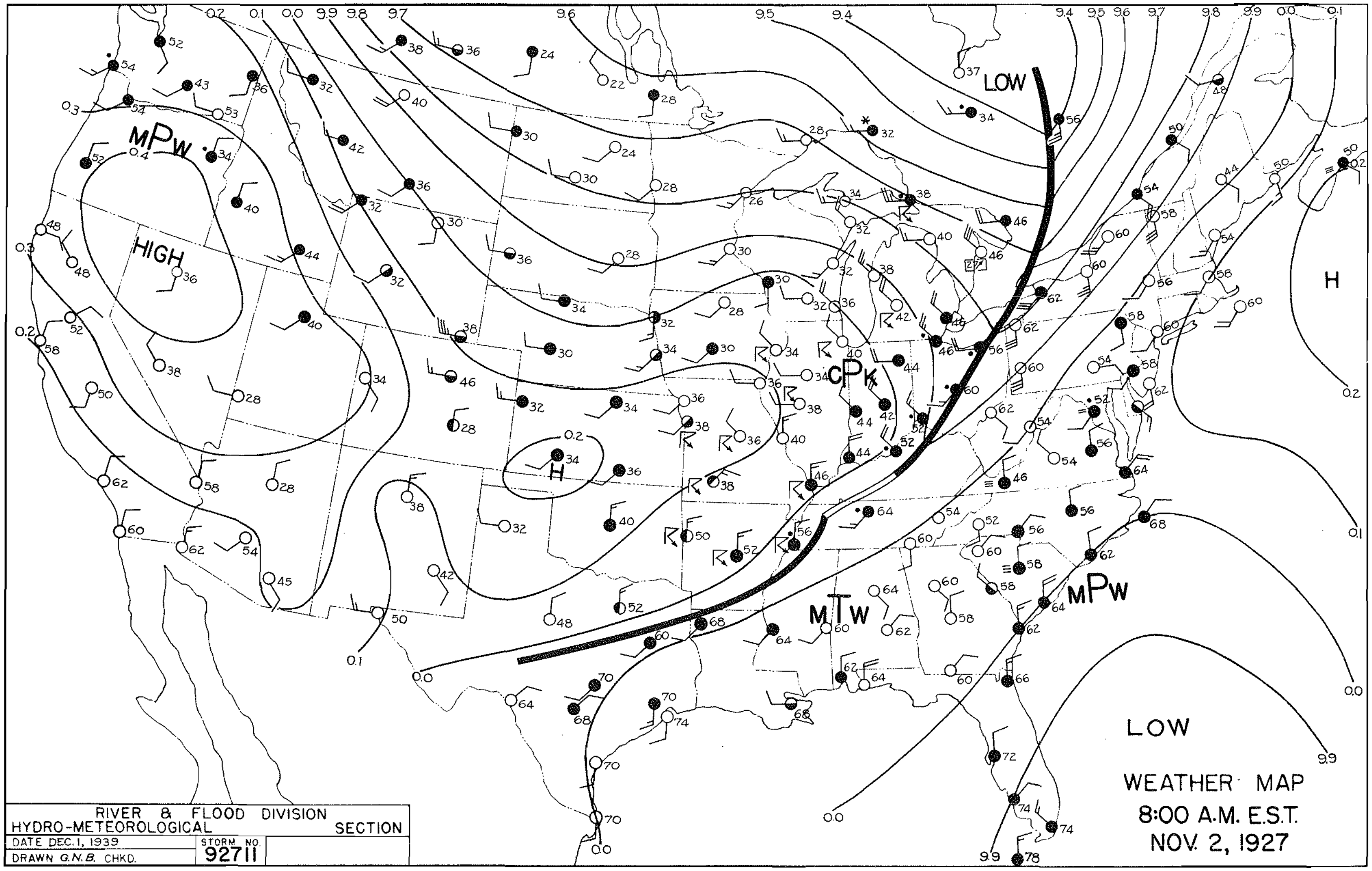

LOW
HIGH
H
mPw
cPk
mTw
mPw
LOW
H
RIVER & FLOOD DIVISION
HYDRO-METEOROLOGICAL SECTION
DATE DEC. 1, 1939
DRAWN G.N.B. CHKD.
STORM NO. 92711
WEATHER MAP
8:00 A.M. E.S.T.
NOV. 2, 1927

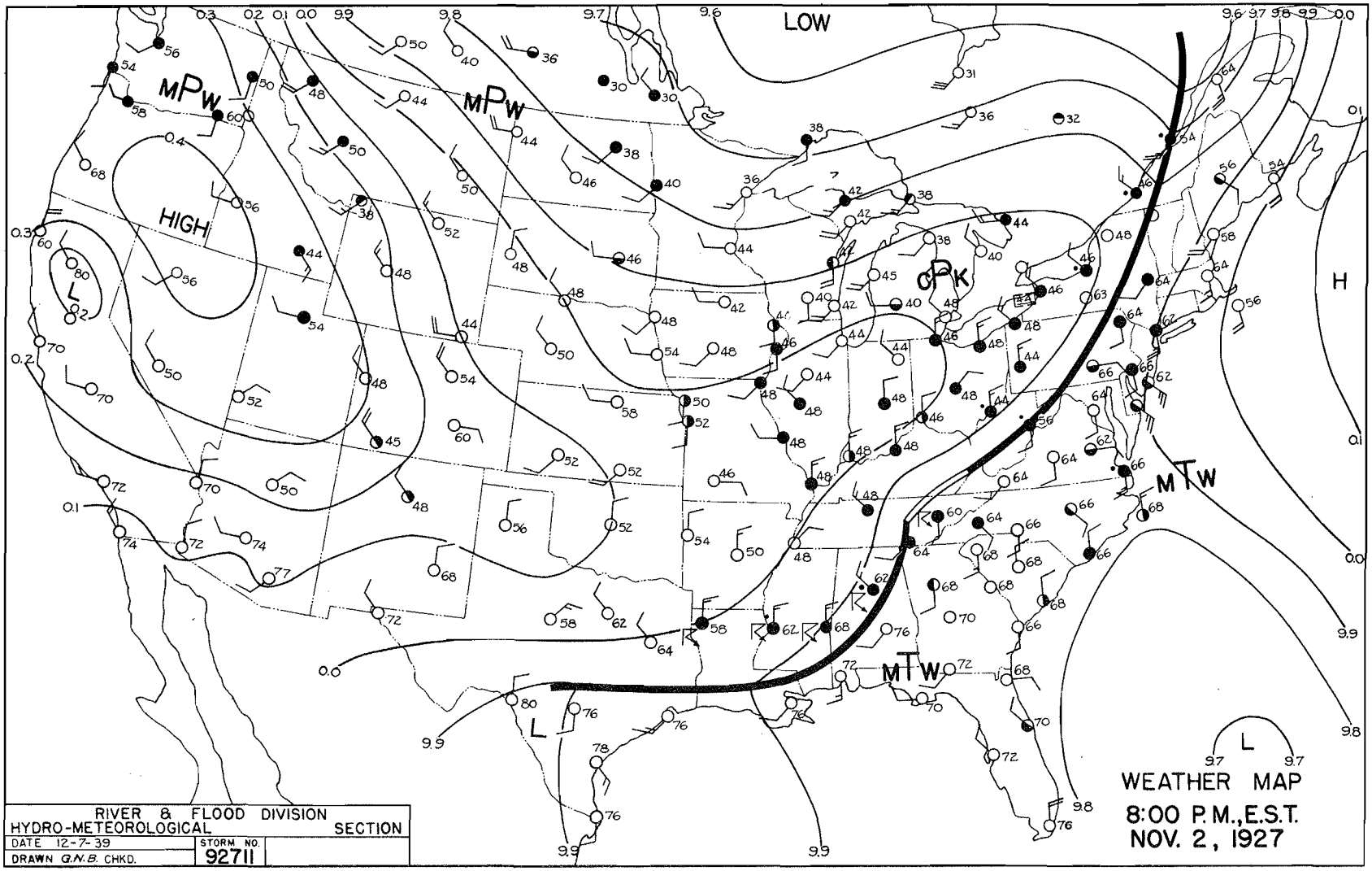
LOW
HIGH
mPw
mPw
cPk
mTw
mTw
L
L
H
WEATHER MAP
8:00 P.M., E.S.T.
NOV. 2, 1927
RIVER & FLOOD DIVISION
HYDRO-METEOROLOGICAL SECTION
DATE 12-7-39
STORM NO. 92711
DRAWN G.N.B. CHKD.

FIGURE A-21

FIGURE A-22

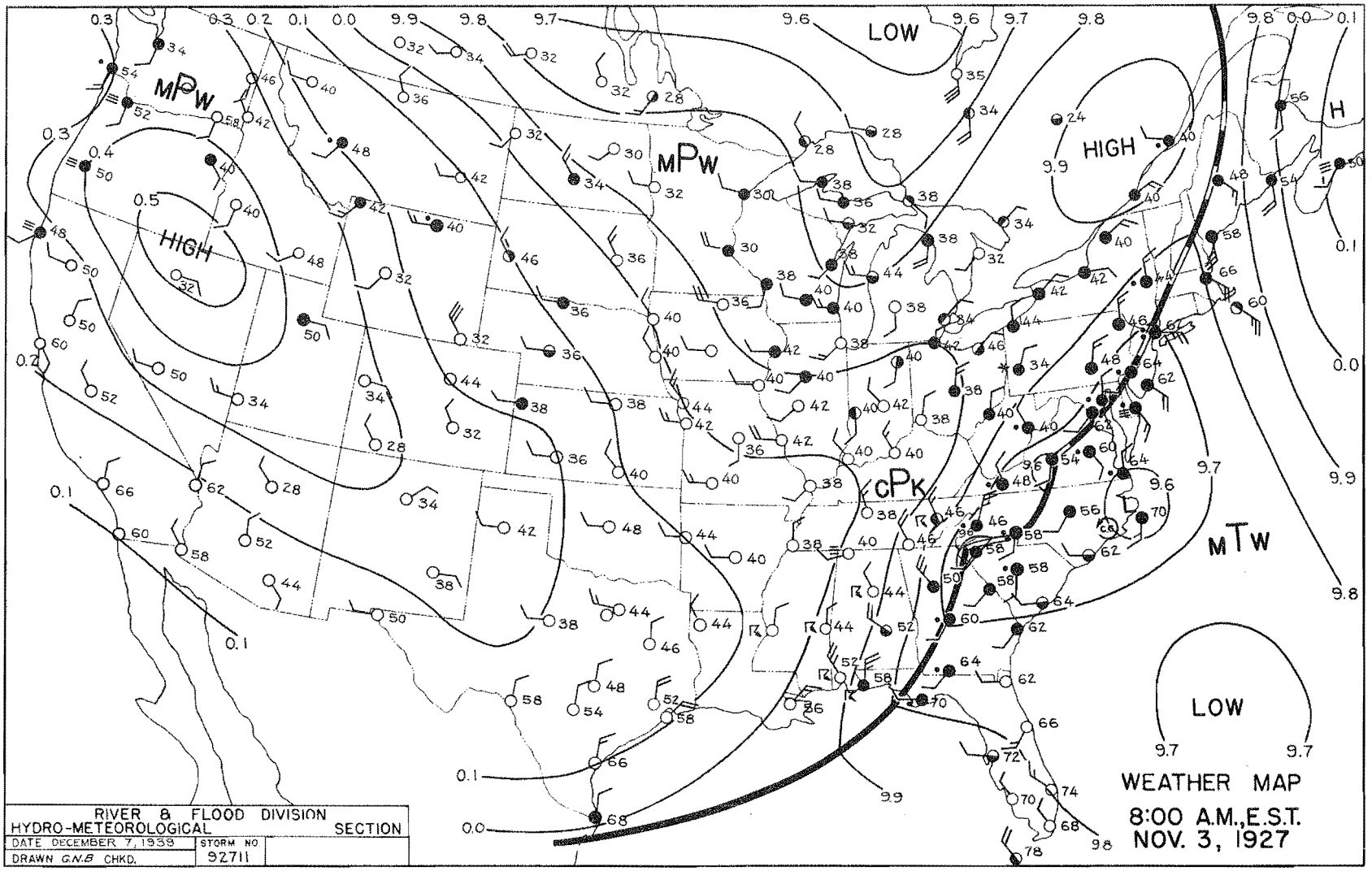
LOW
HIGH
HIGH
LOW
mPw
mPw
cPk
mTw
H
WEATHER MAP
8:00 A.M.,E.S.T.
NOV. 3, 1927
RIVER & FLOOD DIVISION
HYDRO-METEOROLOGICAL SECTION
DATE DECEMBER 7, 1939
STORM NO 92711
DRAWN G.N.B CHKD.

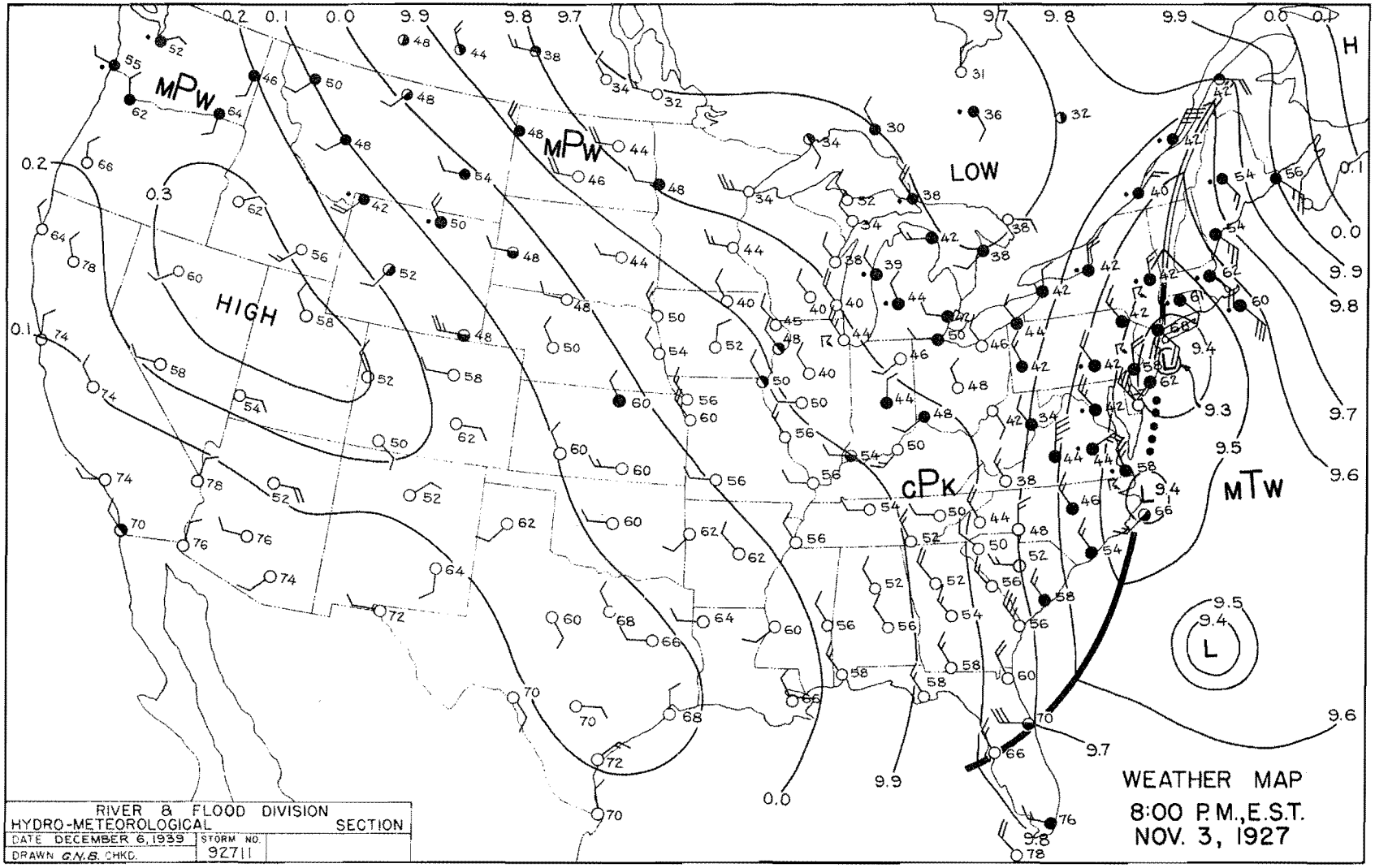
mPw
mPw
HIGH
LOW
cPk
mTw
H
L
L
WEATHER MAP
8:00 P.M.,E.S.T.
NOV. 3, 1927
RIVER & FLOOD DIVISION
HYDRO-METEOROLOGICAL SECTION
DATE DECEMBER 6, 1939
STORM NO. 92711
DRAWN C.N.B. CHKD.

FIGURE A-23

FIGURE A-24

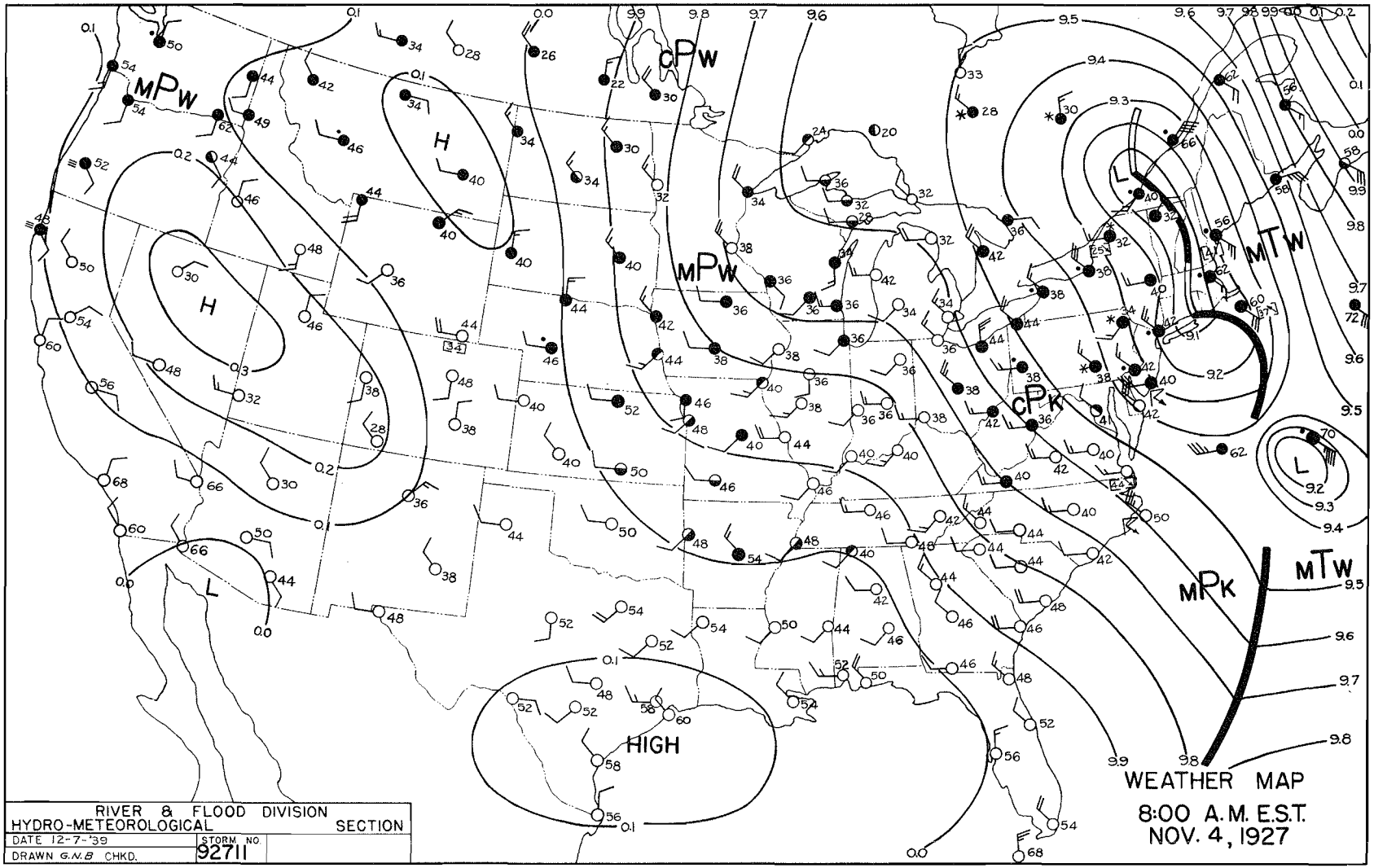
cPw
mPw
mPw
H
H
L
L
HIGH
cPk
mPk
mTw
mTw
WEATHER MAP
8:00 A.M. E.S.T.
NOV. 4, 1927
RIVER & FLOOD DIVISION
HYDRO-METEOROLOGICAL SECTION
DATE 12-7-'39
STORM NO. 92711
DRAWN G.N.B CHKD.

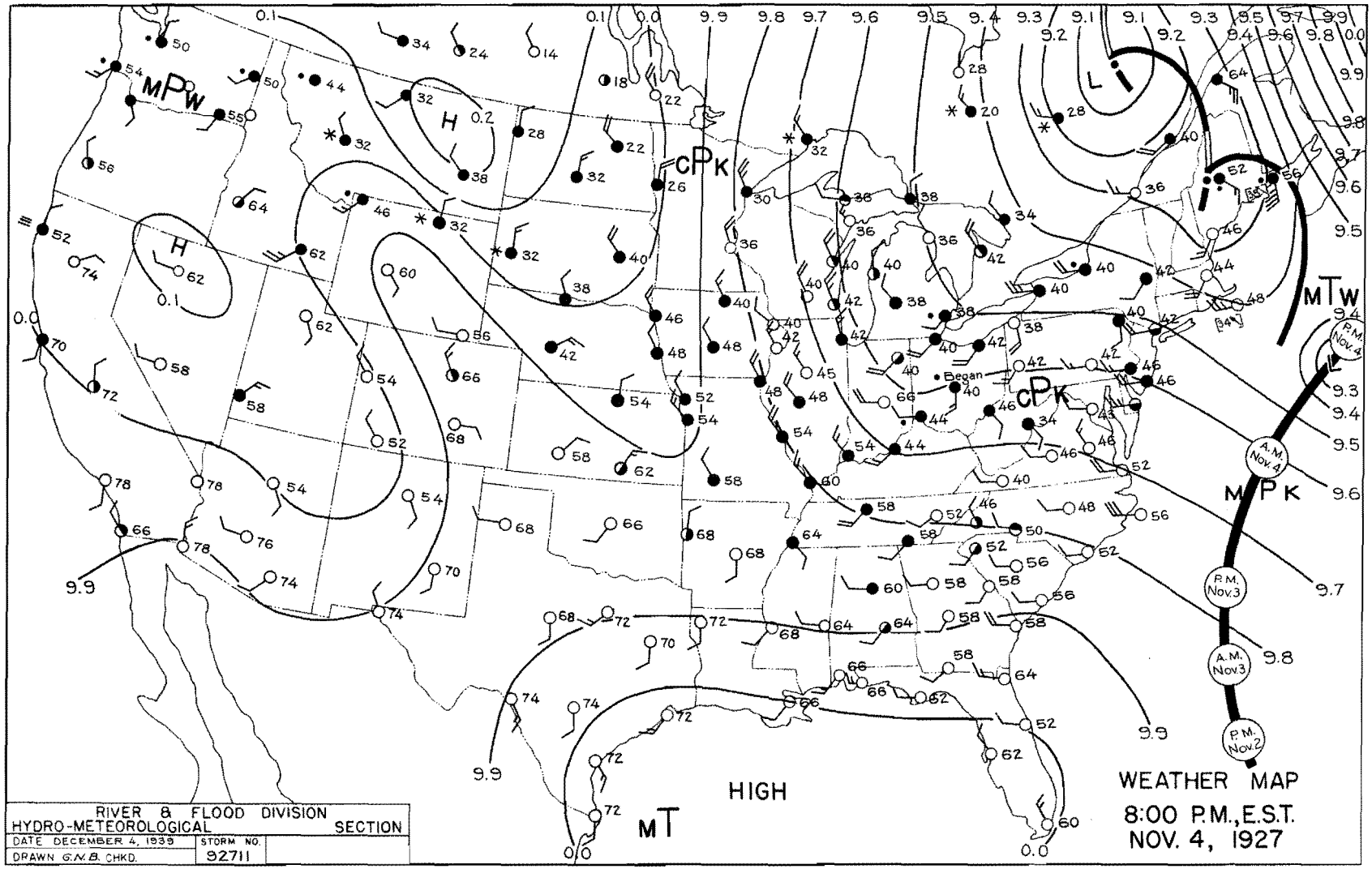
mPw
cPk
H
L
mTw
mPk
Began
HIGH
mT
WEATHER MAP
8:00 P.M.,E.S.T.
NOV. 4, 1927
P.M. Nov.4
A.M. Nov.4
P.M. Nov.3
A.M. Nov.3
P.M. Nov.2
RIVER & FLOOD DIVISION
HYDRO-METEOROLOGICAL SECTION
DATE DECEMBER 4, 1939
STORM NO. 92711
DRAWN G.M.B. CHKD.

FIGURE A-25

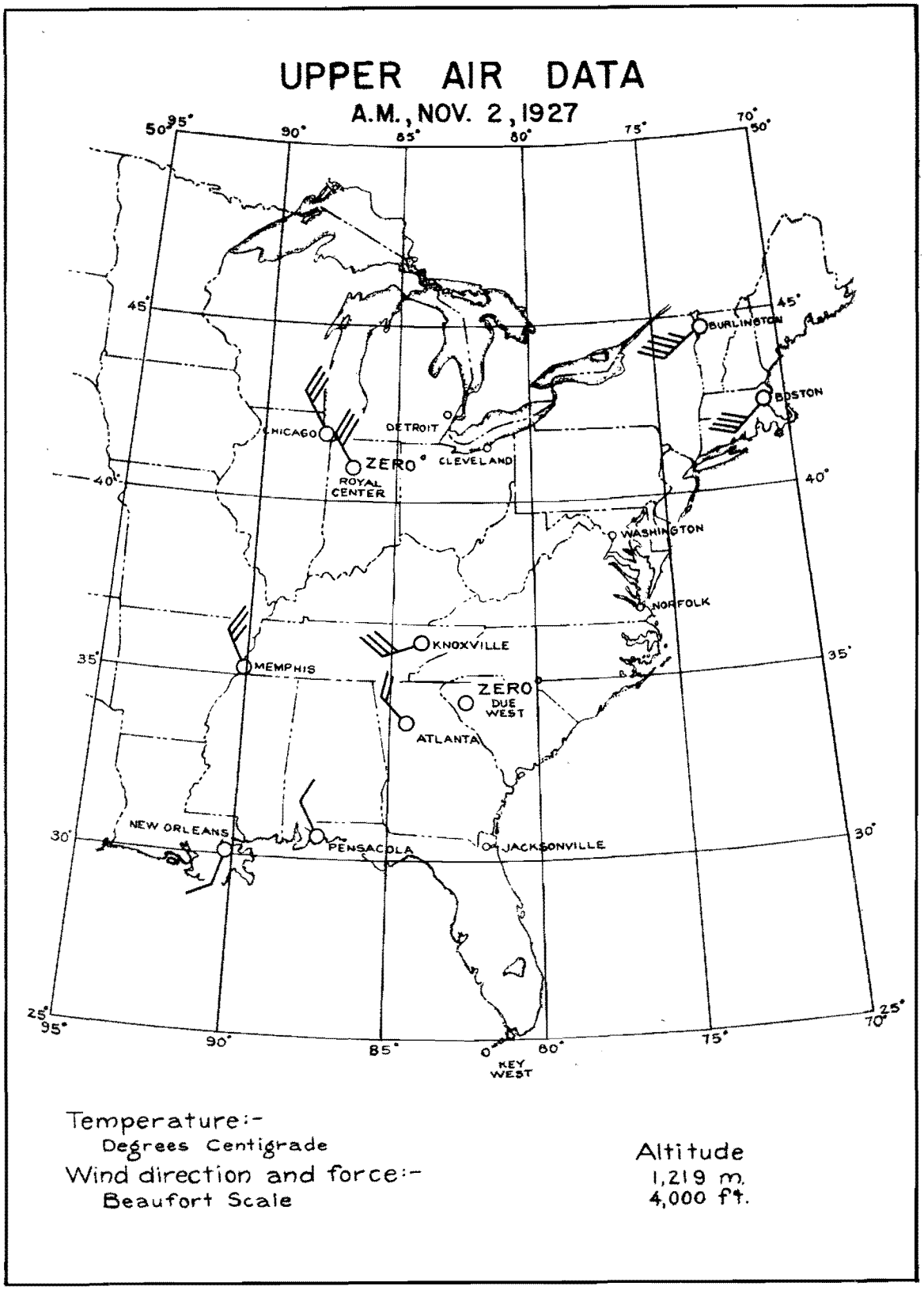
UPPER AIR DATA
A.M., NOV. 2, 1927
95°
90°
85°
80°
75°
70°
50°
45°
40°
35°
30°
25°
BURLINGTON
BOSTON
CHICAGO
DETROIT
CLEVELAND
ZERO
ROYAL CENTER
WASHINGTON
NORFOLK
KNOXVILLE
MEMPHIS
ZERO
DUE WEST
ATLANTA
NEW ORLEANS
PENSACOLA
JACKSONVILLE
KEY WEST
Temperature:-
Degrees Centigrade
Wind direction and force:-
Beaufort Scale
Altitude
1,219 m.
4,000 ft.

FIGURE A-26

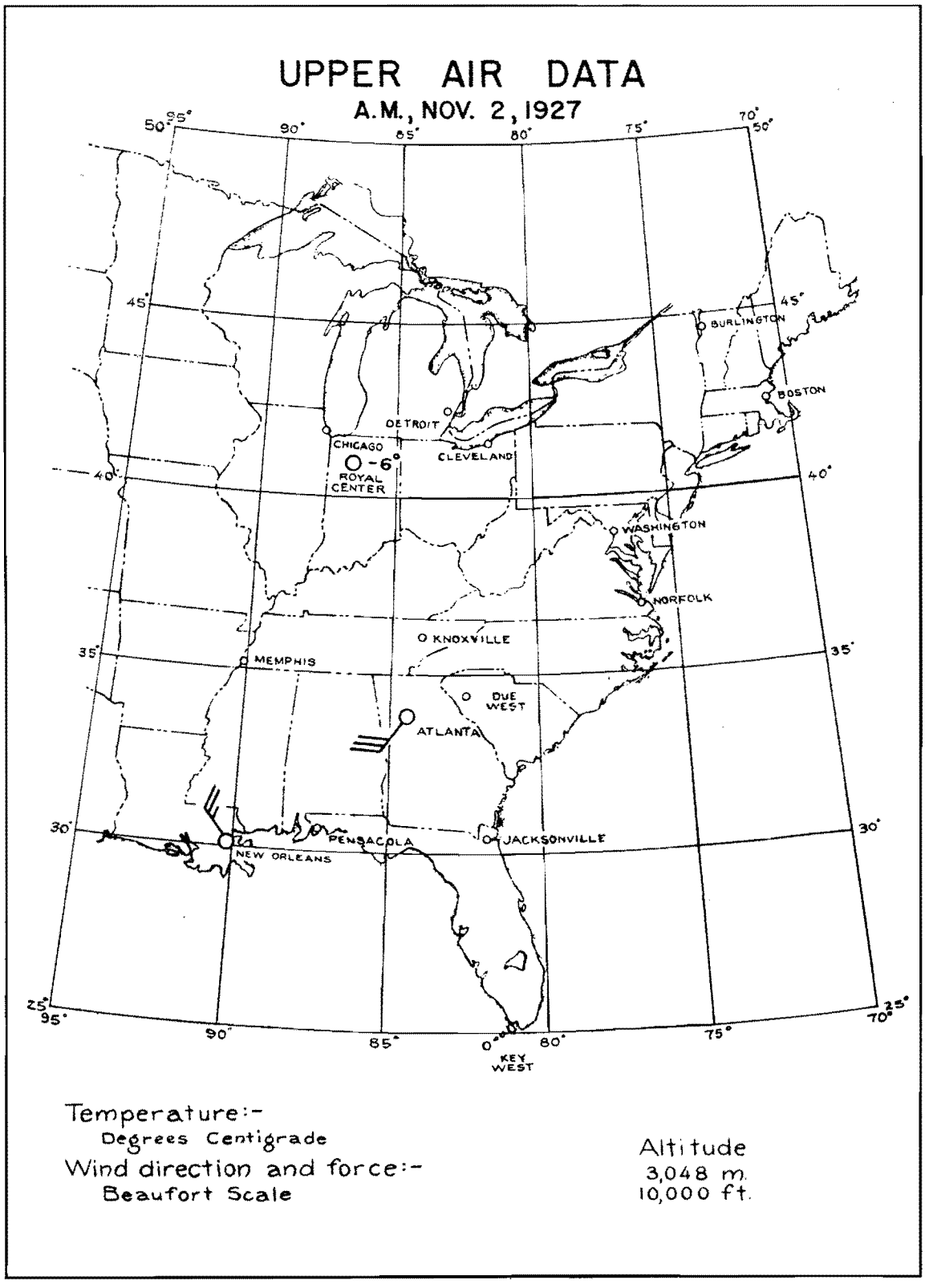
UPPER AIR DATA
A.M., NOV. 2, 1927
95°
90°
85°
80°
75°
70°
50°
45°
40°
35°
30°
25°
BURLINGTON
BOSTON
DETROIT
CHICAGO
O-6°
ROYAL CENTER
CLEVELAND
WASHINGTON
NORFOLK
KNOXVILLE
MEMPHIS
DUE WEST
ATLANTA
PENSACOLA
NEW ORLEANS
JACKSONVILLE
KEY WEST
Temperature:-
Degrees Centigrade
Wind direction and force:-
Beaufort Scale
Altitude
3,048 m.
10,000 ft.

FIGURE A- 27

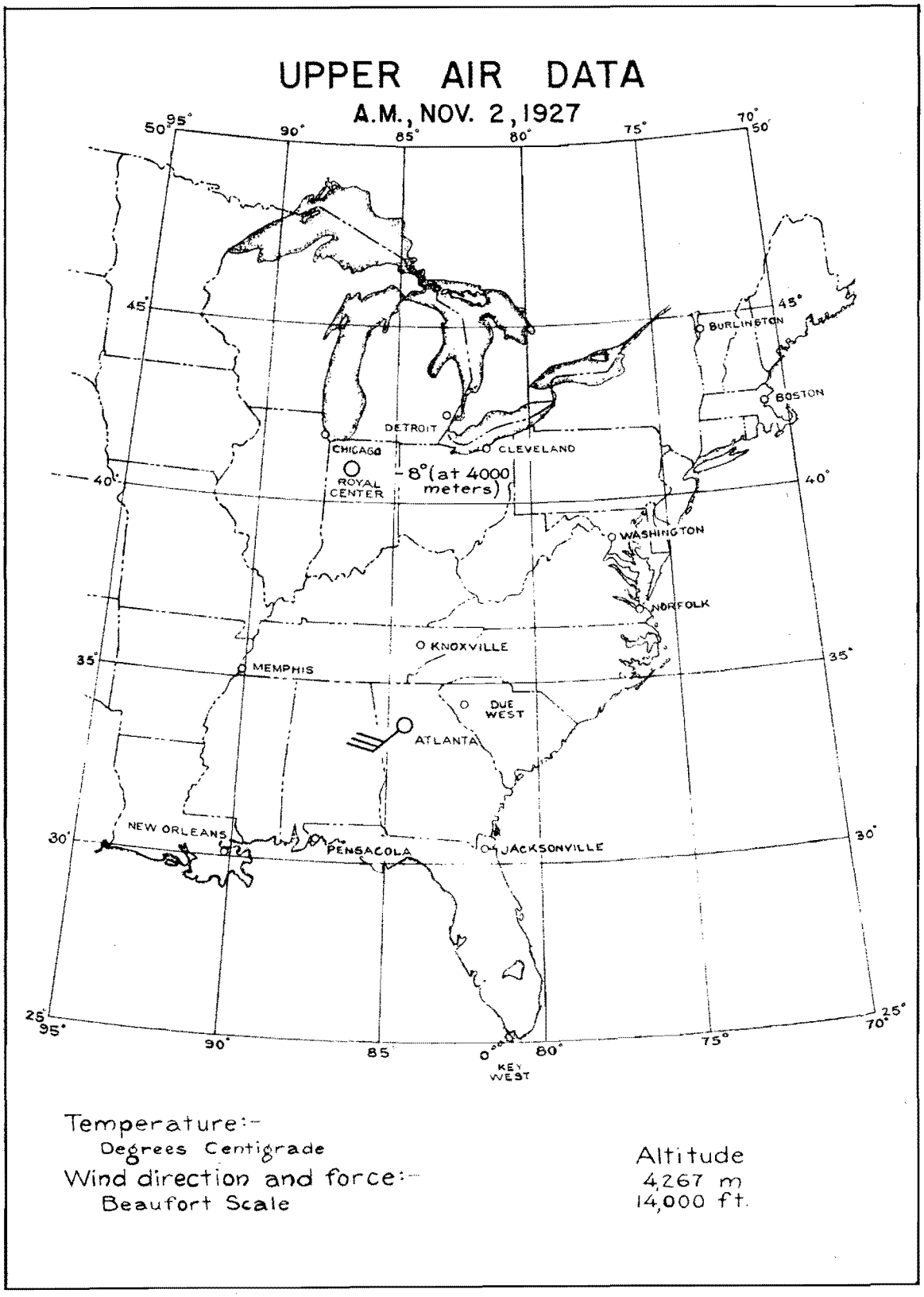
UPPER AIR DATA
A.M., NOV. 2, 1927
95°
90°
85°
80°
75°
70°
50°
45°
40°
35°
30°
25°
BURLINGTON
BOSTON
DETROIT
CHICAGO
CLEVELAND
ROYAL CENTER
-8°(at 4000 meters)
WASHINGTON
NORFOLK
KNOXVILLE
MEMPHIS
DUE WEST
ATLANTA
NEW ORLEANS
PENSACOLA
JACKSONVILLE
KEY WEST
Temperature:-
Degrees Centigrade
Wind direction and force:-
Beaufort Scale
Altitude
4,267 m
14,000 ft.

FIGURE A-28

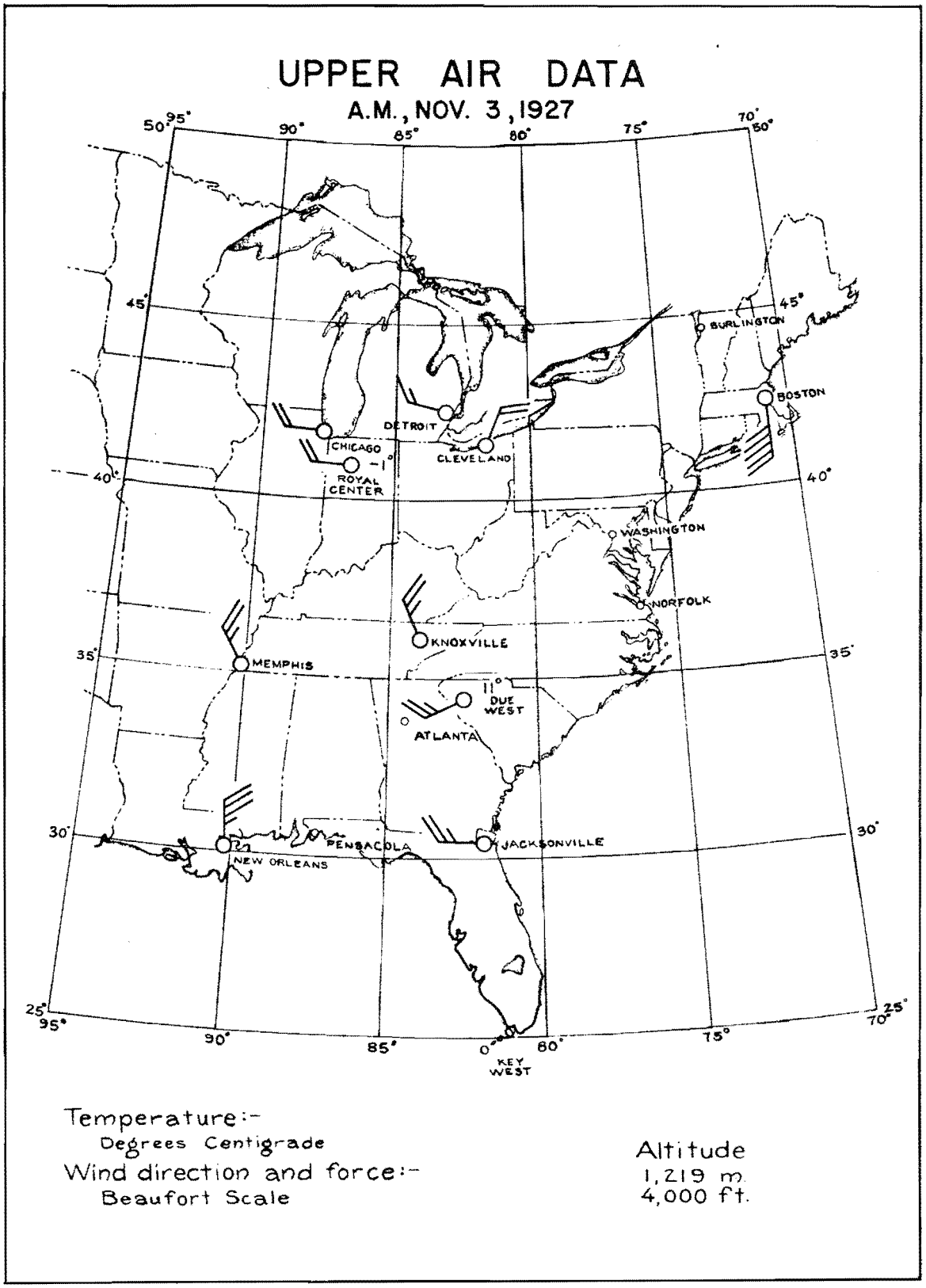
UPPER AIR DATA
A.M., NOV. 3, 1927
50°
95°
90°
85°
80°
75°
70°
45°
40°
35°
30°
25°
BURLINGTON
BOSTON
DETROIT
CHICAGO
-1°
ROYAL CENTER
CLEVELAND
WASHINGTON
NORFOLK
KNOXVILLE
MEMPHIS
11°
DUE WEST
ATLANTA
PENSACOLA
NEW ORLEANS
JACKSONVILLE
0°
KEY WEST
Temperature:-
Degrees Centigrade
Wind direction and force:-
Beaufort Scale
Altitude
1,219 m.
4,000 ft.

FIGURE A-29

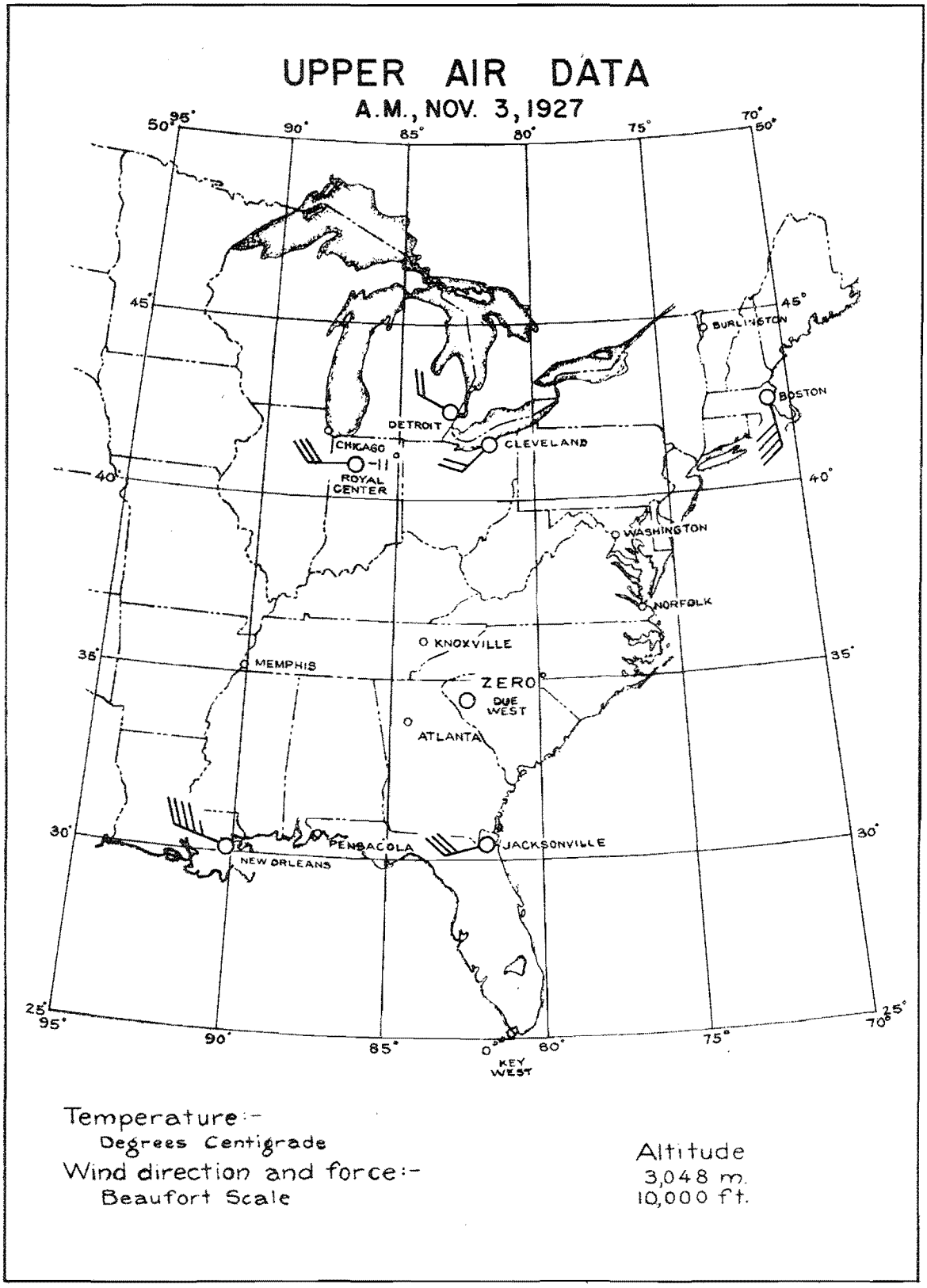
UPPER AIR DATA
A.M., NOV. 3, 1927
95°
90°
85°
80°
75°
70°
50°
45°
40°
35°
30°
25°
BURLINGTON
BOSTON
DETROIT
CHICAGO
CLEVELAND
ROYAL CENTER
WASHINGTON
NORFOLK
KNOXVILLE
MEMPHIS
ZERO
DUE WEST
ATLANTA
PENSACOLA
JACKSONVILLE
NEW ORLEANS
KEY WEST
Temperature:-
Degrees Centigrade
Wind direction and force:-
Beaufort Scale
Altitude
3,048 m.
10,000 ft.

FIGURE A-30

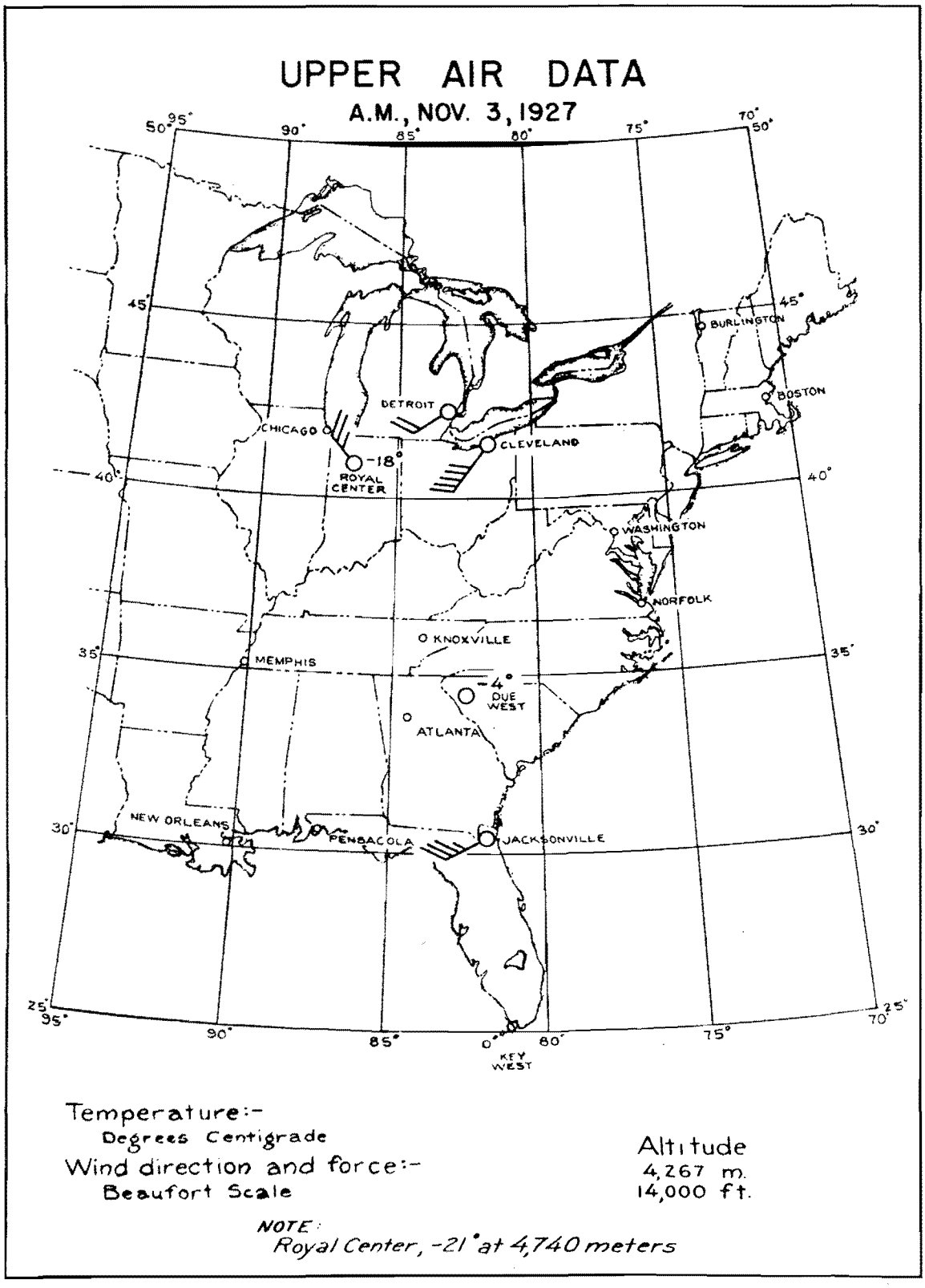
UPPER AIR DATA
A.M., NOV. 3, 1927
95°
90°
85°
80°
75°
70°
50°
45°
40°
35°
30°
25°
BURLINGTON
BOSTON
DETROIT
CHICAGO
CLEVELAND
-18°
ROYAL CENTER
WASHINGTON
NORFOLK
KNOXVILLE
MEMPHIS
-4°
DUE WEST
ATLANTA
NEW ORLEANS
PENSACOLA
JACKSONVILLE
KEY WEST
Temperature:-
Degrees Centigrade
Wind direction and force:-
Beaufort Scale
Altitude
4,267 m.
14,000 ft.
NOTE:
Royal Center, -21° at 4,740 meters

FIGURE A- 31

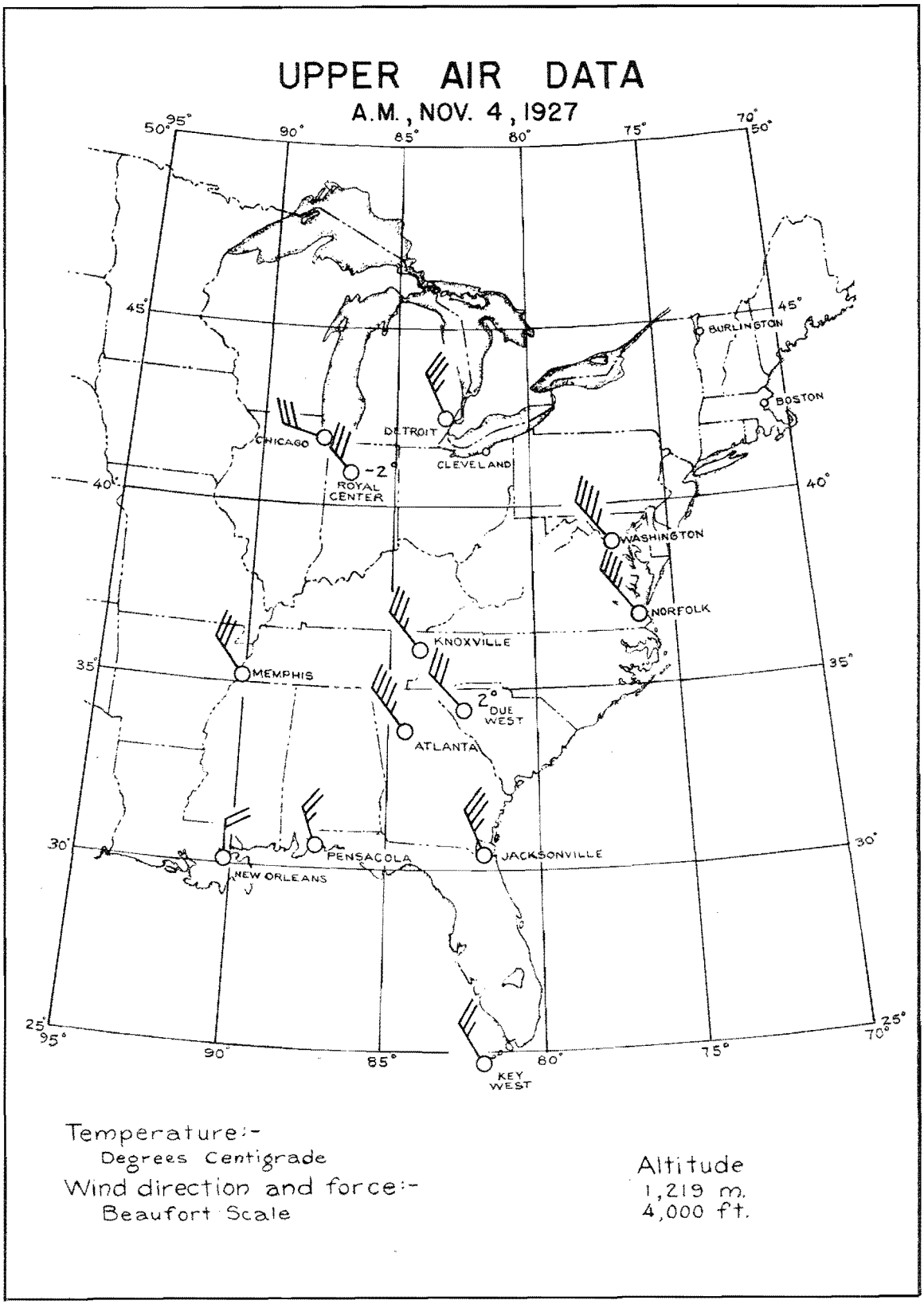
UPPER AIR DATA
A.M., NOV. 4, 1927
95°
90°
85°
80°
75°
70°
50°
45°
40°
35°
30°
25°
BURLINGTON
BOSTON
DETROIT
CHICAGO
CLEVELAND
-2°
ROYAL CENTER
WASHINGTON
NORFOLK
KNOXVILLE
MEMPHIS
2°
DUE WEST
ATLANTA
PENSACOLA
JACKSONVILLE
NEW ORLEANS
KEY WEST
Temperature:-
Degrees Centigrade
Wind direction and force:-
Beaufort Scale
Altitude
1,219 m.
4,000 ft.

FIGURE A-32

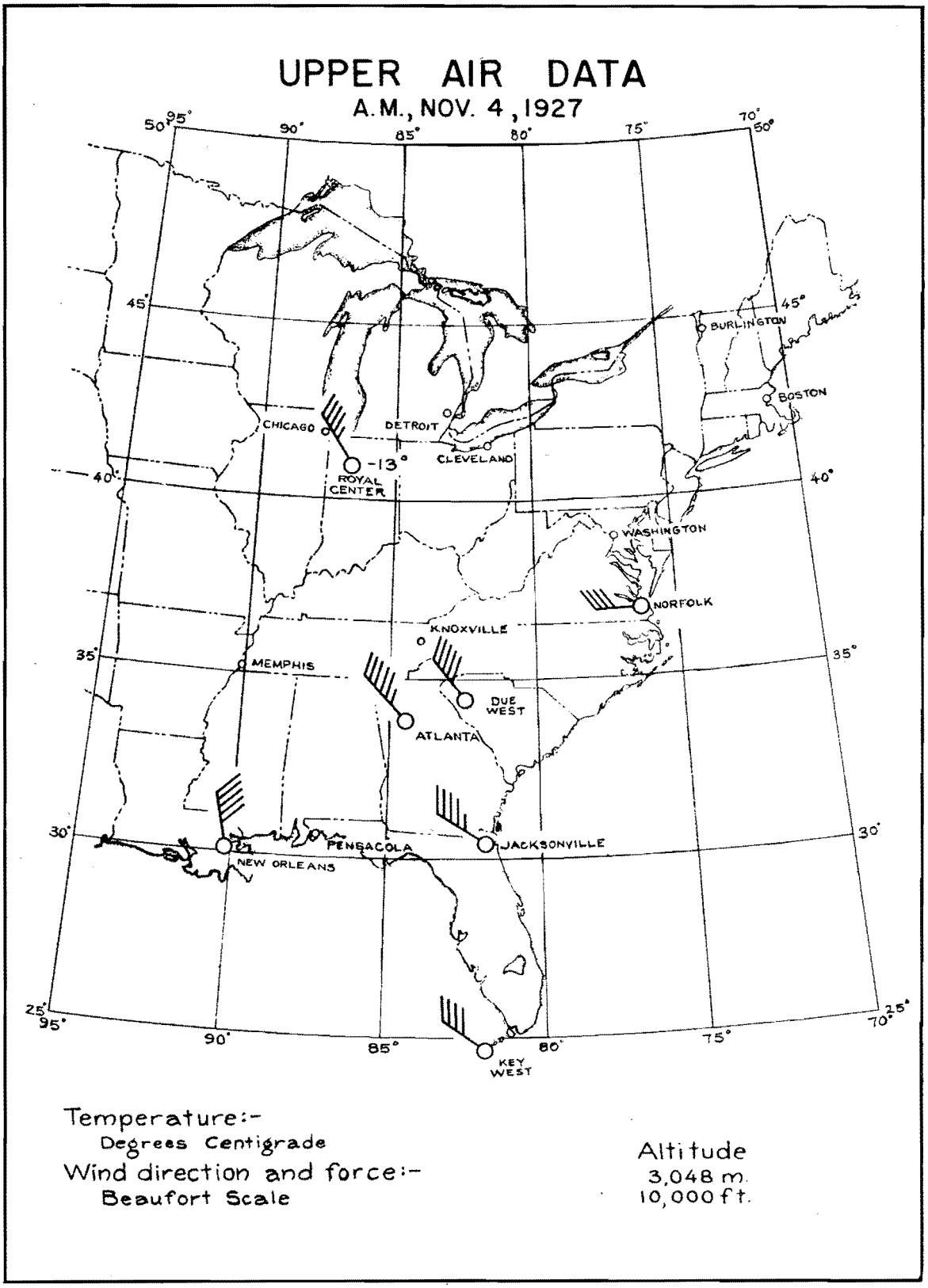
UPPER AIR DATA
A.M., NOV. 4, 1927
95°
90°
85°
80°
75°
70°
50°
45°
40°
35°
30°
25°
CHICAGO
DETROIT
CLEVELAND
-13°
ROYAL CENTER
BURLINGTON
BOSTON
WASHINGTON
NORFOLK
KNOXVILLE
MEMPHIS
DUE WEST
ATLANTA
PENSACOLA
NEW ORLEANS
JACKSONVILLE
KEY WEST
Temperature:-
Degrees Centigrade
Wind direction and force:-
Beaufort Scale
Altitude
3,048 m.
10,000 ft.

FIGURE A-33

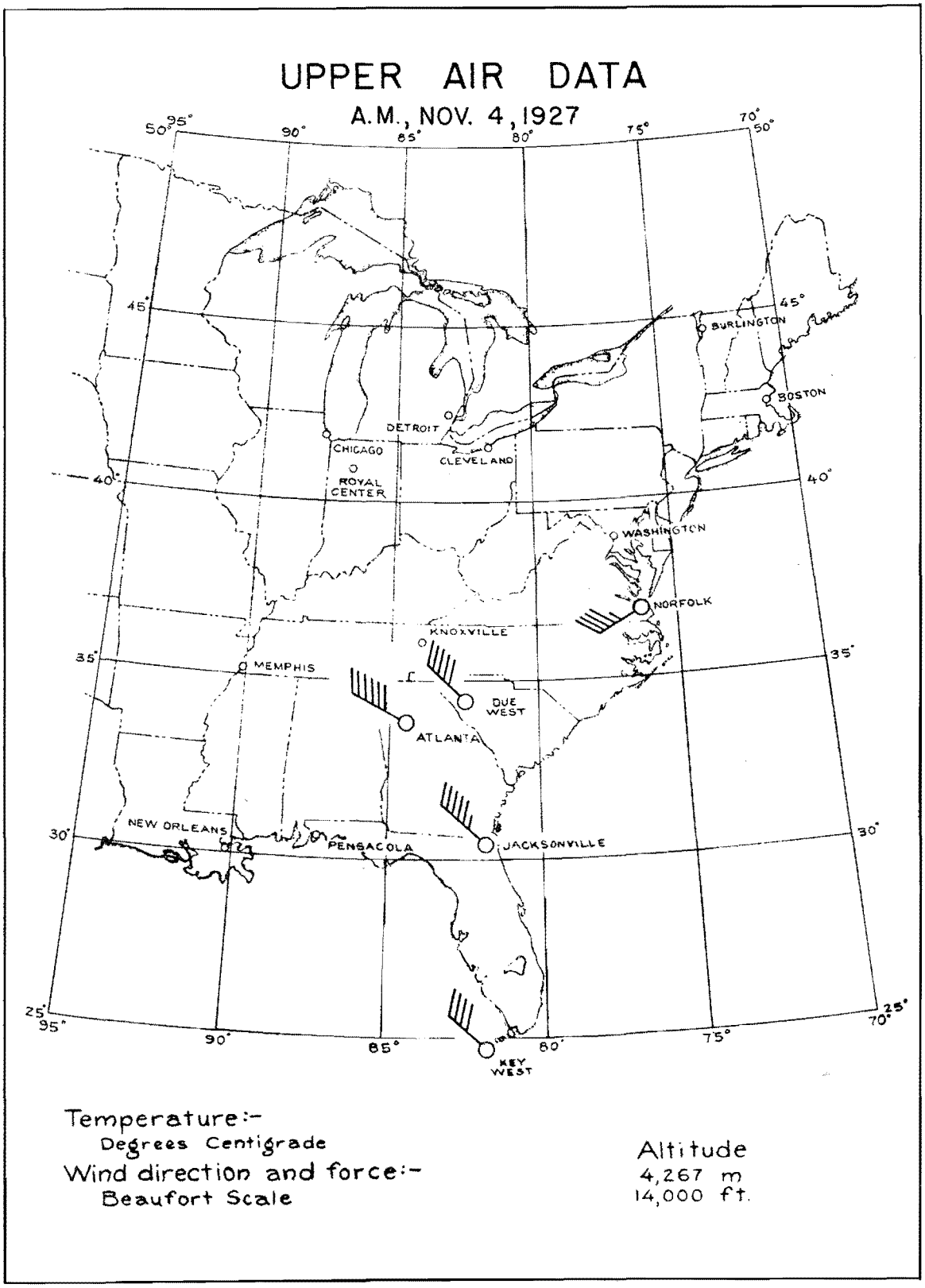
UPPER AIR DATA
A.M., NOV. 4, 1927
50°
95°
90°
85°
80°
75°
70°
45°
40°
35°
30°
25°
BURLINGTON
BOSTON
DETROIT
CHICAGO
CLEVELAND
ROYAL CENTER
WASHINGTON
NORFOLK
KNOXVILLE
MEMPHIS
DUE WEST
ATLANTA
NEW ORLEANS
PENSACOLA
JACKSONVILLE
KEY WEST
Temperature:-
Degrees Centigrade
Wind direction and force:-
Beaufort Scale
Altitude
4,267 m
14,000 ft.

FIGURE A-34

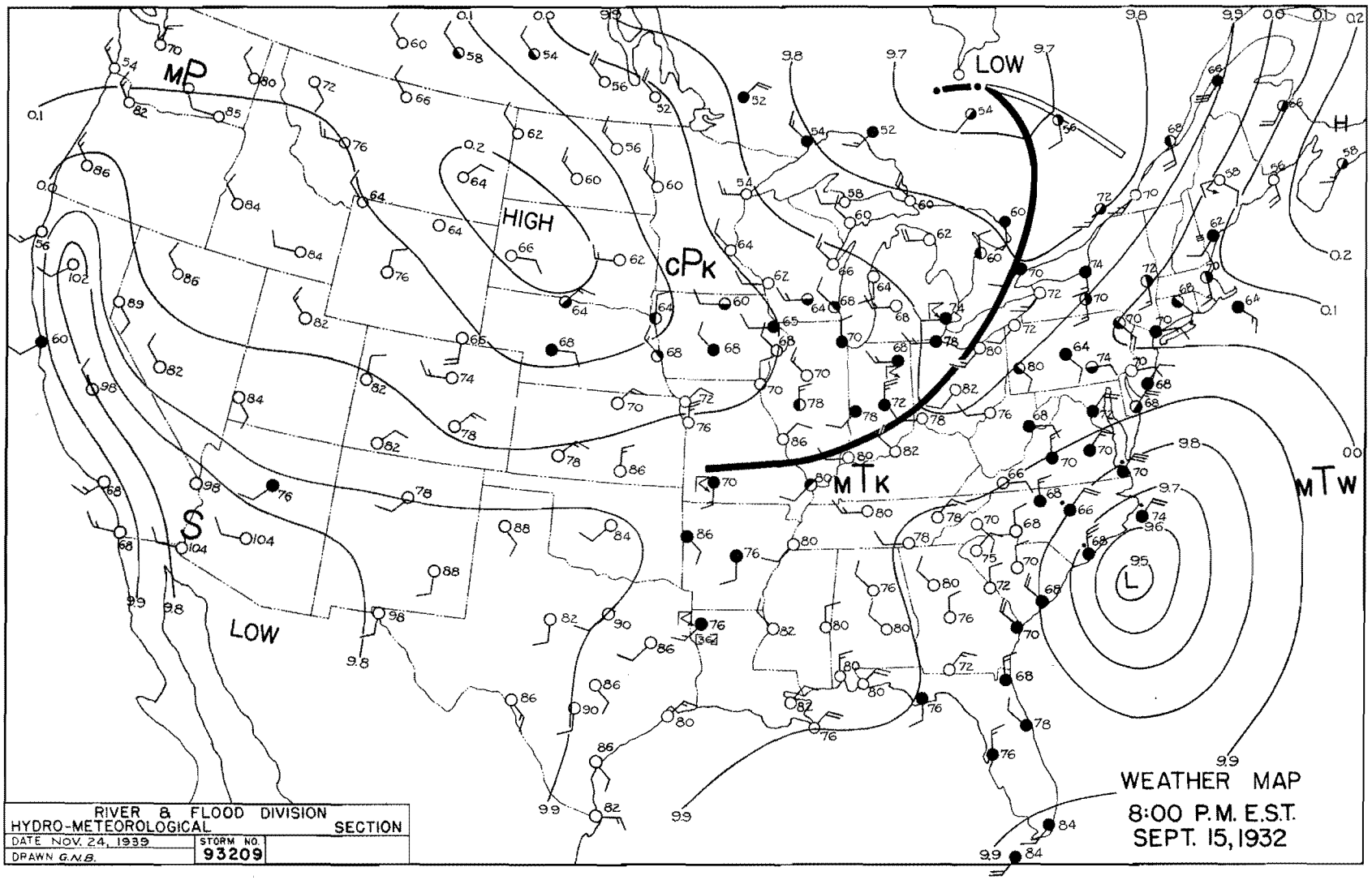
mP
LOW
HIGH
cPk
mTk
mTw
S
LOW
H
L
WEATHER MAP
8:00 P.M. E.S.T.
SEPT. 15, 1932
RIVER & FLOOD DIVISION
HYDRO-METEOROLOGICAL SECTION
DATE NOV. 24, 1939
STORM NO. 93209
DRAWN G.N.B.

FIGURE A-35

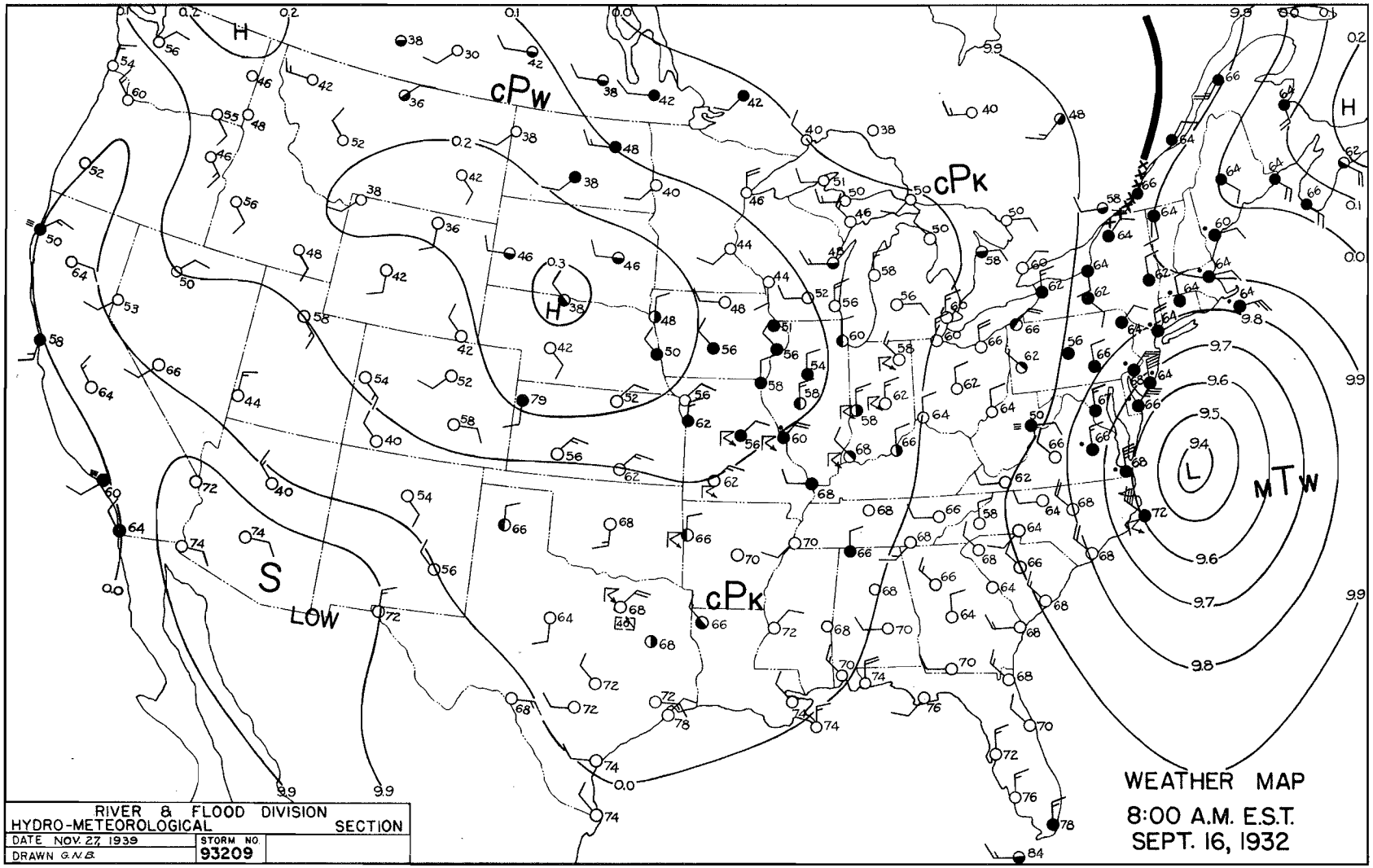
cPw
cPk
cPk
H
H
H
S
LOW
L
MTw
WEATHER MAP
8:00 A.M. E.S.T.
SEPT. 16, 1932
RIVER & FLOOD DIVISION
HYDRO-METEOROLOGICAL SECTION
DATE NOV. 27 1939
STORM NO. 93209
DRAWN G.N.B.

FIGURE A-36

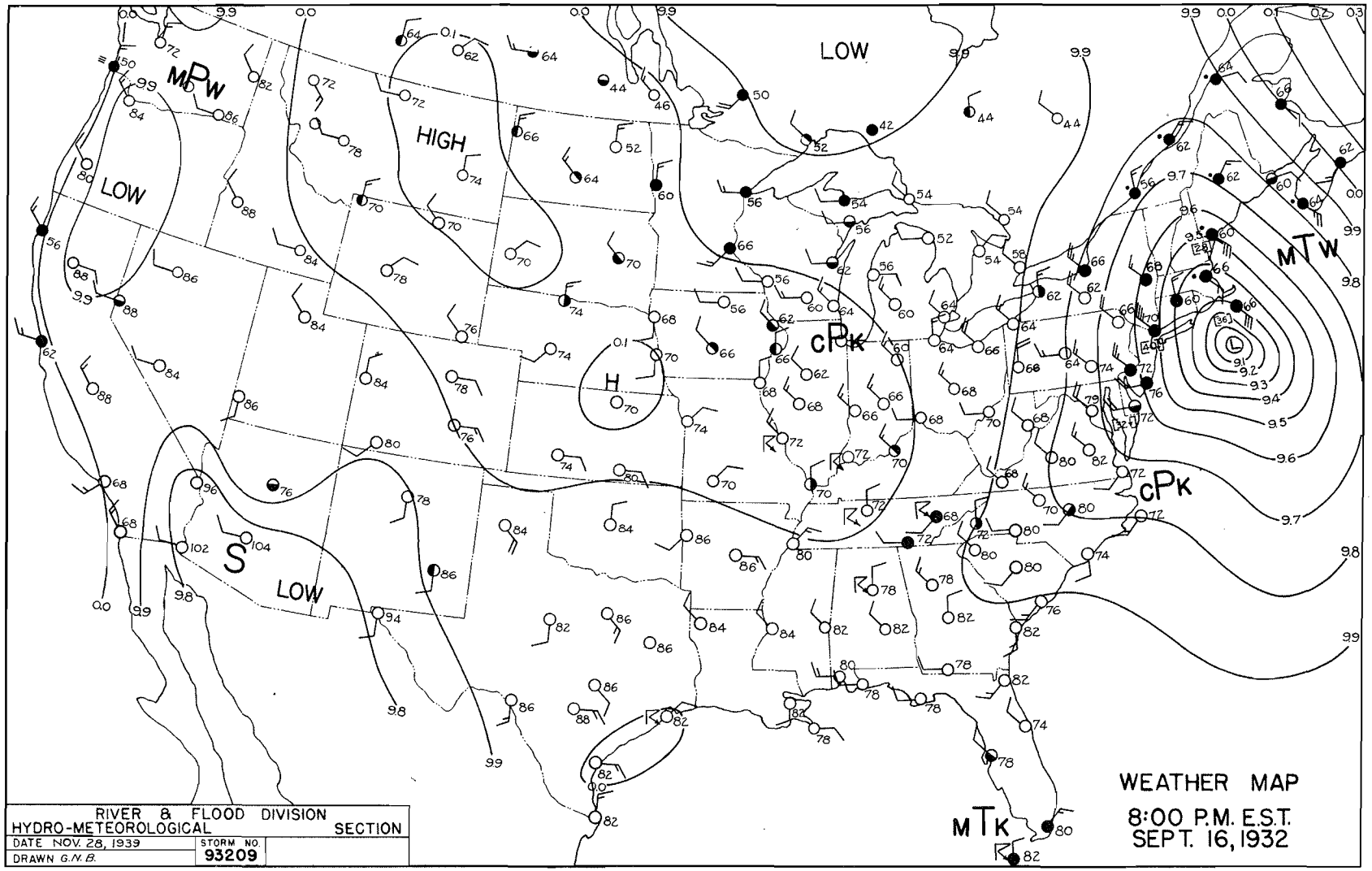
LOW
HIGH
LOW
H
S
LOW
mPw
cPk
cPk
mTw
mTk
WEATHER MAP
8:00 P.M. E.S.T.
SEPT. 16, 1932
RIVER & FLOOD DIVISION
HYDRO-METEOROLOGICAL SECTION
DATE NOV. 28, 1939
STORM NO. 93209
DRAWN G.N.B.

FIGURE A-37

FIGURE A-38

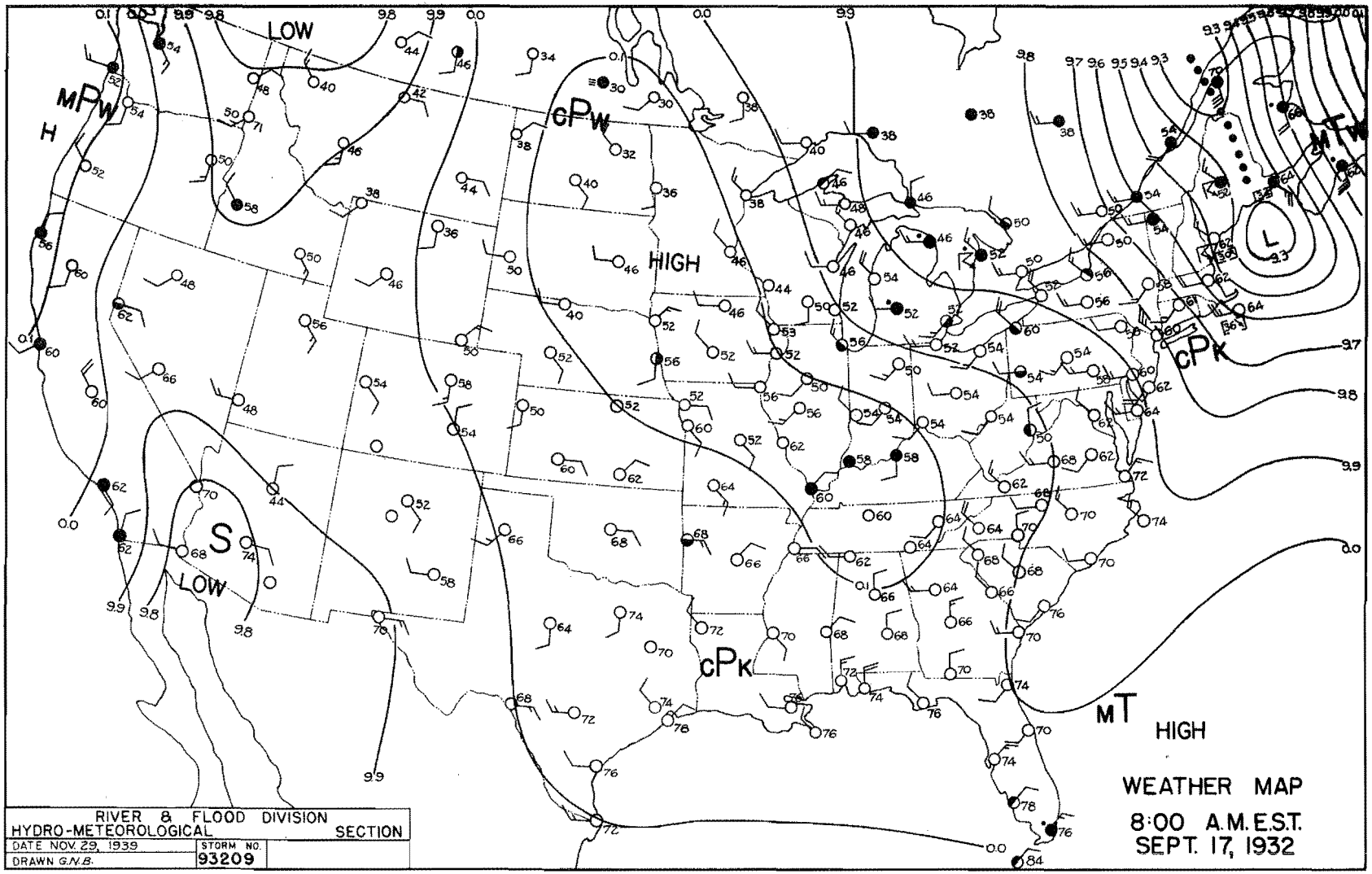
LOW
MPW
H
cPW
HIGH
MTW
L
cPK
S
LOW
cPK
MT
HIGH
WEATHER MAP
8:00 A.M. E.S.T.
SEPT. 17, 1932
RIVER & FLOOD DIVISION
HYDRO-METEOROLOGICAL SECTION
DATE NOV. 29, 1939
STORM NO. 93209
DRAWN G.N.B.

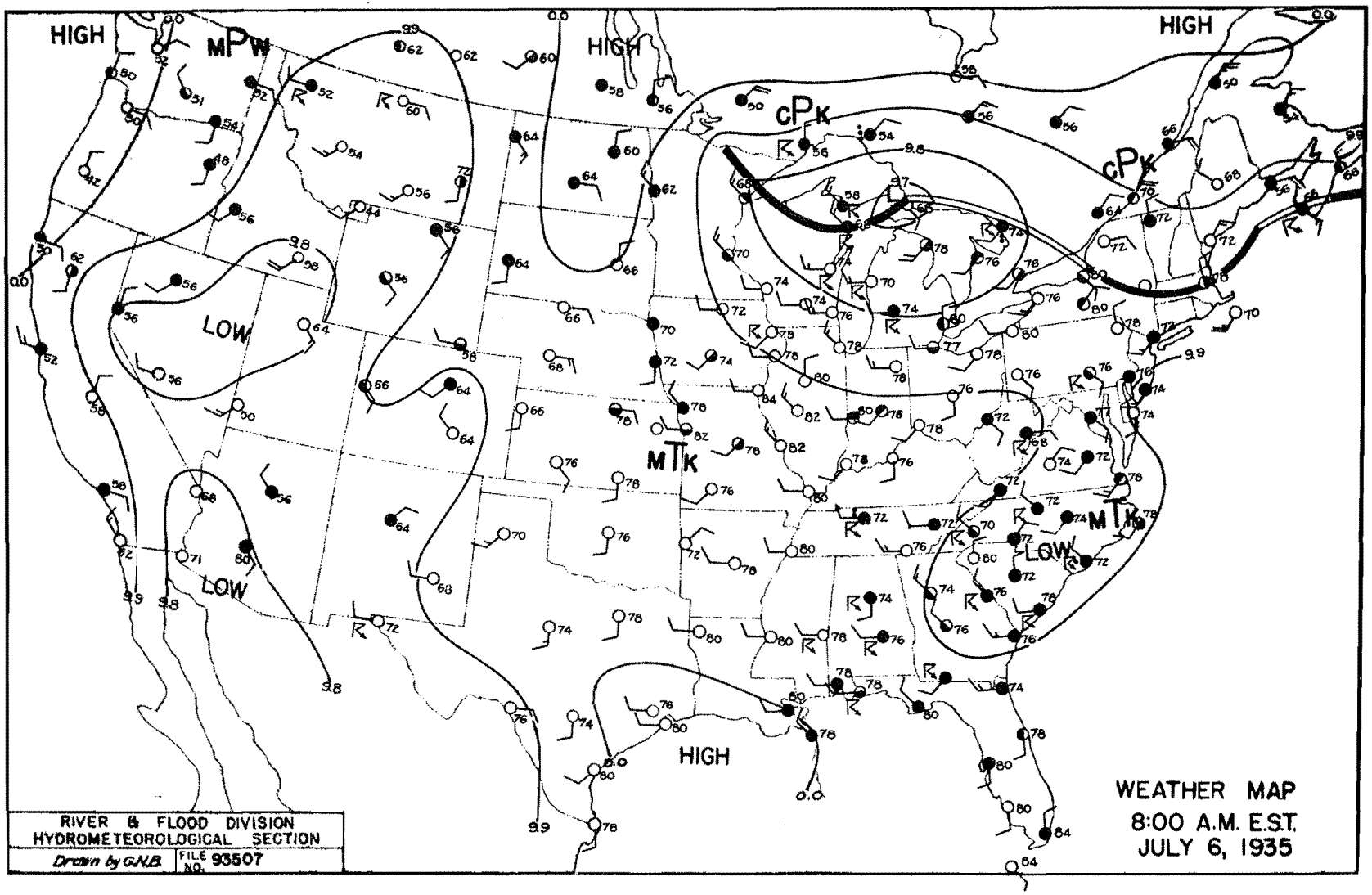
HIGH
mPw
HIGH
HIGH
cPk
cPk
LOW
mTk
mTk
LOW
LOW
HIGH
RIVER & FLOOD DIVISION
HYDROMETEOROLOGICAL SECTION
Drawn by G.N.B.
FILE NO. 93507
WEATHER MAP
8:00 A.M. E.S.T.
JULY 6, 1935

FIGURE A-39

FIGURE A-40

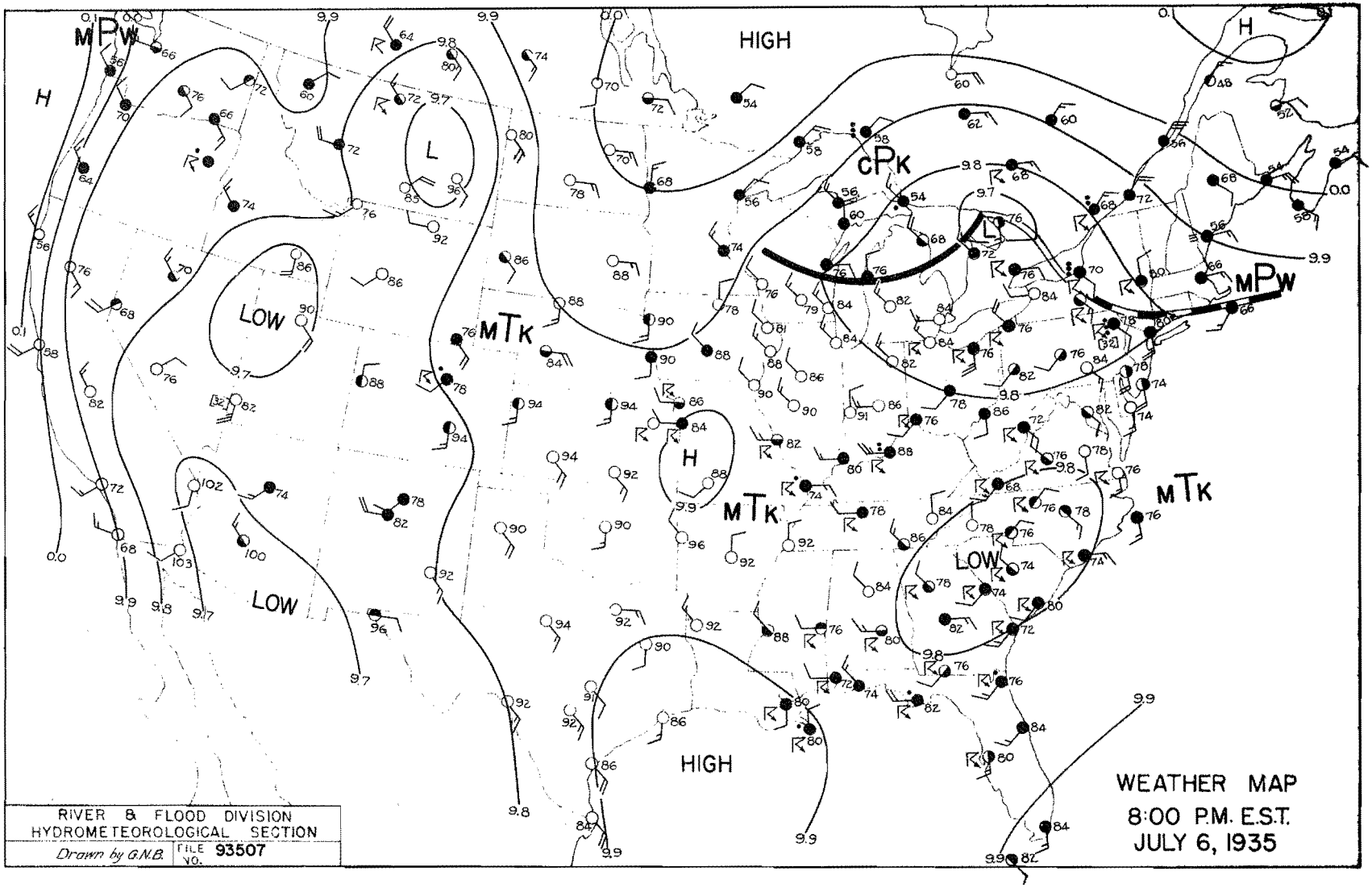
mPw
H
HIGH
cPk
L
LOW
mTk
mPw
H
mTk
mTk
LOW
LOW
HIGH
WEATHER MAP
8:00 P.M. E.S.T.
JULY 6, 1935
RIVER & FLOOD DIVISION
HYDROMETEOROLOGICAL SECTION
Drawn by G.N.B.
FILE NO. 93507

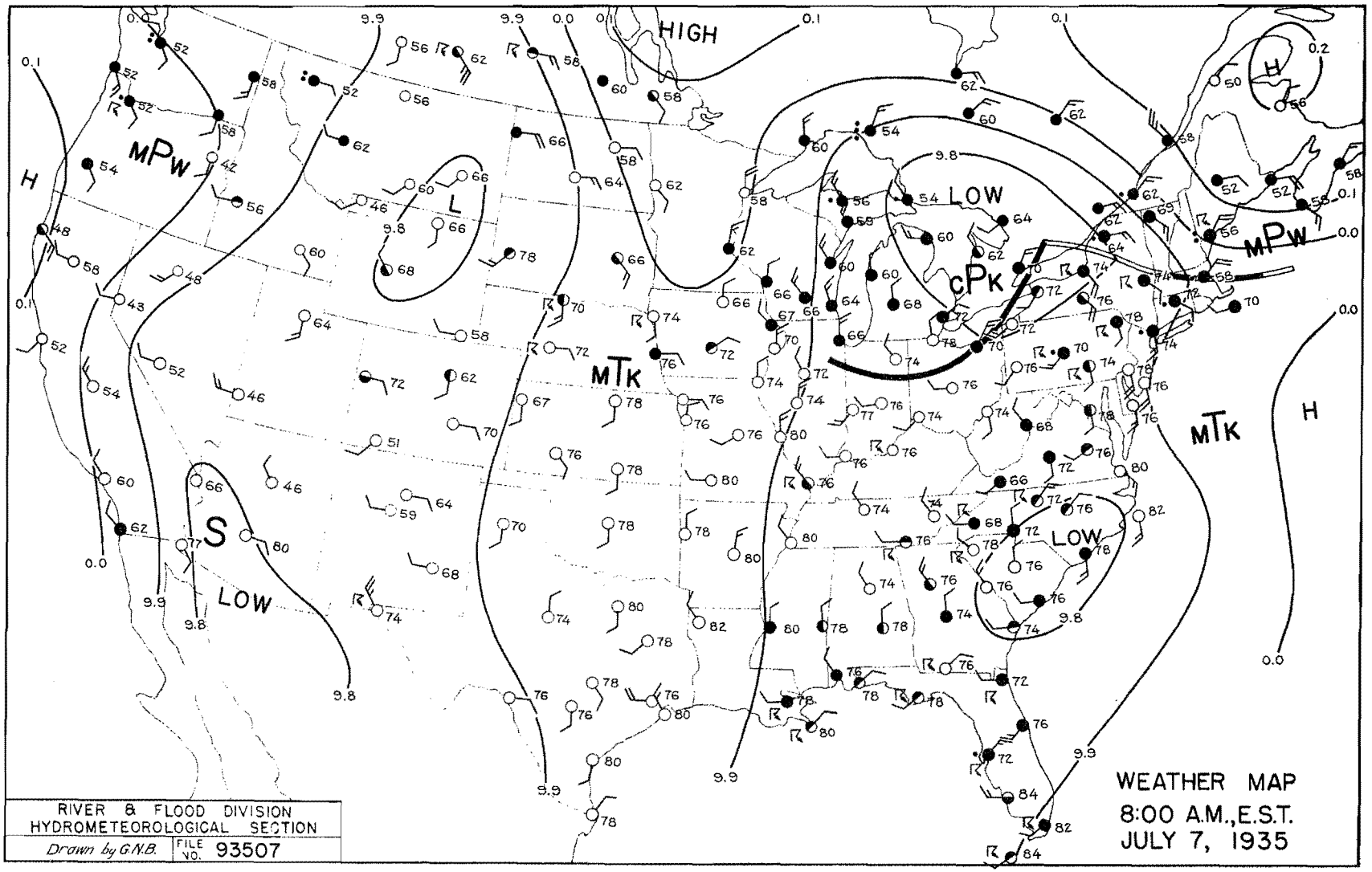
HIGH
LOW
LOW
LOW
mPw
mPw
cPk
mTk
mTk
H
H
H
L
S
RIVER & FLOOD DIVISION
HYDROMETEOROLOGICAL SECTION
Drawn by G.N.B.
FILE NO. 93507
WEATHER MAP
8:00 A.M., E.S.T.
JULY 7, 1935

FIGURE A-41

FIGURE A-42

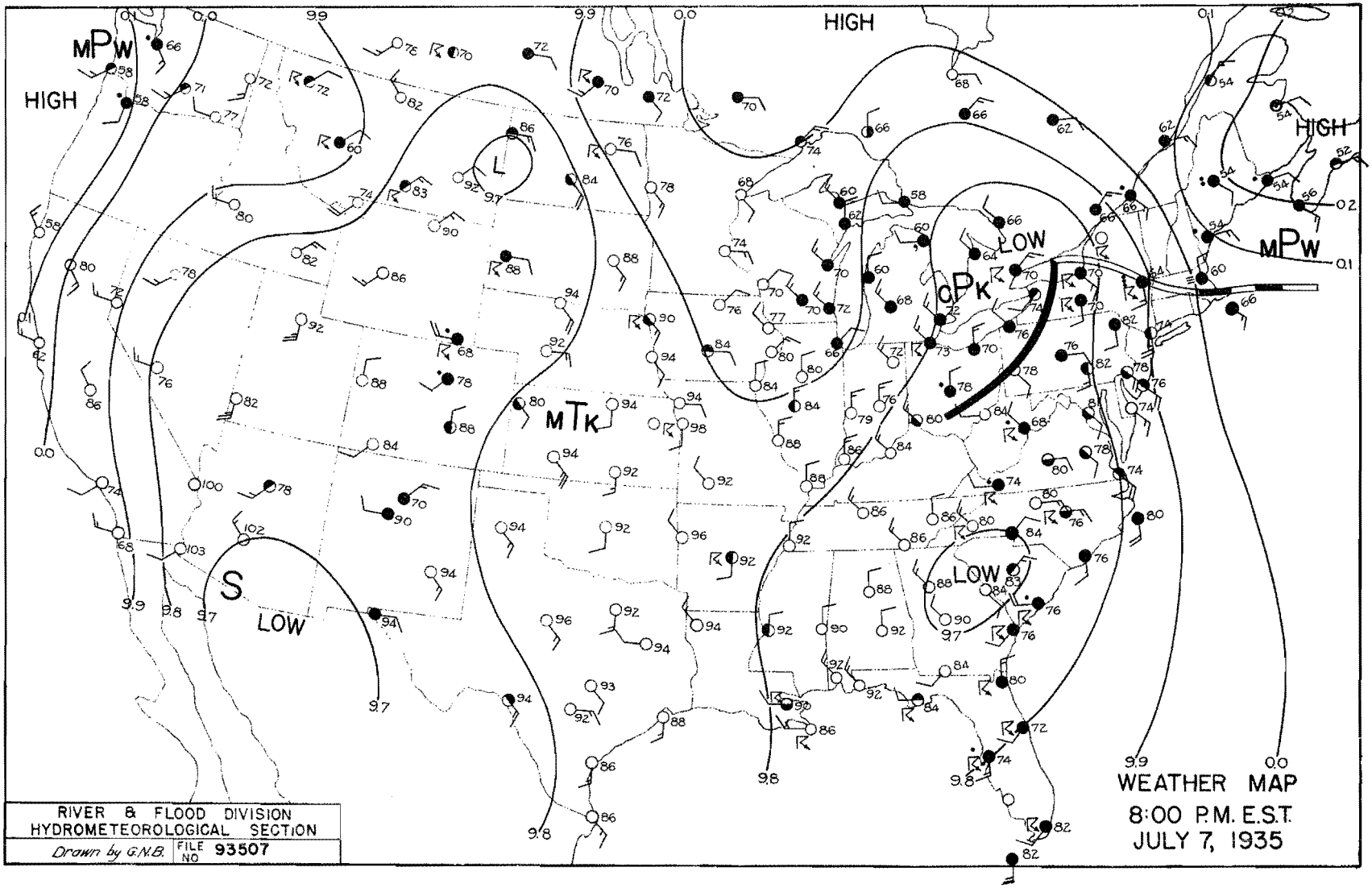
HIGH
HIGH
HIGH
LOW
LOW
LOW
MPW
MPW
MTK
CPK
L
S
RIVER & FLOOD DIVISION
HYDROMETEOROLOGICAL SECTION
Drawn by G.N.B.
FILE NO 93507
WEATHER MAP
8:00 P.M. E.S.T.
JULY 7, 1935

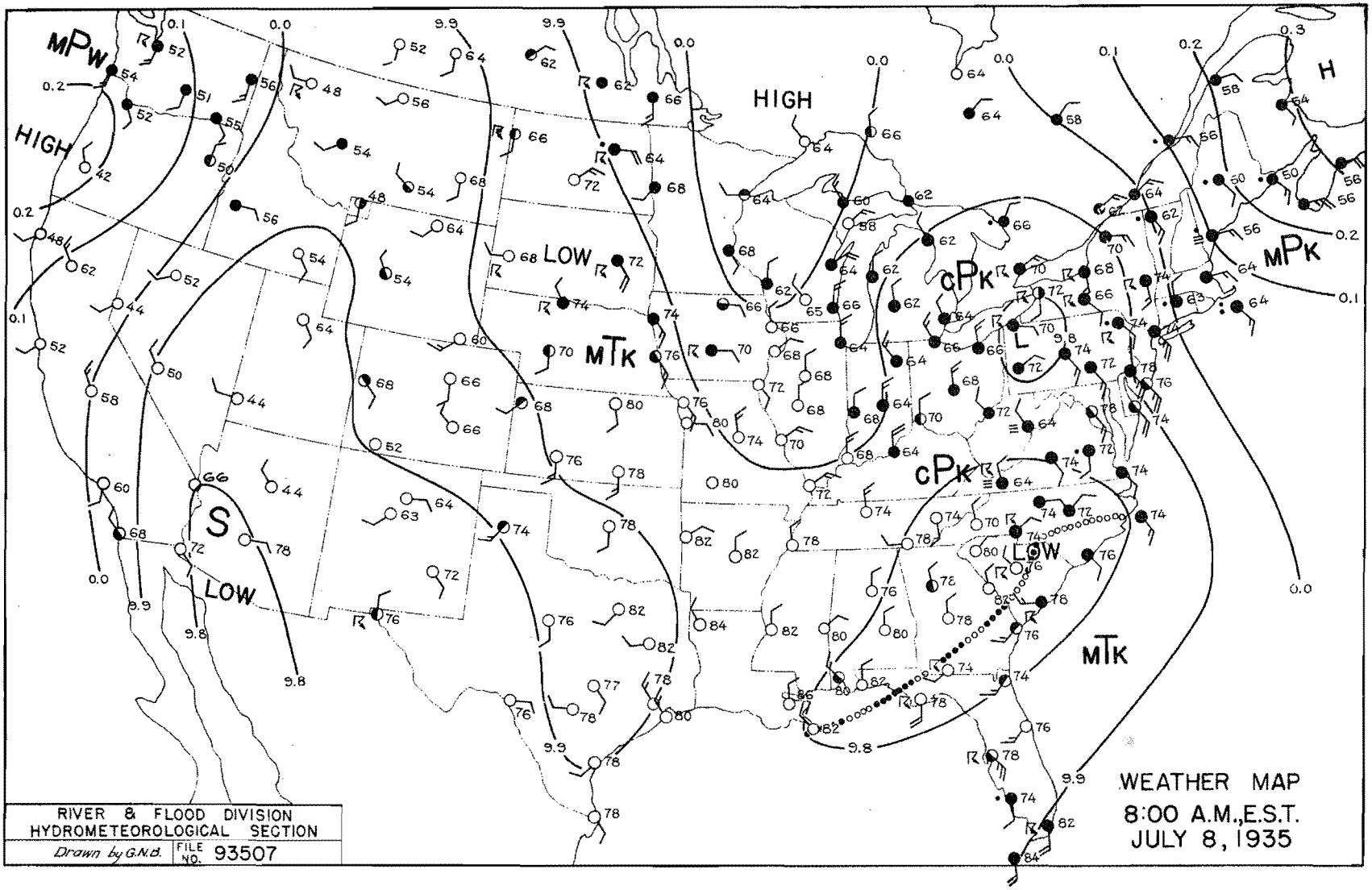
mPw
HIGH
HIGH
LOW
mTk
S
LOW
cPk
cPk
L
LOW
mTk
mPk
H
WEATHER MAP
8:00 A.M.,E.S.T.
JULY 8, 1935
RIVER & FLOOD DIVISION
HYDROMETEOROLOGICAL SECTION
Drawn by G.N.B.
FILE NO. 93507

FIGURE A-43

FIGURE A-44

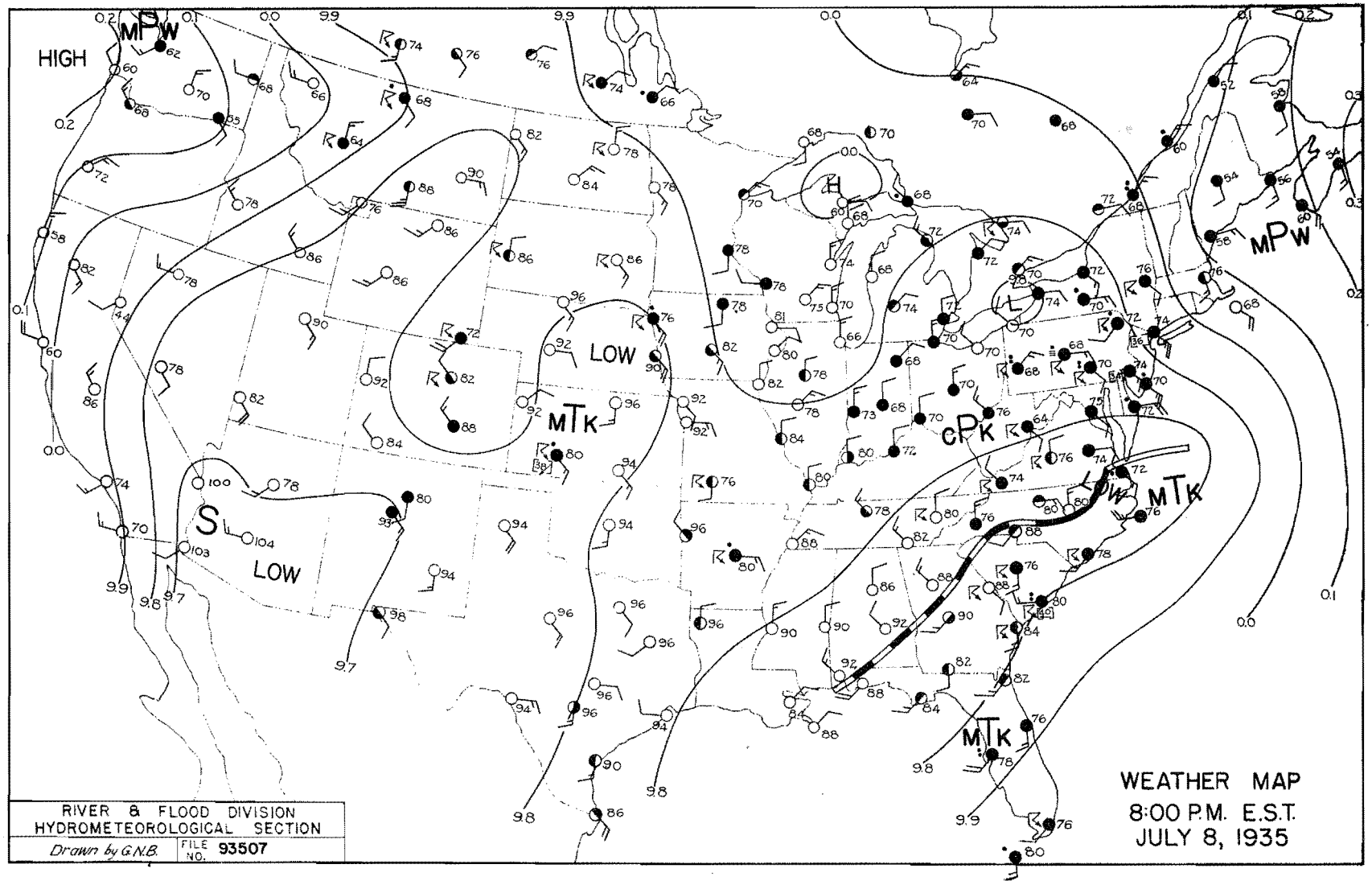
HIGH
mPw
LOW
mTk
S
LOW
cPk
mTk
mPw
mTk
H
WEATHER MAP
8:00 P.M. E.S.T.
JULY 8, 1935
RIVER & FLOOD DIVISION
HYDROMETEOROLOGICAL SECTION
Drawn by G.N.B.
FILE NO. 93507

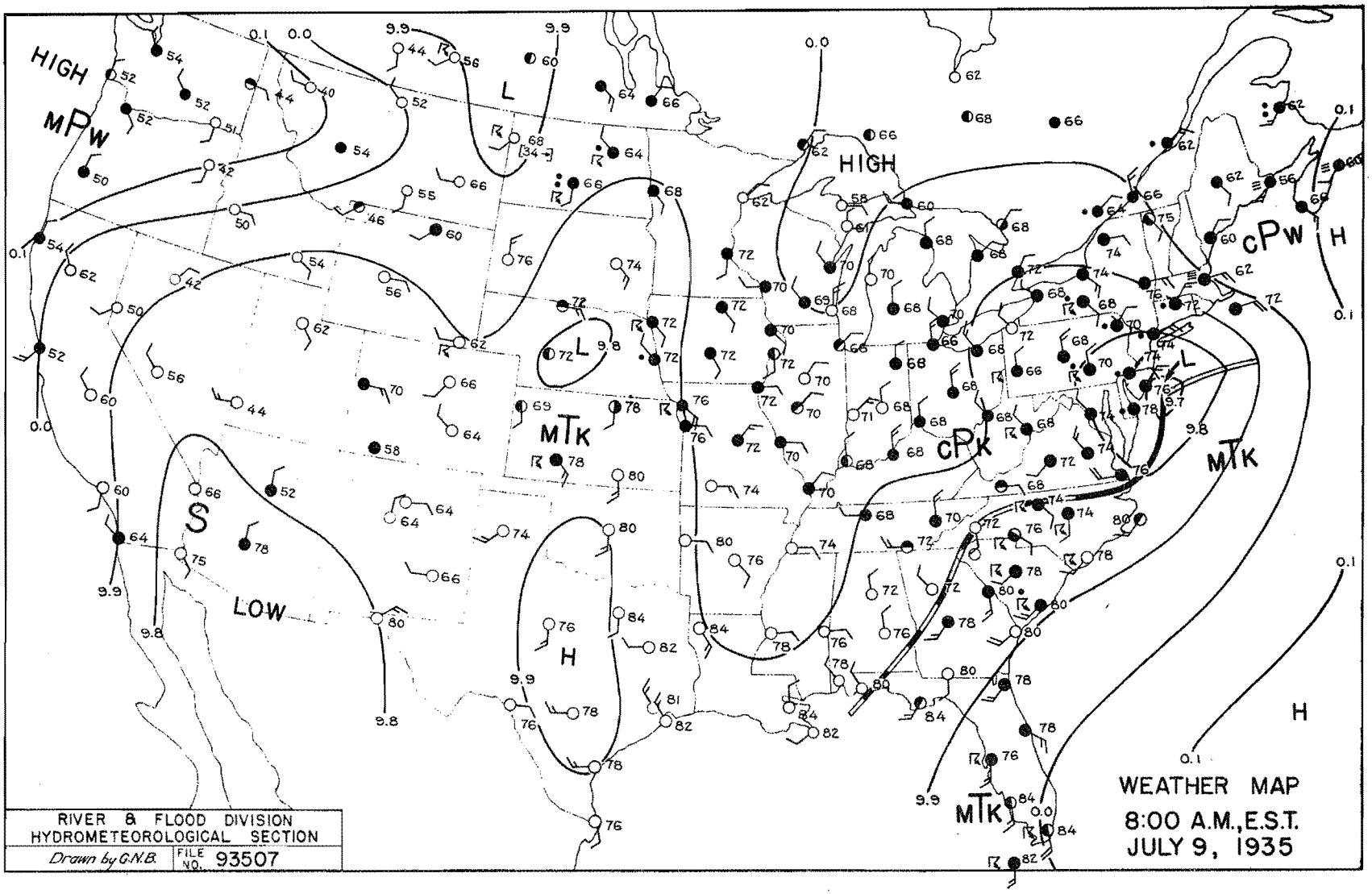
HIGH
mPw
L
HIGH
cPw
H
L
MTk
cPk
MTk
S
LOW
H
L
MTk
H
WEATHER MAP
8:00 A.M., E.S.T.
JULY 9, 1935
RIVER & FLOOD DIVISION
HYDROMETEOROLOGICAL SECTION
Drawn by G.N.B.
FILE NO. 93507

FIGURE A-45

FIGURE A-46

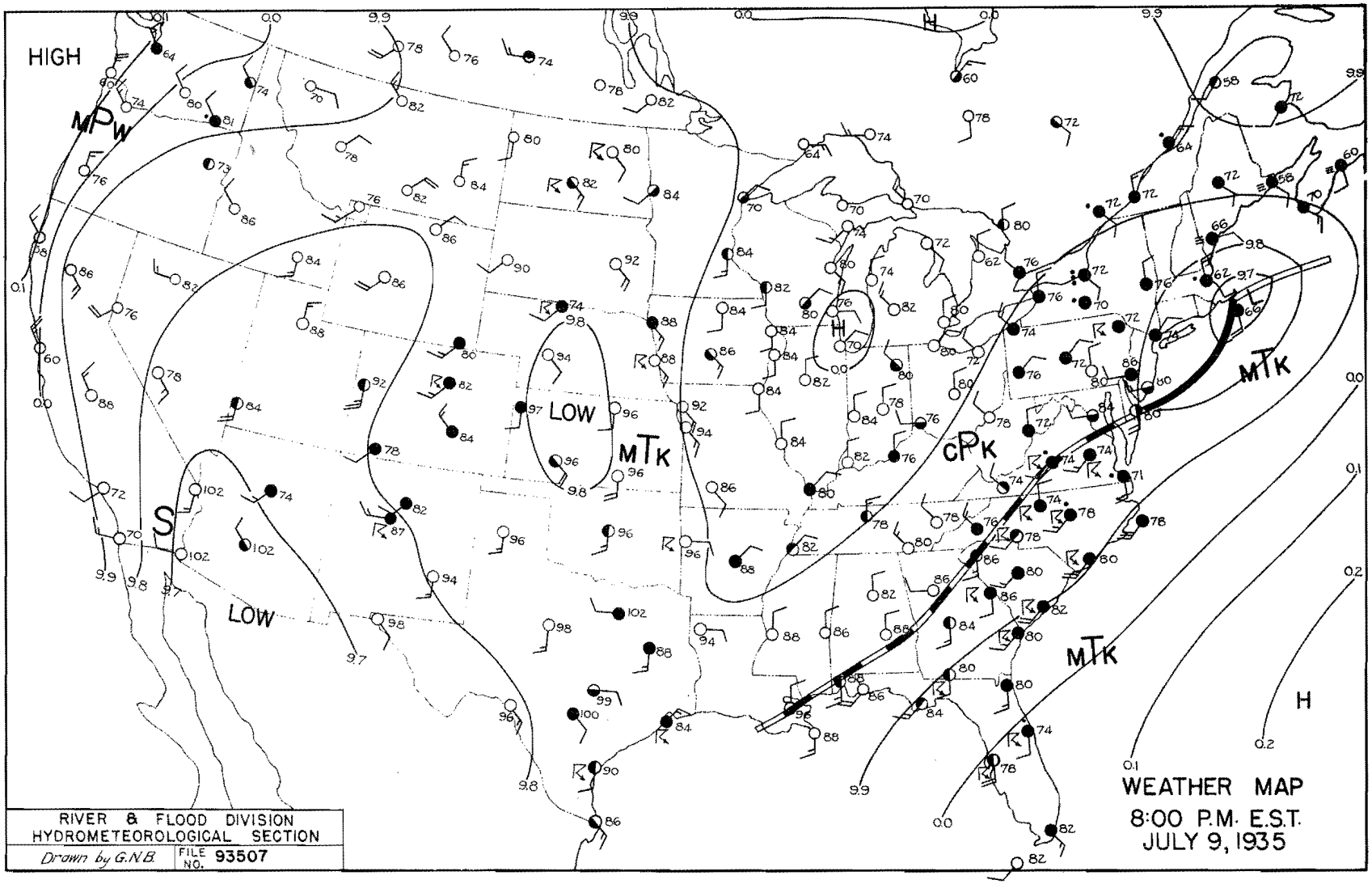
HIGH
mPw
LOW
mTk
cPk
S
LOW
mTk
H
WEATHER MAP
8:00 P.M. E.S.T.
JULY 9, 1935
RIVER & FLOOD DIVISION
HYDROMETEOROLOGICAL SECTION
Drawn by G.N.B.
FILE NO. 93507

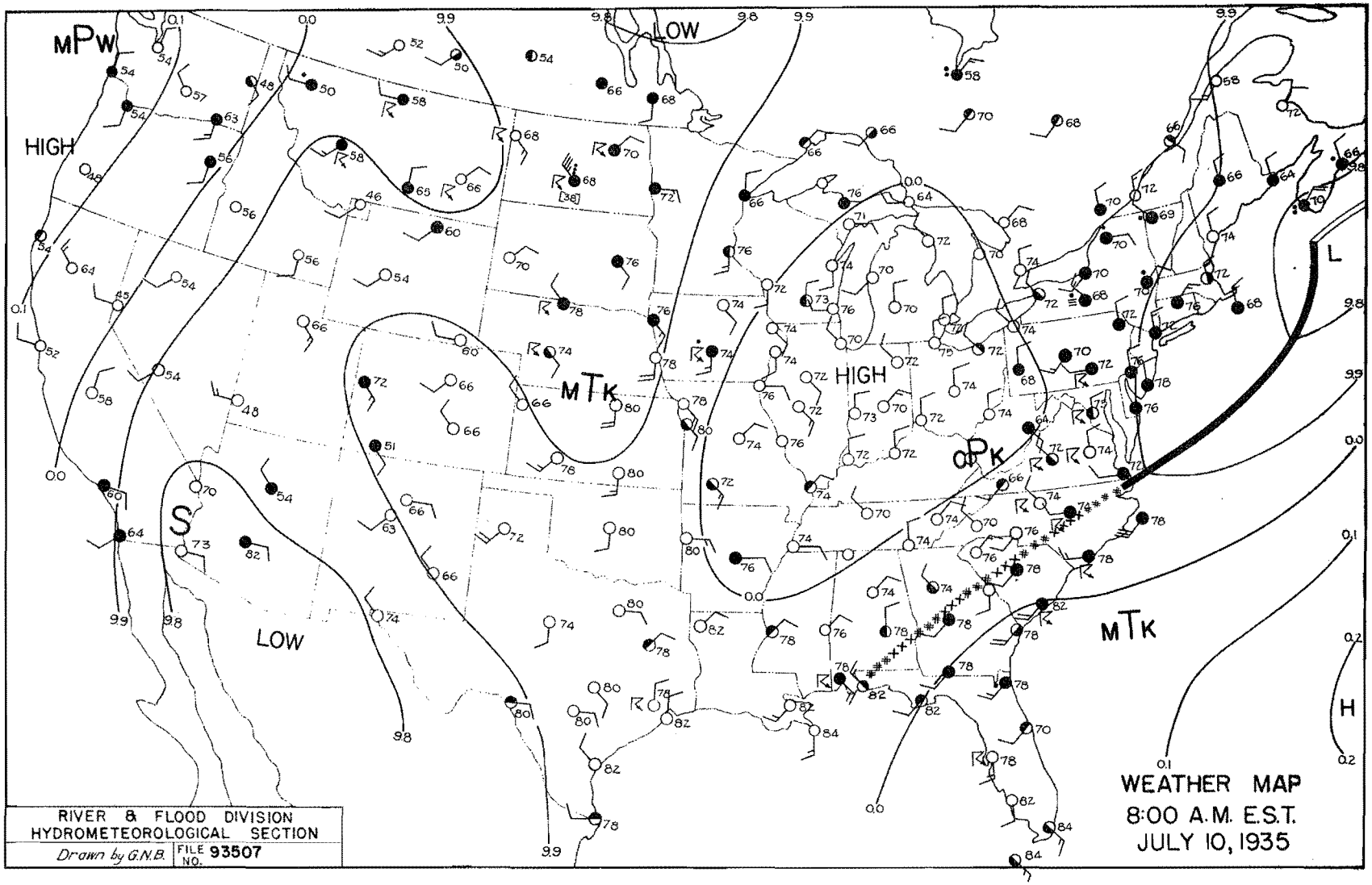
mPw
HIGH
LOW
mTk
HIGH
cPk
S
LOW
mTk
L
H
WEATHER MAP
8:00 A.M. E.S.T.
JULY 10, 1935
RIVER & FLOOD DIVISION
HYDROMETEOROLOGICAL SECTION
Drawn by G.N.B.
FILE NO. 93507

FIGURE A-47

FIGURE A-48

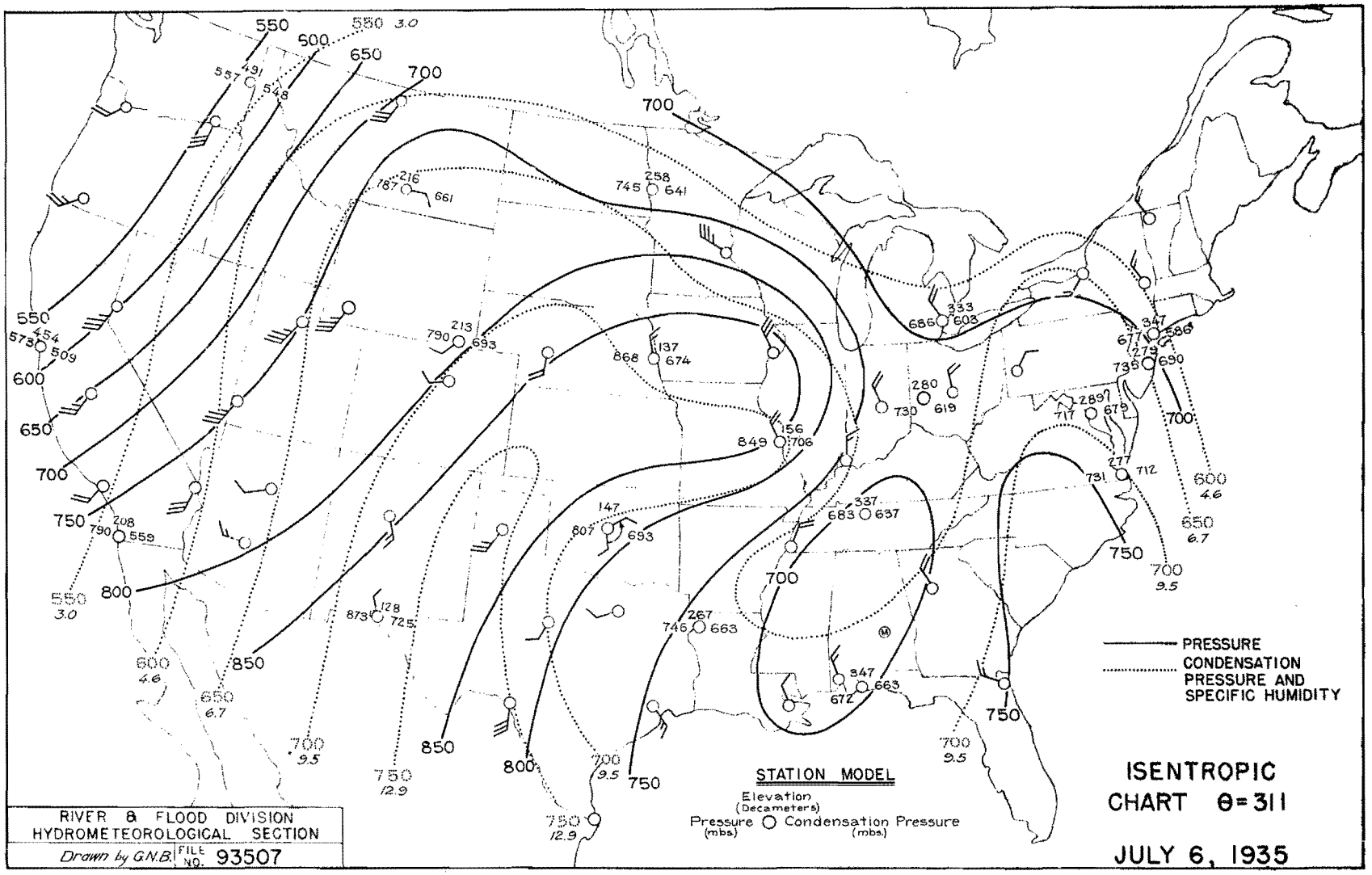
PRESSURE
CONDENSATION PRESSURE AND SPECIFIC HUMIDITY
STATION MODEL
Elevation (Decameters)
Pressure ○ Condensation Pressure (mbs.)
ISENTROPIC CHART θ=311
JULY 6, 1935
RIVER & FLOOD DIVISION
HYDROMETEOROLOGICAL SECTION
Drawn by G.N.B. FILE NO. 93507

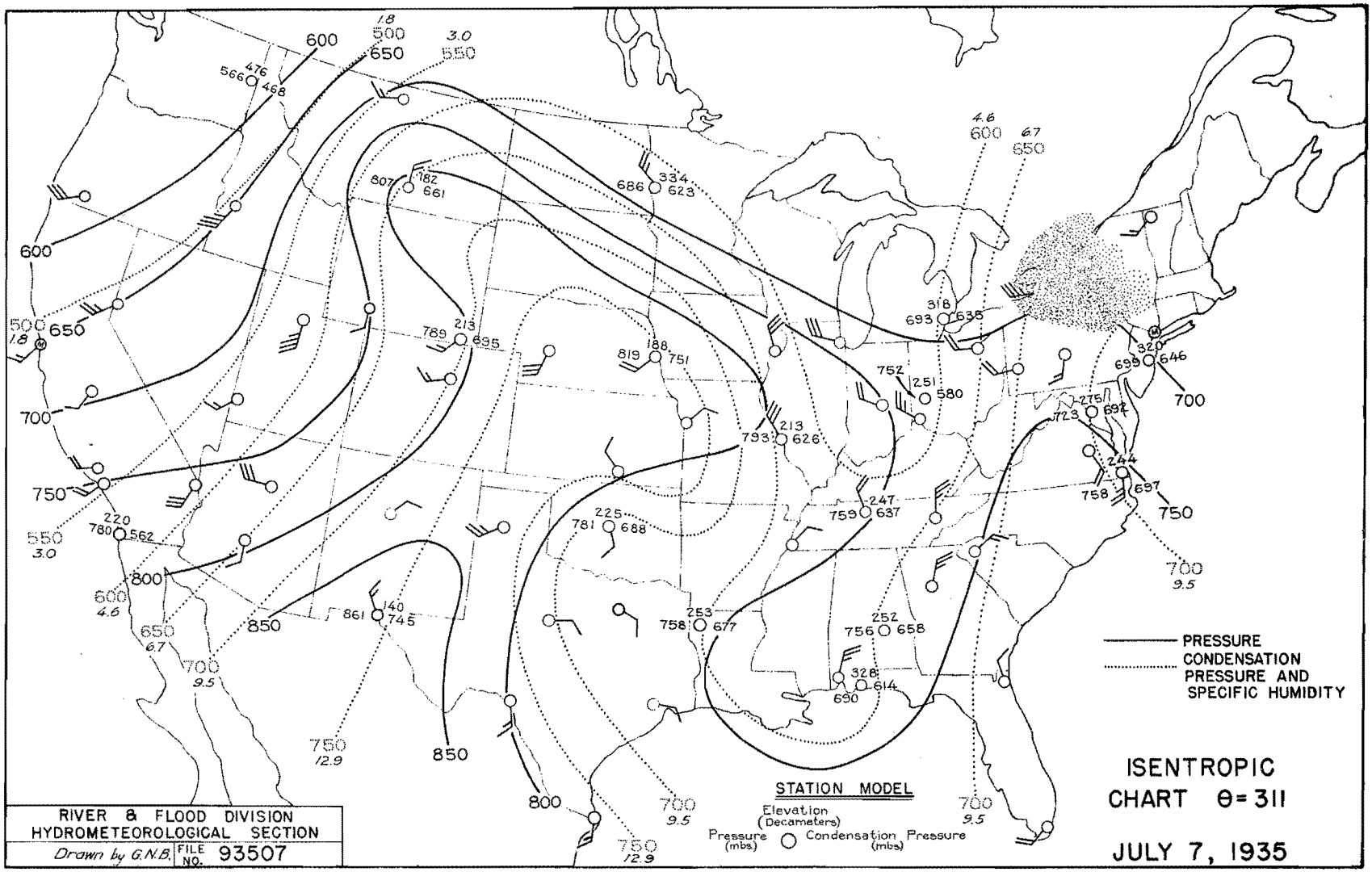
PRESSURE
CONDENSATION PRESSURE AND SPECIFIC HUMIDITY
STATION MODEL
Elevation (Decameters)
Pressure (mbs)
Condensation Pressure (mbs)
ISENTROPIC CHART θ = 311
JULY 7, 1935
RIVER & FLOOD DIVISION
HYDROMETEOROLOGICAL SECTION
Drawn by G.N.B.
FILE NO. 93507

FIGURE A-49

FIGURE A-50

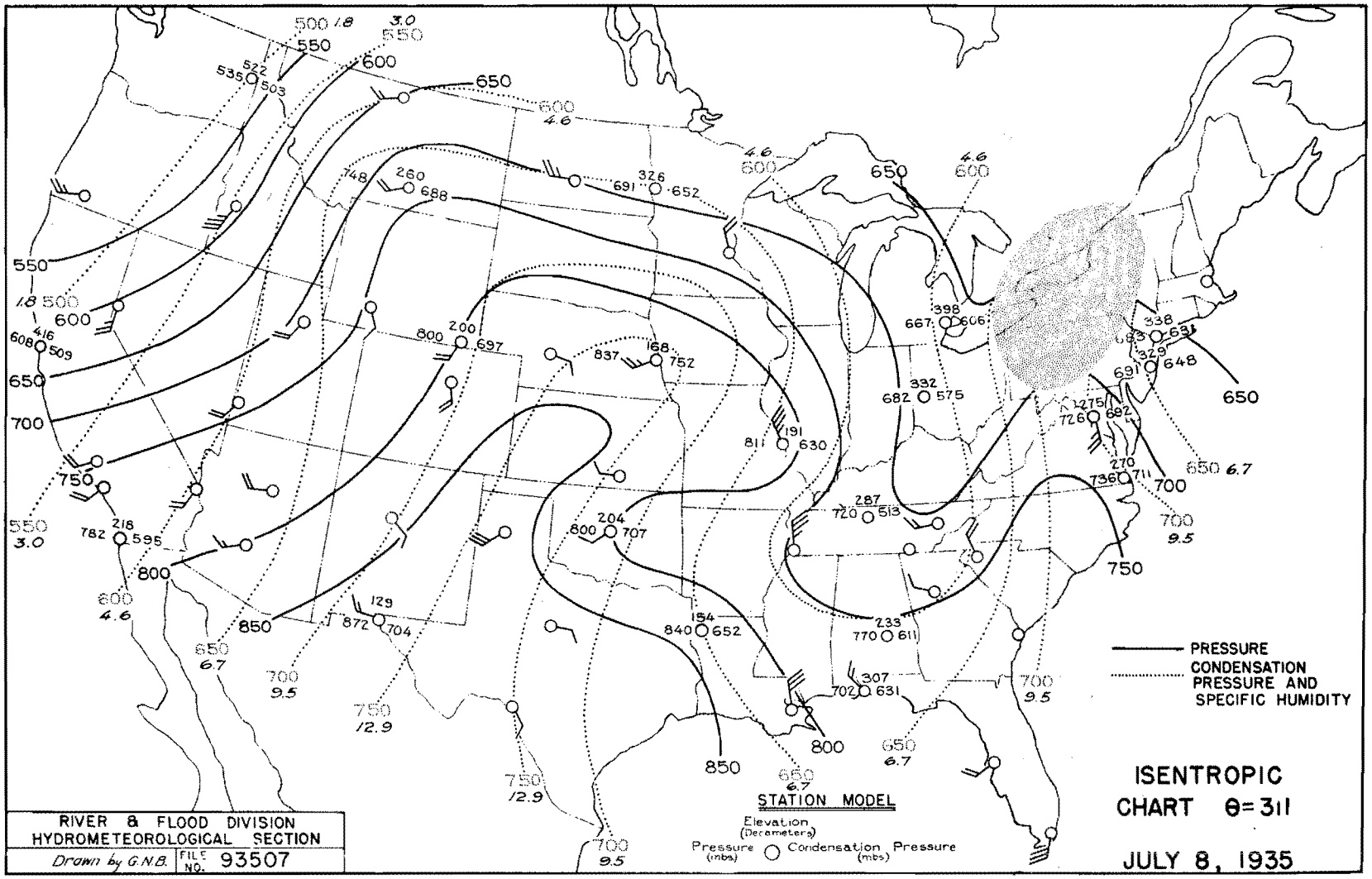
PRESSURE
CONDENSATION PRESSURE AND SPECIFIC HUMIDITY
ISENTROPIC CHART θ=311
JULY 8, 1935
STATION MODEL
Elevation (Decameters)
Pressure (mbs) Condensation Pressure (mbs)
RIVER & FLOOD DIVISION
HYDROMETEOROLOGICAL SECTION
Drawn by G.N.B.
FILE NO. 93507

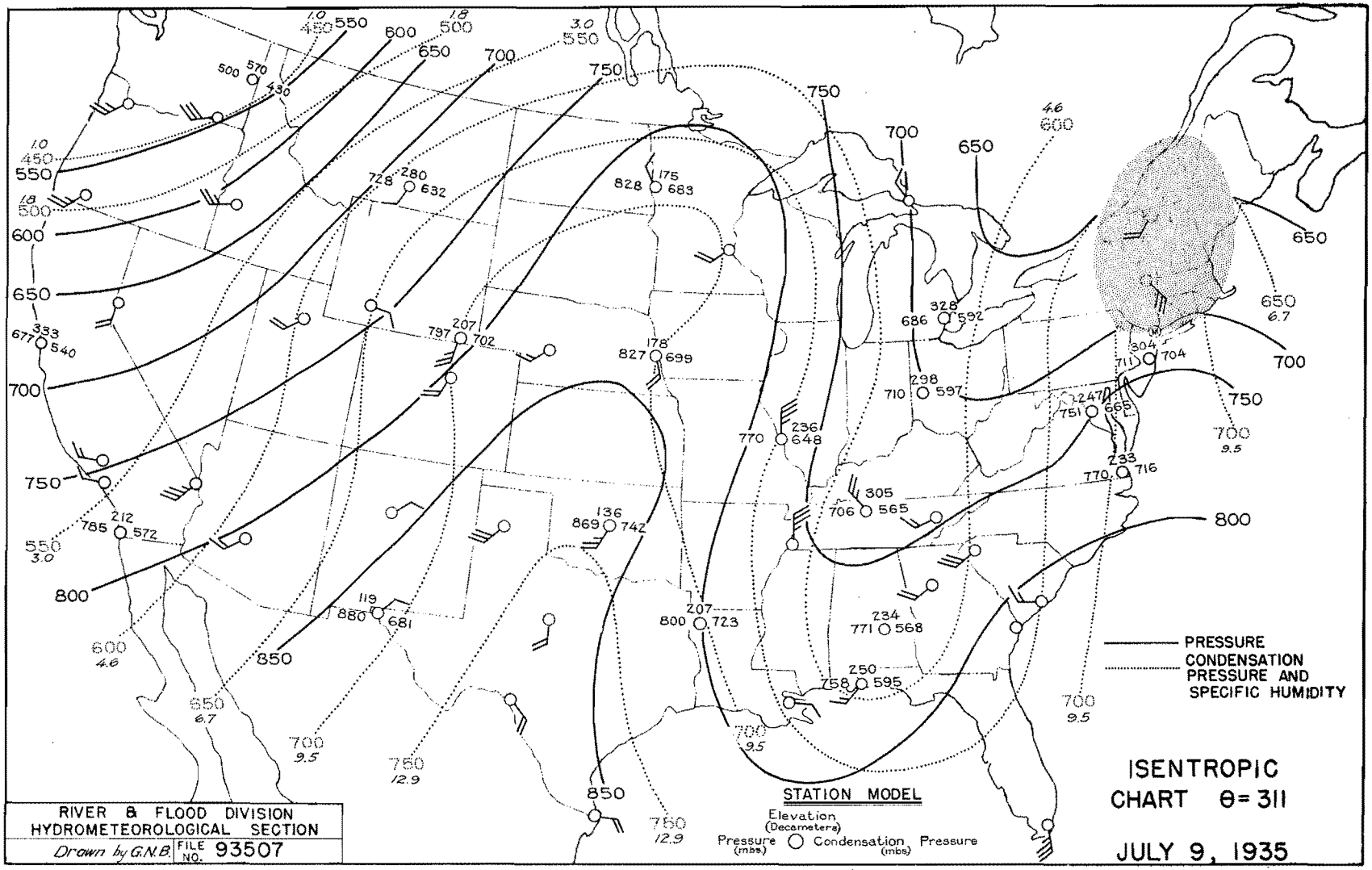
PRESSURE
CONDENSATION PRESSURE AND SPECIFIC HUMIDITY
ISENTROPIC CHART θ= 311
JULY 9, 1935
STATION MODEL
Elevation (Decametere)
Pressure (mbs)
Condensation Pressure (mbs)
RIVER & FLOOD DIVISION
HYDROMETEOROLOGICAL SECTION
Drawn by G.N.B.
FILE NO. 93507

FIGURE A-51

FIGURE A-52

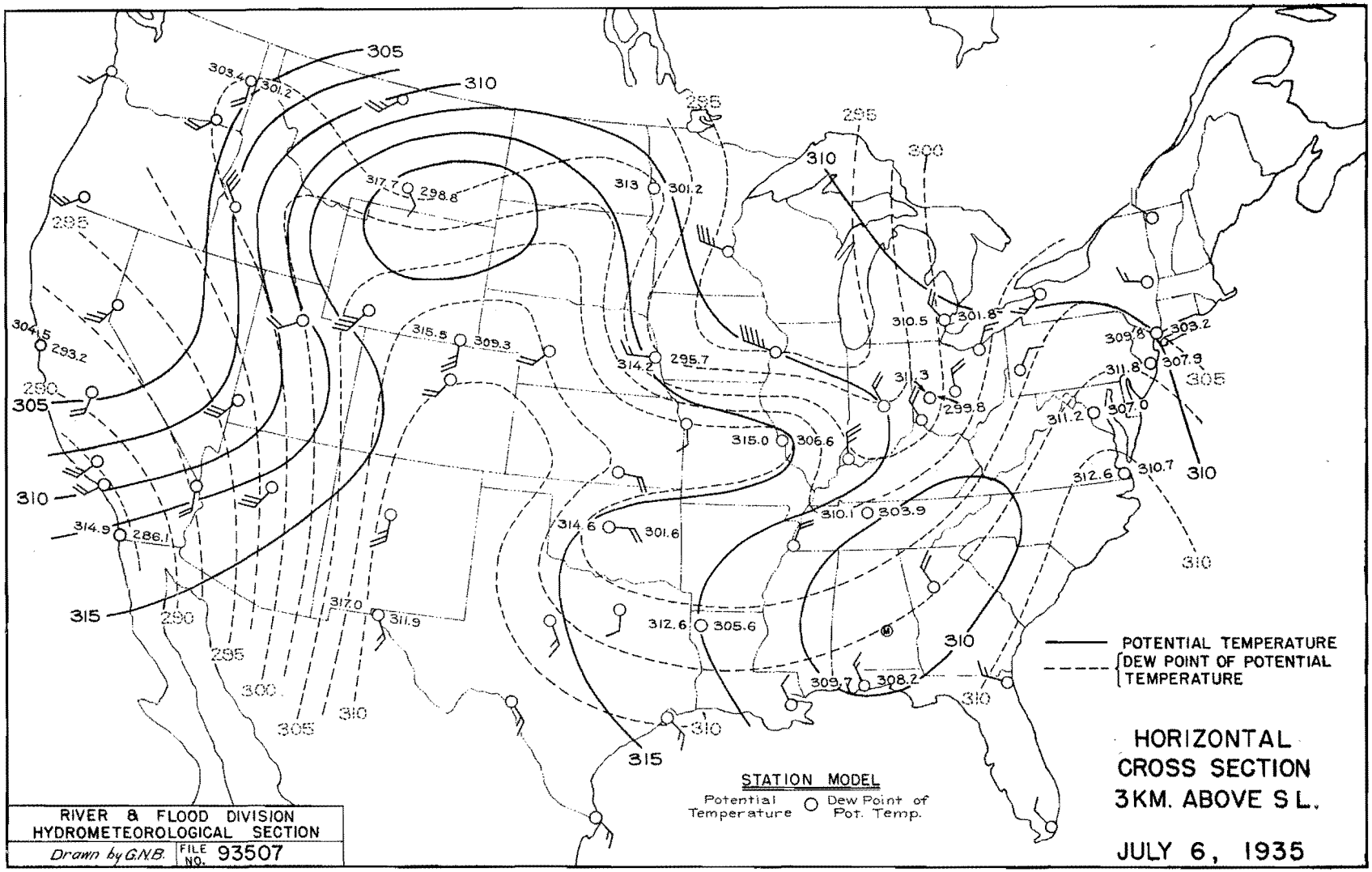
POTENTIAL TEMPERATURE
DEW POINT OF POTENTIAL TEMPERATURE
STATION MODEL
Potential Temperature
Dew Point of Pot. Temp.
HORIZONTAL CROSS SECTION 3KM. ABOVE S.L.
JULY 6, 1935
RIVER & FLOOD DIVISION
HYDROMETEOROLOGICAL SECTION
Drawn by G.N.B.
FILE NO. 93507

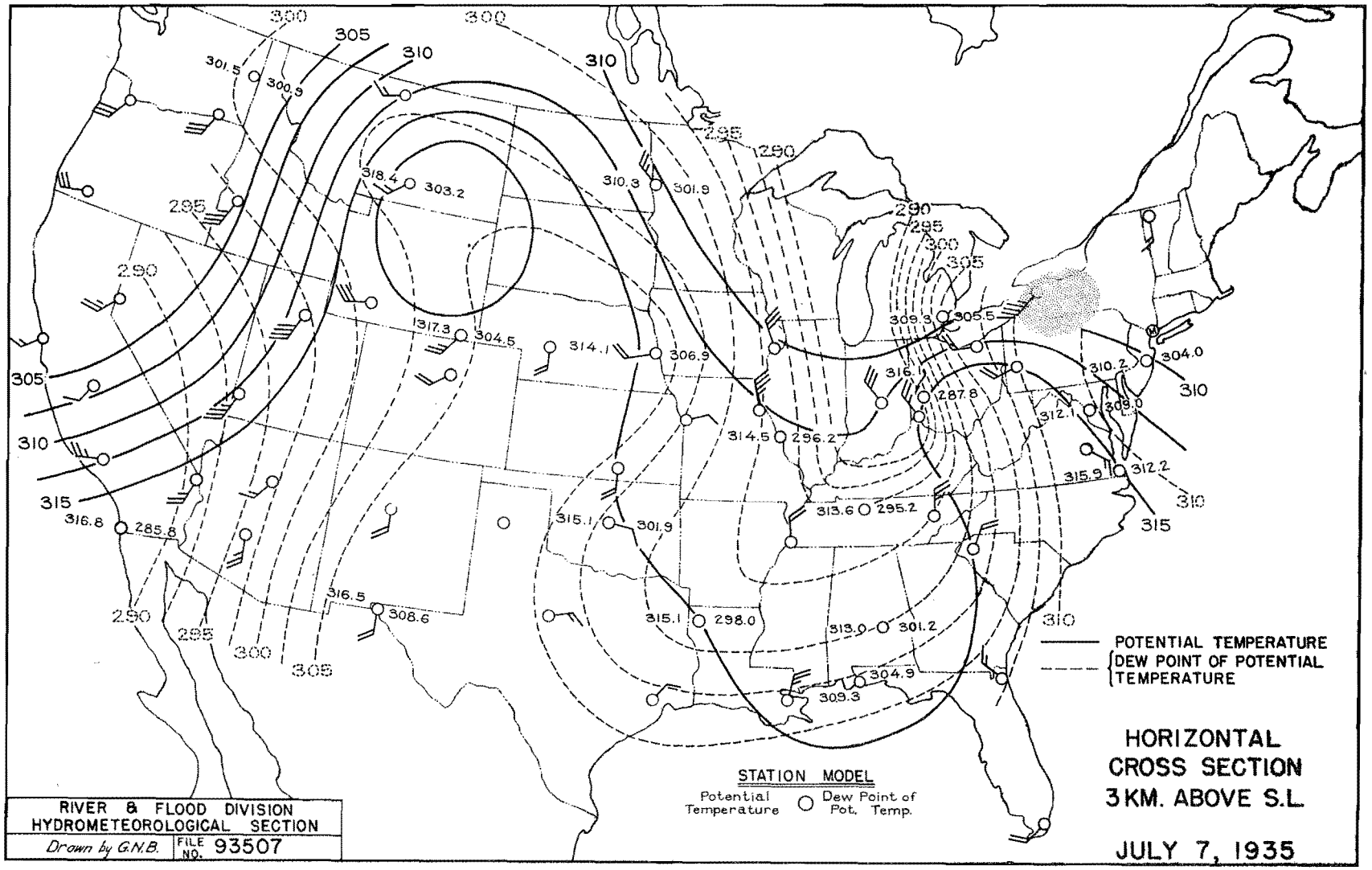
300
305
310
301.5
300.9
318.4
303.2
310.3
301.9
295
290
317.3
304.5
314.1
306.9
314.5
296.2
316.8
285.8
316.5
308.6
315.1
301.9
315.1
298.0
313.0
301.2
304.9
309.3
313.6
295.2
309.3
305.5
316.1
287.8
310.2
304.0
309.0
312.1
315.9
312.2
POTENTIAL TEMPERATURE
DEW POINT OF POTENTIAL TEMPERATURE
STATION MODEL
Potential Temperature
Dew Point of Pot. Temp.
HORIZONTAL CROSS SECTION 3 KM. ABOVE S.L.
JULY 7, 1935
RIVER & FLOOD DIVISION
HYDROMETEOROLOGICAL SECTION
Drawn by G.N.B.
FILE NO. 93507

FIGURE A-53

FIGURE A-54

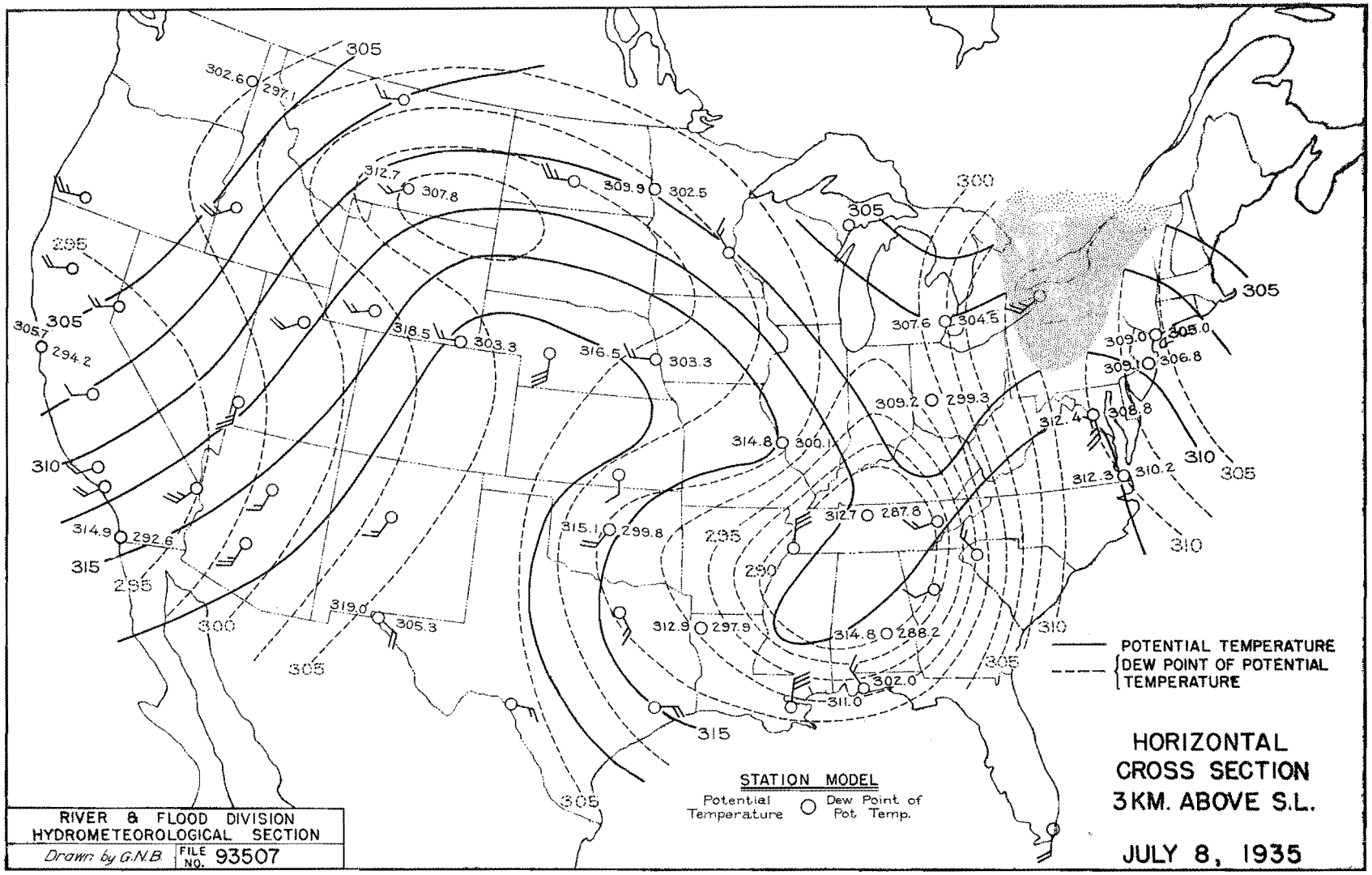
305
302.6
297.1
312.7
307.8
309.9
302.5
300
305
307.6
304.5
305
309.0
305.0
309.1
306.8
309.2
299.3
312.4
308.8
310
305
314.8
300.1
312.3
310.2
310
305.7
294.2
318.5
303.3
316.5
303.3
310
314.9
292.6
315
295
315.1
299.8
312.7
287.8
295
290
300
319.0
305.3
312.9
297.9
314.8
288.2
310
305
305
302.0
311.0
315
305
STATION MODEL
Potential Temperature
Dew Point of Pot Temp.
POTENTIAL TEMPERATURE
DEW POINT OF POTENTIAL TEMPERATURE
HORIZONTAL CROSS SECTION 3KM. ABOVE S.L.
JULY 8, 1935
RIVER & FLOOD DIVISION
HYDROMETEOROLOGICAL SECTION
Drawn by G.N.B.
FILE NO. 93507

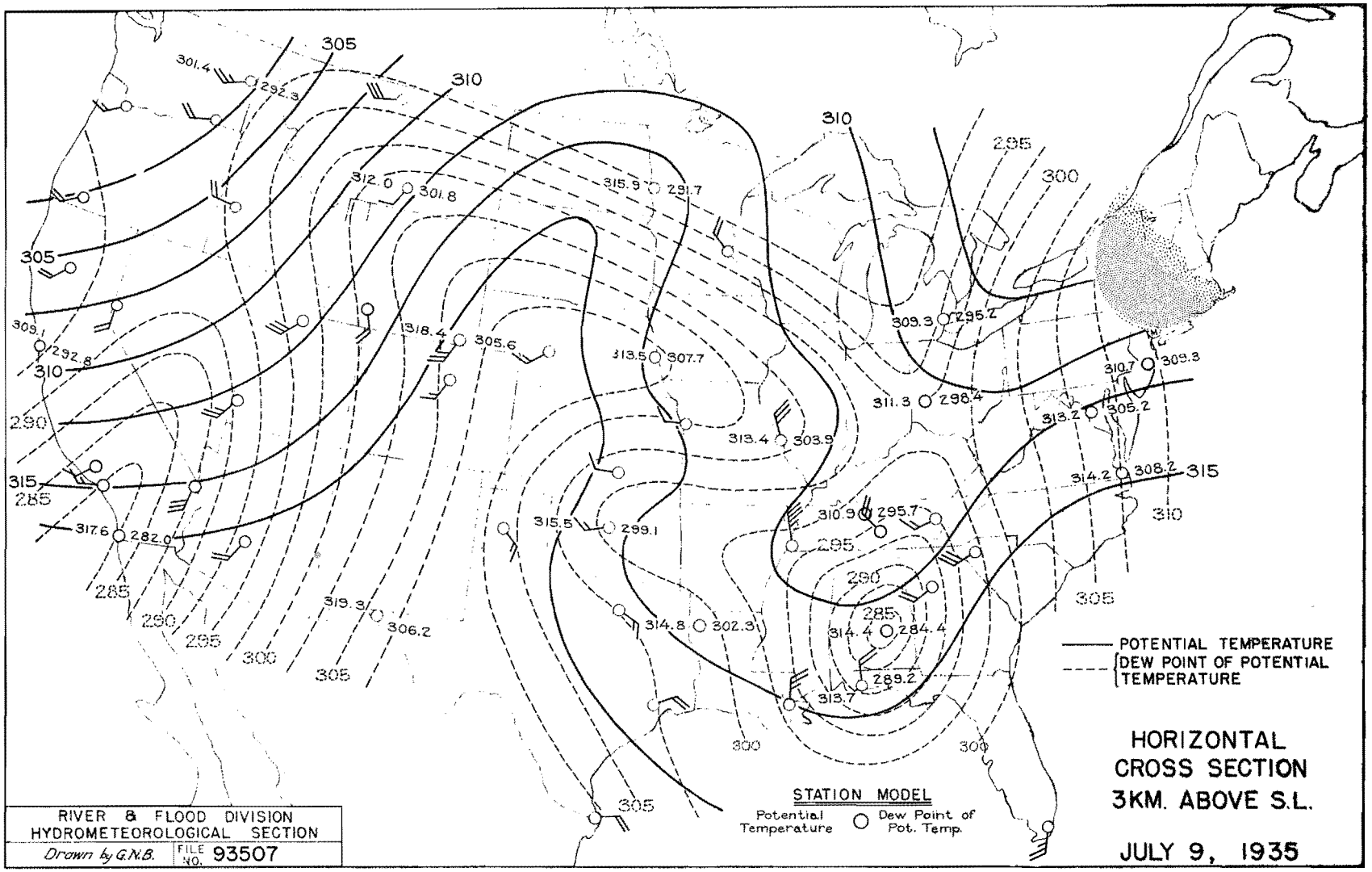
HORIZONTAL
CROSS SECTION
3KM. ABOVE S.L.
JULY 9, 1935
POTENTIAL TEMPERATURE
DEW POINT OF POTENTIAL TEMPERATURE
STATION MODEL
Potential Temperature
Dew Point of Pot. Temp.
RIVER & FLOOD DIVISION
HYDROMETEOROLOGICAL SECTION
Drawn by G.N.B.
FILE NO. 93507

FIGURE A-55

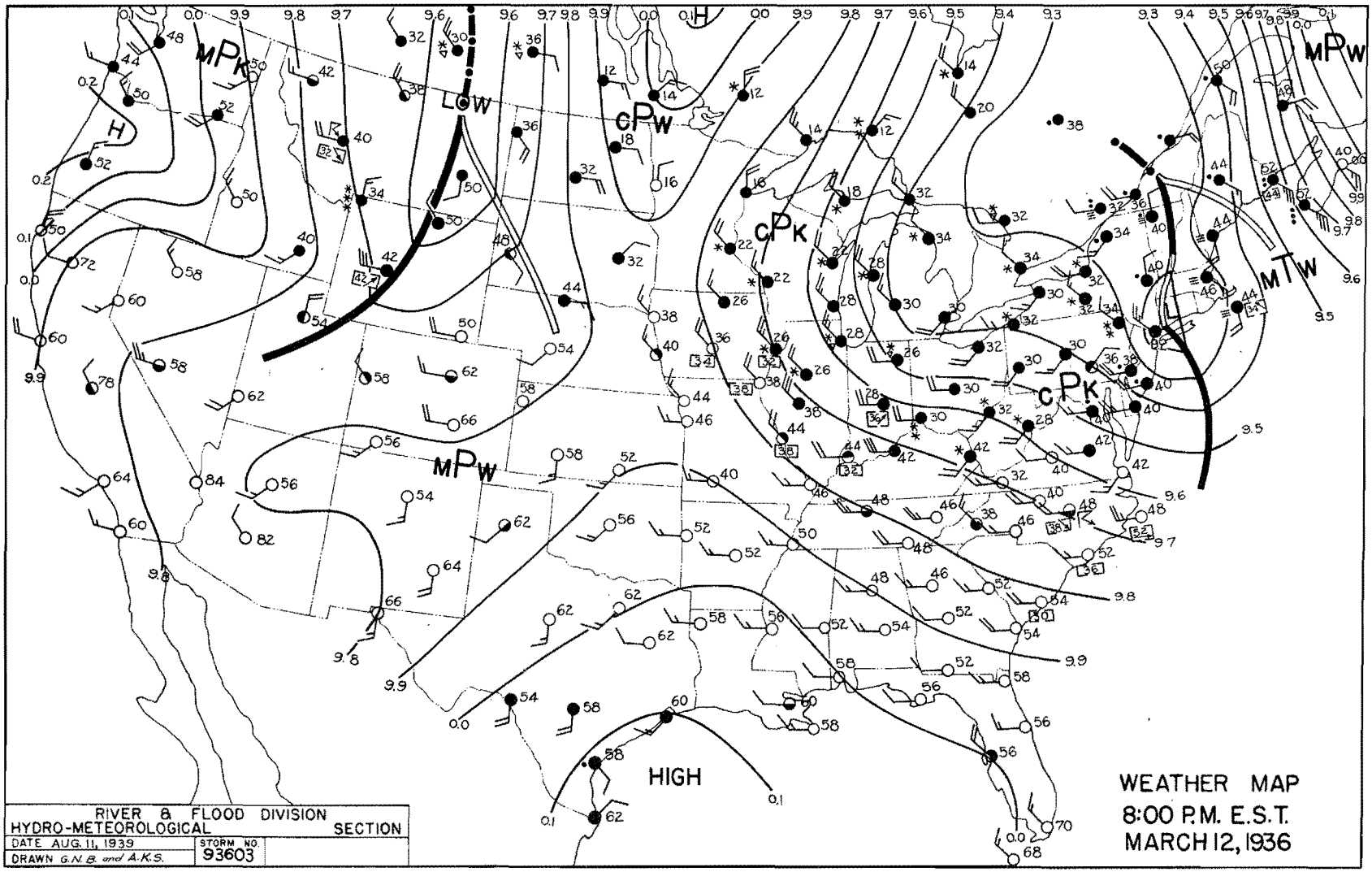
mPk
LOW
cPw
H
cPk
mPw
mTw
cPk
mPw
HIGH
WEATHER MAP
8:00 P.M. E.S.T.
MARCH 12, 1936
RIVER & FLOOD DIVISION
HYDRO-METEOROLOGICAL SECTION
DATE AUG. 11, 1939
STORM NO. 93603
DRAWN G.N.B. and A.K.S.

FIGURE A-57

FIGURE A-58

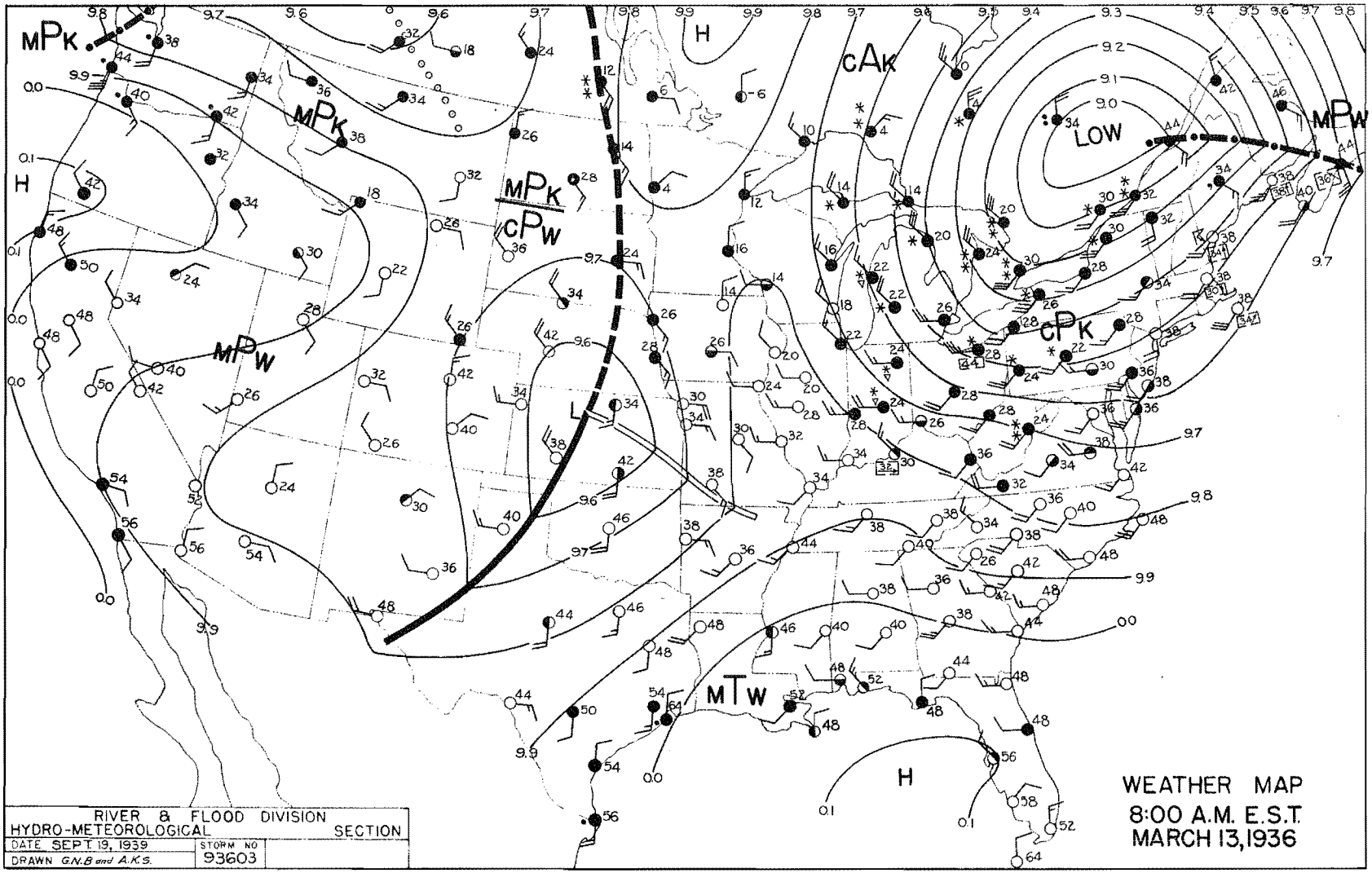
mPk
mPk
mPk
cPw
mPw
mPw
H
L
cAk
LOW
cPk
mTw
H
H
WEATHER MAP
8:00 A.M. E.S.T.
MARCH 13,1936
RIVER & FLOOD DIVISION
HYDRO-METEOROLOGICAL SECTION
DATE SEPT. 19, 1939
STORM NO 93603
DRAWN G.N.B and A.K.S.

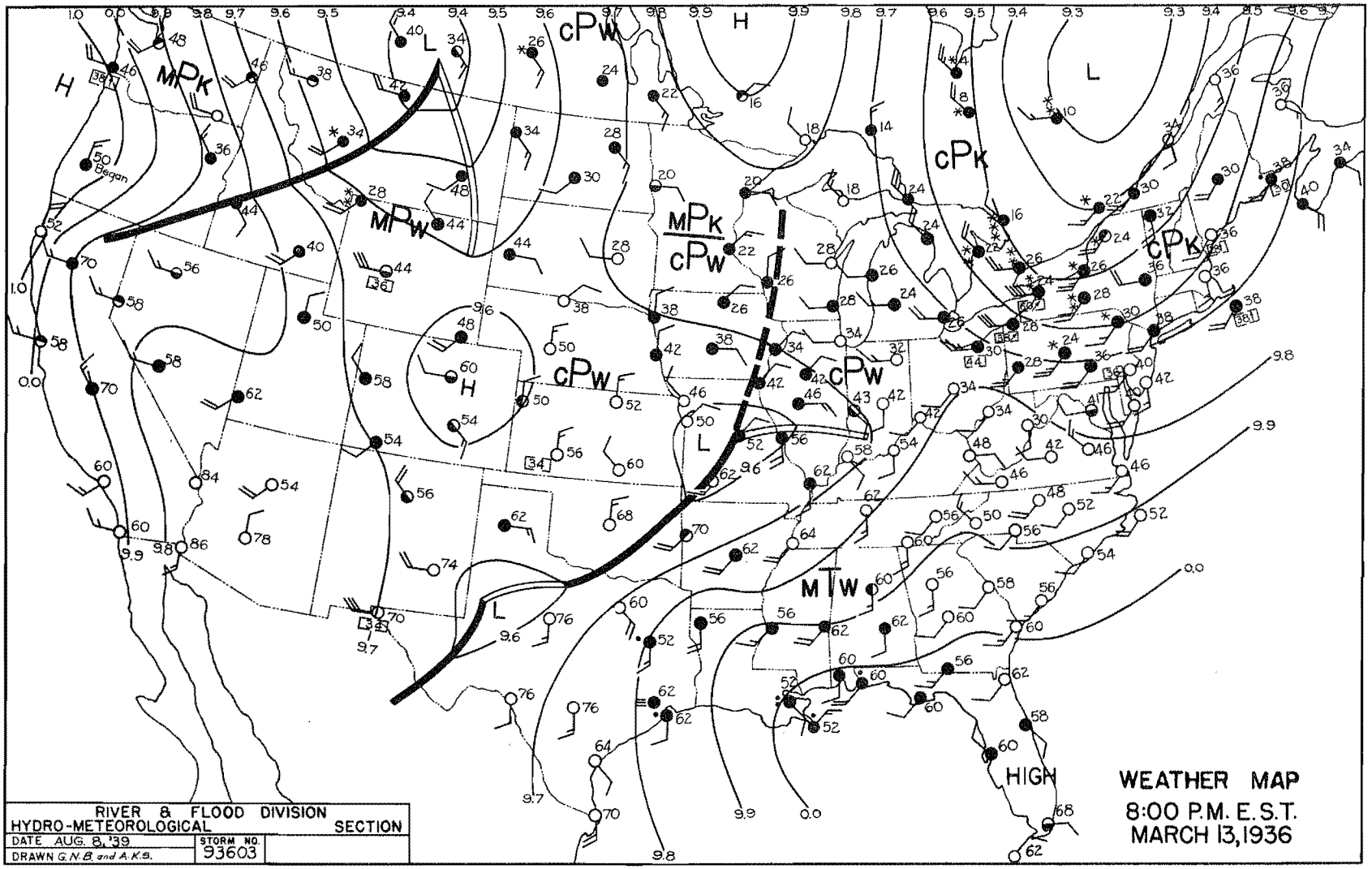
WEATHER MAP
8:00 P.M. E.S.T.
MARCH 13,1936
RIVER & FLOOD DIVISION
HYDRO-METEOROLOGICAL SECTION
DATE AUG. 8, '39
STORM NO. 93603
DRAWN G.N.B. and A.K.S.
cPw
mPk
mPw
cPk
mTw
HIGH
Began

FIGURE A-59

FIGURE A-60

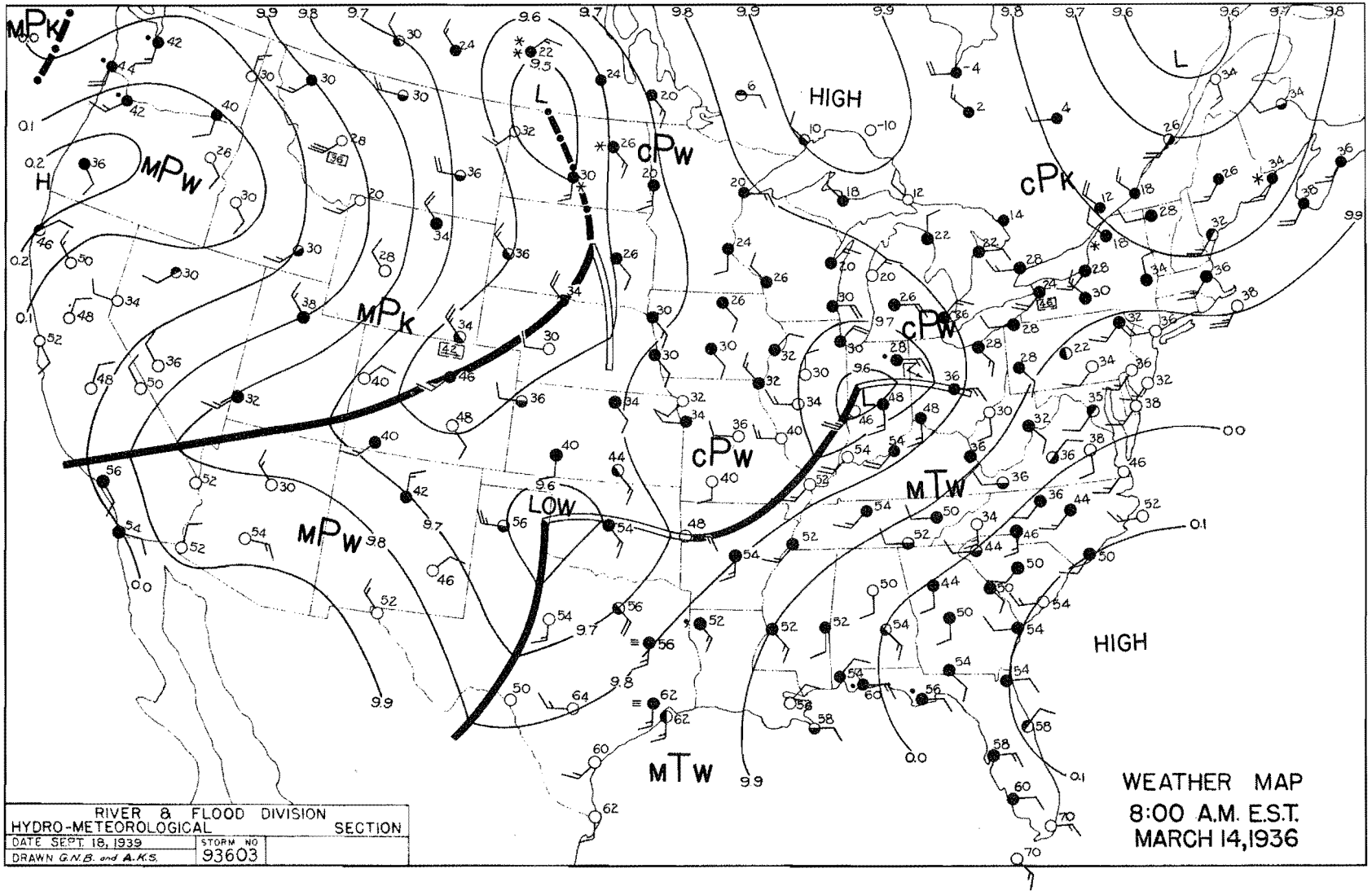
mPk
mPw
H
mPk
mPw
L
cPw
HIGH
cPw
cPk
L
cPw
L
mTw
LOW
mPw
HIGH
mTw
RIVER & FLOOD DIVISION
HYDRO-METEOROLOGICAL SECTION
DATE SEPT. 18, 1939
STORM NO 93603
DRAWN G.N.B. and A.K.S.
WEATHER MAP
8:00 A.M. E.S.T.
MARCH 14, 1936

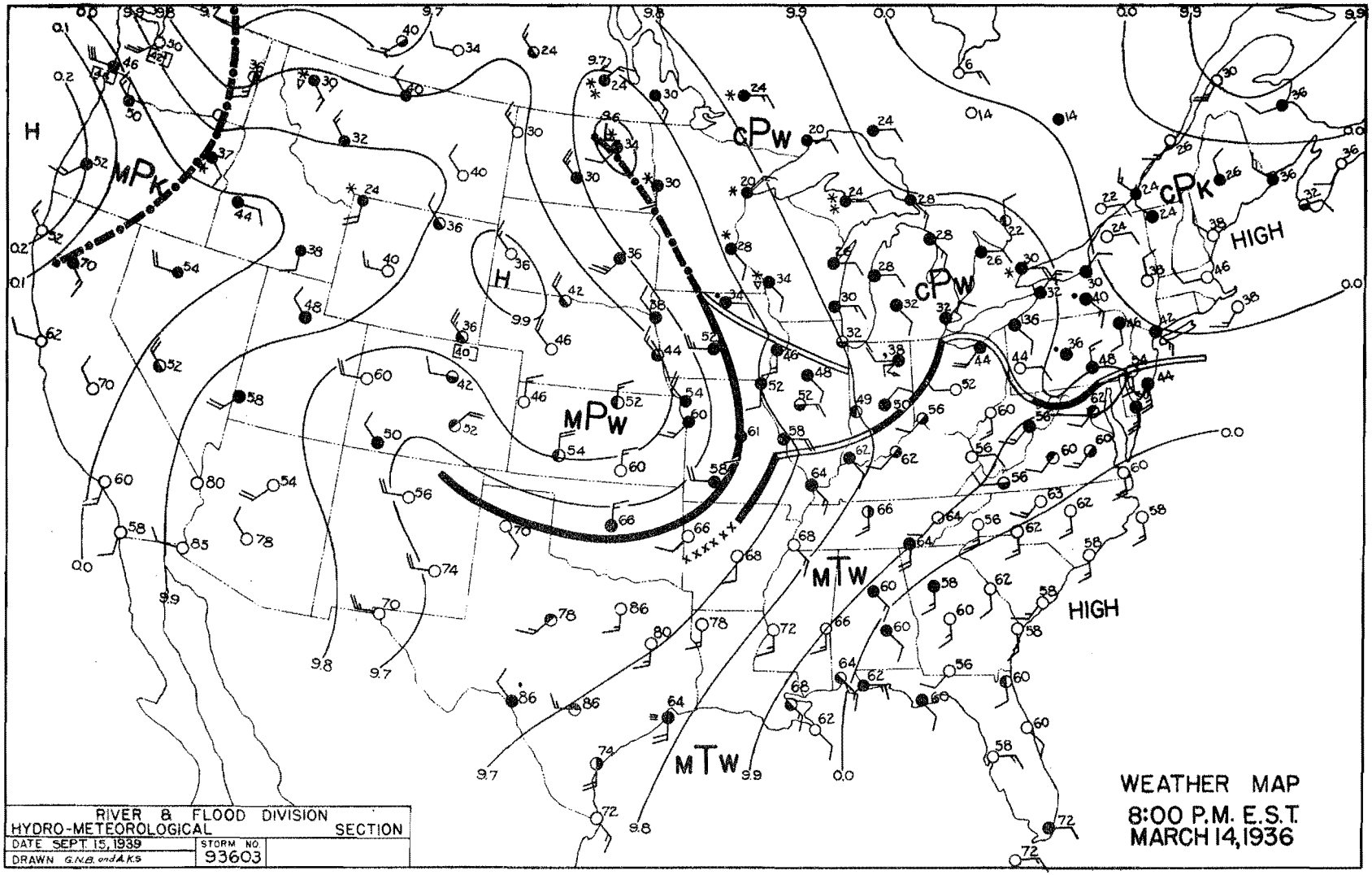
H
mPk
cPw
H
mPw
cPw
cPk
HIGH
mTw
HIGH
mTw
WEATHER MAP
8:00 P.M. E.S.T.
MARCH 14, 1936
RIVER & FLOOD DIVISION
HYDRO-METEOROLOGICAL SECTION
DATE SEPT. 15, 1939
STORM NO. 93603
DRAWN G.N.B. and A.K.S

FIGURE A-61

FIGURE A-62

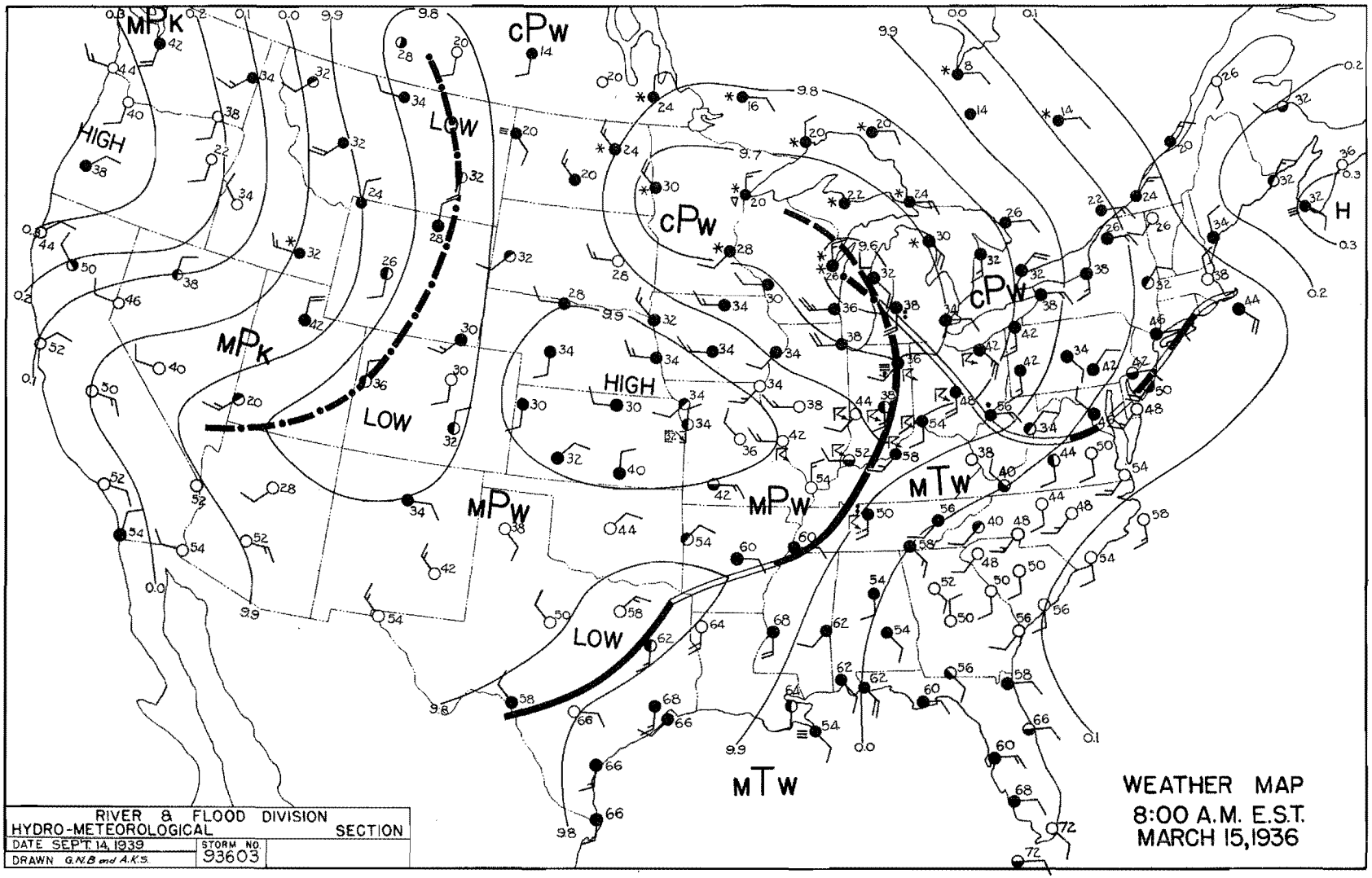
mPk
cPw
HIGH
LOW
mPw
mTw
H
WEATHER MAP
8:00 A.M. E.S.T.
MARCH 15,1936
RIVER & FLOOD DIVISION
HYDRO-METEOROLOGICAL SECTION
DATE SEPT. 14, 1939
STORM NO. 93603
DRAWN G.N.B and A.K.S.

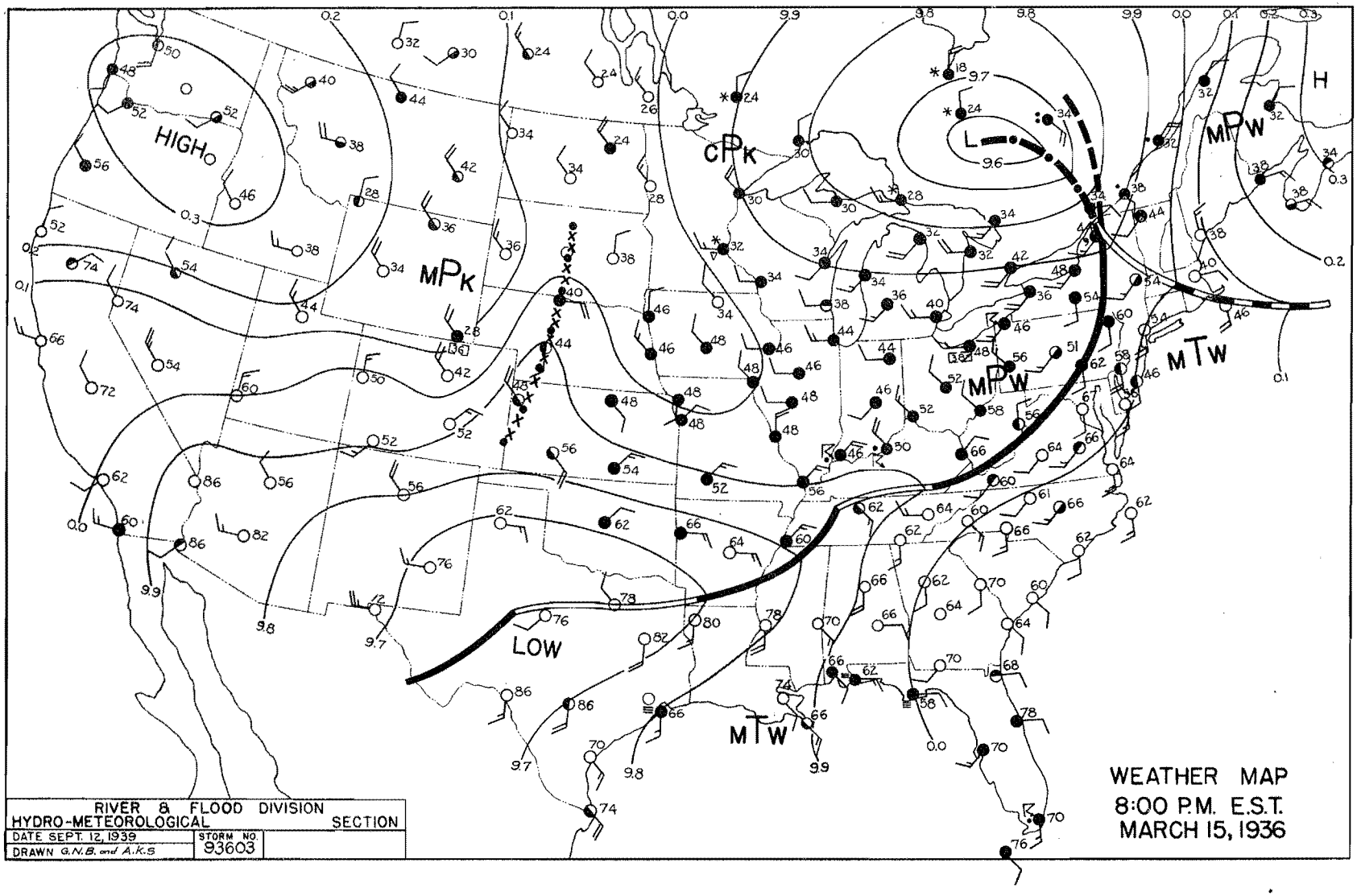
HIGH
MPK
CPK
L
MPW
MPW
MTW
H
LOW
MTW
WEATHER MAP
8:00 P.M. E.S.T.
MARCH 15, 1936
RIVER & FLOOD DIVISION
HYDRO-METEOROLOGICAL SECTION
DATE SEPT. 12, 1939
STORM NO. 93603
DRAWN G.N.B. and A.K.S

FIGURE A-63

FIGURE A-64

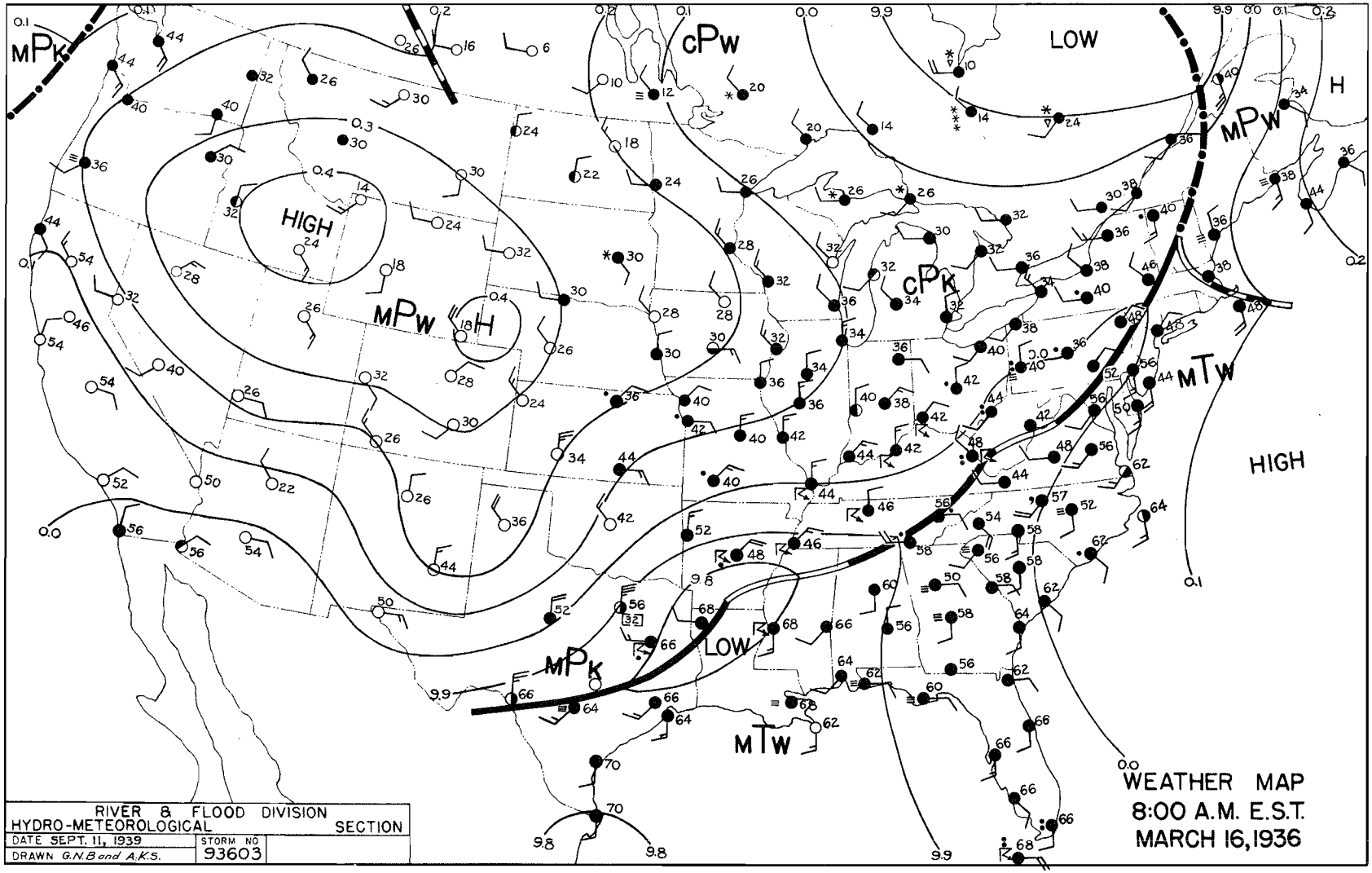
mPk
cPw
LOW
H
mPw
HIGH
cPk
mTw
HIGH
LOW
mPk
mTw
WEATHER MAP
8:00 A.M. E.S.T.
MARCH 16, 1936
RIVER & FLOOD DIVISION
HYDRO-METEOROLOGICAL SECTION
DATE SEPT. 11, 1939
STORM NO 93603
DRAWN G.N.B and A.K.S.

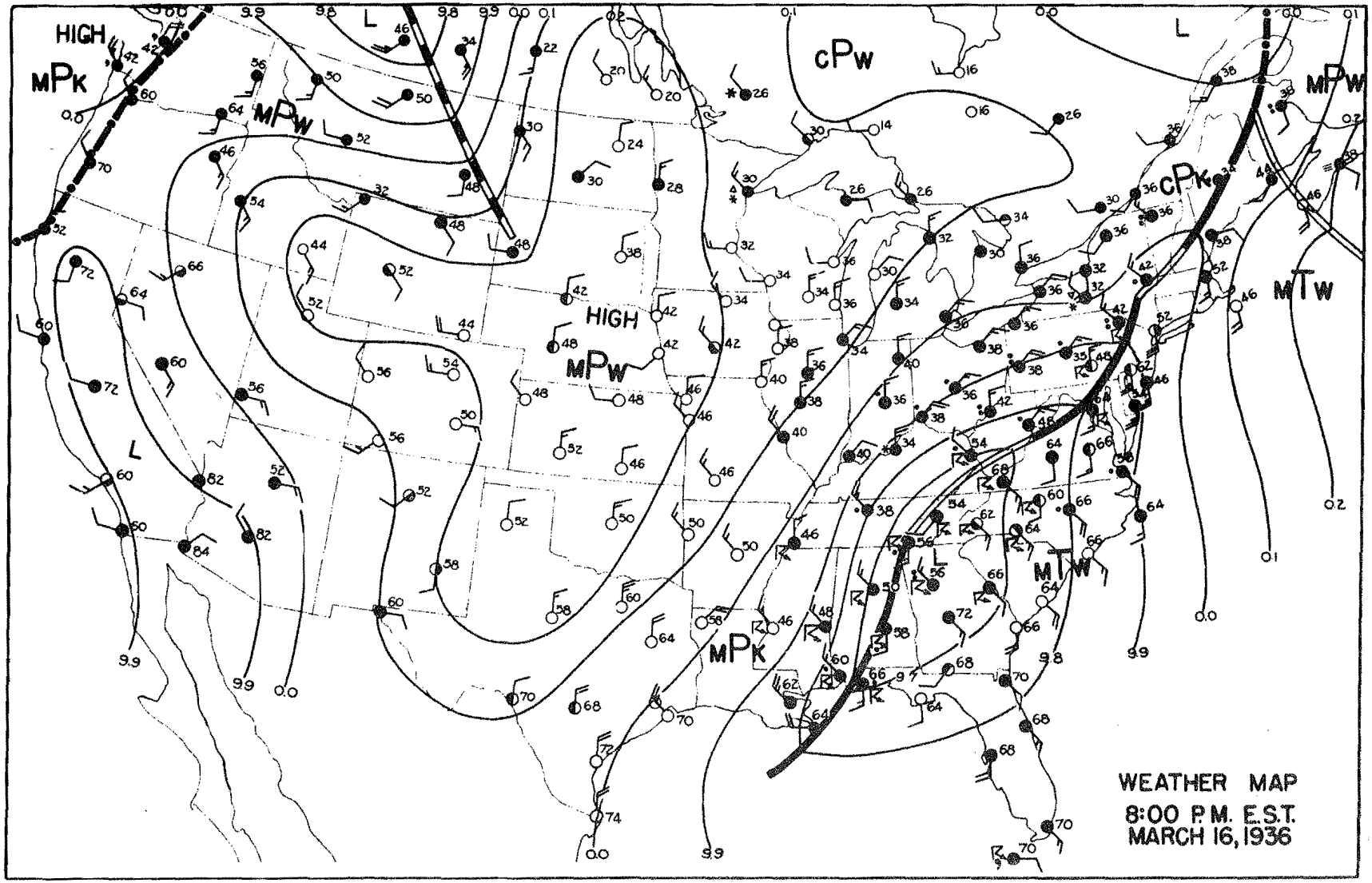
HIGH
mPK
mPW
L
cPW
cPK
mTW
HIGH
mPW
L
mTW
mPK
WEATHER MAP
8:00 P.M. E.S.T.
MARCH 16, 1936

FIGURE A-65

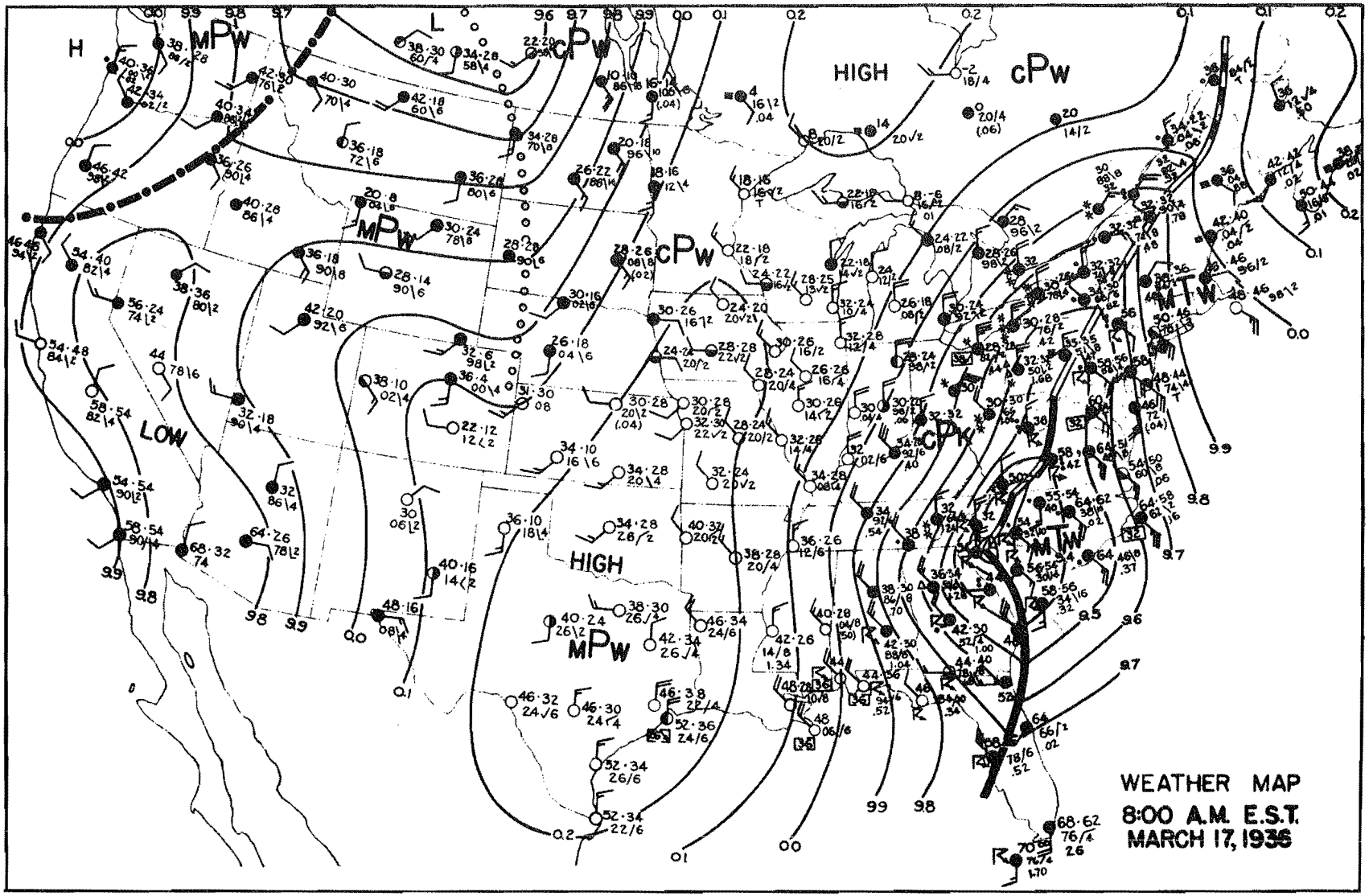
H
L
HIGH
HIGH
LOW
cPw
cPw
cPw
cPk
MPw
MPw
MPw
MTW
MTW
WEATHER MAP
8:00 A.M. E.S.T.
MARCH 17, 1936

FIGURE A-66

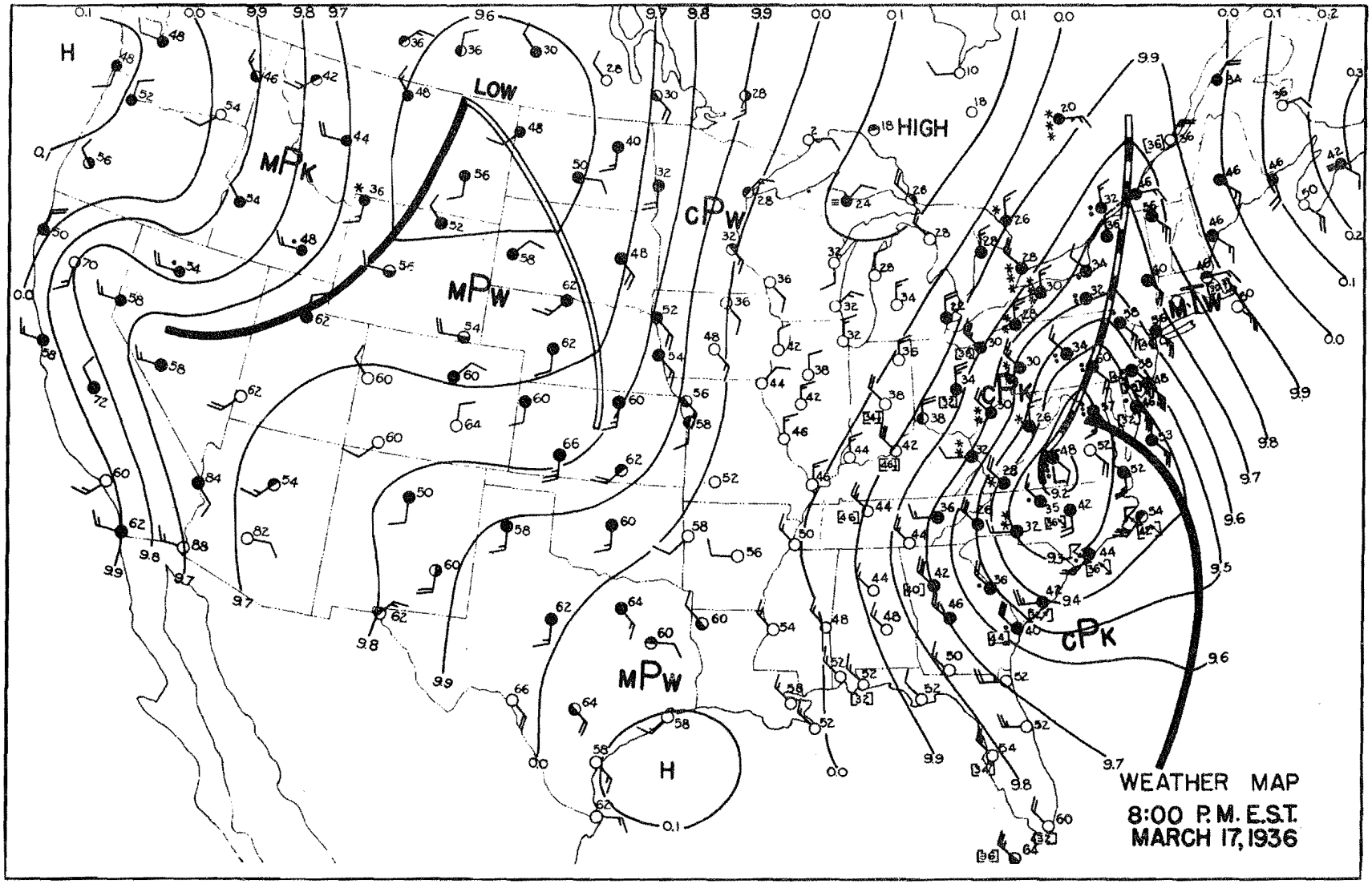
H
LOW
HIGH
mPk
mPw
cPw
cPk
mPw
H
WEATHER MAP
8:00 P.M. E.S.T.
MARCH 17, 1936

FIGURE A-67

FIGURE A-68

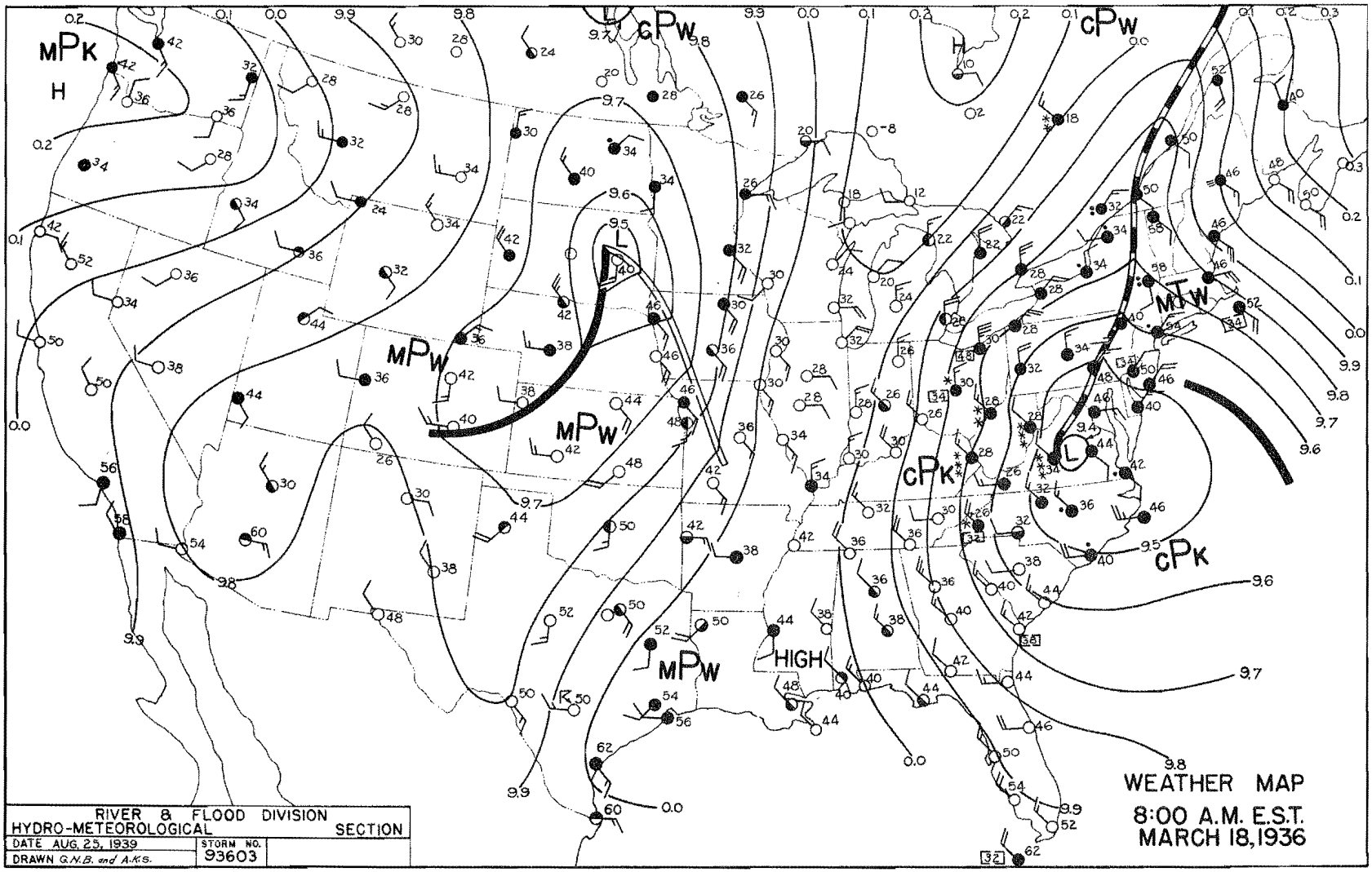
mPK
H
cPW
9.7
9.8
9.9
0.0
0.1
0.2
mPW
9.6
9.5
L
cPW
H
MTW
cPK
9.4
L
9.5
cPK
9.6
9.7
9.8
HIGH
mPW
mPW
9.9
0.0
WEATHER MAP
8:00 A.M. E.S.T.
MARCH 18,1936
RIVER & FLOOD DIVISION
HYDRO-METEOROLOGICAL SECTION
DATE AUG. 25, 1939
STORM NO. 93603
DRAWN G.N.B. and A.K.S.

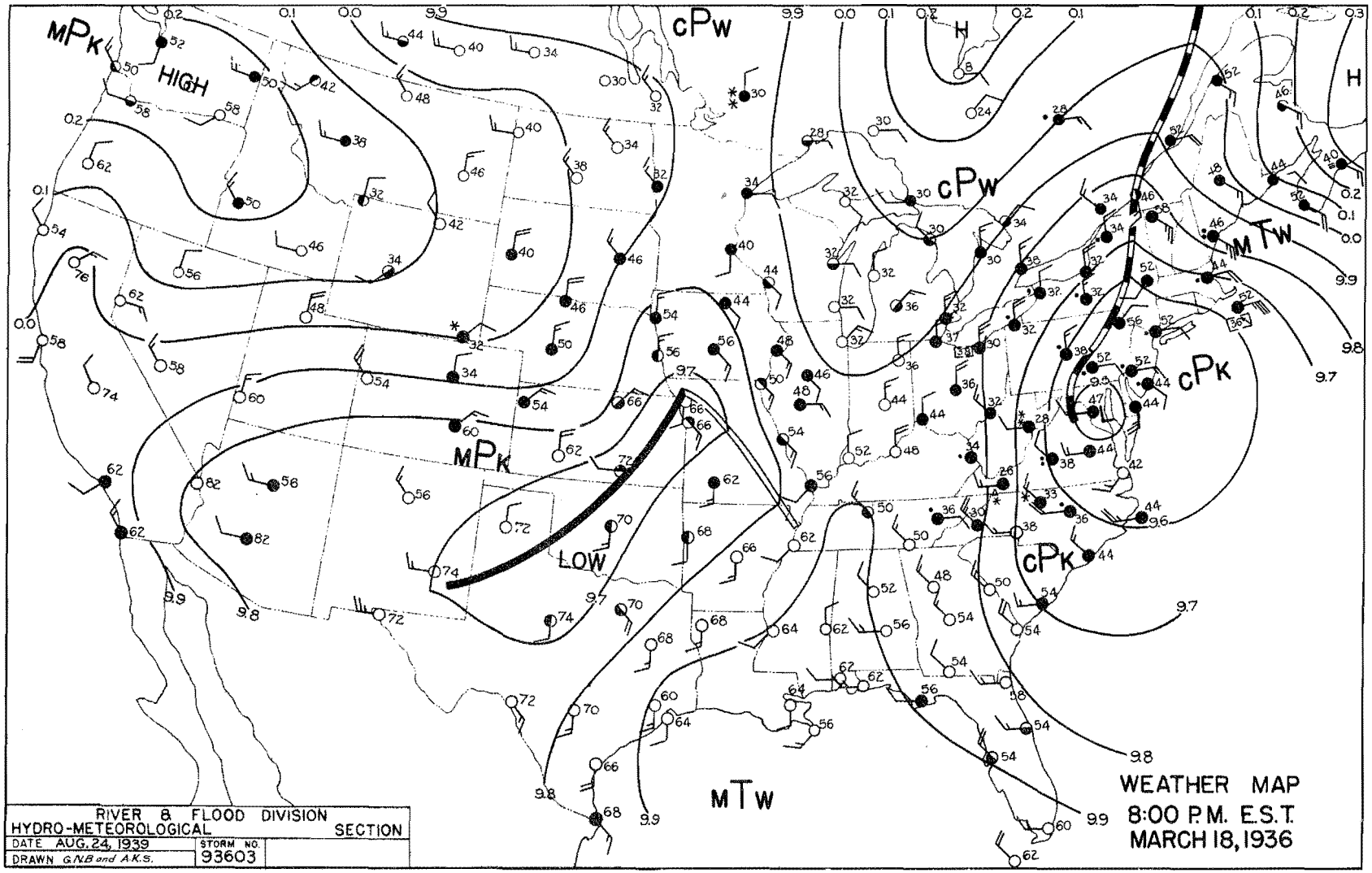
mPK
HIGH
cPW
H
cPW
mTW
cPK
mPK
LOW
cPK
mTW
WEATHER MAP
8:00 P.M. E.S.T.
MARCH 18, 1936
RIVER & FLOOD DIVISION
HYDRO-METEOROLOGICAL SECTION
DATE AUG. 24, 1939
STORM NO. 93603
DRAWN G.N.B and A.K.S.

FIGURE A-69

FIGURE A-70

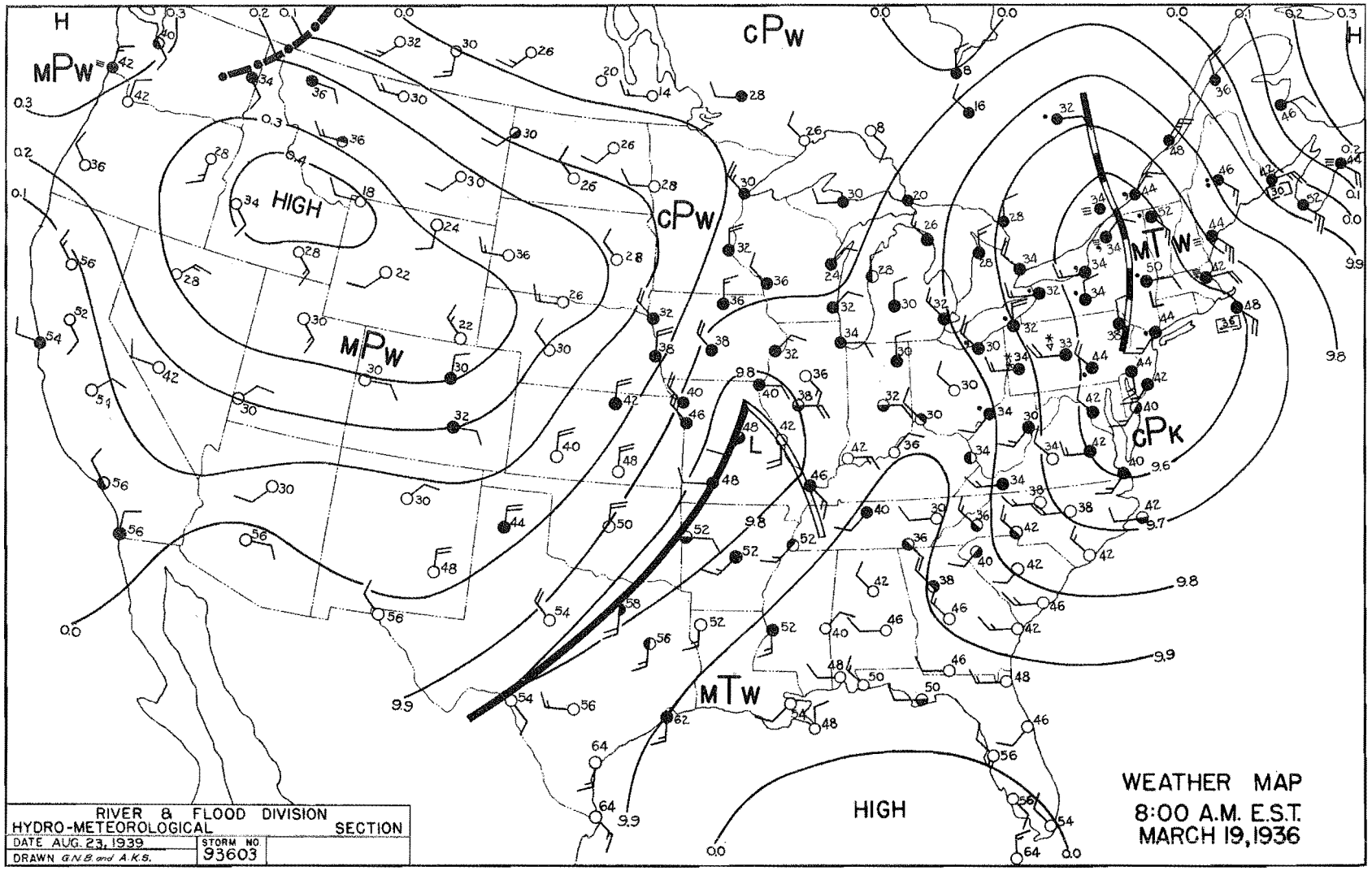
H
mPw
HIGH
cPw
mPw
cPw
L
mTw
mTw
L
cPk
HIGH
H
WEATHER MAP
8:00 A.M. E.S.T.
MARCH 19, 1936
RIVER & FLOOD DIVISION
HYDRO-METEOROLOGICAL SECTION
DATE AUG. 23, 1939
STORM NO 93603
DRAWN G.N.B. and A.K.S.

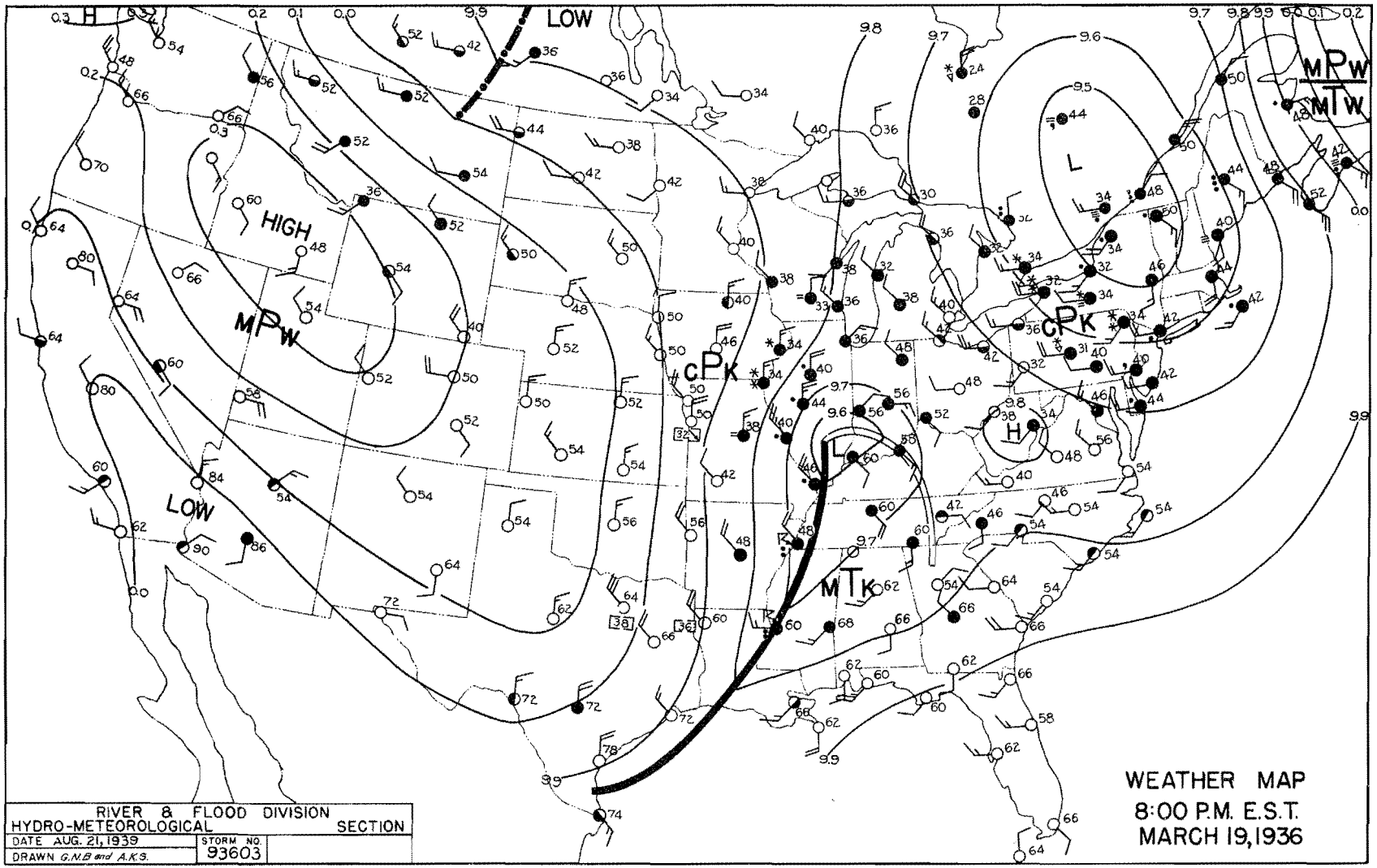
LOW
HIGH
MPW
LOW
cPK
cPK
MTK
L
H
L
MPW
MTW
WEATHER MAP
8:00 P.M. E.S.T.
MARCH 19,1936
RIVER & FLOOD DIVISION
HYDRO-METEOROLOGICAL SECTION
DATE AUG. 21, 1939
STORM NO. 93603
DRAWN G.N.B and A.K.S.

FIGURE A-71

FIGURE A-72

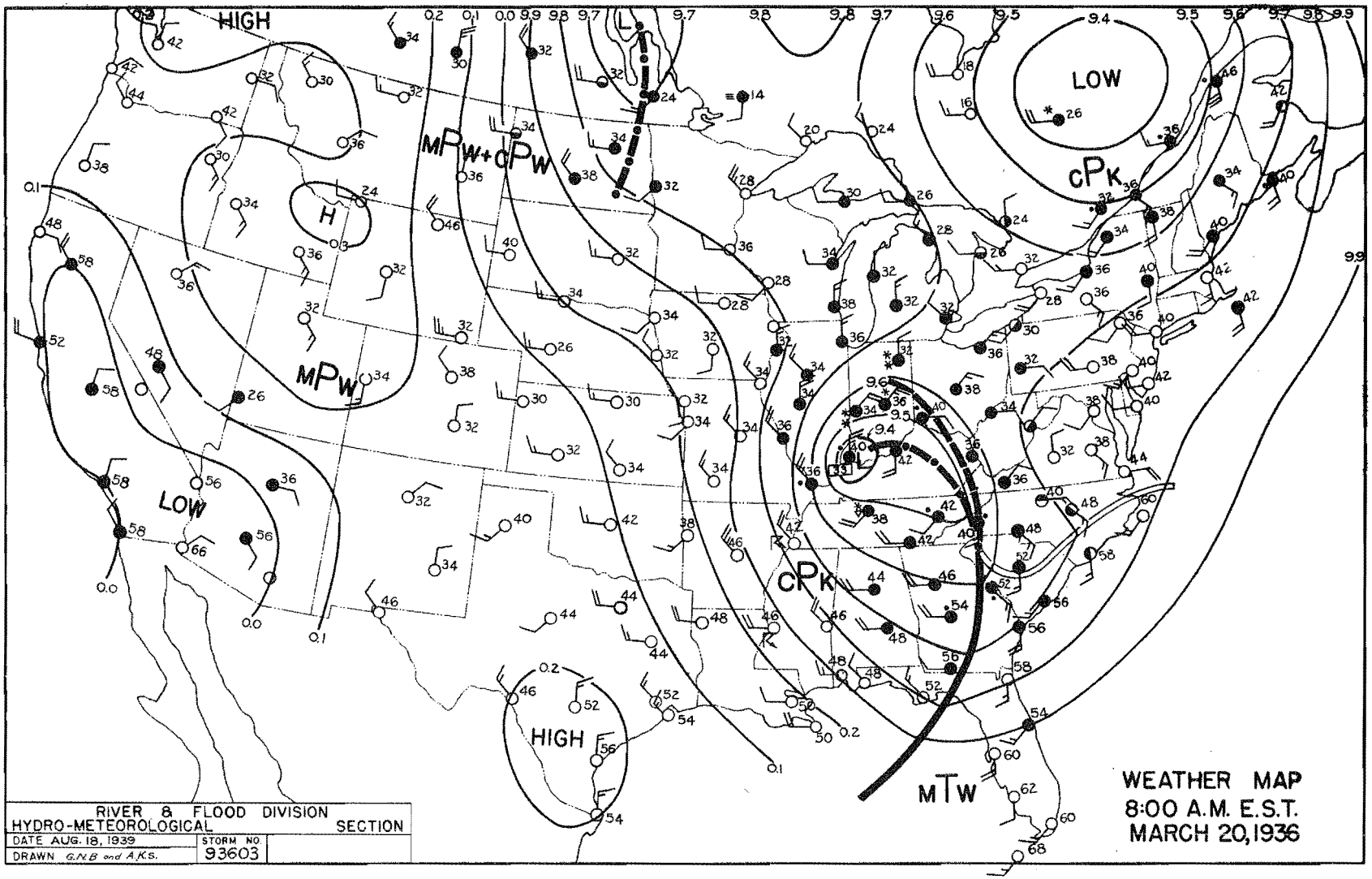
HIGH
LOW
H
mPw+cPw
mPw
cPk
LOW
cPk
HIGH
mTw
WEATHER MAP
8:00 A.M. E.S.T.
MARCH 20,1936
RIVER & FLOOD DIVISION
HYDRO-METEOROLOGICAL SECTION
DATE AUG. 18, 1939
STORM NO. 93603
DRAWN G.N.B and A.K.S.

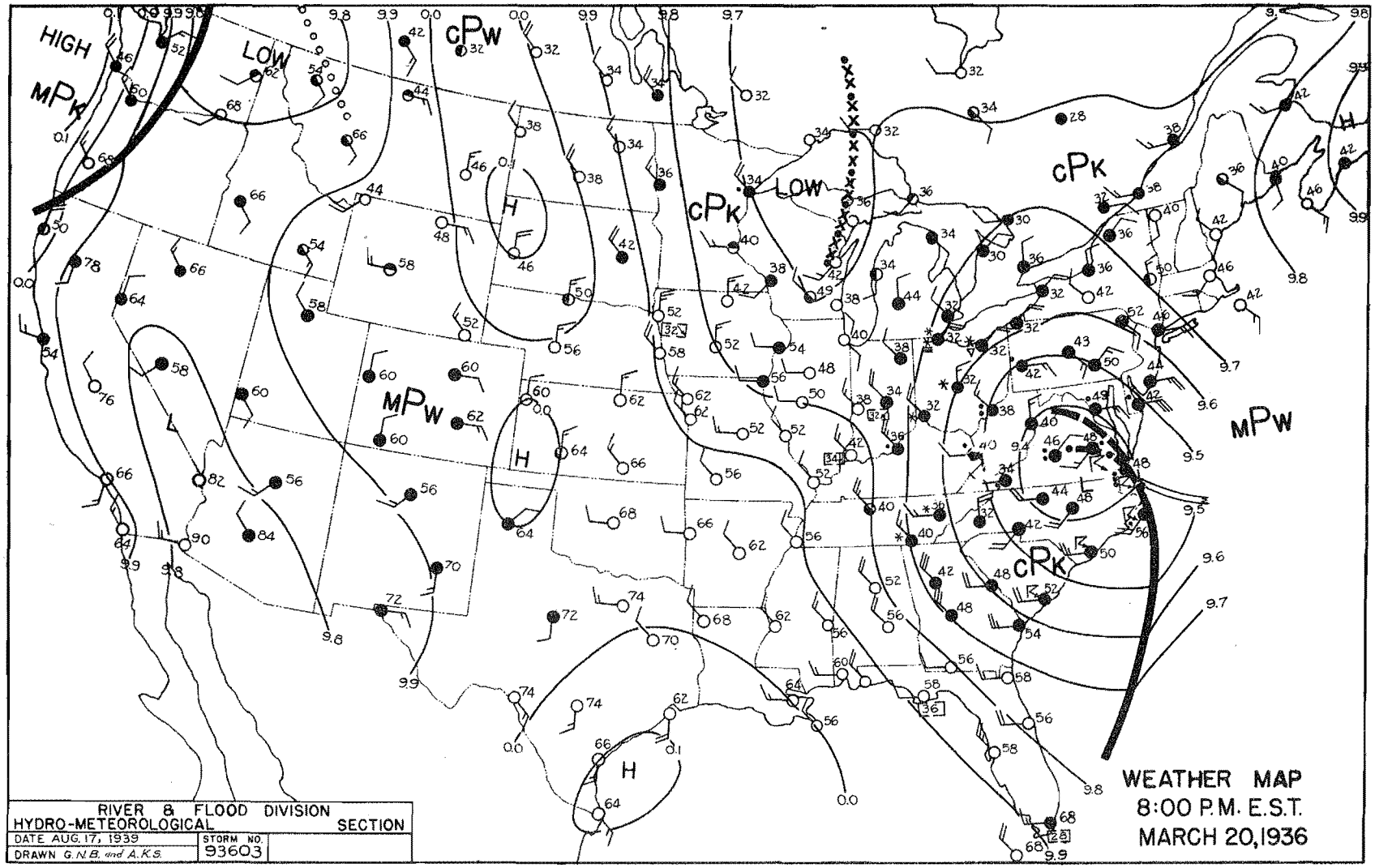
HIGH
MPK
LOW
cPW
H
cPK
LOW
cPK
MPW
H
MPW
H
cPK
WEATHER MAP
8:00 P.M. E.S.T.
MARCH 20,1936
RIVER & FLOOD DIVISION
HYDRO-METEOROLOGICAL SECTION
DATE AUG. 17, 1939
STORM NO. 93603
DRAWN G.N.B. and A.K.S.

FIGURE A-73

FIGURE A-74

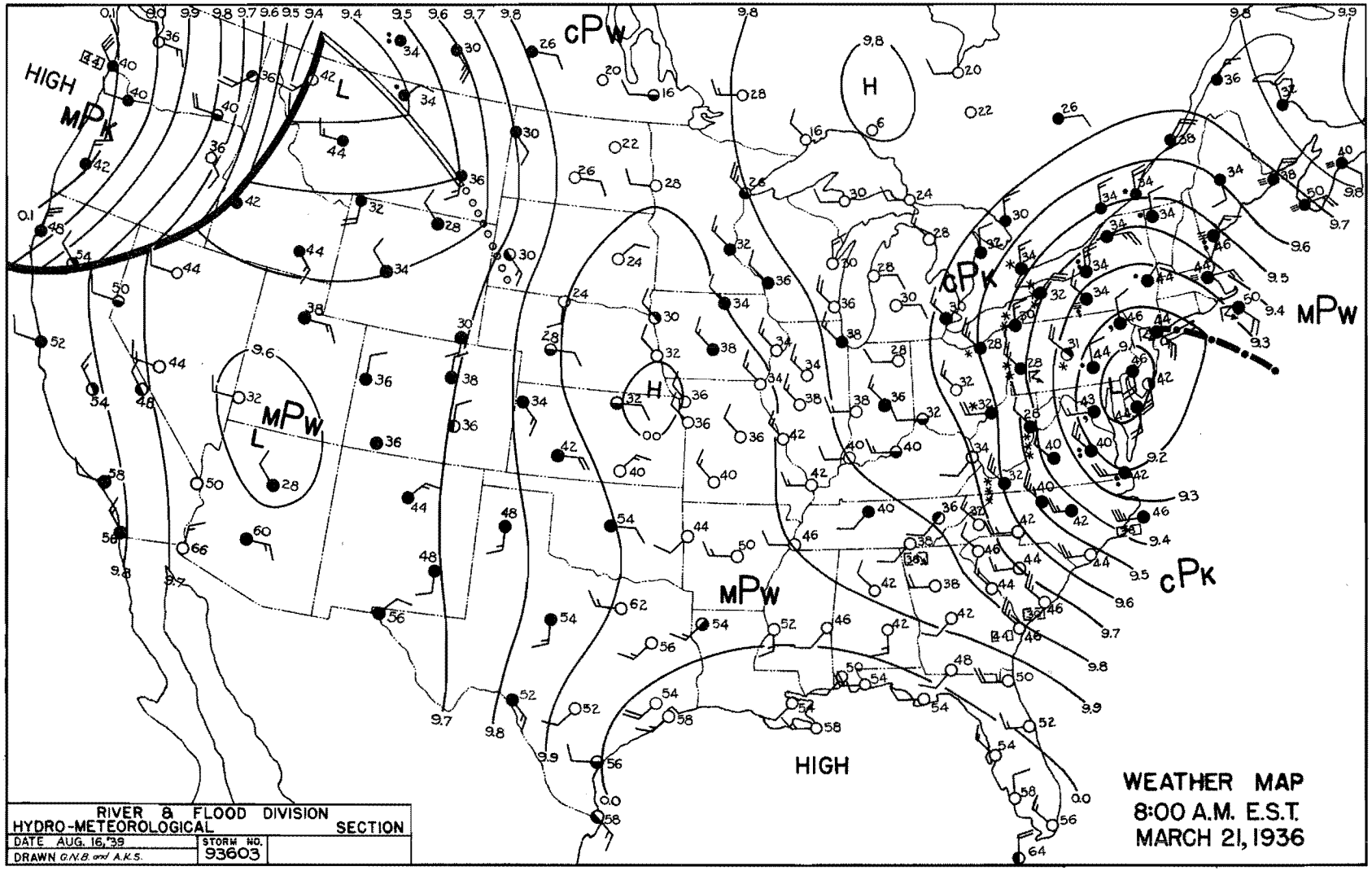
HIGH
MPK
L
cPW
H
cPK
MPW
L
H
MPW
cPK
HIGH
WEATHER MAP
8:00 A.M. E.S.T.
MARCH 21, 1936
RIVER & FLOOD DIVISION
HYDRO-METEOROLOGICAL SECTION
DATE AUG. 16, '39
STORM NO. 93603
DRAWN G.N.B. and A.K.S.

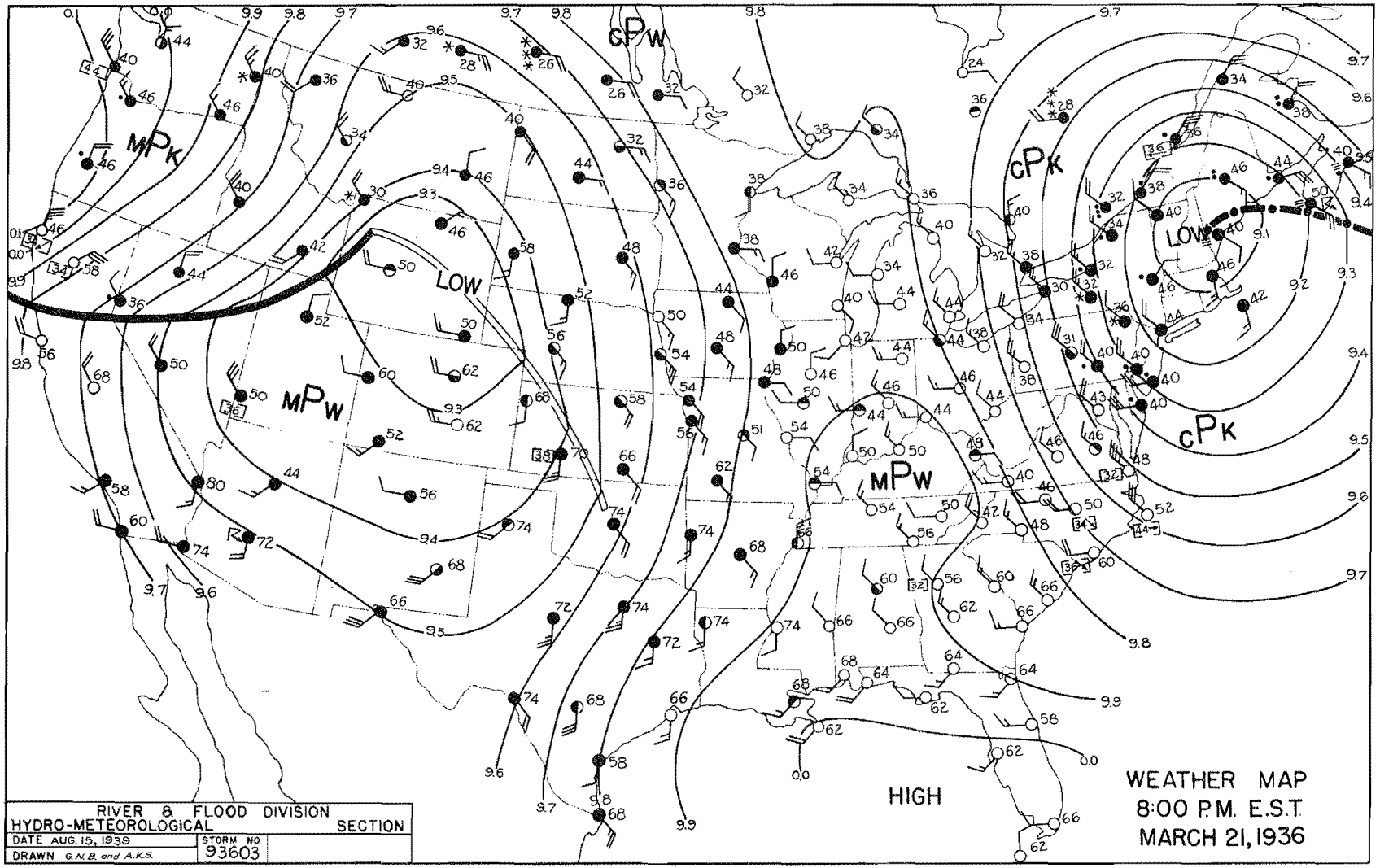
mPK
cPW
LOW
mPW
cPK
LOW
cPK
mPW
HIGH
WEATHER MAP
8:00 P.M. E.S.T.
MARCH 21, 1936
RIVER & FLOOD DIVISION
HYDRO-METEOROLOGICAL SECTION
DATE AUG. 15, 1939
STORM NO. 93603
DRAWN G.N.B. and A.K.S.

FIGURE A-75

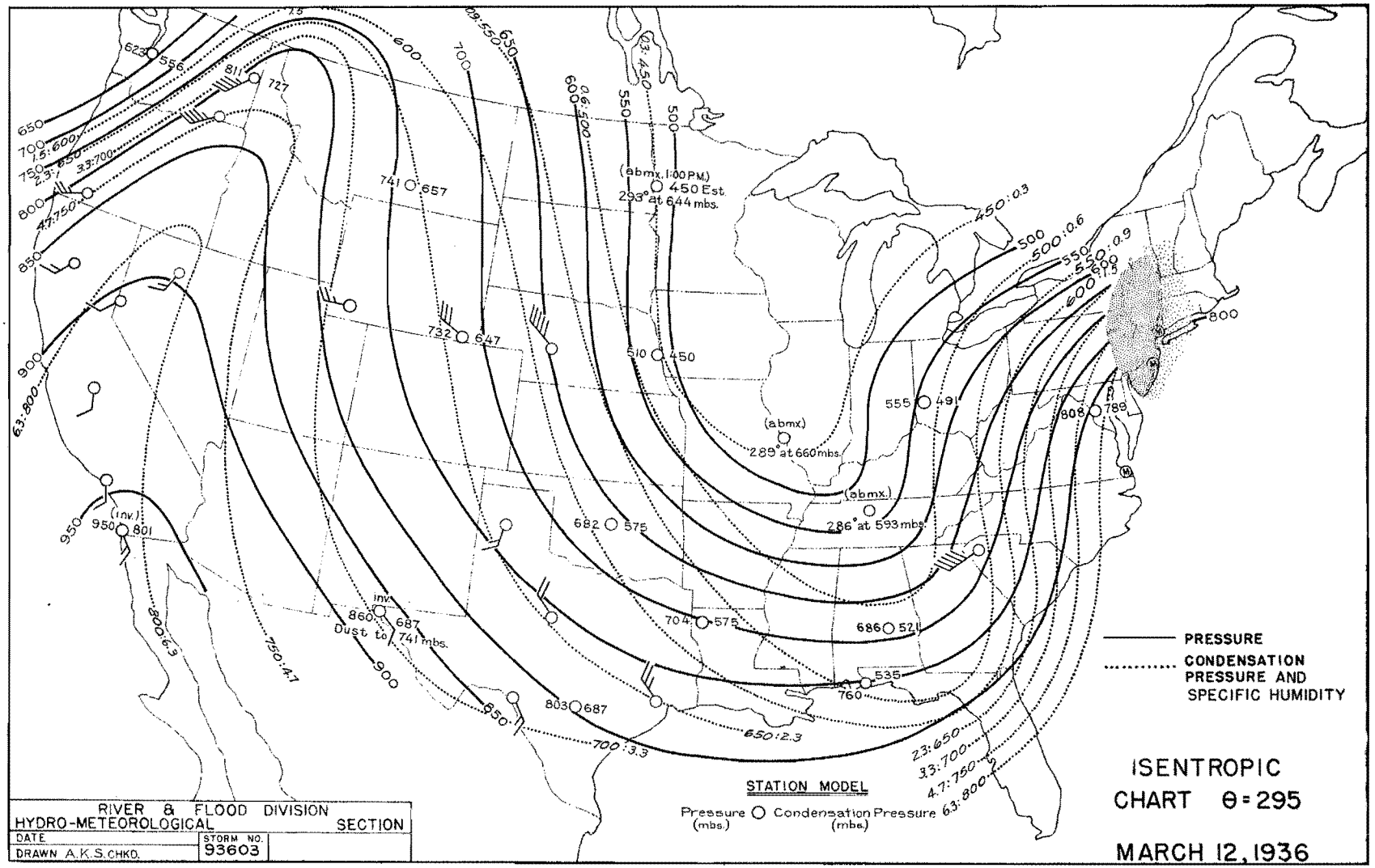
PRESSURE
CONDENSATION PRESSURE AND SPECIFIC HUMIDITY
STATION MODEL
Pressure (mbs.) O Condensation Pressure (mbs.)
ISENTROPIC CHART θ = 295
MARCH 12, 1936
RIVER & FLOOD DIVISION
HYDRO-METEOROLOGICAL SECTION
DATE
DRAWN A.K.S. CHKD.
STORM NO. 93603
(abmx. 1:00 P.M.) 450 Est. 293° at 644 mbs.
(abmx) 289° at 660 mbs.
(abmx) 286° at 593 mbs.
Dust to 741 mbs.

FIGURE A-76

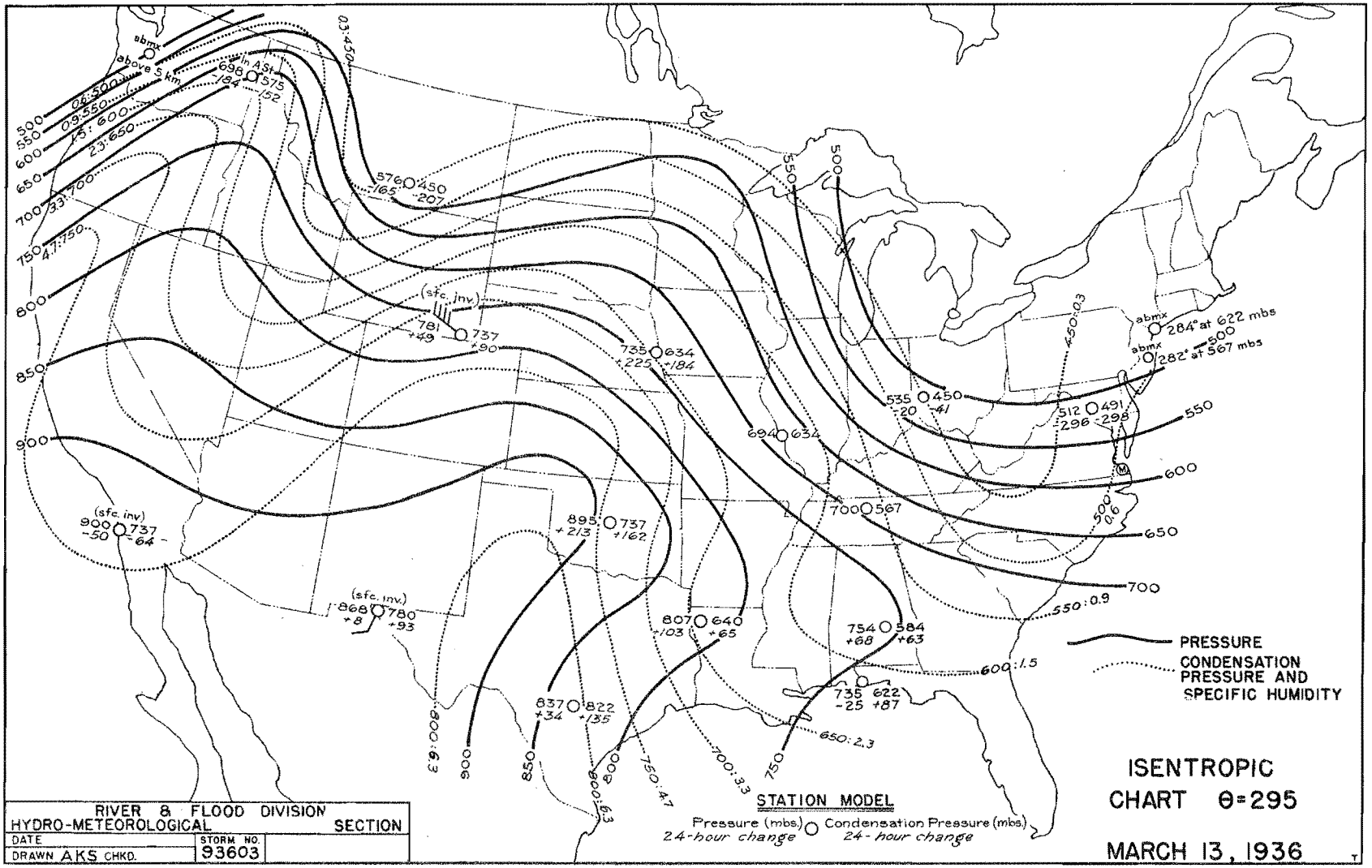
abmx
above 5 km
06:500
09:550
13:600
23:650
33:700
47:750
03:450
698 -184
575 -152
576 -165
450 -207
(sfc. inv.)
781 +49
737 +90
735 +225
634 +184
694
634
535 -20
450 -41
512 -296
491 -298
abmx
284° at 622 mbs
abmx
282° at 567 mbs
450:03
500
550
600
650
700
850
900
700 567
500 -0.6
550:0.9
600:1.5
650:2.3
700:3.3
750:4.7
800:6.3
850
900
(sfc. inv.)
900 737 -50 -64
(sfc. inv.)
868 780 +8 +93
895 737 +213 +162
807 640 +103 +65
754 584 +68 +63
735 622 -25 +87
837 822 +34 +135
PRESSURE
CONDENSATION PRESSURE AND SPECIFIC HUMIDITY
STATION MODEL
Pressure (mbs.) 24-hour change
Condensation Pressure (mbs.) 24-hour change
ISENTROPIC CHART θ=295
MARCH 13, 1936
RIVER & FLOOD DIVISION
HYDRO-METEOROLOGICAL SECTION
DATE
DRAWN AKS CHKD.
STORM NO. 93603

FIGURE A-77

FIGURE A-78

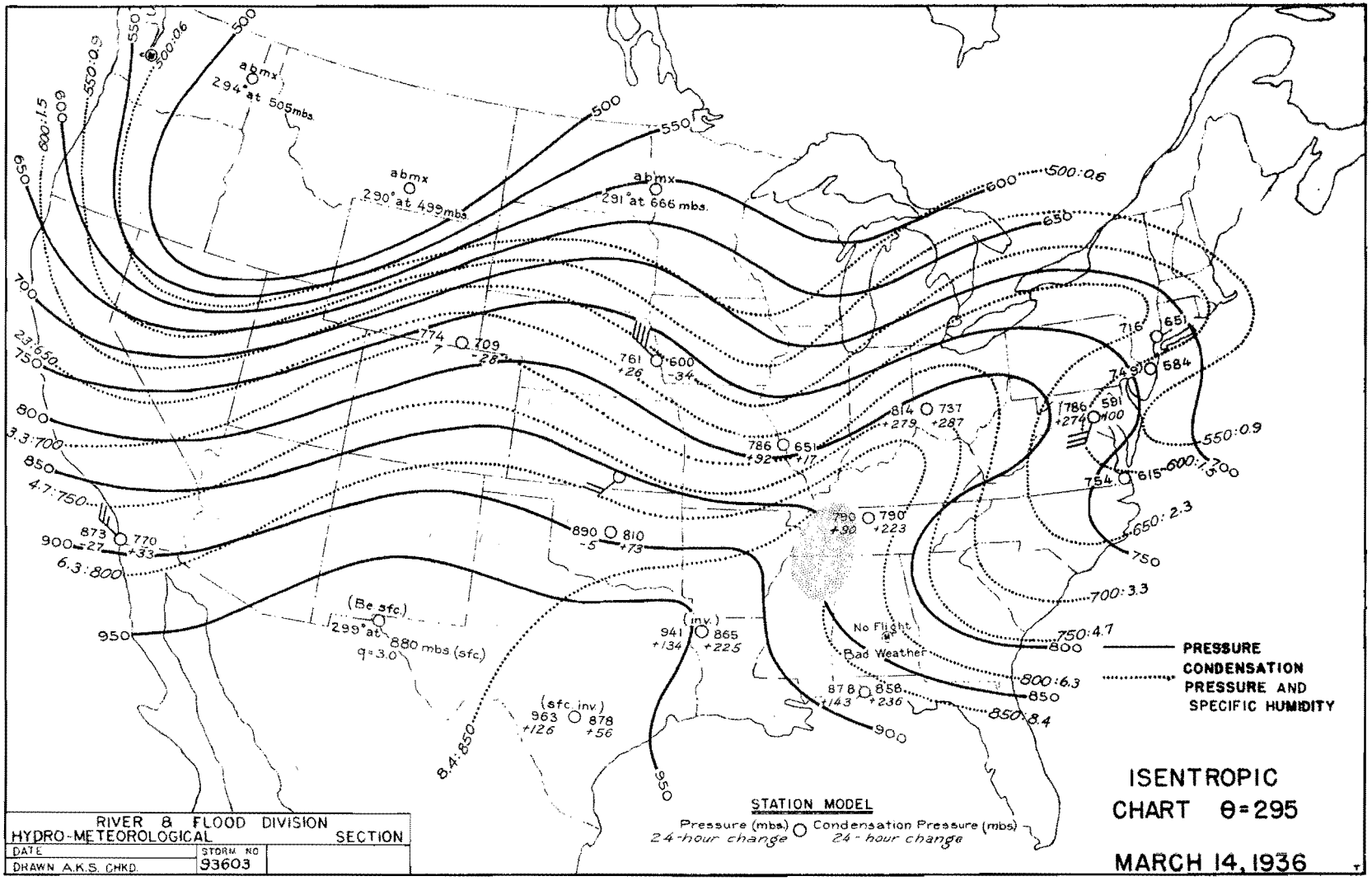
abmx
294° at 505mbs.
abmx
290° at 499mbs.
abmx
291° at 666 mbs.
(Be sfc.)
299° at 880 mbs (sfc.)
q=3.0
(inv.)
(sfc inv)
No Flight
Bad Weather
PRESSURE
CONDENSATION PRESSURE AND SPECIFIC HUMIDITY
STATION MODEL
Pressure (mbs.) Condensation Pressure (mbs.)
24-hour change 24-hour change
RIVER & FLOOD DIVISION
HYDRO-METEOROLOGICAL SECTION
DATE
DRAWN A.K.S. CHKD.
STORM NO 93603
ISENTROPIC
CHART θ=295
MARCH 14, 1936

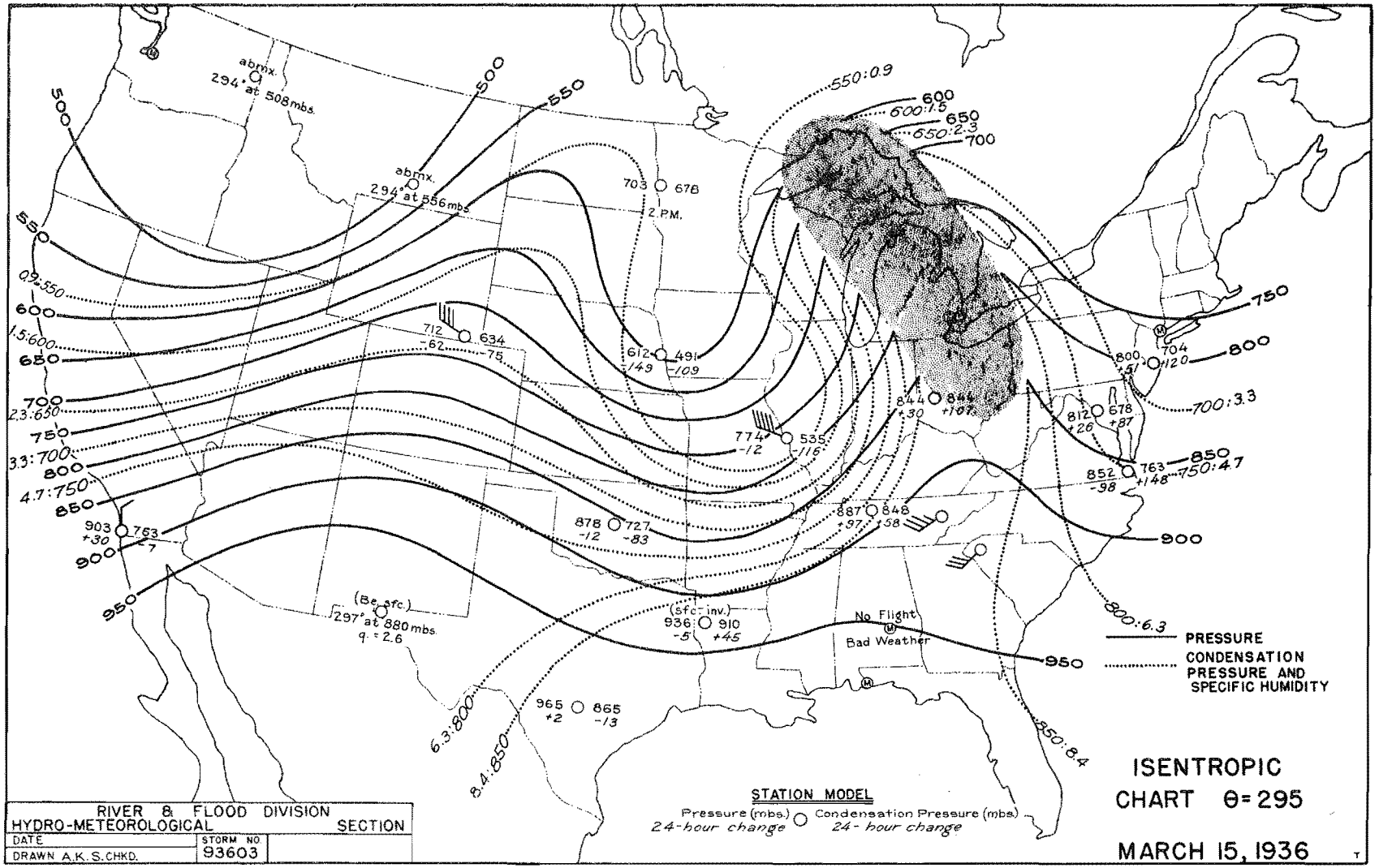
abmx. 294° at 508mbs.
abmx. 294° at 556mbs.
703 678
2 P.M.
712 634 -62 -75
612 491 -149 -109
774 535 -12 -116
844 844 +30 +107
800 704 +51 +120
812 678 +26 +87
852 763 -98 +148
887 848 +97 +58
878 727 -12 -83
903 763 +30 -7
(Be sfc.) 297° at 880mbs. q = 2.6
(sfc-inv.) 936 910 -5 +45
965 865 +2 -13
No Flight
Bad Weather
500
550
550:0.9
600
600:1.5
650
650:2.3
700
700:3.3
750
750:4.7
800
800:6.3
850
850:8.4
900
950
PRESSURE
CONDENSATION PRESSURE AND SPECIFIC HUMIDITY
STATION MODEL
Pressure (mbs.) 24-hour change
Condensation Pressure (mbs.) 24-hour change
ISENTROPIC CHART θ=295
MARCH 15, 1936
RIVER & FLOOD DIVISION
HYDRO-METEOROLOGICAL SECTION
DATE
STORM NO. 93603
DRAWN A.K.S. CHKD.

FIGURE A-79

FIGURE A-80

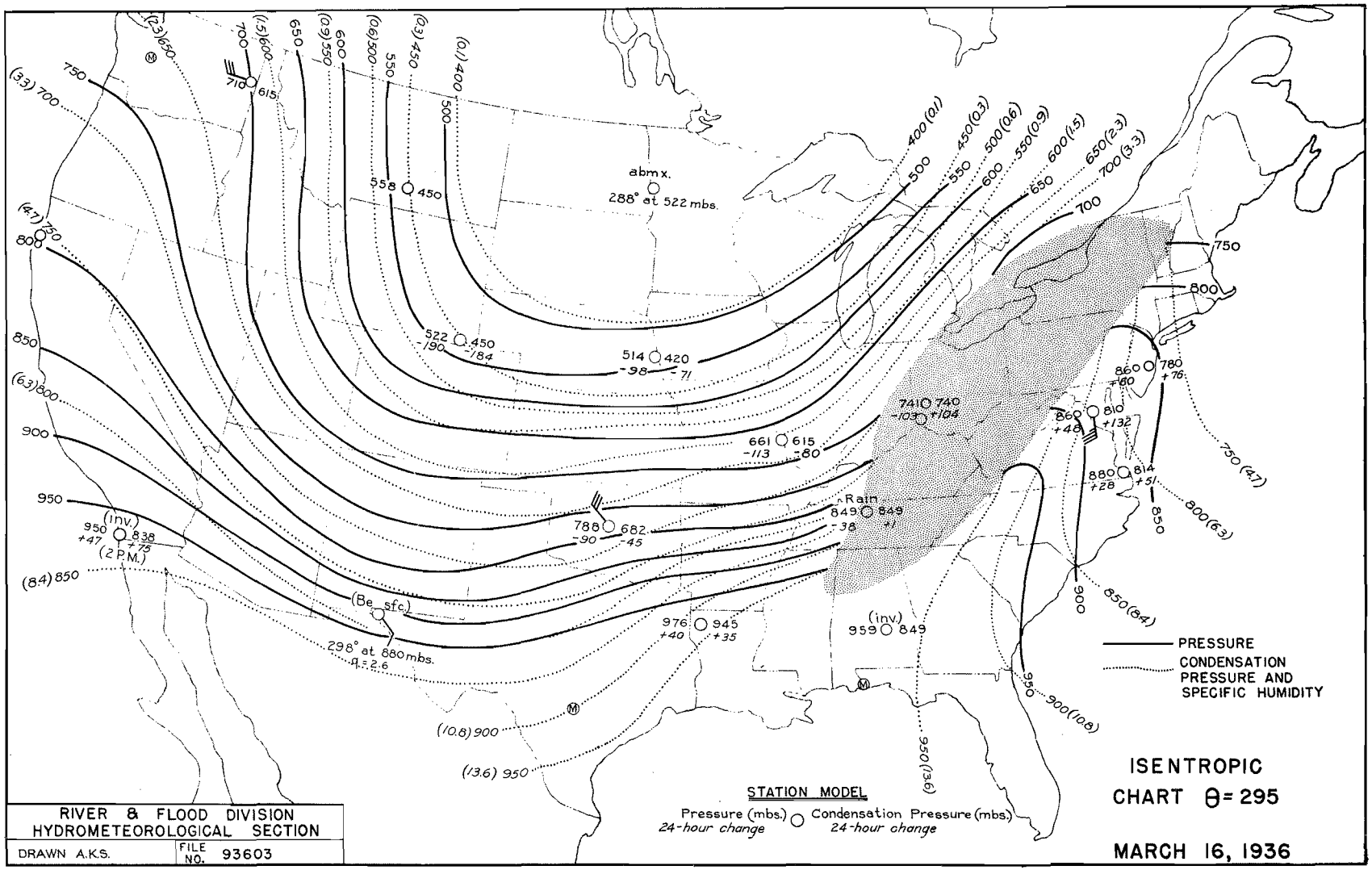
abmx.
288° at 522 mbs.
298° at 880 mbs.
n = 2.6
Rain
(Be sfc)
(inv.)
(2 P.M.)
PRESSURE
CONDENSATION PRESSURE AND SPECIFIC HUMIDITY
STATION MODEL
Pressure (mbs.) 24-hour change
Condensation Pressure (mbs.) 24-hour change
ISENTROPIC CHART θ = 295
MARCH 16, 1936
RIVER & FLOOD DIVISION
HYDROMETEOROLOGICAL SECTION
DRAWN A.K.S.
FILE NO. 93603

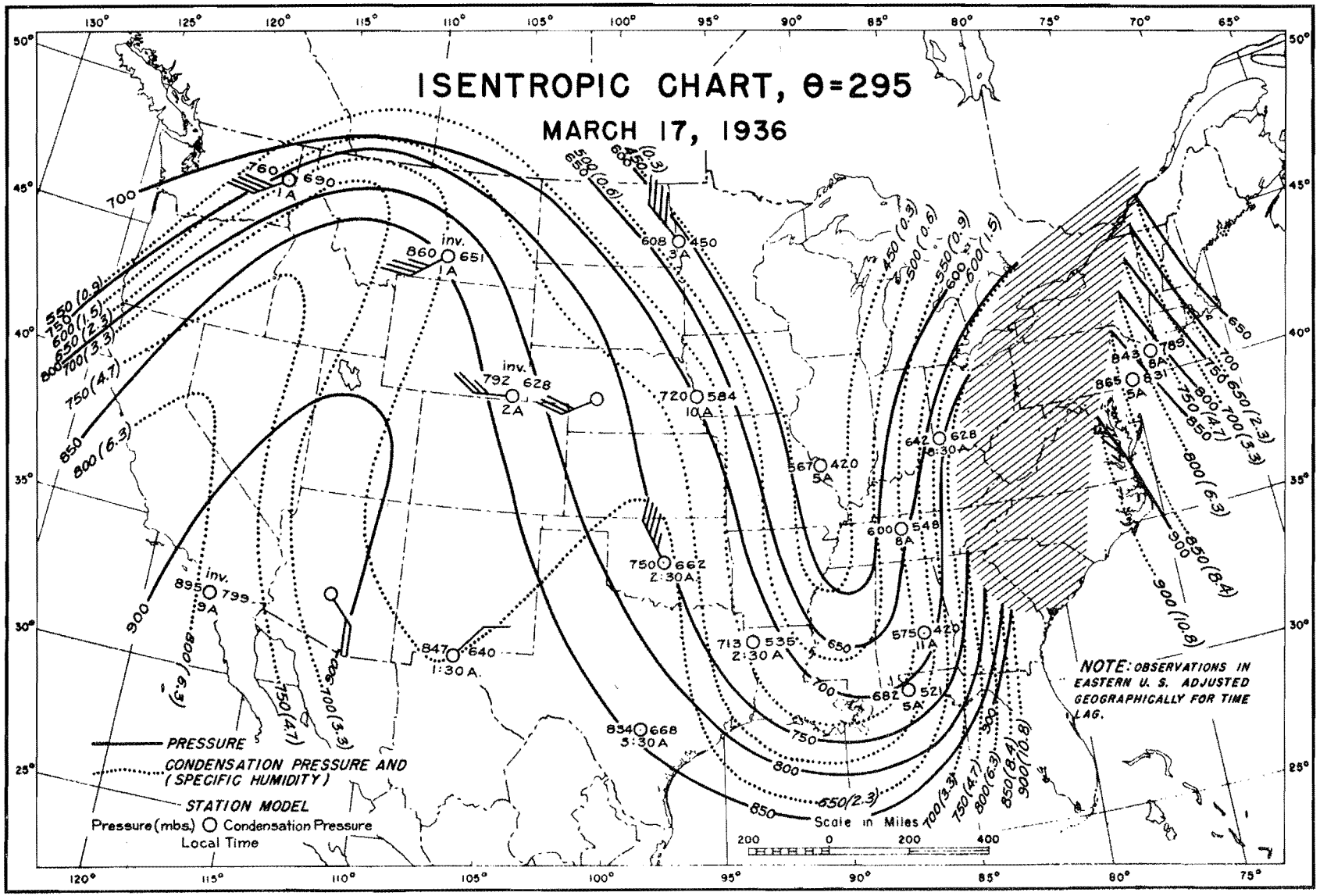
ISENTROPIC CHART, θ=295
MARCH 17, 1936
NOTE: OBSERVATIONS IN EASTERN U. S. ADJUSTED GEOGRAPHICALLY FOR TIME LAG.
PRESSURE
CONDENSATION PRESSURE AND (SPECIFIC HUMIDITY)
STATION MODEL
Pressure (mbs.) ○ Condensation Pressure
Local Time
Scale in Miles
200 0 200 400

FIGURE A-81

FIGURE A-82

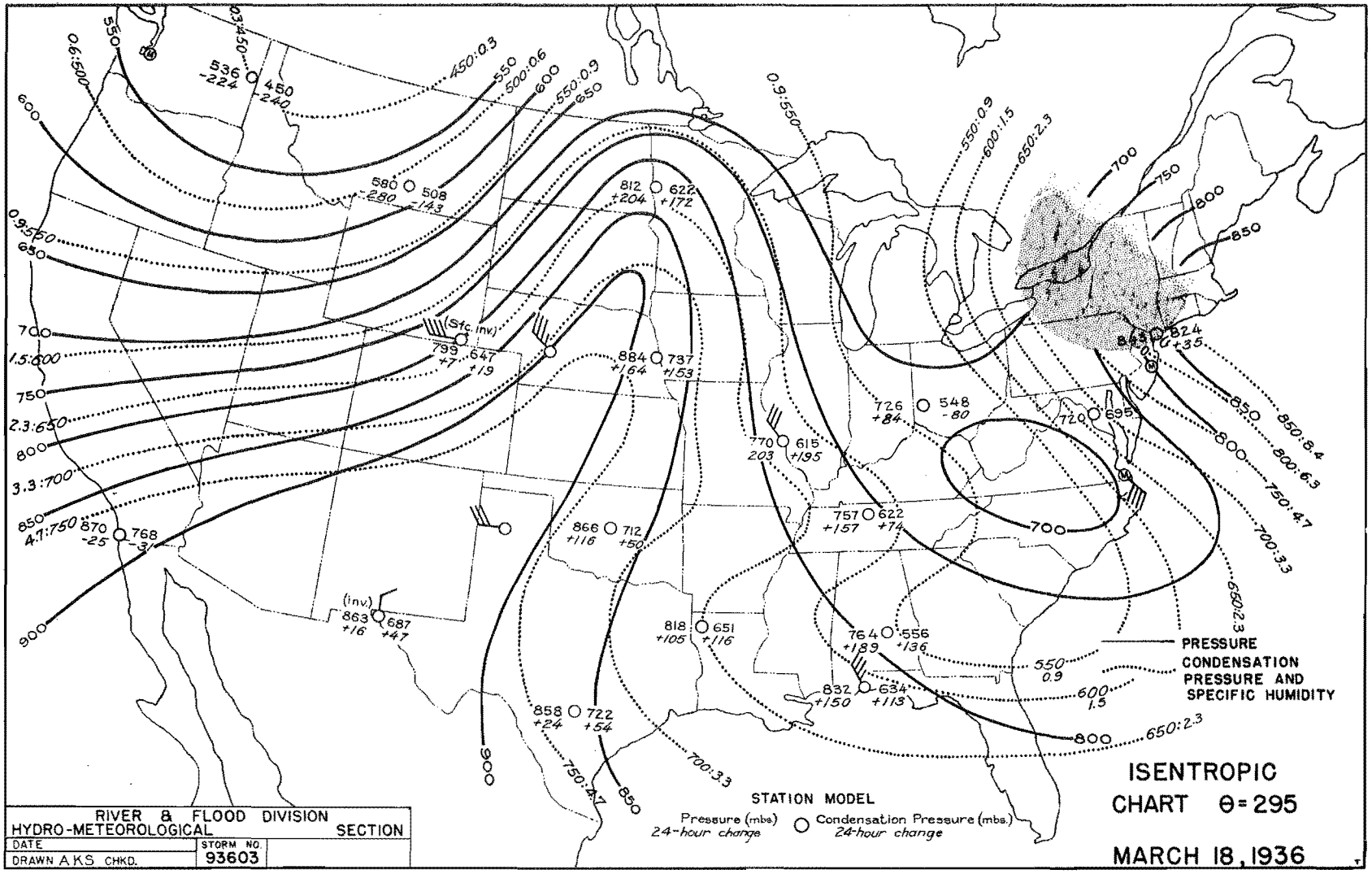
ISENTROPIC
CHART θ = 295
MARCH 18, 1936
PRESSURE
CONDENSATION PRESSURE AND SPECIFIC HUMIDITY
STATION MODEL
Pressure (mbs) 24-hour change
Condensation Pressure (mbs.) 24-hour change
RIVER & FLOOD DIVISION
HYDRO-METEOROLOGICAL SECTION
DATE
DRAWN A.K.S. CHKD.
STORM NO. 93603

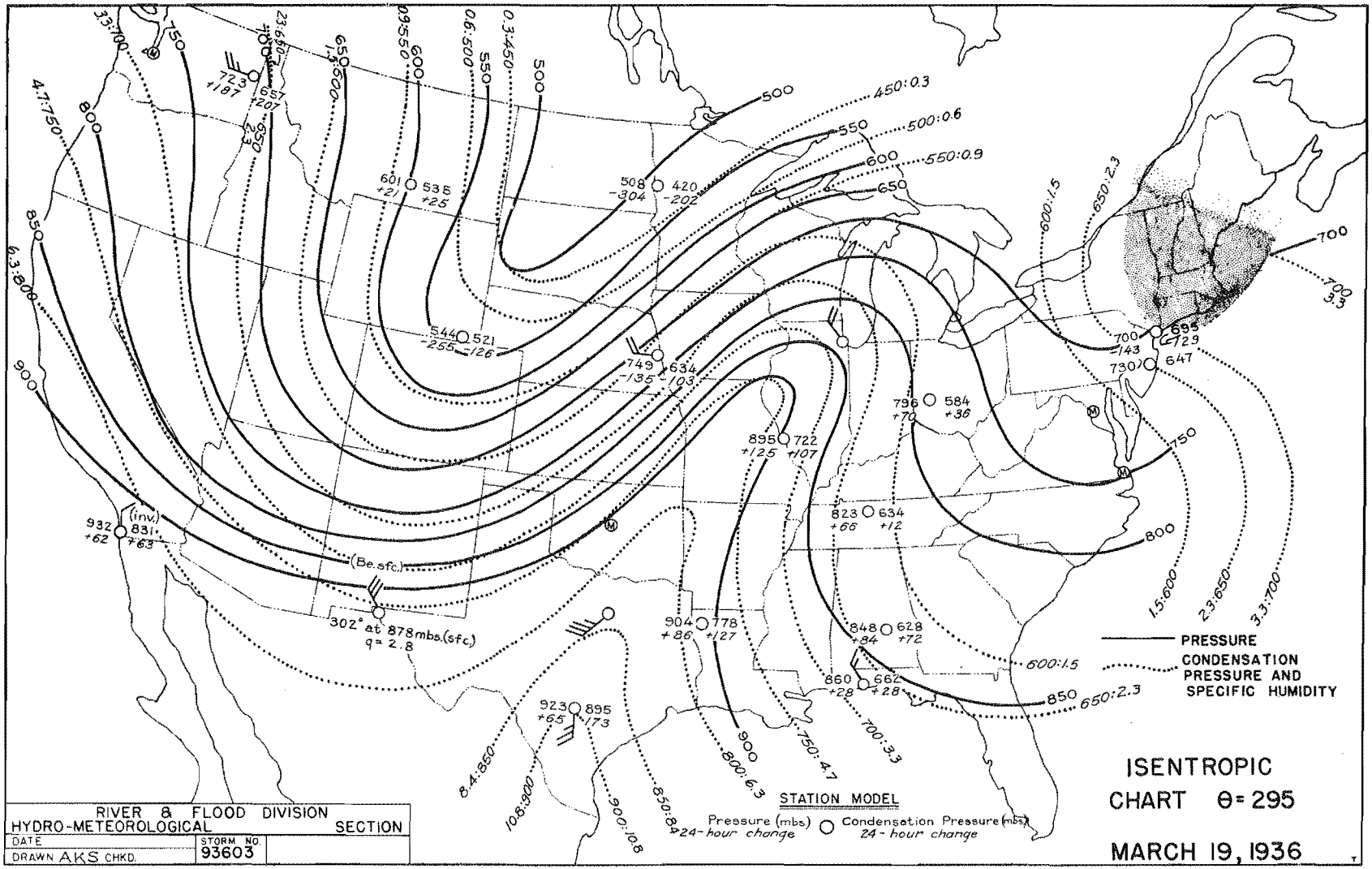
ISENTROPIC
CHART θ= 295
MARCH 19, 1936
PRESSURE
CONDENSATION PRESSURE AND SPECIFIC HUMIDITY
STATION MODEL
Pressure (mbs) 24-hour change
Condensation Pressure (mbs) 24-hour change
RIVER & FLOOD DIVISION
HYDRO-METEOROLOGICAL SECTION
DATE
STORM NO. 93603
DRAWN AKS CHKD.
302° at 878 mbs. (sfc.) q= 2.8
(Be. sfc.)
(inv.)

FIGURE A-83

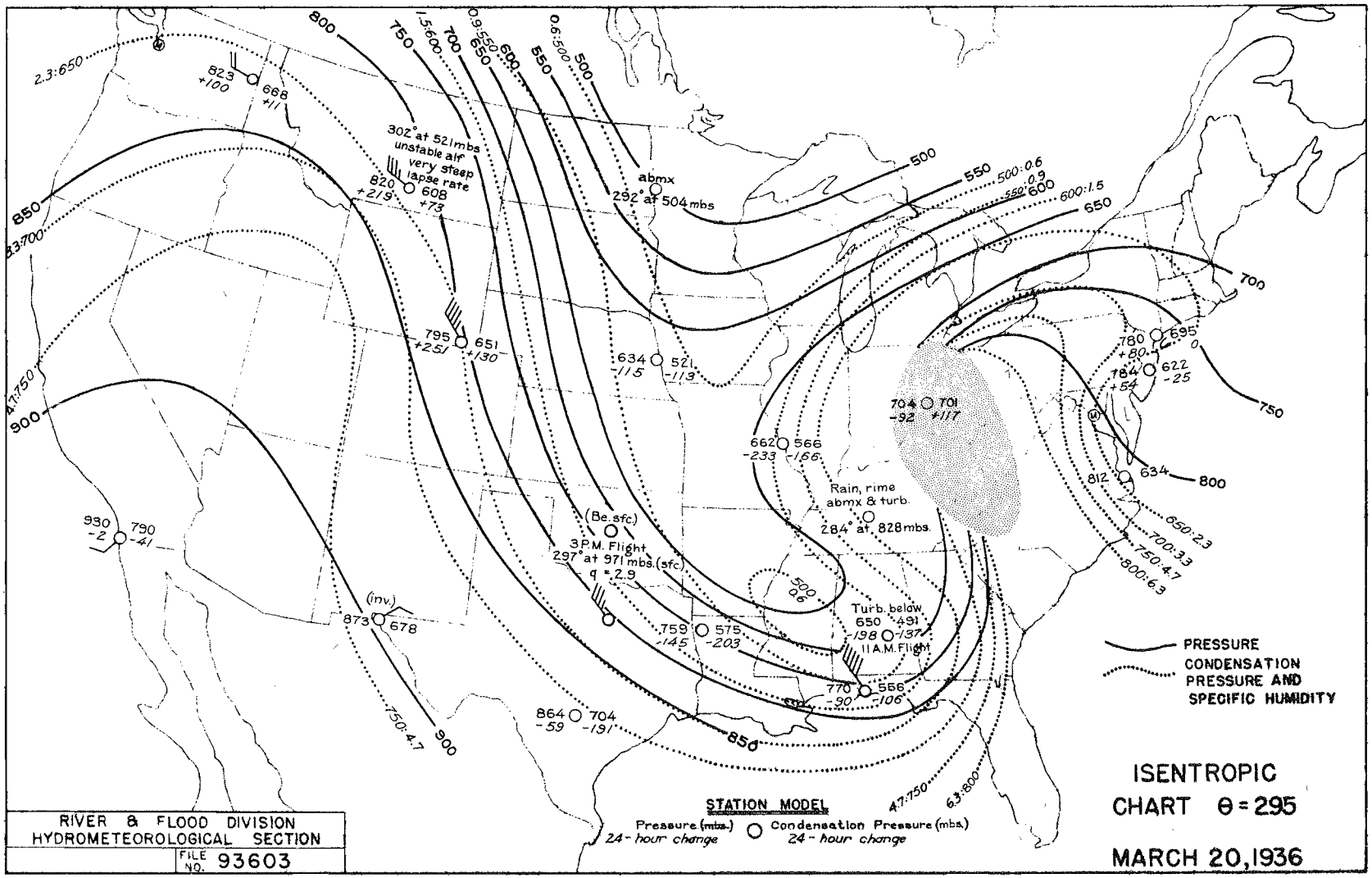
800
750
700
650
600
550
500
850
900
2.3:650
4.7:750
823
+100
668
+11
820
+219
302° at 521 mbs
unstable air
very steep
lapse rate
608
+73
abmx
292° at 504 mbs
795
+251
651
+130
634
-115
521
-113
662
-233
566
-166
704
-92
701
+117
780
+80
695
0
784
+54
622
-25
812
634
930
-2
790
-41
(Be. sfc)
3 P.M. Flight
297° at 971 mbs. (sfc)
q = 2.9
Rain, rime
abmx & turb.
284° at 828 mbs
(inv.)
873
678
759
145
575
-203
Turb. below
650
491
198
-137
11 A.M. Flight
770
-30
556
-106
864
-59
704
-191
0.9:550
1.5:600
0.6:500
500:0.6
550:0.9
600:1.5
650:2.3
700:3.3
750:4.7
800:6.3
PRESSURE
CONDENSATION PRESSURE AND SPECIFIC HUMIDITY
STATION MODEL
Pressure (mbs.) 24-hour change
Condensation Pressure (mbs.) 24-hour change
RIVER & FLOOD DIVISION
HYDROMETEOROLOGICAL SECTION
FILE NO. 93603
ISENTROPIC
CHART θ = 295
MARCH 20, 1936

FIGURE A-84

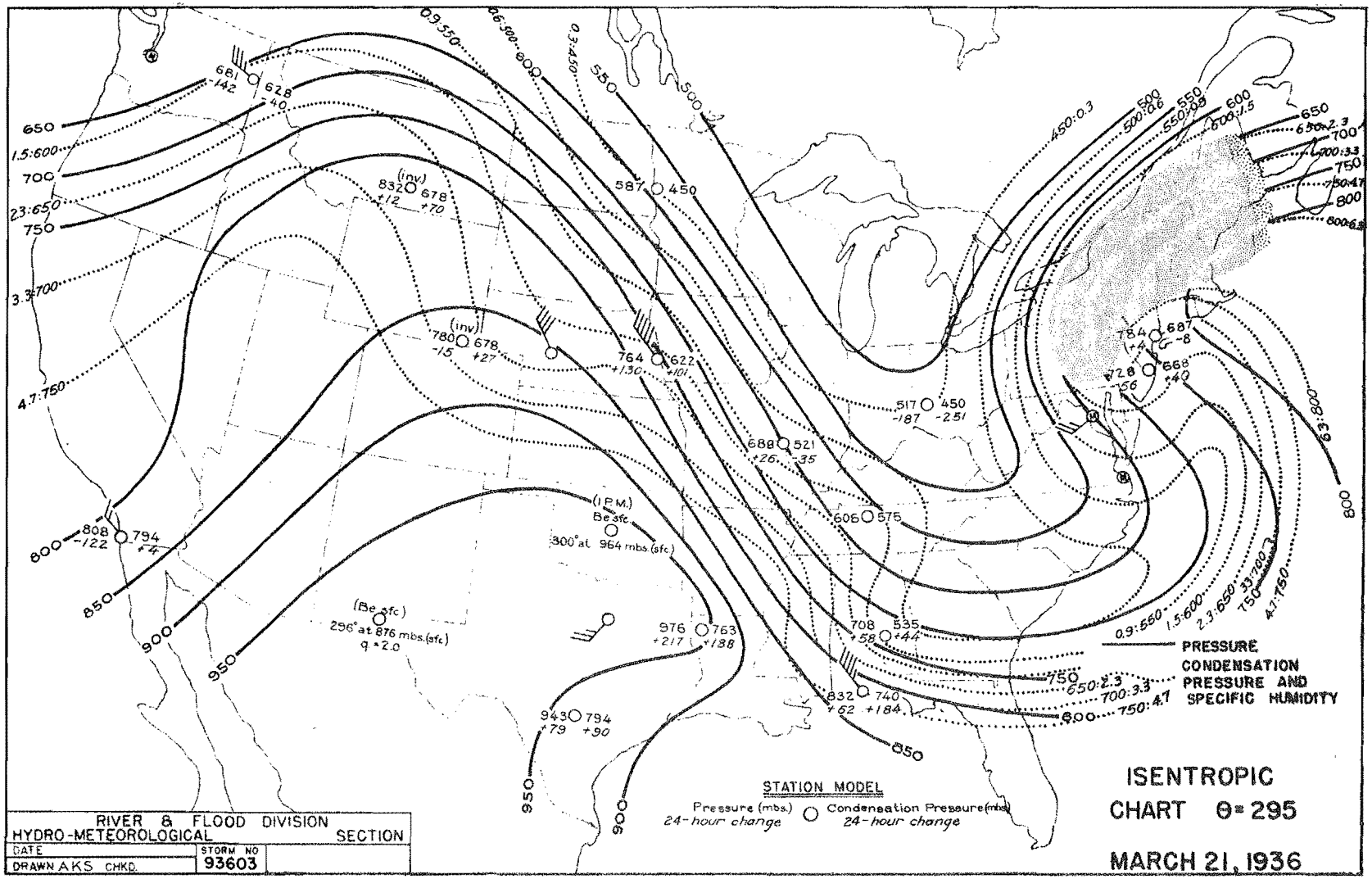
ISENTROPIC
CHART θ = 295
MARCH 21, 1936
PRESSURE
CONDENSATION PRESSURE AND SPECIFIC HUMIDITY
STATION MODEL
Pressure (mbs.) 24-hour change
Condensation Pressure (mbs.) 24-hour change
RIVER & FLOOD DIVISION
HYDRO-METEOROLOGICAL SECTION
DATE
DRAWN AKS CHKD.
STORM NO 93603

FIGURE A-85

FIGURE A-86

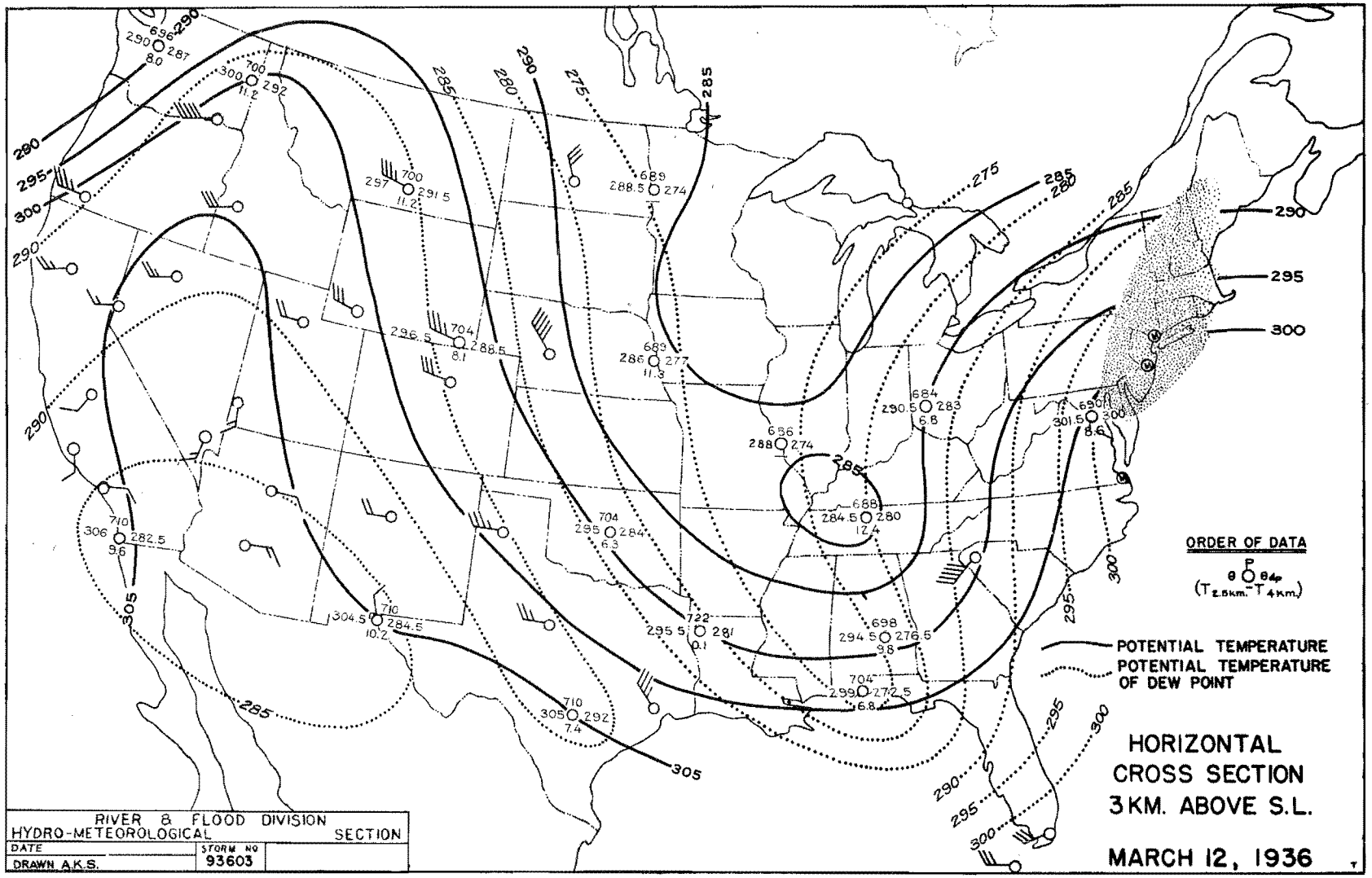
ORDER OF DATA
θ P 84p
(T2.5km.-T4km.)
POTENTIAL TEMPERATURE
POTENTIAL TEMPERATURE OF DEW POINT
HORIZONTAL CROSS SECTION 3KM. ABOVE S.L.
MARCH 12, 1936
RIVER & FLOOD DIVISION
HYDRO-METEOROLOGICAL SECTION
DATE
DRAWN A.K.S.
STORM NO 93603

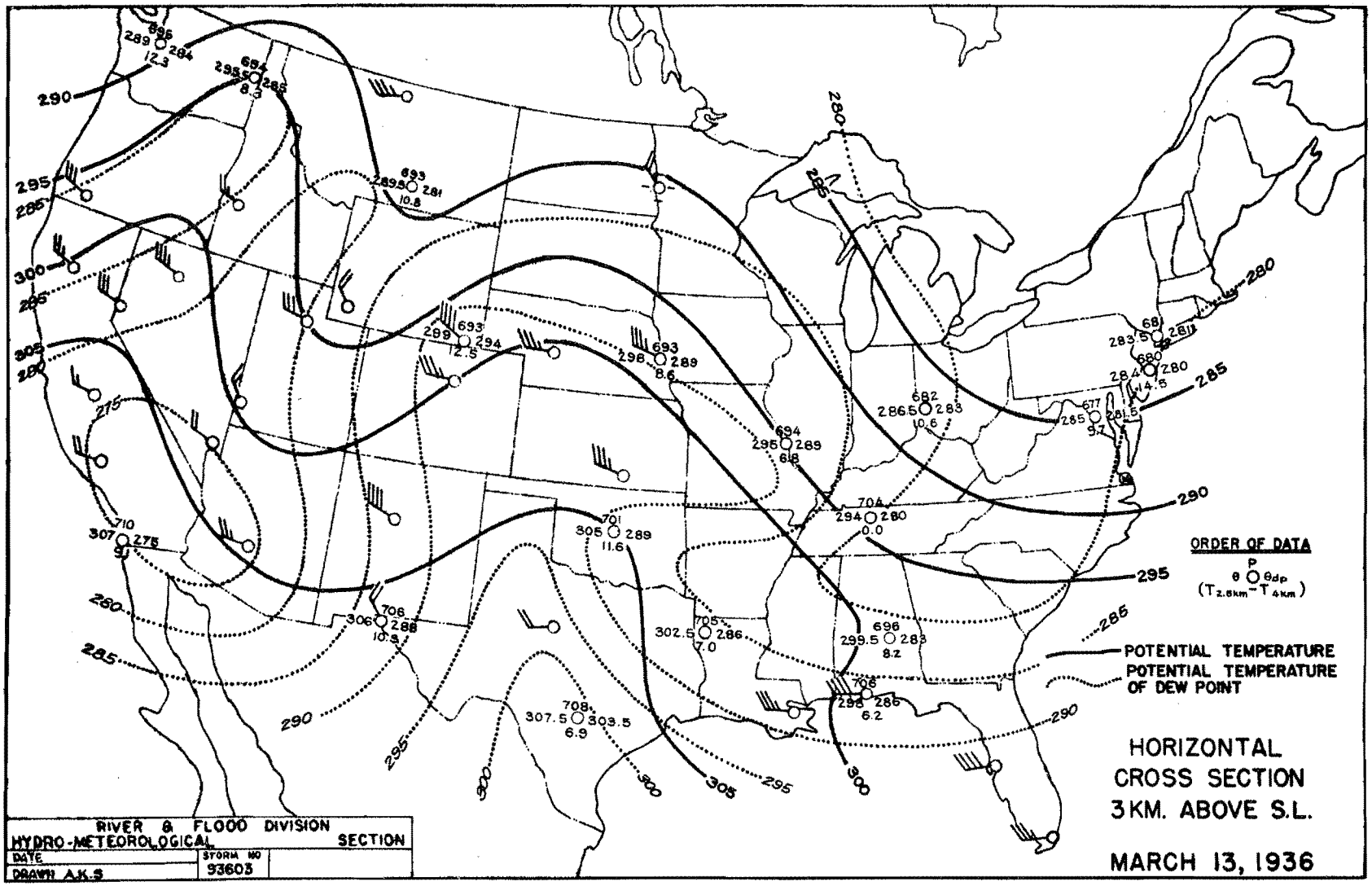
ORDER OF DATA
P
θ θdp
(T2.6km − T4km)
POTENTIAL TEMPERATURE
POTENTIAL TEMPERATURE OF DEW POINT
HORIZONTAL CROSS SECTION 3KM. ABOVE S.L.
MARCH 13, 1936
RIVER & FLOOD DIVISION
HYDRO-METEOROLOGICAL SECTION
DATE
STORM NO 53603
DRAWN A.K.S

FIGURE A-87

FIGURE A-88

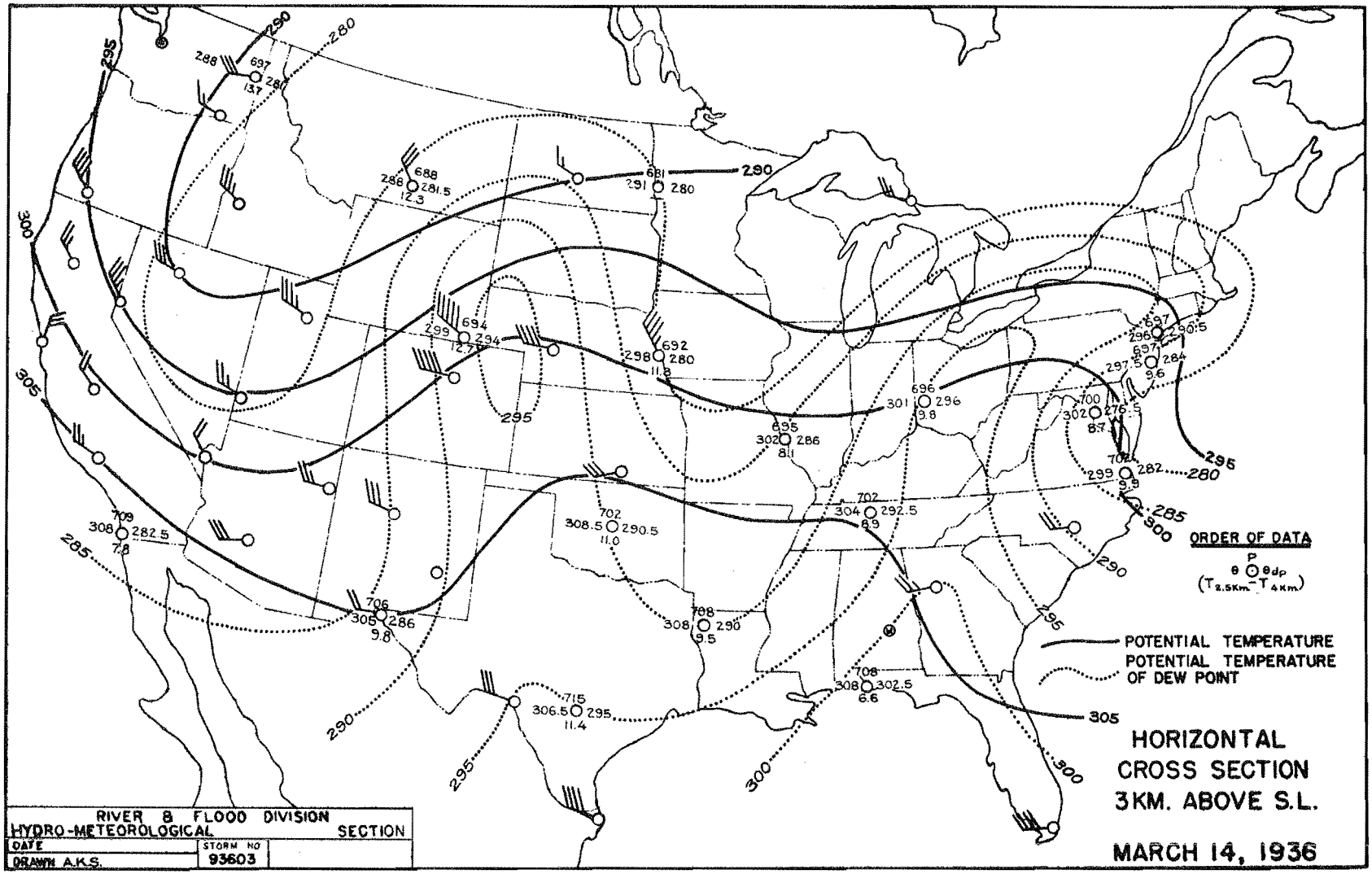
ORDER OF DATA
P
θ θdp
(T2.5Km − T4Km)
POTENTIAL TEMPERATURE
POTENTIAL TEMPERATURE OF DEW POINT
HORIZONTAL CROSS SECTION 3KM. ABOVE S.L.
MARCH 14, 1936
RIVER & FLOOD DIVISION
HYDRO-METEOROLOGICAL SECTION
DATE
DRAWN A.K.S.
STORM NO
93603

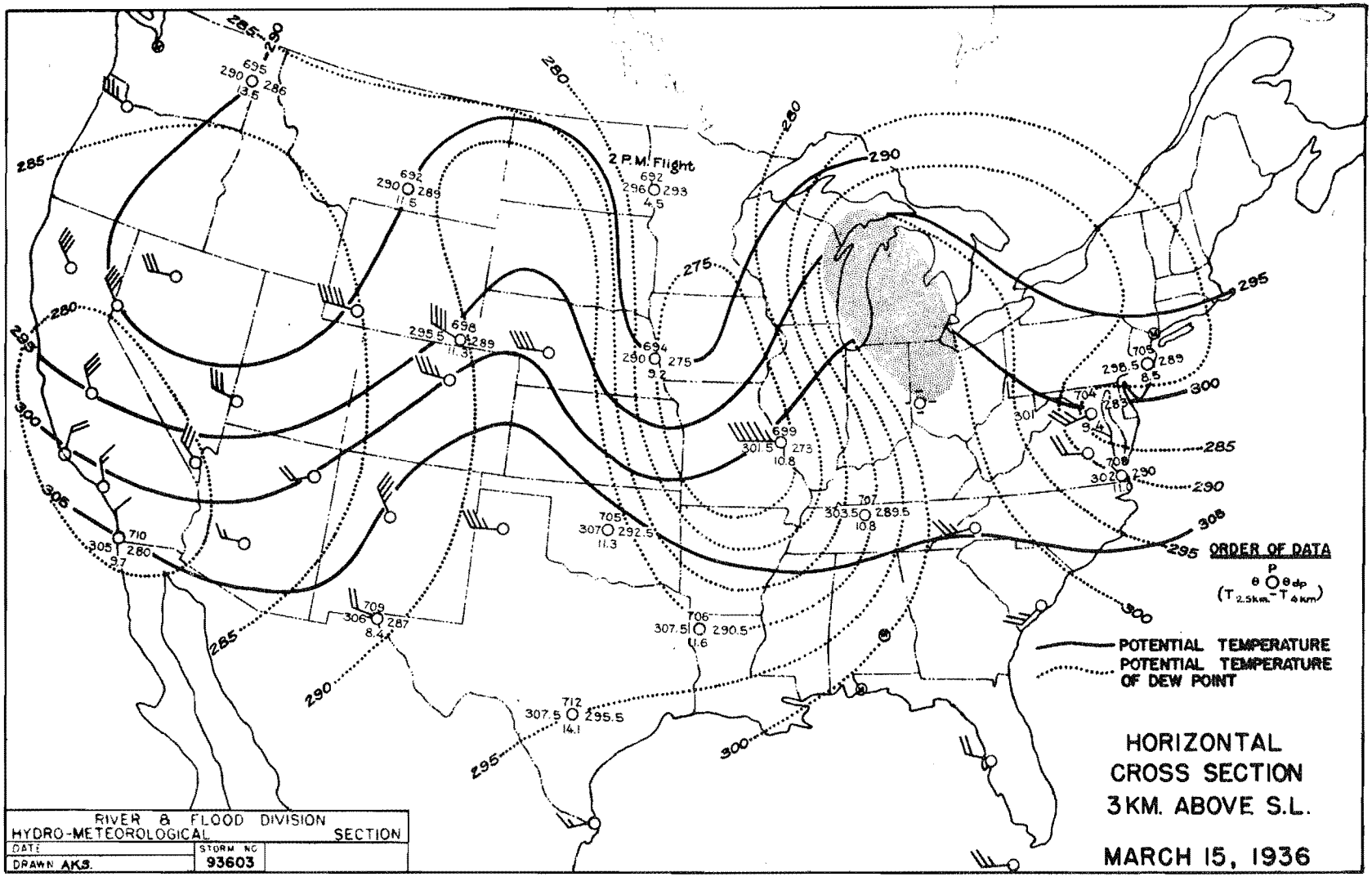
2 P.M. Flight
ORDER OF DATA
$\theta^{p}_{\theta dp}$
$(T_{2.5km.} - T_{4km})$
POTENTIAL TEMPERATURE
POTENTIAL TEMPERATURE OF DEW POINT
HORIZONTAL CROSS SECTION 3 KM. ABOVE S.L.
MARCH 15, 1936
RIVER & FLOOD DIVISION
HYDRO-METEOROLOGICAL SECTION
DATE
DRAWN AKS.
STORM NO 93603

FIGURE A-89

FIGURE A-90

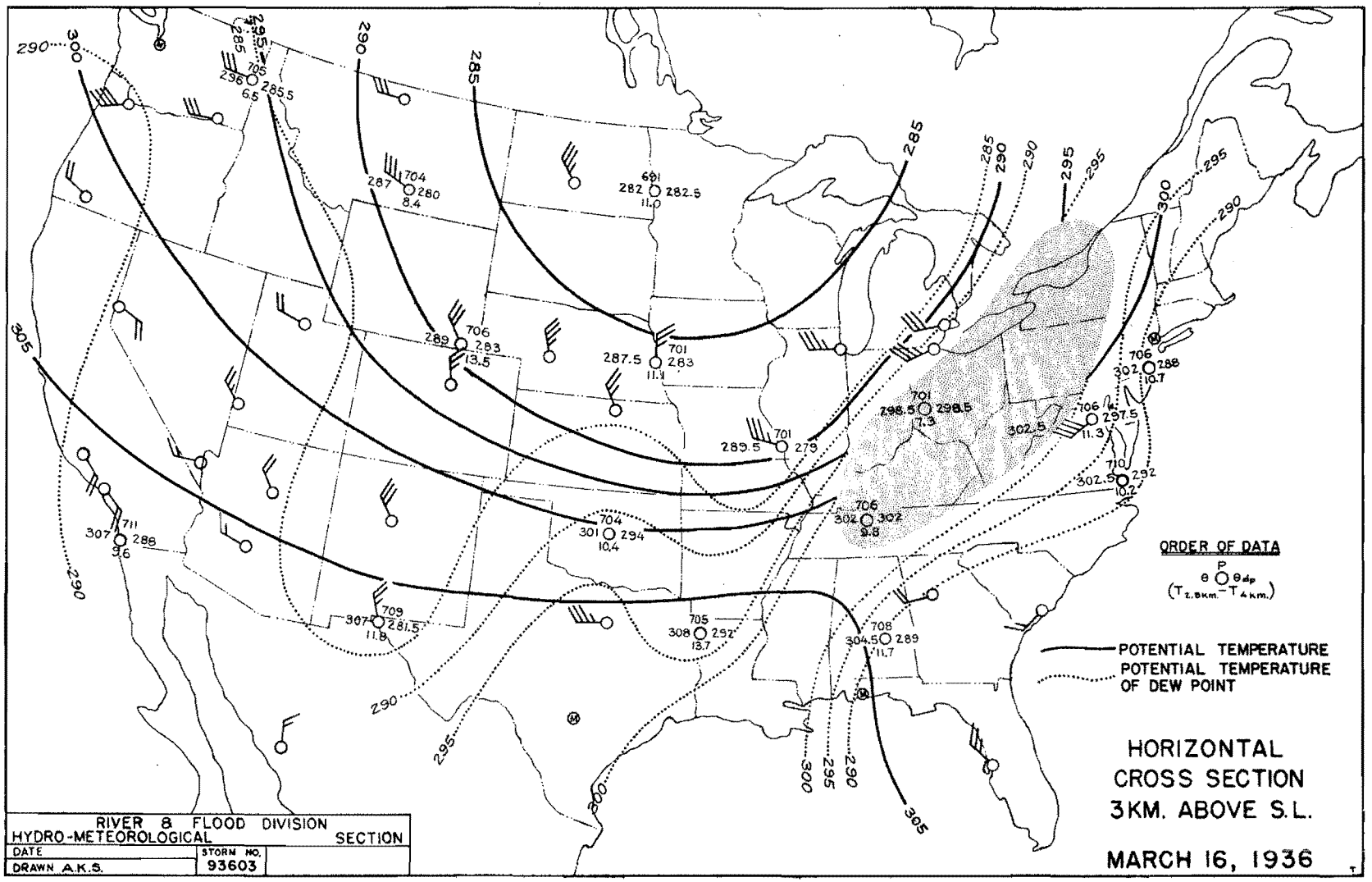
ORDER OF DATA
$e \overset{P}{O} \theta_{dp}$
$(T_{2.8km.} - T_{4km.})$
POTENTIAL TEMPERATURE
POTENTIAL TEMPERATURE OF DEW POINT
HORIZONTAL CROSS SECTION 3KM. ABOVE S.L.
MARCH 16, 1936
RIVER & FLOOD DIVISION
HYDRO-METEOROLOGICAL SECTION
DATE
DRAWN A.K.S.
STORM NO. 93603

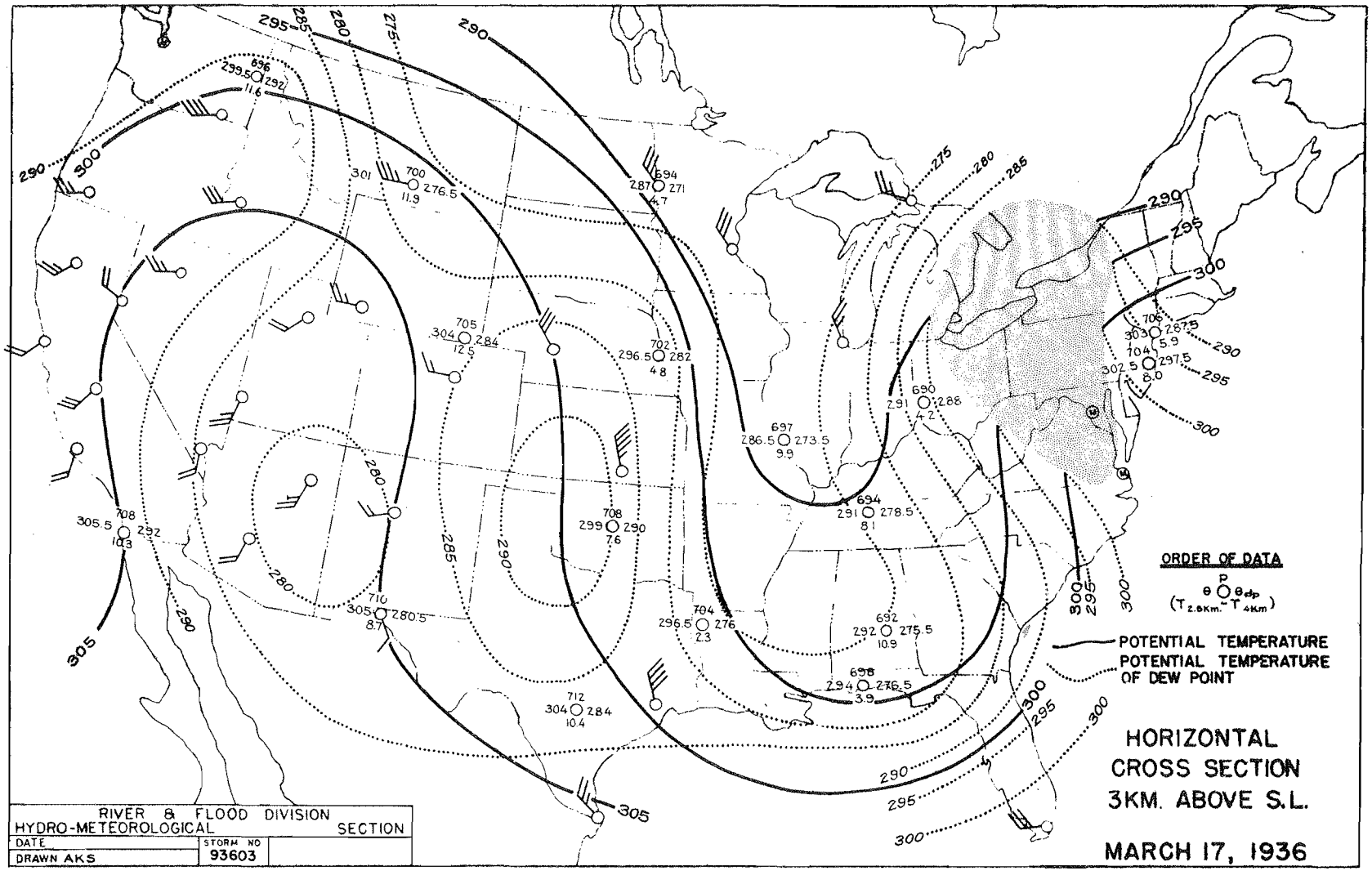
ORDER OF DATA
P
θ θdp
(T 2.5Km. ~ T 4Km)
POTENTIAL TEMPERATURE
POTENTIAL TEMPERATURE OF DEW POINT
HORIZONTAL CROSS SECTION 3KM. ABOVE S.L.
MARCH 17, 1936
RIVER & FLOOD DIVISION
HYDRO-METEOROLOGICAL SECTION
DATE
STORM NO 93603
DRAWN AKS

FIGURE A-91

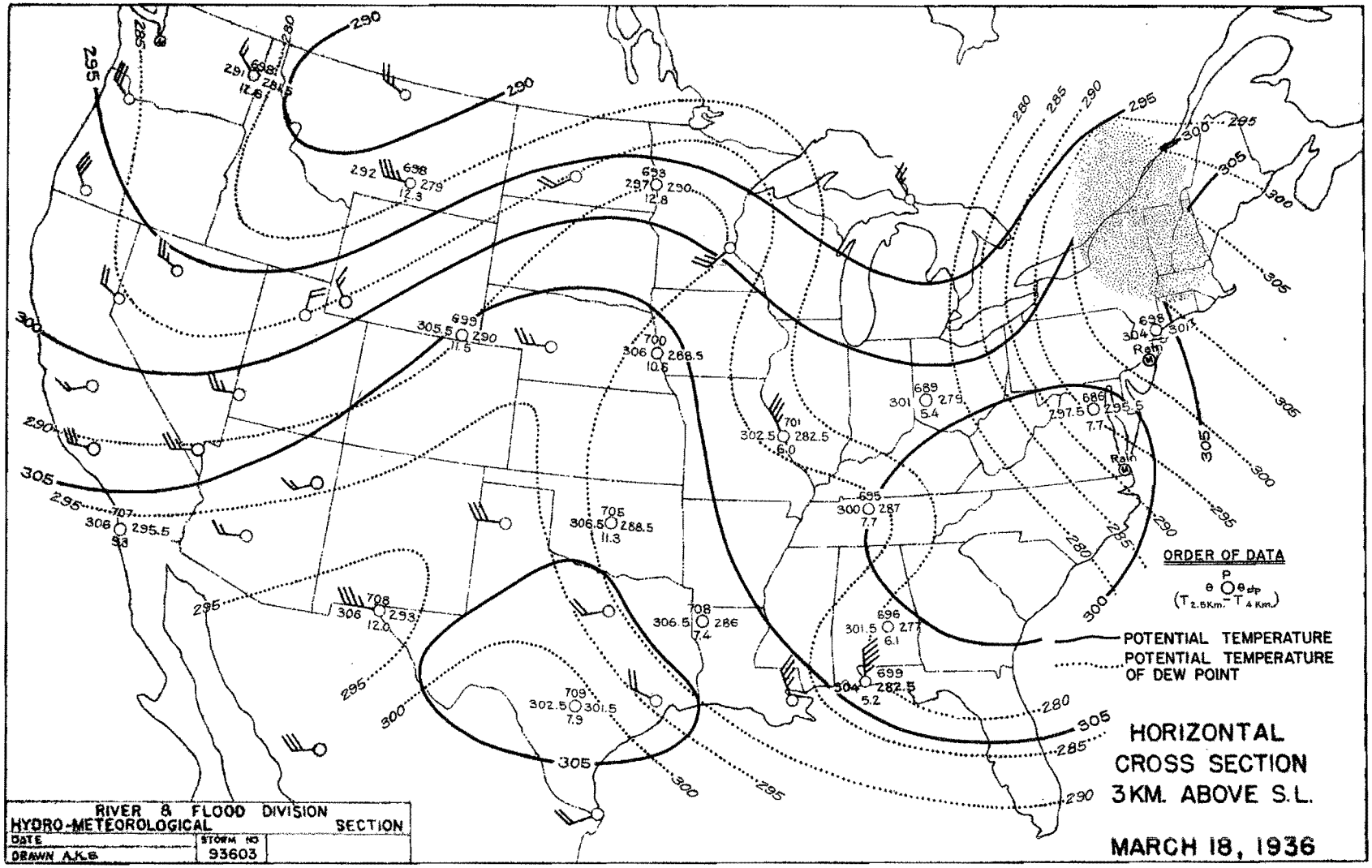
ORDER OF DATA
P
θ θdp
(T2.5Km.-T4Km.)
POTENTIAL TEMPERATURE
POTENTIAL TEMPERATURE OF DEW POINT
HORIZONTAL CROSS SECTION 3KM. ABOVE S.L.
MARCH 18, 1936
RIVER & FLOOD DIVISION
HYDRO-METEOROLOGICAL SECTION
DATE
DRAWN A.K.B.
STORM NO 93603

FIGURE A-92

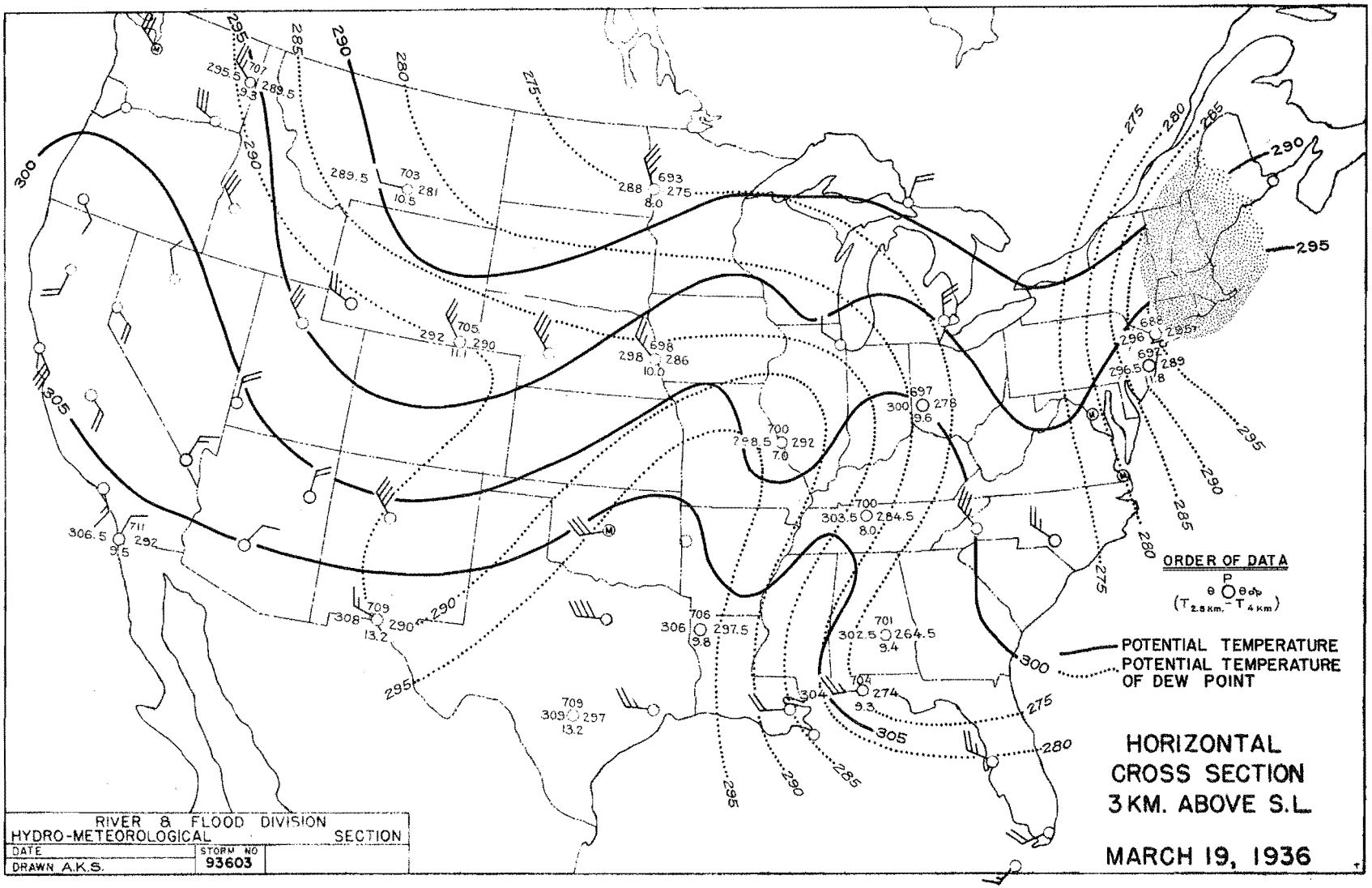
ORDER OF DATA
P
θ θdp
(T2.5Km. - T4Km.)
POTENTIAL TEMPERATURE
POTENTIAL TEMPERATURE OF DEW POINT
HORIZONTAL CROSS SECTION 3 KM. ABOVE S.L.
MARCH 19, 1936
RIVER & FLOOD DIVISION
HYDRO-METEOROLOGICAL SECTION
DATE
DRAWN A.K.S.
STORM NO 93603

FIGURE A-93

FIGURE A-94

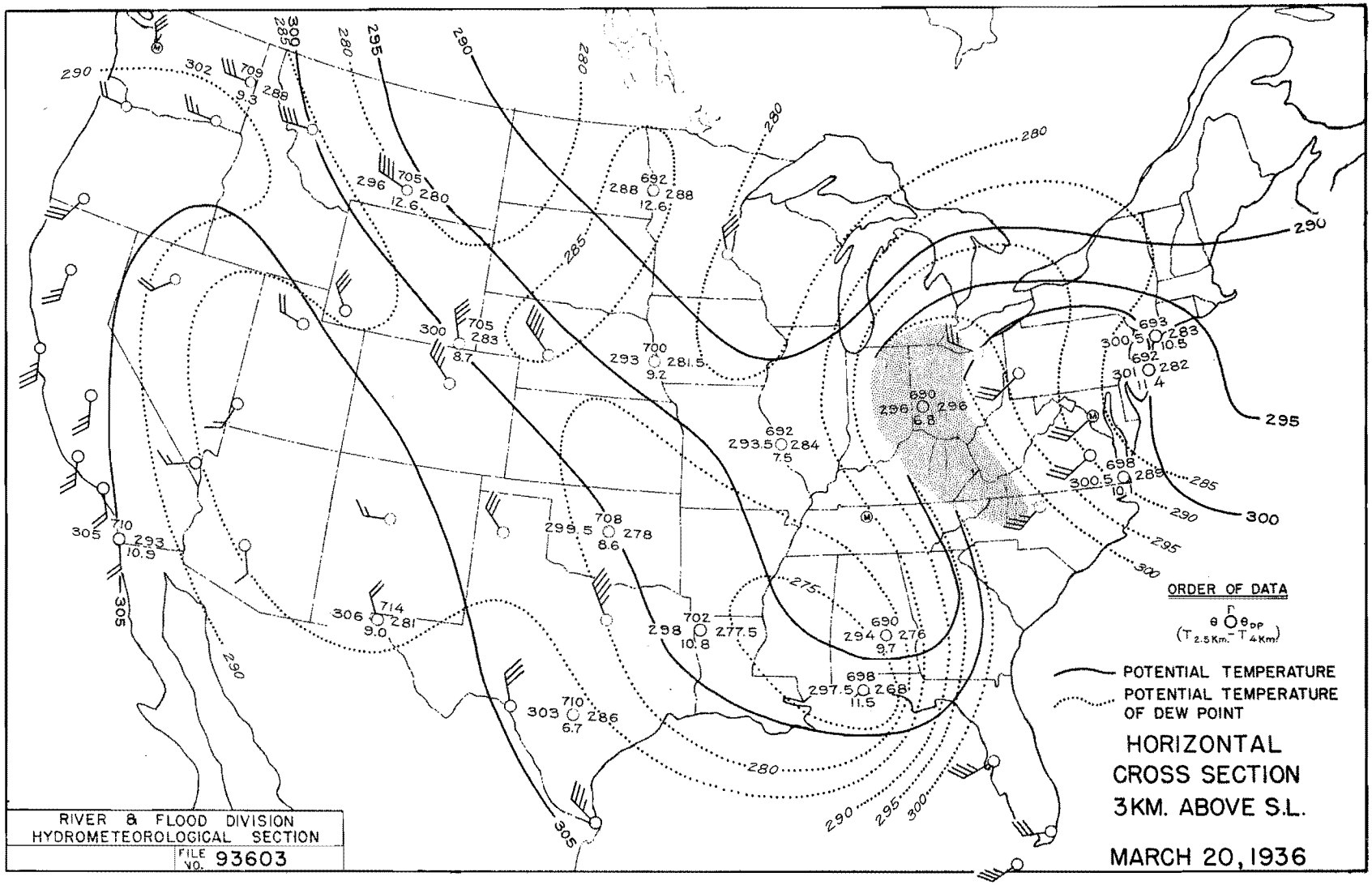
ORDER OF DATA
θ θpp
(T2.5Km.- T4Km.)
POTENTIAL TEMPERATURE
POTENTIAL TEMPERATURE OF DEW POINT
HORIZONTAL CROSS SECTION 3KM. ABOVE S.L.
MARCH 20, 1936
RIVER & FLOOD DIVISION
HYDROMETEOROLOGICAL SECTION
FILE NO. 93603

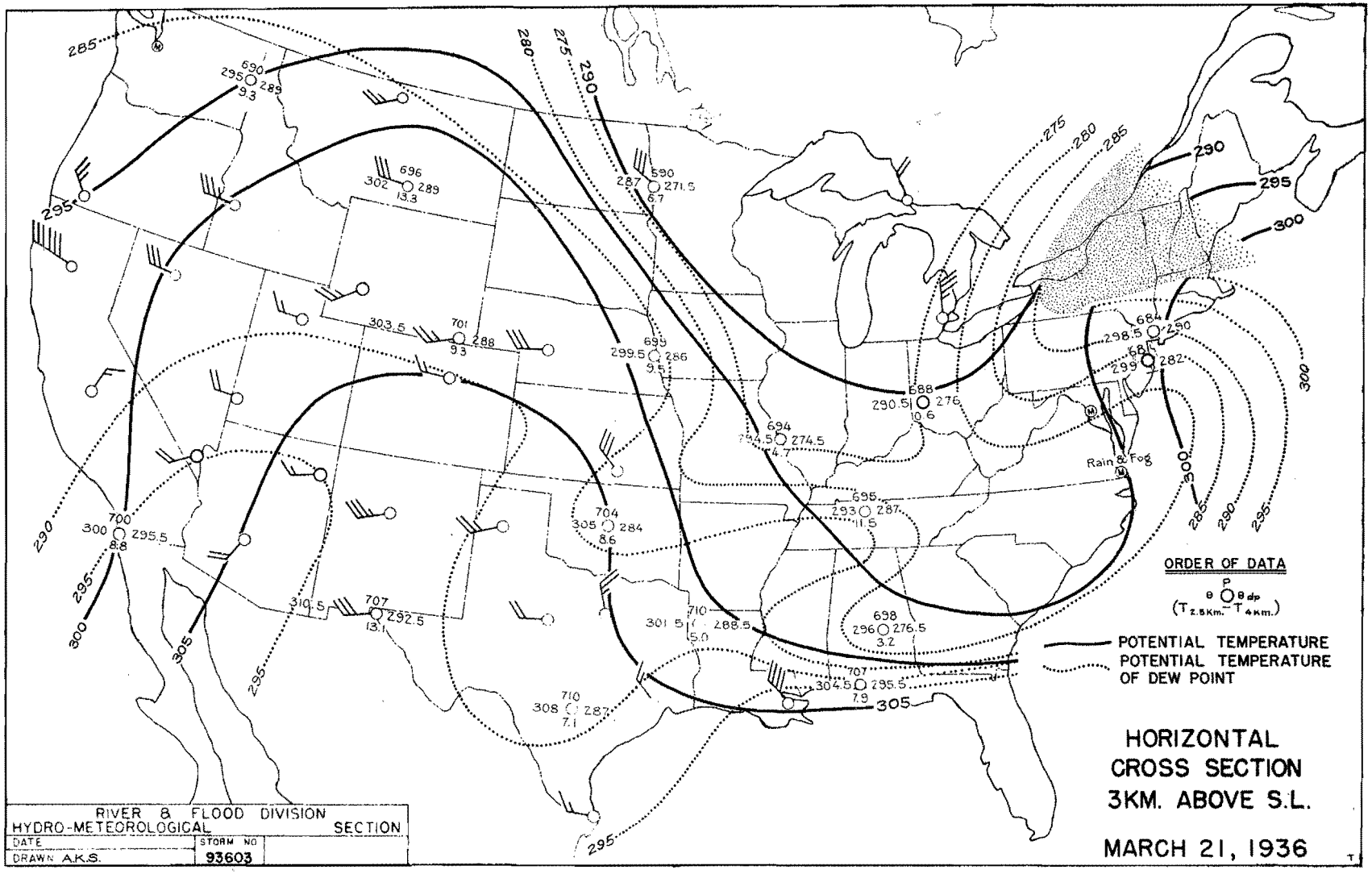
ORDER OF DATA
θ dp
(T 2.5Km. − T 4Km.)
POTENTIAL TEMPERATURE
POTENTIAL TEMPERATURE OF DEW POINT
HORIZONTAL CROSS SECTION 3KM. ABOVE S.L.
MARCH 21, 1936
Rain & Fog
RIVER & FLOOD DIVISION
HYDRO-METEOROLOGICAL SECTION
DATE
DRAWN A.K.S.
STORM NO
93603

FIGURE A-95

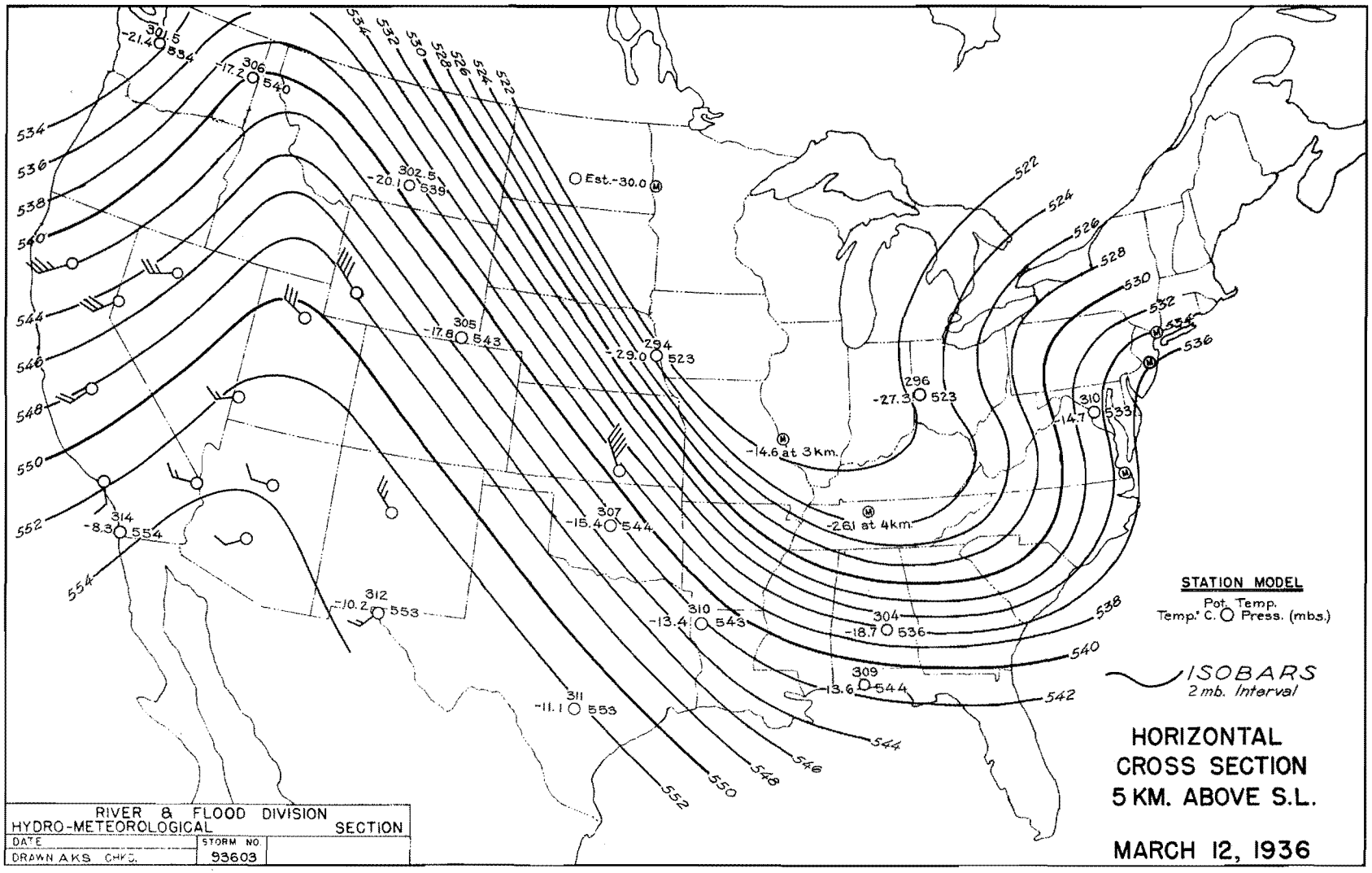
534
532
530
528
526
524
522
301.5
-21.4
854
306
-17.2
540
534
536
538
540
544
546
548
550
552
554
302.5
-20.1
539
Est.-30.0
305
-17.8
543
294
-29.0
523
522
524
526
528
530
532
534
536
296
-27.3
523
310
-14.7
533
-14.6 at 3km.
-26.1 at 4km.
314
-8.3
554
307
-15.4
544
312
-10.2
553
310
-13.4
543
304
-18.7
536
538
540
542
309
-13.6
544
311
-11.1
553
544
546
548
550
552
STATION MODEL
Pot. Temp.
Temp.° C. Press. (mbs.)
ISOBARS
2 mb. Interval
HORIZONTAL
CROSS SECTION
5 KM. ABOVE S.L.
MARCH 12, 1936
RIVER & FLOOD DIVISION
HYDRO-METEOROLOGICAL SECTION
DATE
STORM NO.
93603
DRAWN AKS CHKD.

FIGURE A-96

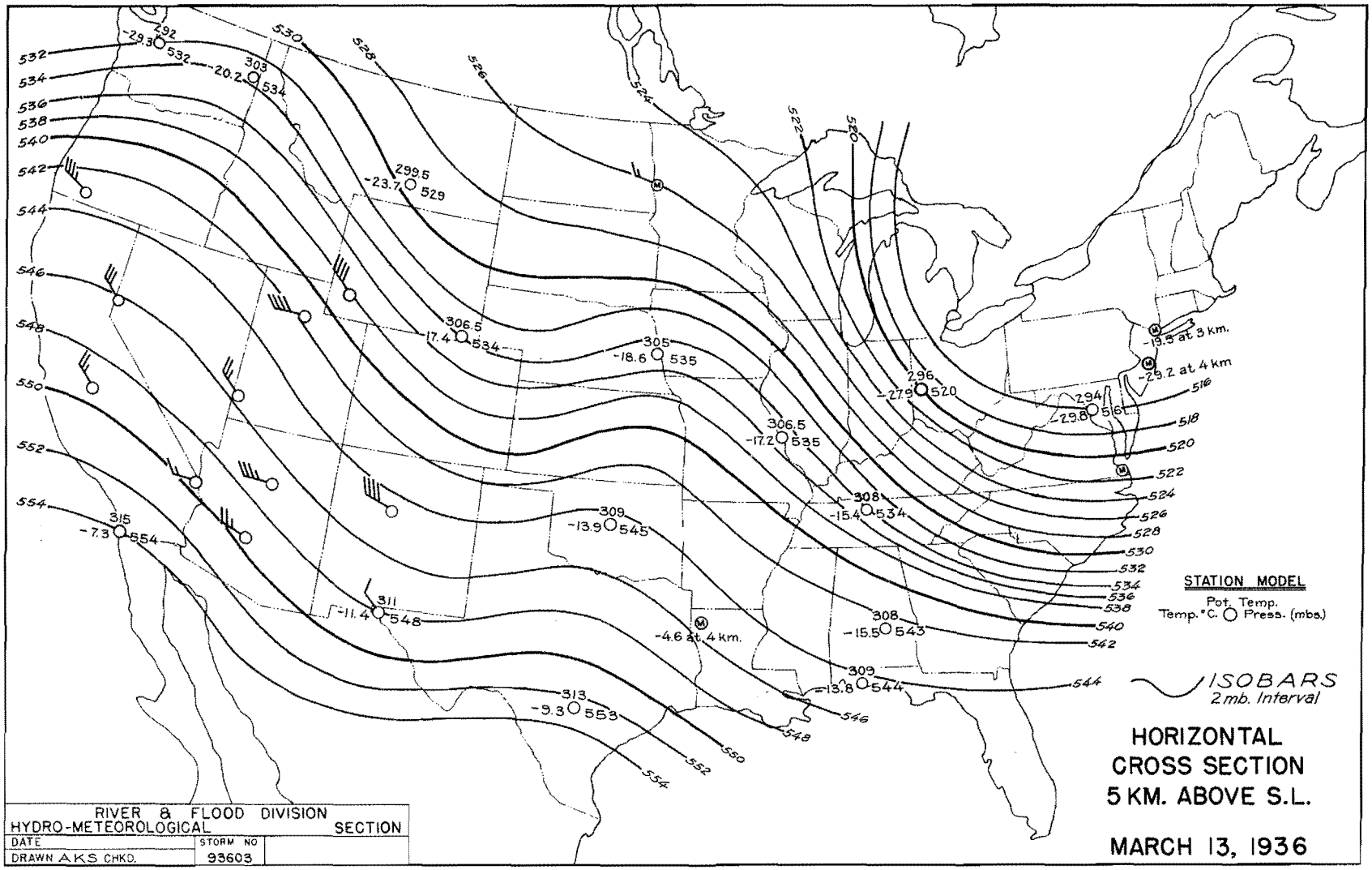
532
534
536
538
540
542
544
546
548
550
552
554
530
528
526
524
522
520
292
-29.3
532
303
-20.2
534
299.5
-23.7
529
306.5
-17.4
534
305
-18.6
535
306.5
-17.2
535
309
-13.9
545
315
-7.3
554
311
-11.4
548
313
-9.3
553
-4.6 at 4 km.
309
-13.8
544
308
-15.5
543
308
-15.4
534
296
-27.9
520
294
-29.8
516
-13.5 at 3 km.
-25.2 at 4 km
516
518
520
522
524
526
528
530
532
534
536
538
540
542
544
546
548
550
552
554
STATION MODEL
Pot. Temp.
Temp. °C. ○ Press. (mbs.)
ISOBARS
2 mb. Interval
HORIZONTAL
CROSS SECTION
5 KM. ABOVE S.L.
MARCH 13, 1936
RIVER & FLOOD DIVISION
HYDRO-METEOROLOGICAL SECTION
DATE
STORM NO
93603
DRAWN AKS CHKD.

FIGURE A-97

FIGURE A-98

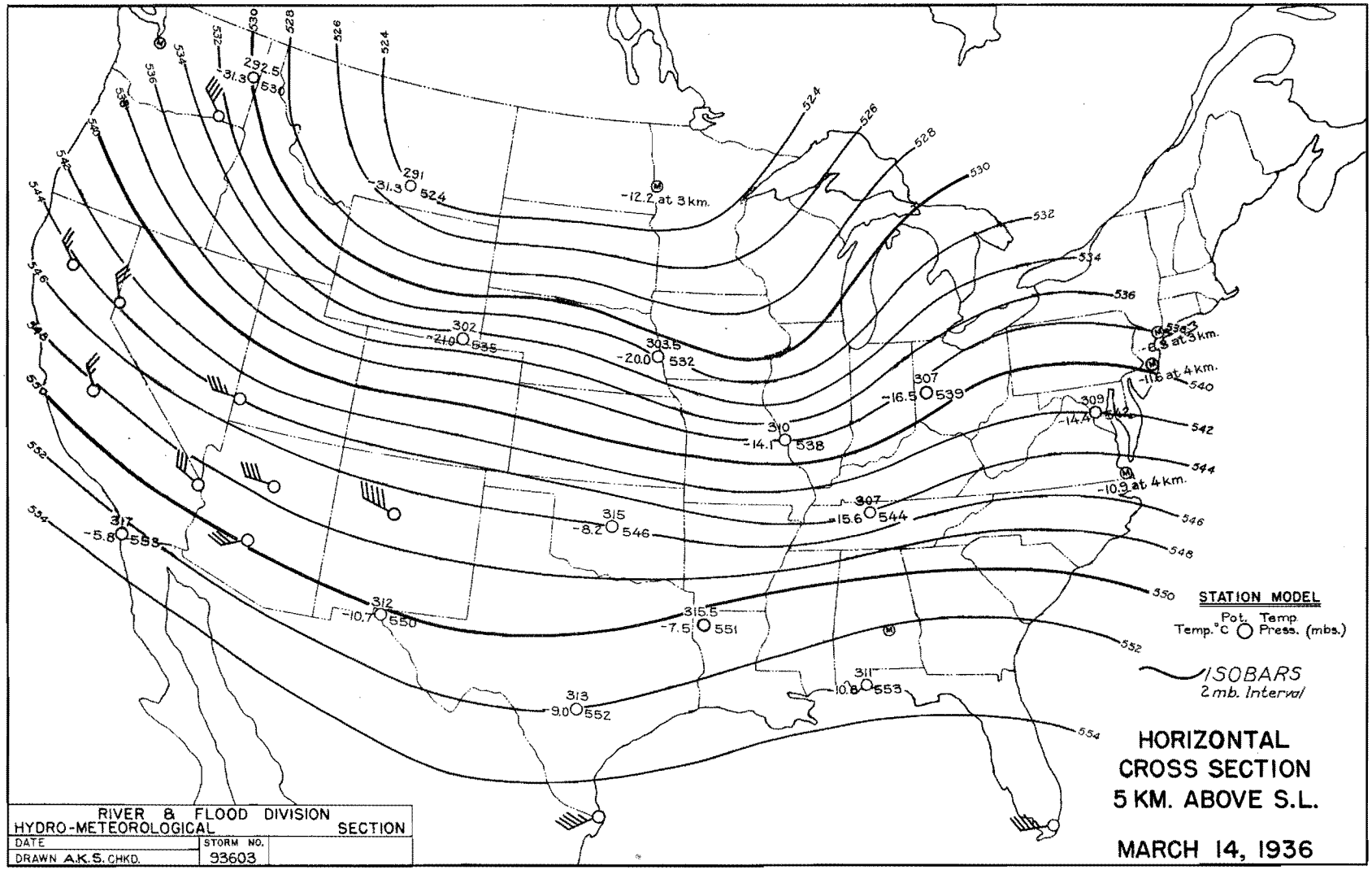
STATION MODEL
Pot. Temp
Temp. °C
Press. (mbs.)
ISOBARS
2 mb. Interval
HORIZONTAL
CROSS SECTION
5 KM. ABOVE S.L.
MARCH 14, 1936
RIVER & FLOOD DIVISION
HYDRO-METEOROLOGICAL SECTION
DATE
STORM NO.
93603
DRAWN A.K.S. CHKD.
-12.2 at 3 km.
-6.8 at 3 km.
-11.6 at 4 km.
-10.9 at 4 km.

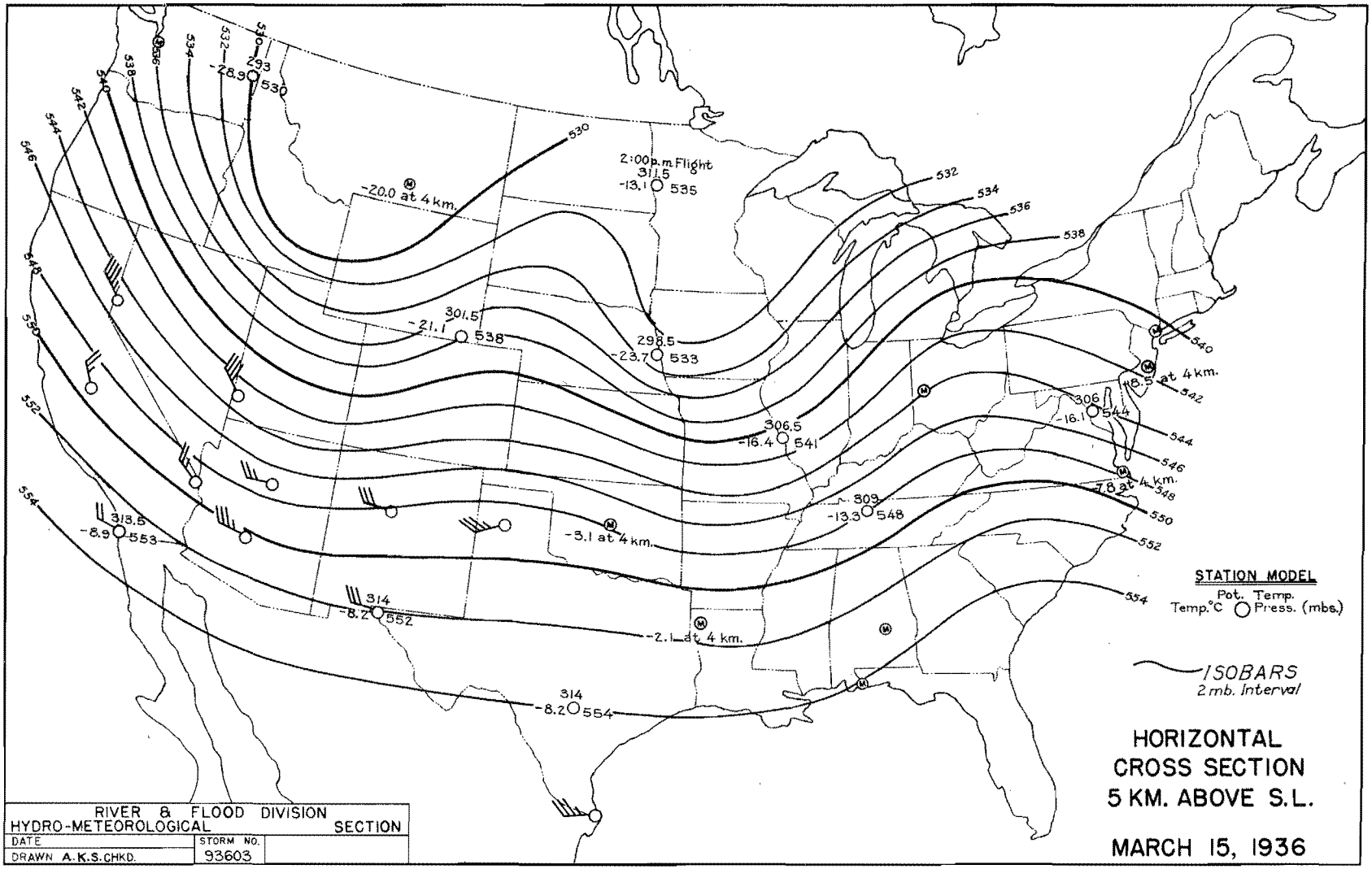
2:00 p.m. Flight
311.5
-13.1
535
-20.0 at 4 km.
301.5
-21.1
538
298.5
-23.7
533
306.5
-16.4
541
306
-16.1
544
309
-13.3
548
-3.1 at 4 km.
-2.1 at 4 km.
-8.5 at 4 km.
-7.8 at 4 km.
313.5
-8.9
553
314
-8.2
552
314
-8.2
554
530
532
534
536
538
540
542
544
546
548
550
552
554
STATION MODEL
Pot. Temp.
Temp.°C
Press. (mbs.)
ISOBARS
2 mb. Interval
HORIZONTAL
CROSS SECTION
5 KM. ABOVE S.L.
MARCH 15, 1936
RIVER & FLOOD DIVISION
HYDRO-METEOROLOGICAL SECTION
DATE
STORM NO.
93603
DRAWN A.K.S. CHKD.

FIGURE A-99

FIGURE A-100

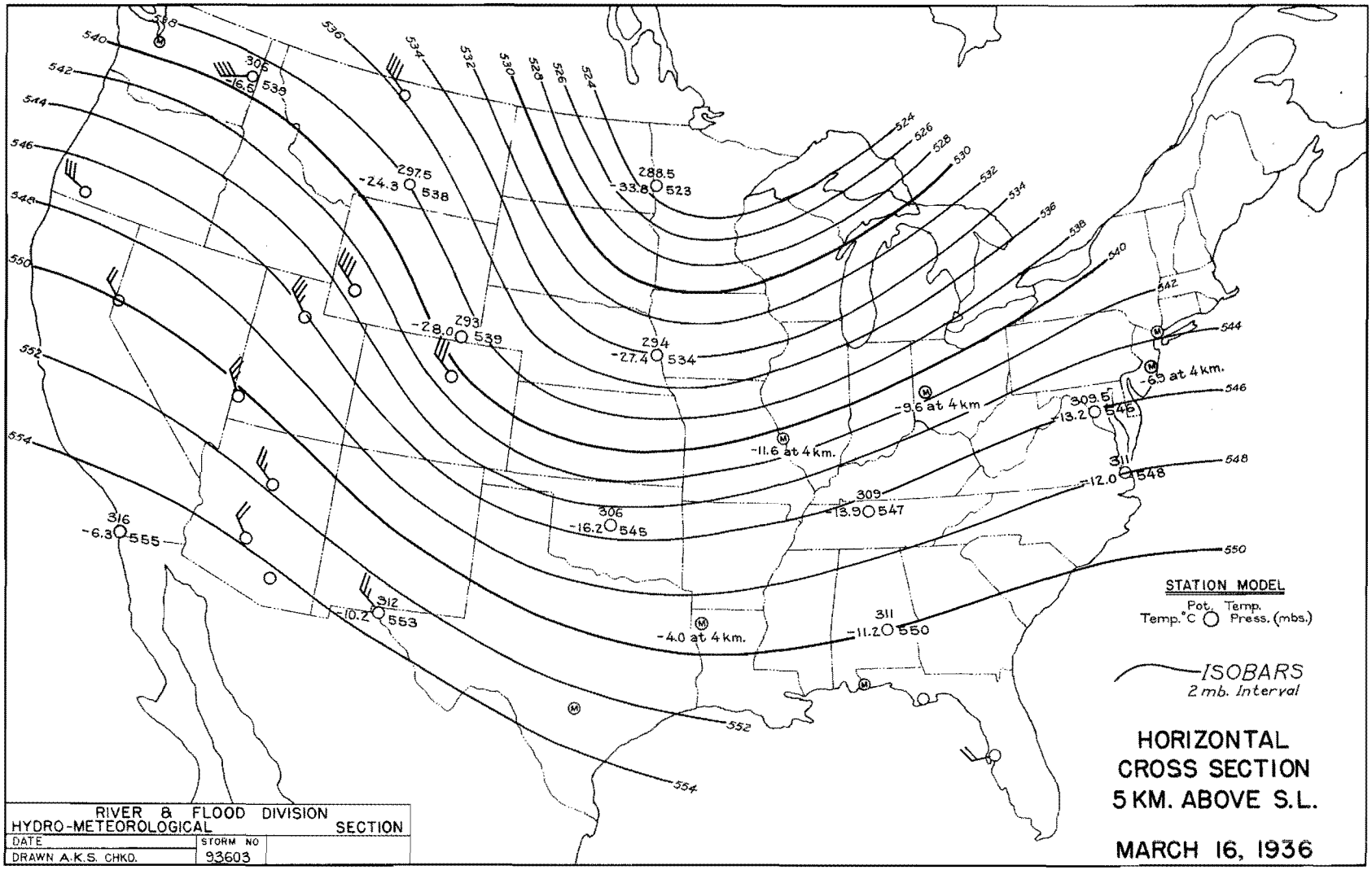
STATION MODEL
Pot. Temp.
Temp.°C Press. (mbs.)
ISOBARS
2 mb. Interval
HORIZONTAL
CROSS SECTION
5 KM. ABOVE S.L.
MARCH 16, 1936
RIVER & FLOOD DIVISION
HYDRO-METEOROLOGICAL SECTION
DATE
STORM NO
93603
DRAWN A.K.S. CHKD.
-24.3
-28.0
-27.4
-33.8
-16.6
-9.6 at 4 km.
-11.6 at 4 km.
-6.9 at 4 km.
-4.0 at 4 km.
-13.2
-12.0
-13.9
-16.2
-6.3
-10.2
-11.2

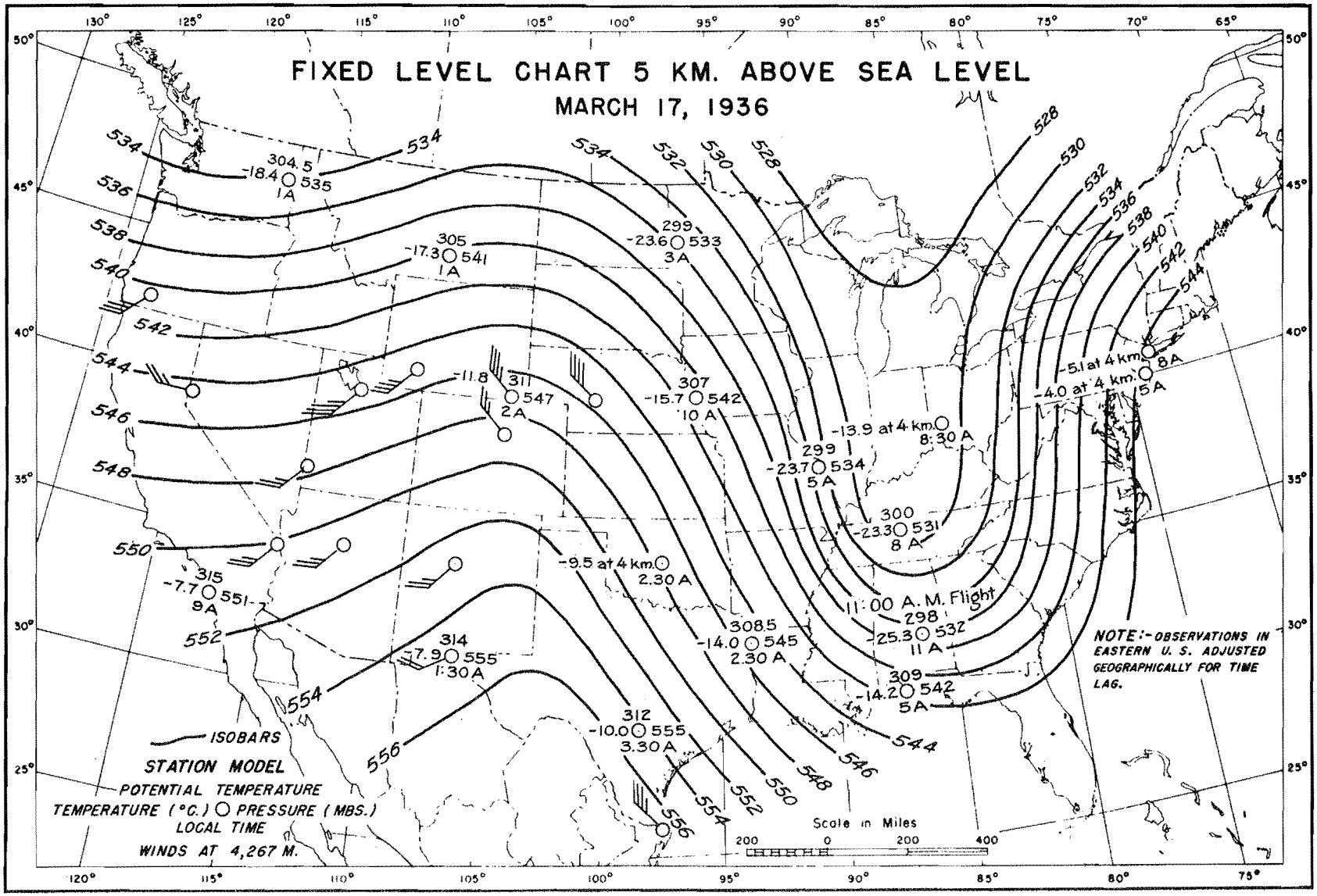
FIXED LEVEL CHART 5 KM. ABOVE SEA LEVEL
MARCH 17, 1936
ISOBARS
STATION MODEL
POTENTIAL TEMPERATURE
TEMPERATURE (°C.) O PRESSURE (MBS.)
LOCAL TIME
WINDS AT 4,267 M.
Scale in Miles
200 0 200 400
11:00 A.M. Flight
NOTE:- OBSERVATIONS IN EASTERN U. S. ADJUSTED GEOGRAPHICALLY FOR TIME LAG.

FIGURE A-101

FIGURE A-102

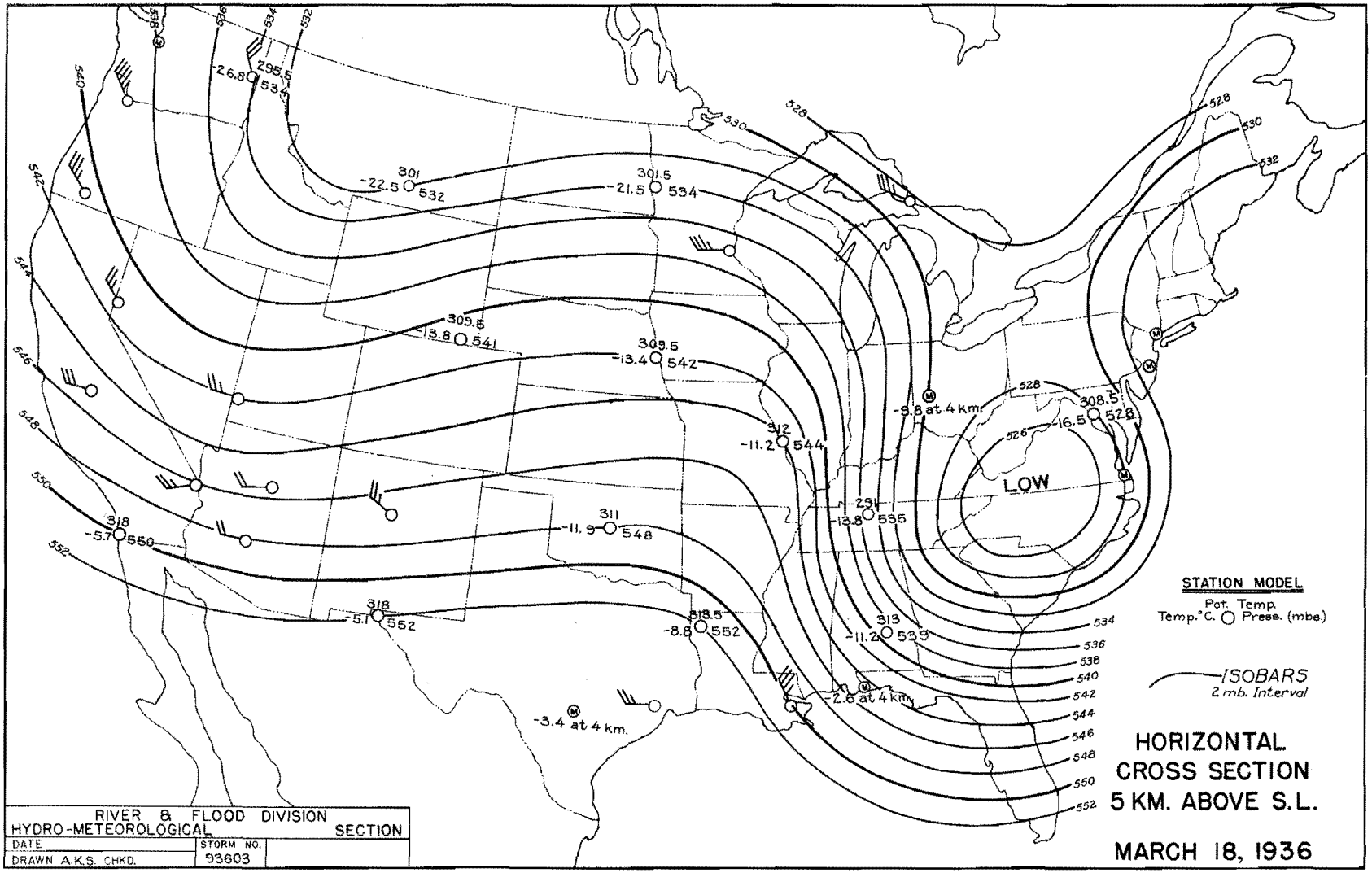
LOW
-9.8 at 4 km.
-2.6 at 4 km.
-3.4 at 4 km.
-26.8 295.5 534
-22.5 301 532
-21.5 301.5 534
-13.8 309.5 541
-13.4 309.5 542
-11.2 312 544
-13.8 291 535
-11.9 311 548
-5.7 318 550
-5.1 318 552
-8.8 318.5 552
-11.2 313 539
16.5 308.5 528
STATION MODEL
Pot. Temp.
Temp.°C. Press. (mbs.)
ISOBARS
2 mb. Interval
HORIZONTAL
CROSS SECTION
5 KM. ABOVE S.L.
MARCH 18, 1936
RIVER & FLOOD DIVISION
HYDRO-METEOROLOGICAL SECTION
DATE
STORM NO. 93603
DRAWN A.K.S. CHKD.

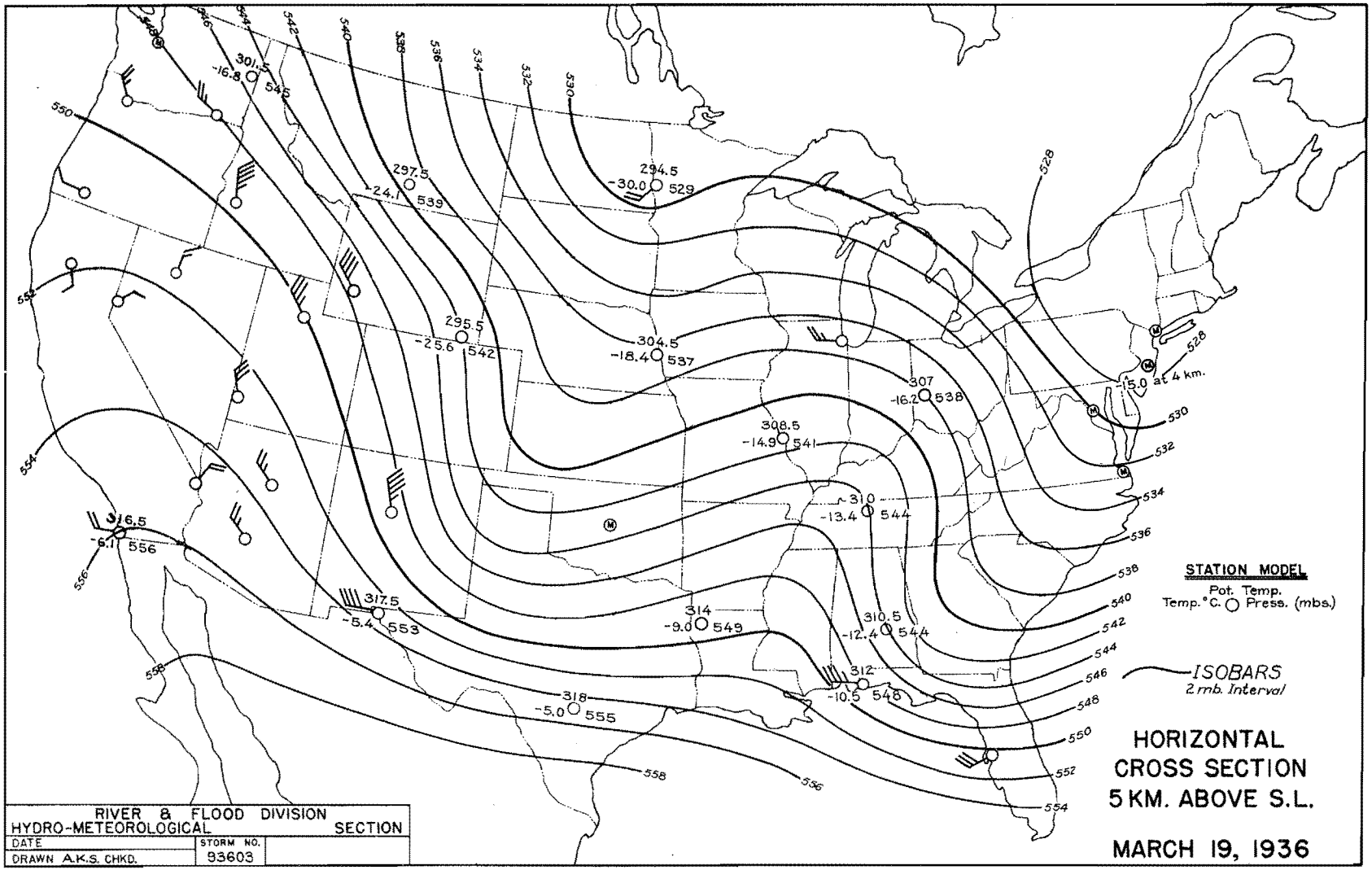
STATION MODEL
Pot. Temp.
Temp. °C. ○ Press. (mbs.)
ISOBARS
2 mb. Interval
HORIZONTAL
CROSS SECTION
5 KM. ABOVE S.L.
MARCH 19, 1936
RIVER & FLOOD DIVISION
HYDRO-METEOROLOGICAL SECTION
DATE
STORM NO. 93603
DRAWN A.K.S. CHKD.
316.5
-6.1 556
317.5
-5.4 553
318
-5.0 555
314
-9.0 549
310.5
-12.4 544
312
-10.5 548
310
-13.4 544
308.5
-14.9 541
307
-16.2 538
304.5
-18.4 537
297.5
-24.1 539
295.5
-25.6 542
294.5
-30.0 529
301.5
-16.8 549
-15.0 at 4 km.

FIGURE A-103

FIGURE A-104

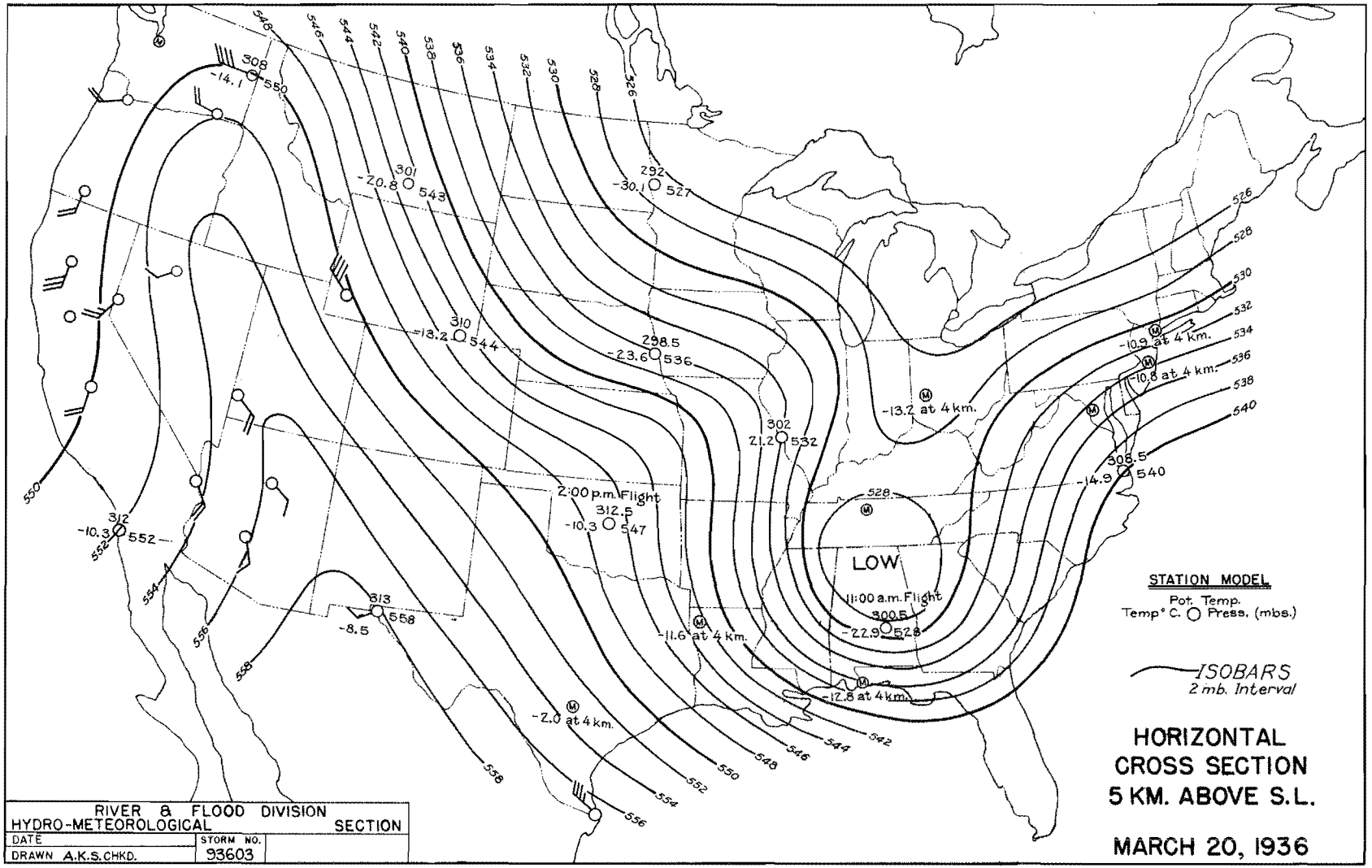
LOW
2:00 p.m. Flight
11:00 a.m. Flight
-13.2 at 4 km.
-10.9 at 4 km.
-10.8 at 4 km.
-11.6 at 4 km.
-12.8 at 4 km.
-2.0 at 4 km.
STATION MODEL
Pot. Temp.
Temp° C. Press. (mbs.)
ISOBARS
2 mb. Interval
HORIZONTAL
CROSS SECTION
5 KM. ABOVE S.L.
MARCH 20, 1936
RIVER & FLOOD DIVISION
HYDRO-METEOROLOGICAL SECTION
DATE
DRAWN A.K.S. CHKD.
STORM NO.
93603

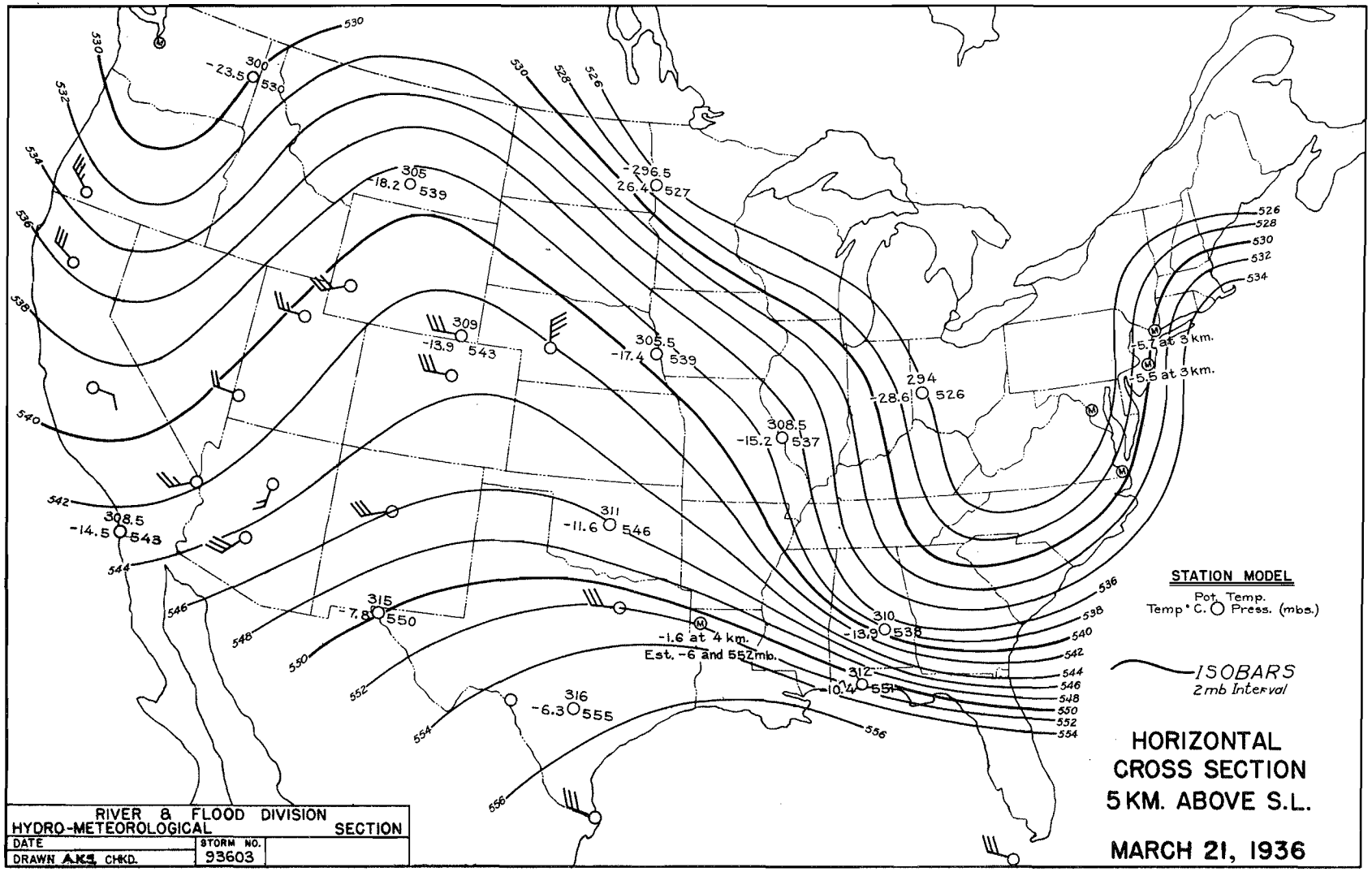
STATION MODEL
Pot. Temp.
Temp° C. Press. (mbs.)
ISOBARS
2mb Interval
HORIZONTAL
CROSS SECTION
5 KM. ABOVE S.L.
MARCH 21, 1936
RIVER & FLOOD DIVISION
HYDRO-METEOROLOGICAL SECTION
DATE
DRAWN AKS CHKD.
STORM NO. 93603
-23.5 300 530
-18.2 305 539
-13.9 309 543
-14.5 308.5 543
-7.8 315 550
-6.3 316 555
-11.6 311 546
-17.4 305.5 539
-26.5 296.5
26.4 527
-28.6 294 526
-15.2 308.5 537
-13.9 310 538
-10.4 312 551
-1.6 at 4 km.
Est. -6 and 55Zmb.
-5.7 at 3km.
-5.5 at 3km.

FIGURE A-105

FIGURE A-106

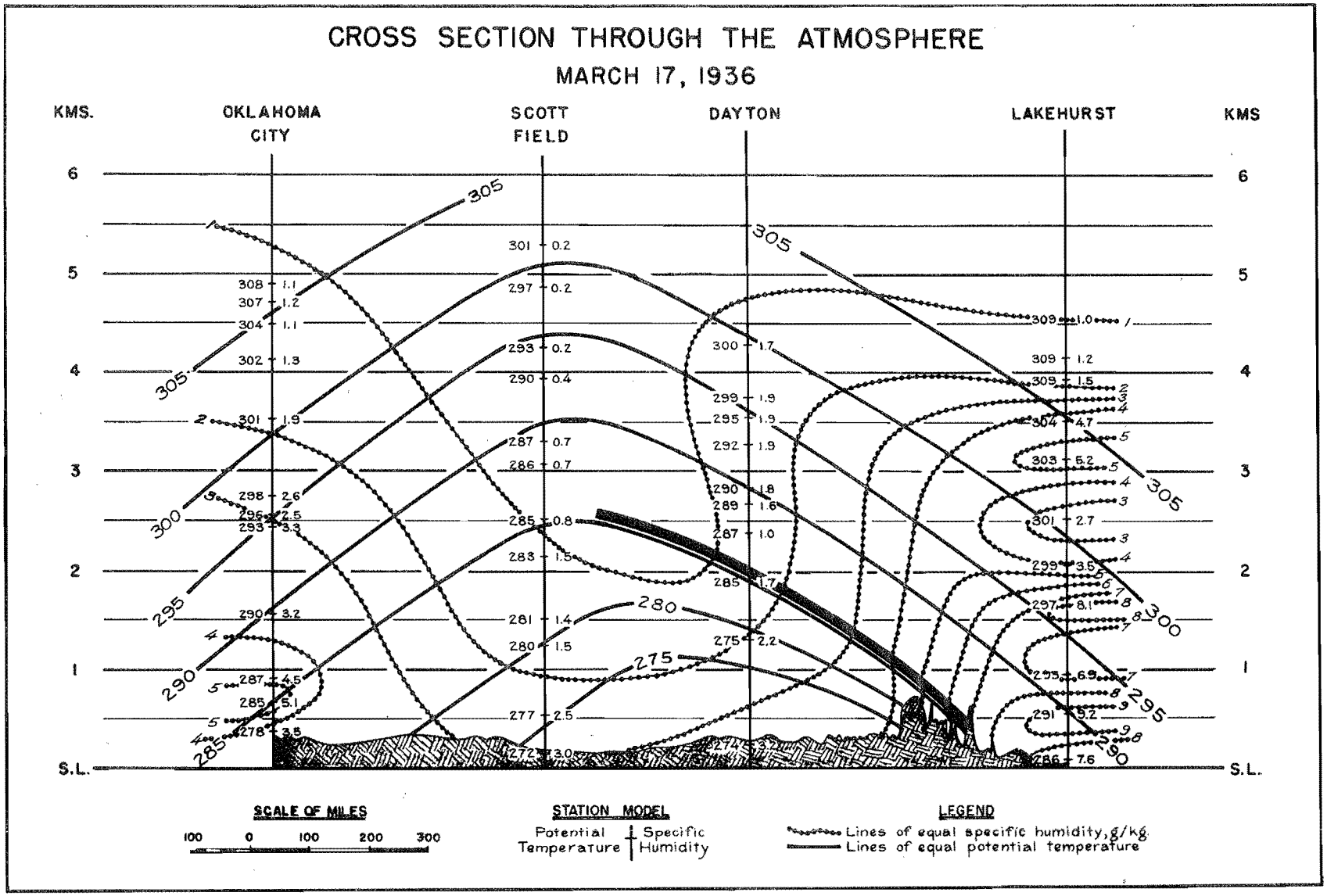
CROSS SECTION THROUGH THE ATMOSPHERE
MARCH 17, 1936
KMS.
OKLAHOMA CITY
SCOTT FIELD
DAYTON
LAKEHURST
KMS
S.L.
SCALE OF MILES
100 0 100 200 300
STATION MODEL
Potential Temperature
Specific Humidity
LEGEND
Lines of equal specific humidity, g/kg
Lines of equal potential temperature

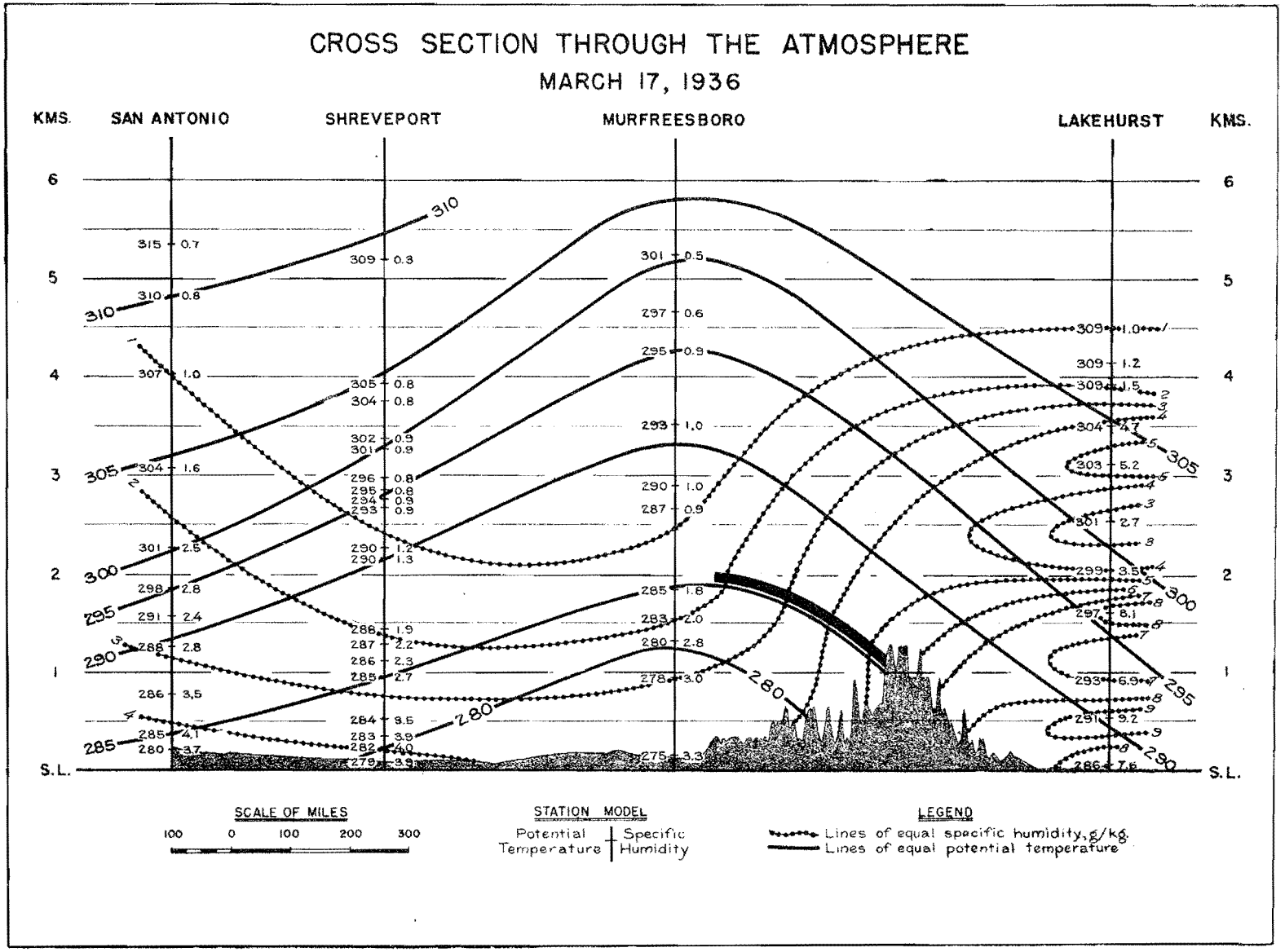
CROSS SECTION THROUGH THE ATMOSPHERE
MARCH 17, 1936
KMS.
SAN ANTONIO
SHREVEPORT
MURFREESBORO
LAKEHURST
KMS.
S.L.
S.L.
SCALE OF MILES
100 0 100 200 300
STATION MODEL
Potential Temperature
Specific Humidity
LEGEND
Lines of equal specific humidity, g/kg.
Lines of equal potential temperature

FIGURE A-107